

# HYDROGEOLOGY OF DEKE ISLAND PINGELAP ATOLL EASTERN CAROLINE ISLANDS

Jerry F. Ayers  
H. Len Vacher  
Russell N. Clayshulte  
David Strout  
Richard Stebnisky

*Water and Energy Research Institute  
of the  
Western Pacific*

**UNIVERSITY OF GUAM**

**Technical Report No. 52**

**July, 1984**



Contents of this publication do not necessarily reflect the views and policies of the United States Department of the Interior nor does mention of trade names or commercial products constitute their endorsement or recommendation for use by the United States Government.

HYDROGEOLOGY OF DEKE ISLAND, PINGELAP ATOLL,  
EASTERN CAROLINE ISLANDS

By

Jerry F. Ayers  
H. Len Vacher  
Russell N. Clayshulte  
David Strout  
Richard Stebnisky

UNIVERSITY OF GUAM

*Water and Energy Research Institute  
of the  
Western Pacific*

Technical Report No. 52

July, 1984

Project Completion Report

for

A HYDROGEOLOGIC INVESTIGATION OF ATOLL ISLANDS,  
PONAPE STATE, EASTERN CAROLINE ISLANDS

U.S.G.S. Project No. G-837-02  
T.T.P.I. Contract No. CT410036

Principal Investigators: Jerry F. Ayers and H. L. Vacher

U.S.G.S. Project Period: October 1, 1983 to September 30, 1984  
T.T.P.I. Project Period: February 1, 1984 to December 31, 1984

The research on which this report is based was financed in part by the United States Department of the Interior as authorized under the Water Research and Development Act of 1978 (P.L. 95-467) and by the Trust Territory of the Pacific Islands.

## ABSTRACT

An extensive hydrogeological investigation was conducted on Deke Island located on Pingelap Atoll, Ponape State. Field work included installation of observation wells, water-level monitoring, installation of a tidal gage, core drilling, surface geological and topographical mapping, geophysical surveys, and water-quality analysis. Results from the work performed on the study island indicate a number of previously unknown aspects of atoll island hydrology. The most significant of these aspects is the partial confinement of the fresh-water lens system beneath the landward extension of the reef-flat plate. Where the plate is absent water-table conditions are prevalent. The plate acts as a leaky confining layer which allows some rainwater to enter the flow system by downward movement under gravity. Approximately 2/3 of Deke overlies the reef-flat plate; the remainder overlies sediments deposited behind the reef-flat depositional environment.

In addition to the documentation of hydraulic conditions within the lens system the behavior of the ground-water resource was studied and a method of reducing observed water levels in wells to actual sea level was developed. Also, several subsurface hydrogeologic units were identified and their roles within the overall hydrology of Deke were defined. In general, the size and extent of the lens was mapped. Based on the interpretation of study results an atoll island hydrogeologic (conceptual) model is presented. Finally, some practical implications of the study findings are discussed and recommendations for further work are made.

## TABLE OF CONTENTS

	Page
LIST OF FIGURES.....	vii
LIST OF TABLES.....	x
INTRODUCTION.....	1
Purpose and Scope of the Study.....	1
Location and Description of the Study Island.....	3
METHODS OF INVESTIGATION.....	7
Water-Level Monitoring Program.....	7
The Piezometer Study.....	9
Elevation Control.....	9
Weather Data.....	10
Geomorphology and Surface Geology Mapping Program.....	10
Topographic Mapping.....	11
Grain-Size Analysis.....	11
Measurement of Stratigraphic Sections.....	12
Subsurface Geologic Investigation.....	12
Core Drilling Operations.....	12
Sampling Methods.....	13
Core and Sample Examination.....	13
Water-Quality Determination.....	13
Surface-Based Geophysical Surveys.....	15
Seismic-Refraction Profiling.....	15
Earth-Resistivity Sounding.....	18
RESULTS OF THE INVESTIGATION.....	20
Water-Level Monitoring Program.....	20
Lagoon Tides.....	20
Ground-Water Tides.....	28
Areal Patterns.....	28
Standpipe vs. Piezometers.....	33
Ocean Shore Tide Pipe.....	36
Day-to-Day Variations.....	36
14-Day Time Series.....	36
Reduced Levels.....	39
Standpipes vs. Piezometers.....	46
Areal Patterns.....	46
Water-Level Maps.....	49
Geomorphology and Surface Geology of Deke.....	53
Geomorphology.....	53
Grain-Size Distribution.....	56

## Tables of Contents Continued.

	Page
Surface Geology.....	56
Stratigraphic Sections.....	63
Subsurface Geologic Investigation.....	63
Core Drilling.....	63
Reef-Flat and Hard-Layer Samples.....	68
Geophysical Surveys.....	68
Seismic-Refraction Profiling.....	70
Earth-Resistivity Soundings.....	77
Water Quality.....	89
DISCUSSION.....	89
Interpretation of Water-Level Data.....	89
Reduced Levels.....	90
Constant-Sea-Level Water-Level Hydrograph.....	95
Hydrogeological Framework of Deke.....	100
The Fresh-Water Lens System.....	107
Practical Implications of the Study Results.....	109
Guidelines for Further Study.....	113
SUMMARY.....	117
Water-Level Monitoring Program.....	117
Geomorphology and Geology.....	118
Hydrogeology and Groundwater Occurrence.....	119
ACKNOWLEDGMENT.....	120
REFERENCES CITED.....	122
TABLE OF CONTENTS APPENDIX A: Water-Level Data.....	123
TABLE OF CONTENTS APPENDIX B: Geophysical Data.....	164
TABLE OF CONTENTS APPENDIX C: Drilling Logs and Sample Description.....	288
TABLE OF CONTENTS APPENDIX D: Relative-Salinity Data.....	353

## LIST FIGURES

	Page
1. Map of Micronesia showing the location of Pingelap Atoll.....	4
2. Aerial view of Pingelap Atoll.....	5
3. Map of Deke Island showing the location of various types of observation sites.....	8
4. Map of a portion of Pingelap Atoll showing the collection sites for reef-flat and taro-pit rock samples.....	14
5. Map of Deke Island showing the locations of seismic-refraction lines and earth-resistivity stations.....	16
6. Graphs showing the tidal highs and lows and the daily mean at the lagoon recorder station.....	21
7. Graphs showing daily mean sea level at the lagoon recorder station and barometric pressure.....	22
8. Graph showing a representative week-long recording of the semidiurnal tides in the lagoon.....	24
9. Graphs showing a tidal cycle in the lagoon and at a deep piezometer (B5) located near the ocean shore.....	26
10. Map of Deke Island showing the geographical variations of high-to-low and low-to-high tidal time.....	30
11. Map of Deke Island showing the time lag of the tidal highs.....	31
12. Map of Deke Island showing the geographical distributions of tidal efficiency.....	32
13. Graphs showing the simultaneous tidal variations at piezometer-standpipe pairs.....	34
14. Simultaneous continuous recordings at two observation wells....	35
15. Graph showing the tidal high at two nearshore inland piezometers and at a standpipe installed in an ocean-facing beach.....	37
16. Hydrographs from observation wells located within the western portion of Deke Island.....	40
17. Hydrographs from observation wells located within the eastern portion of Deke Island.....	41
18. Graphs of ground-water levels, daily lagoon level, and daily rainfall.....	44

List of Figures Continued.	Page
19. Graphs of reduced well hydrographs, daily mean lagoon level, and daily rainfall.....	45
20. Graph of daily water levels at two observation wells.....	47
21. Map of Deke Island showing the distribution of standard deviations for a 21-day series of water levels.....	50
22. Map of Deke Island showing the geographic distribution of the range of the 21-day series of water levels.....	51
23. Map of Deke Island showing the geographical distribution of the average water level measured in observation wells.....	52
24. Map of Deke Island showing the geographical distribution on ground-water levels for two measurement days.....	54
25. Topographic map of Deke Island.....	55
26. Contour map of the sediment distribution at the surface of Deke Island.....	57
27. Grain-size distribution of surface sediment samples within three mapped zones.....	58
28. Example graphs of polymodal grain-size distributions for sieve samples.....	60
29. Results of sieve analyses on samples collected from stratigraphic test pits.....	61
30. Map of Deke Island showing the distribution of surface sediments.....	62
31. Map of Deke Island showing the traverse used in topographic profiling and surface sediment sampling.....	64
32. Profiles showing topographic cross sections and sediment-size zones.....	65
33. Geologic and drilling logs for all cored boreholes across Deke Island.....	67
34. Geologic logs of selected cored boreholes across Deke Island...	69
35. Seismic profiles across Deke Island.....	75
36. Map of Deke Island showing the geographic distribution of chloride-ion concentration in observation wells.....	84
37. Map of Deke Island showing the geographic distribution of total hardness measured in observation wells.....	85



## List of Figures Continued.

	Page
38. Graph of specific conductance versus time at observation well D <sub>s</sub> 4.....	87
39. Probability plot of relative salinity measurements from observation well D4.....	88
40. Hydrographs of three observation wells on Deke Island.....	91
41. Graphs of reduced hydrographs at three observation wells.....	92
42. Graphs of smoothed reduced water levels at three observation wells, daily mean lagoon level, and daily rainfall.....	93
43. Comparison of constant sea-level hydrographs and reduced hydrographs at three observation wells.....	98
44. Graphs of reduced ground-water levels, daily lagoon level, and rainfall for a 21-day measurement period.....	99
45. Generalized observation well hydrograph and rainfall.....	101
46. Hydrogeologic cross section along seismic profile A.....	102
47. Hydrogeologic cross section along seismic profile C.....	103
48. Generalized conceptual model of the Deke Island groundwater-flow system.....	108
49. Probability plots of relative-salinity profiles at D53.....	111

## LIST OF TABLES

	Page
1. Tidal data from continuous recordings.....	25
2. Results of the tide studies of March 18, 19, 20.....	27
3. Combined results of the tidal studies.....	29
4. The 14-well time series.....	38
5. 14-well time series: well statistics.....	42
6. 14-well time series: day statistics.....	43
7. Expanded time series: well statistics.....	48
8. Statistical parameter calculated from sieved samples.....	59
9. Seismic velocities determined from the computer analysis of first arrival times for 2-layer seismographs.....	71
10. Seismic velocities determined from the computer analysis of first arrival times for 3-layer seismographs.....	72
11. Summary statistics for seismic velocities determined by computer analysis of 2- and 3- layer seismographs.....	73
12. Layer thickness and resistance determined from matching field vertical electrical sounding (VES) curves with computer- generated VES curves.....	78
13. Water quality data for samples collected from observation wells.....	79
14. Depth related specific-conductance and estimated chloride-ion data for DS3.....	80
15. Depth related specific-conductance and estimated chloride-ion data for DS4.....	82
16. Relative-salinity profile data for DS3.....	83
17. Correlation of measured water levels, reduced water levels, and "constant-sea-level hydrographs" with the lagoon record....	94
18. Calculation of CSL hydrograph at C2.....	97
19. Legend to Figures 46 and 47.....	104

## INTRODUCTION

Many atoll island communities in Micronesia face continual problems of potable water-supply shortages and water-quality deterioration. The level of severity of these problems is demonstrated by the recent outbreaks of water-borne diseases in Truk State, the Marshall Islands, and elsewhere. It is obvious that effective measures to control these problems must be initiated as soon as possible. It is equally obvious, in light of the findings of this investigation, that a thorough understanding of the hydrogeologic framework and ground-water occurrence for a given island is necessary to ensure success in addressing the numerous water-related problems experienced by island inhabitants.

Information obtained from field work on the study island of Deke indicates a much more complex hydrogeology than would ordinarily be expected for such a small, and seemingly uncomplicated, island. Discovery of a hard substrate underlying much of the island and documentation of its profound effect on the occurrence and behavior of groundwater may force a re-evaluation of earlier-held views of atoll island hydrology.

A number of practical aspects have already come to light based on the work in Deke. For instance, on islands similar to Deke, such as Nukuoro (Ayers and Clayshulte, 1983), it is now obvious why salt-water intrusion occurs in areas of root-crop cultivation (e.g., taro). Steps necessary to control the problem are also obvious. We have a somewhat better understanding of flow paths within the lens system and why fresh groundwater occurs where it does. We also have a better understanding of how to deal with the interpretation of field data, particularly water-level information. Finally, a well-developed set of guidelines for directing future studies of atoll island hydrogeology has also been produced as a result of the field work associated with this investigation.

### Purpose and Scope of the Study

Fresh groundwater is the most reliable source of drinking water on islands where there is a pronounced dry season -- as is the case for most atolls in Micronesia. It is also easily contaminated and therefore has the potential for spreading water-borne disease. Presently, the level of understanding related to atoll geology and hydrology is rather limited. Because of this, the present investigation was initiated with the primary purpose of defining the hydrogeologic framework and ground-water occurrence within the atoll island setting. Specific objectives of the study were to:

1. Determine the size and extent of the fresh-water lens and the zone of mixing between fresh groundwater and underlying saltwater;
2. Characterize the behavior of the lens as it relates to short-term sea-level fluctuations and rainfall events.
3. Define flow directions within the fresh-water lens;

4. Determine the geological makeup of the island and the reef complex upon which it is situated;
5. Map the physiographic features of the island that may influence water quality, recharge rates, and subsurface flow patterns.
6. Assess the ground-water quality within the lens; and
7. Provide a set of guidelines for directing future work on atoll islands.

Accomplishment of these objectives required a year of planning and logistical support from Ponape State government agencies. In addition, field operations required the transport of a large amount of equipment and supplies, the expertise of a 5-member research team, and a 6-week field study program. The latter aspect of the study was conducted during the dry season (February to May) of 1984.

Numerous activities associated with both field work and data analysis were necessary to achieve the above objectives. Among the field work activities were:

1. Establishment of a camp site on the study island;
2. Installation of a continuous recording tide station in the lagoon;
3. Installation of water-level monitoring wells across the study island, some of which were equipped with recorders;
4. Establishment of an elevation control network using standard surveying techniques;
5. Mapping topographic features and the surficial geology;
6. Utilization of surface geophysical techniques (seismic refraction and electrical resistivity) to map subsurface conditions;
7. Drilling to confirm geophysical observations, collect subsurface material, monitor water levels, collect water samples, and perform additional tests.

A considerable amount of data was collected during the field work. Activities associated with the analyses of data were:

1. Reduction of water-level data relative to a fixed datum;
2. Computer analysis of data obtained from surface-based geophysical surveys;
3. Examination of core, rock, and sediment samples;
4. Standard sieve analyses of collected sediment samples;

5. Compilation of salinity profiles and other water-quality data; and,
6. Data interpretation and report preparation.

Some additional activities associated with this study but not part of the original scope of work include:

1. Bathymetric surveys of the lagoon;
2. Mapping the fracture system of the reef complex;
3. Conducting permeability-plug tests on a number of core samples;
4. Petrographic examination of thin sections (prepared from core and rock samples) to determine cement fabrics; and,
5. X-ray (and possible SEM) analysis of selected core and rock samples to determine cement composition.

Results from the latter three activities will not be available until a later date.

#### Location and Description of the Study Island

The study island of Deke is located on Pingelap Atoll which is some 175 miles east of Ponape, Eastern Caroline Islands (Figure 1). (Pingelap Atoll is a political entity of Ponape State, Federated States of Micronesia). Deke is one of three islands situated atop the atoll platform. The aerial photograph of Figure 2 shows the geographical setting of Deke and the general character of Pingelap Atoll. It is worth noting that the bathymetry of the lagoon is somewhat atypical of other atolls in the Western Pacific region. A ribbon-type reef extends across the central portion of the lagoon. Similar reef development is present on Mokil, an atoll between Pingelap and Ponape, however most atoll lagoons are relatively free of structures except for the occasional patch reef. No doubt the reef across the lagoon of Pingelap significantly affects water circulation and sediment transport, not to mention navigation, inside the margin of the reef complex.

Deke Island was selected as the study site for a number of reasons. First and foremost, the configuration and size of the island is such that a substantial fresh-water lens would be present. Second, the island appeared to be typical of other atoll islands located elsewhere in the Western Pacific. Third, the island is uninhabited and therefore the groundwater-flow system could be studied in its pristine environment without the affects of human activities. Results of this study could then be compared to altered but similar hydrogeologic settings in order to evaluate the affects of settlement. Finally, air service would be available in case of emergency and equipment replacement or repair.

Deke island is situated along the north-western margin of the atoll platform. The island is typical in the sense that it is low lying, densely

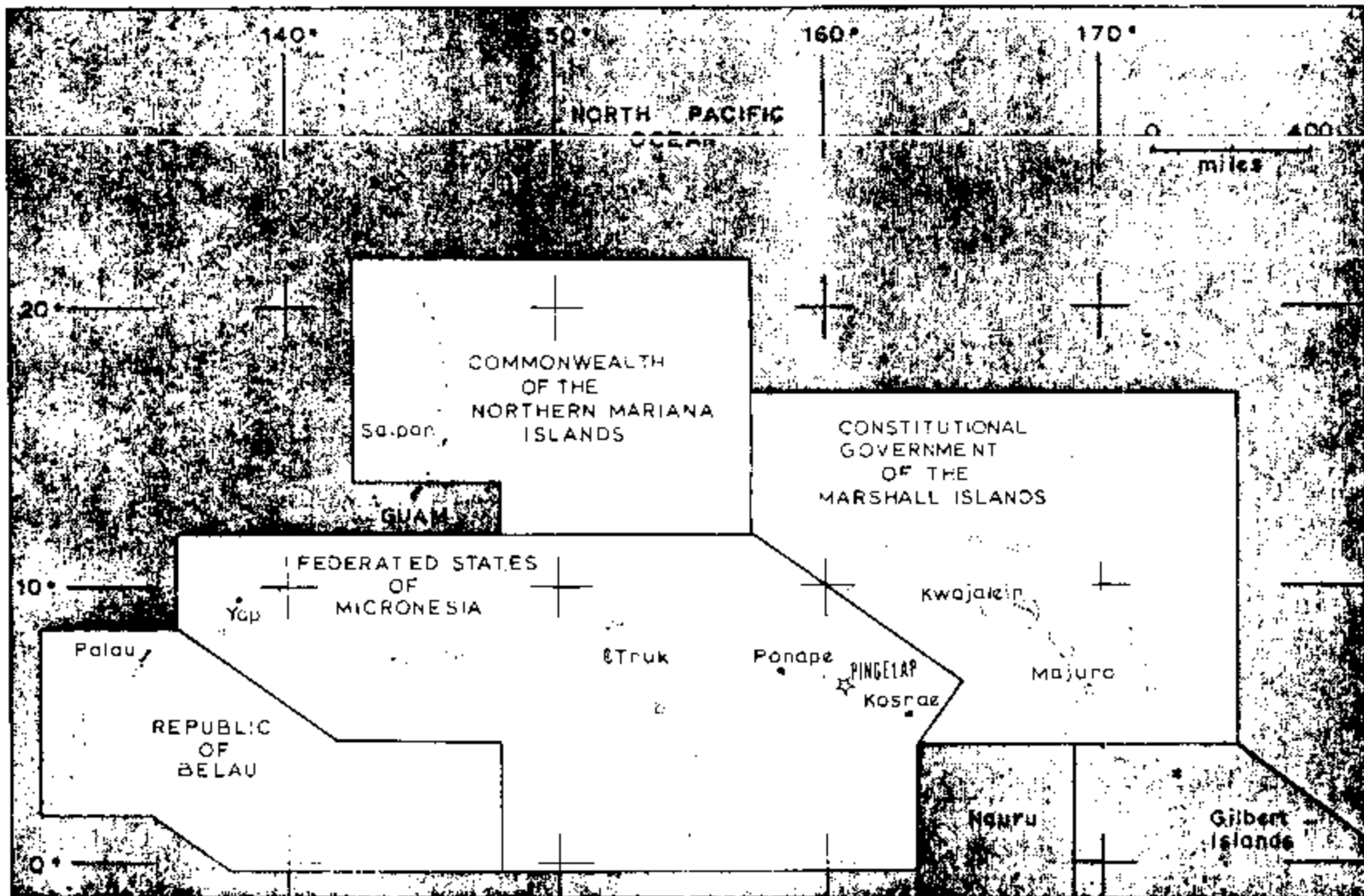


Figure 1. Map of Micronesia showing the location of Pingelap Atoll. Pingelap Atoll is a political entity of Ponape State, Federated States of Micronesia.

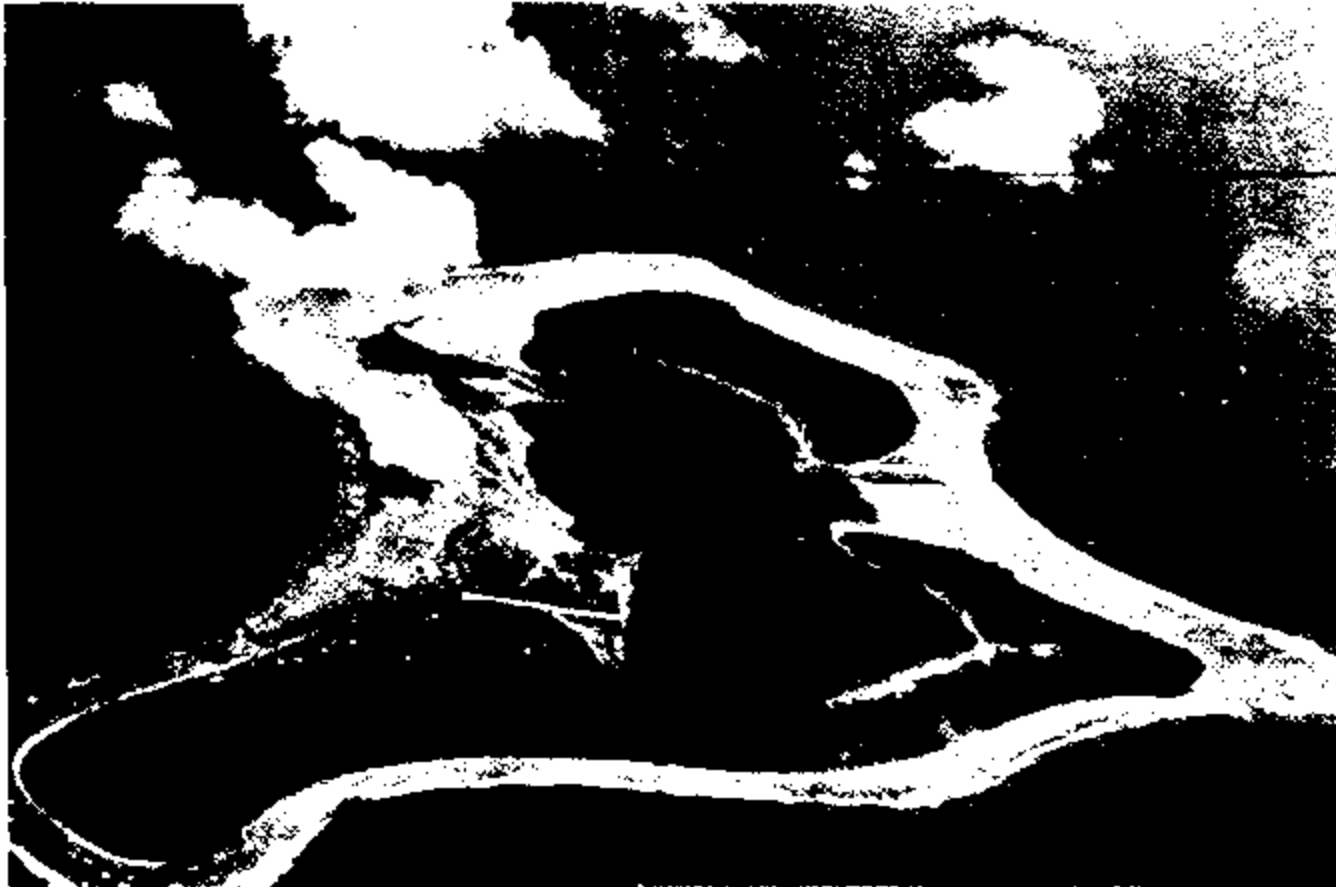


Figure 2. Aerial view of Pingelap Atoll. The study area, Deke Island, is located in the background of the photograph.

vegetated, and composed primarily of reef- and lagoon-derived sediment. Deke is approximately 1300 m (4264 ft) long, on the average is 400 m (1312 ft) wide, and is somewhat arcuate in shape. The ocean shoreline, for the most part, is exposed to wind-driven waves generated by the northeast trades.

A primary use of Deke by the inhabitants of Pingelap Island is for coconut harvesting (for the purpose of copra production). Other uses include materials collection (for building and fishing) and food gathering. Banana, papaya, pandanus, and taro are, more or less, cultivated on Deke. The latter is grown within hand-dug pits located along the lagoon side of the island. These pits, apparently dug shortly after WWII, provided the study with convenient sites to install water-level observation wells.



## METHODS OF THE INVESTIGATION

A variety of field and analytical techniques were used during the course of the hydrogeologic study of Deke. In this section, the various investigative approaches are presented.

### Water-Level Monitoring Program

The main part of the water-level investigation was monitoring water-level elevations at 22 sites in the southern part of the island (Figure 3). Development of these observation sites began shortly after arrival on Deke. Monitoring of the depth to water began as soon as the site was developed.

The first of the sites to be developed was a tide gauge installed in a 8-inch diameter standpipe along the shore of the lagoon. The other 21 observation sites were for ground-water monitoring. Two of these (wells E3 and E4) were hand-dug wells remaining from the Japanese occupation. Two were drill holes from the early stages of the drilling program (B3, an auger hole, and D1, which was drilled). The remaining 16 sites were standpipes installed in taro pits which had long ago been dug down to the water table.

The 22 sites are located in the southern part of the island. This distribution reflects the limited occurrence of the taro pits, which are sites where observation wells could be installed relatively quickly. As the monitoring of these southern wells proceeded, observation wells were being drilled and hand dug in the northern part of the island. As a result of these activities, it was soon learned that the northern region is underlain by the hard layer at about the depth that the water table had been expected. This finding explained the limited occurrence of the taro pits and also pointed to the need of an additional study to document the confining-bed effects of the hard layer. This study is the piezometer study described below.

Water-level monitoring of the main program involved discrete-time measurements and continuous recordings. In the discrete-time measurements, the depth to water was measured twice each day at each of the observation sites that were not being continuously recorded. Two measurements were taken 6hr to 6hr 15m apart, with the intention that the average of the two would have the effects of semidiurnal tidal variations removed and thus be representative of the daily level. Depth to water was measured by standard chalked-tape methods.

Continuous recording was by Stevens Type-F recorders, 4 of which were used in the investigation. One of these was on permanent station at the lagoon tide gauge; the other 3 were rotated around the well network in order to get tidal signatures at as many places as possible. Continuous recordings were thus obtained at 6 ground-water sites; durations range from 1 to 3 weeks.

Water levels were recorded on 1-wk chart paper and 1-to-1 vertical scale except for the lagoon recorder which was scaled down by a factor of

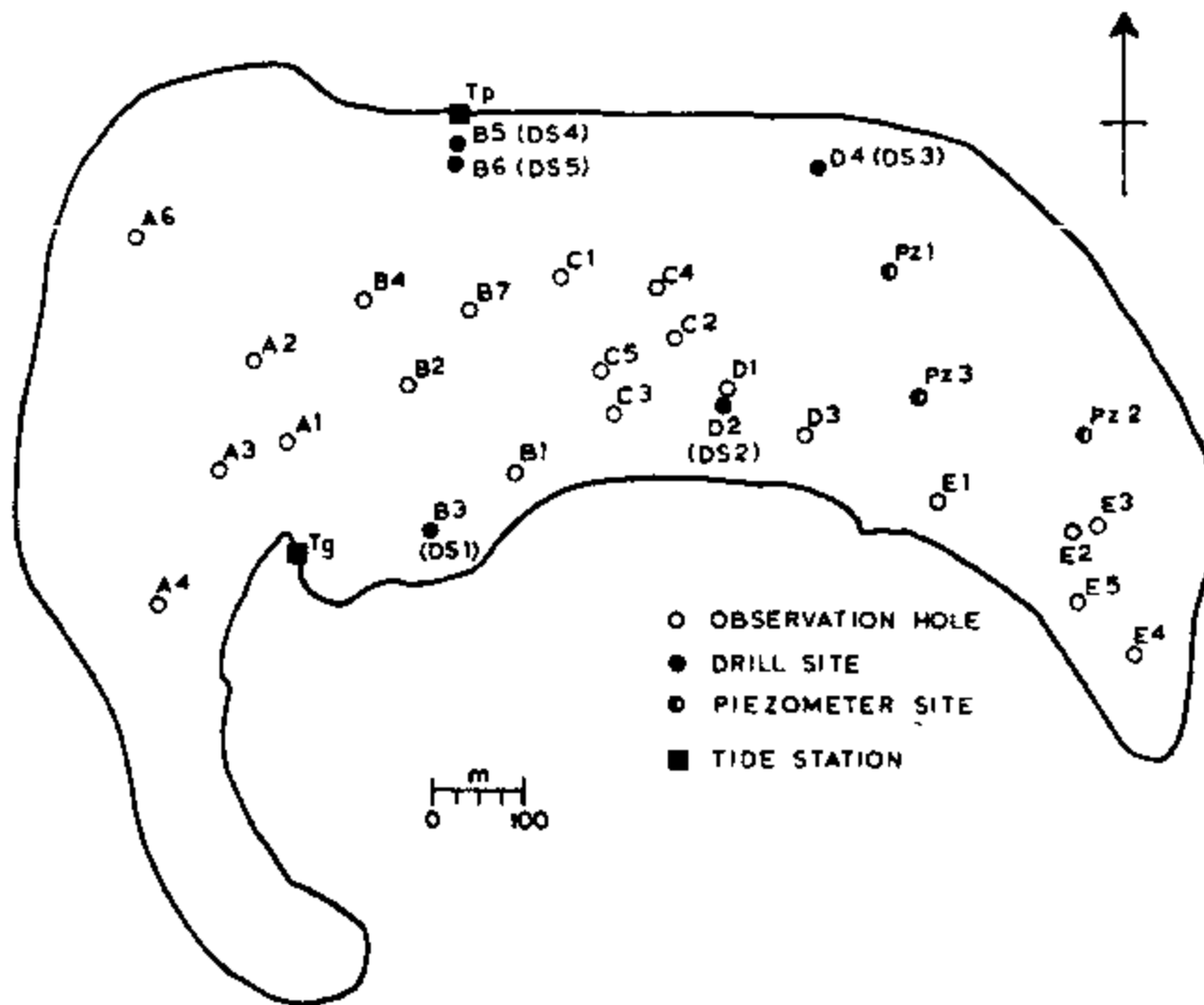


Figure 3. Map of Deke Island showing the location of various types of observation sites.

5. Depth to water and time were noted on the paper at the beginning and end of each 7-day recording period. For days in between, the time was marked on the paper daily, as a part of the water-level rounds for the discrete-time measurements. In the office, the graphs were redrawn to eliminate the time drift that was documented from these daily markings.

### The Piezometer Study

Deep drilling in the northern part of the Island resulted in 3 piezometers (B5, B6, D4). As a part of the drilling operation, the ground was dug to 8 or so feet down to the hard layer and a 2.5-inch diameter casing was tightly cemented to it before the hand-dug hole was backfilled. After the drilling, the casing was the piezometer for an observation well.

In addition to the 3 deep piezometers, 3 piezometer-standpipe pairs were installed to enable comparison of head above and below the hard layer. From these, the ground was again dug down to a bared hard layer. At low ground-water tide (so the hole would be dry), the hard layer was drilled through with a small portable core drill. A 2.5-inch-diameter PVC pipe was tightly cemented to the hard layer in position over the 1-inch-diameter hole; this PVC pipe became the piezometer. Next to the piezometer a standpipe was positioned by piling up a collection of the ubiquitous coral rubble.

In addition to these 6 piezometers, a PVC standpipe was installed in the beach directly north of B5 and B6. This "tide pipe" was set by partially burying it in the sand and, again, piling up coral rubble around the standpipe.

The study itself involved discrete-time depth-to-water measurements at the 6 piezometers and the tide pipe. The intention was to establish the characteristics of tidal behavior in piezometers and relate them to the behavior in the standpipes and, to the extent possible, to the wells of the taro-pit network. On March 18, repeated depth-to-water measurements were taken to define the low and succeeding high at B5, D4 and the 3 piezometer-standpipe pairs. On March 19, the tide pipe was installed in the morning; in the afternoon and night, discrete-time depth-to-water measurements were made to define the high at the 3 deep piezometers, the tide pipe, and 4 taro-pit wells. On March 20, the last field day of the study, water levels were taken by the twice-per-day routine at all taro pit wells and all piezometers; in the evening, closely-spaced repeated depth-to-water measurements were taken at B5, B6 and the tide pipe to precisely determine the time lags at those sites.

By necessity the water-level monitoring of the main program was suspended during the piezometer study and the few days before it while the piezometer sites were being prepared.

### Elevation Control

One of the most time-consuming components of the water-level investigation was the survey required to determine the elevation at all the

measuring sites. These elevations are necessary in order to convert depth-to-water measurements to water-level elevations.

Standard leveling techniques (transit and rod) were utilized by the survey. A network of 31 benchmarks was established at 100- to 200-m intervals and in a system of 5 partly nested loops. Elevation differences were determined by leveling out-and-back between successive benchmarks. Closures between successive benchmarks ranged up to 0.028 ft, with one at that figure; 4 in the 0.20 to 0.22 range, 4 at 0.10 or 0.11, and the rest, 25 of them, less than 0.01 ft. The five loops closed at -0.050, -0.032, 0.024, -0.016, and -0.004 ft, so the net overall closure, from one end of the island to the other is 0.086 ft (2.5 cm).

The net of benchmarks was used to level out and back to each of the water-level observation sites. In nearly all cases these sites were within a single instrument setting of a benchmark, so the closure between benchmark and observation well was a few thousandths of a foot. Exceptions, where the observation well was further from a benchmark of the interlooped net, include A3, A4, B5, B6, D4, E4 and E5.

The net of benchmarks was also the basis for the profile leveling from which the topographic map and profiles were drawn.

Datum for the elevation survey was taken as the lagoon low tide at 1337hr on March 6, 1984. The datum was measured, at the time of low tide, by leveling out-and-back with one instrument setting (and 0.002 ft closure), from a benchmark to the water line on a quiet-water beach next to the lagoon recorder station. This low tide was chosen as a datum so that all elevations, both topographic and water level, would be positive.

#### Weather Data

A small weather station is maintained on Pingelap Island. Data collected at this station are rainfall and barometric pressure at 3 times during the day. These data were made available to the water investigation. In addition, rainfall was measured at 0700hr, daily, by use of a standard rain gauge on Deke. As a part of the daily water-level monitoring, the amount of rain in the gauge was recorded during each of the two rounds, and general observations regarding wind direction, speed, and cloud cover were recorded between rounds.

#### Geomorphology and Surface Geology Mapping Program

Various techniques were utilized to document the geomorphology and surface geology of the study island. These techniques included profile leveling, grain-size analysis of surface material, compass-and-tape mapping of the surface geology, and measurement of stratigraphic sections in test pits.

## Topographic Mapping

Field work associated with mapping the topography of Beke utilized the established benchmark network for elevation control. Profile levels were measured between and beyond the net of benchmarks with transit and rod. Elevations were measured to within a hundredth (0.01) of a foot at 12.5-meter spacing along trails. Data from this field exercise provided the basis for construction of a topographic map.

## Grain-Size Analysis

Grain-size distributions of gravel-sized surface material were measured at 135 locations. These sample sites were located near the cut trails and spaced about 50 meters apart. Data were collected by measuring the longest axis of 100 clasts, systematically selected using a 1-m<sup>2</sup> grid consisting of a string mesh on a wooden frame.

Grain-size distributions of sand-size material were determined at 10 representative surface locations. In addition, grain-size distributions were measured for 18 samples collected from 3 stratigraphic test pits. Each sample was sieved for 15 minutes using a sieve shaker. The fraction retained on each sieve was then weighed to within 0.01 grams.

Sediment sizes were measured in terms of phi ( $\phi$ ) units. Phi sizes are defined by

$$\phi = -\log d/d_0,$$

where  $d$ , the grain diameter, and  $d_0$ , the standard particle diameter (1.0), are in mm. Phi units increase with decreasing grain size.

Data presentation is in terms of moments which characterize the distributions. These statistical moments are defined by:

$$\text{First Moment } M_1 = \sum m_p / 100$$

$$\text{Second Moment } M_2 = \sum f(m_p - M_1)^2 / 100$$

$$\text{Third Moment } M_3 = \sum f(m_p - M_1)^3 / 100,$$

where  $f$  is the frequency in per cent of each size class, and  $m$  is the midpoint of each  $\phi$ -size sieve class. By definition,  $M_1$  is the mean of the distribution.  $M_2$  is the variance, so the standard deviation ( $\sigma$ ) is the square root of  $M_2$ .  $M_3$  is related to the skewness of the distribution by

$$\text{skewness} = M_3 / \sigma^3.$$

The second and third moments, therefore, represent the dispersion about the mean and the asymmetry of the distribution respectively.

## Measurement of Stratigraphic Sections

Stratigraphic sections through the unconsolidated sediments above the hard layer were measured at two drill sites, two piezometer sites, and one stratigraphic test pit. The depth of each stratigraphic unit was measured, and various features such as grain size, sediment type, bedding relationships, and sedimentary structures were noted. These data and the statistical data from 18 sediment samples from 3 of the sites were used to construct graphic logs of the stratigraphy at the various sites.

## Subsurface Geologic Investigation

An important aspect of any hydrogeologic investigation is the collection of direct information related to the physical make up, chemical composition, and structural framework of subsurface units. The goal of all of this is to gain a better understanding of the water-bearing and transmittal properties of the aquifer. Several methods were utilized by the study in an attempt at gathering relevant subsurface data. These methods are described below.

## Core Drilling Operations

Core drilling on Deke was aimed at achieving two main objectives. Specifically, these objectives were (1) to retrieve in situ samples from subsurface units and (2) to provide direct information for calibrating and confirming geophysical data. In addition, finished boreholes serve as observation wells in which water levels are measured, specific-conductance profiles are obtained, and water samples are collected.

Two drilling units were used during the course of the field work. A portable, so-called one-person "Packsack" core drill (Acker Drilling Company) was employed in the drilling of shallow holes (usually less than 10 feet). This unit proved useful in sampling the hard layer at a number of sites in a relatively short time period. It was also useful in the installation of piezometers, as mentioned above. Core samples obtained from the packsack unit are 7/8 inches in diameter. The second unit, also manufactured by Acker, was used to drill deeper holes and retrieve a slightly larger diameter core (model 1200 PM pipe-mounted core drill). Each unit requires an appropriate pump station, drill bits, drill rod, and assorted tools.

Because of unanticipated problems, the number of successful deep drill sites was limited to three, all located along the ocean shoreline (see Figure 3). Depths of 70 and 80 feet were obtained at two of the sites; drilling at the remaining site was terminated at 25 feet due to excessive caving and loss of circulation. The primary problem encountered was the rather unconsolidated nature of the material both above and below the hard layer. Although the problem of unconsolidated overburden was solved by installing casing, the unindurated nature of the substrate below the hard layer was a complete surprise. All indications suggested a relatively well cemented carbonate sediment would be encountered and that casing and drilling mud would not be necessary.

## Sampling Methods

As the field work progressed and the hydrogeologic importance of the hard layer was recognized, the subsurface investigation was expanded to include a program of sampling the reef flat in addition to the hard layer. The main objective was to determine the relationship, if any, between the occurrence of the reef flat substrate and its characteristics and the occurrence of the hard layer and its similar characteristics.

Additional objectives, and of equal importance, were to determine the inland extent of the hard layer and to define the character of its lagoonward boundary.

Figure 4 shows a location map of samples collected from the oceanside reef flat and the hard layer beneath Deke. Samples were obtained by what ever means it took to break the very resistant substrate.

## Core and Sample Examination

All cores from the drilling operation were logged at the time of collection and later split (by sawing) for detailed examination and analysis. Each core was described in terms of its constituent particles, lithology, and physical characteristics. In addition a graphic log was constructed. A number of core samples were selected for permeability-plug tests, X-ray analyses, and possible scanning-electron-microscope work. Results from these analyses, however, will be available at a later date.

Samples of the reef flat and the hard layer were treated in a similar manner. Polished slabs were prepared and examined in terms of composition, lithology, and physical characteristics that relate to the properties of porosity and permeability.

## Water-Quality Determination

Field measurements of selected physical and chemical water-quality parameters were made for groundwater samples collected from observation wells and boreholes. Specific conductance ( $\mu\text{mhos/cm}$ ), temperature ( $^{\circ}\text{C}$ ), and chloride-ion ( $\text{mg/l}$ ) measurements were performed on samples from observation wells between March 17 and 20. Additional parameters analyzed on March 18 on samples from selected observation wells were pH, alkalinity, calcium hardness (as  $\text{mgCa/l}$  and  $\text{mgCaCO}_3/\text{l}$ ), and total hardness. Specific conductance readings were obtained with a field meter and probe which has a range from 0 to 100,000  $\mu\text{mhos/cm}$ . Chloride-ion and pH measurements were made with a specific-ion meter and probes. Alkalinity was determined by potentiometric titration with a standard acid to a pre-selected end-point pH (Standard Methods, 1980). Hardness was determined by EDTA titration (Standard Methods, 1980).

Specific conductance profiles within the groundwater body were obtained from observation wells DS3 and DS4. Measurements were made at 1-foot intervals as the probe was slowly lowered into the water column.

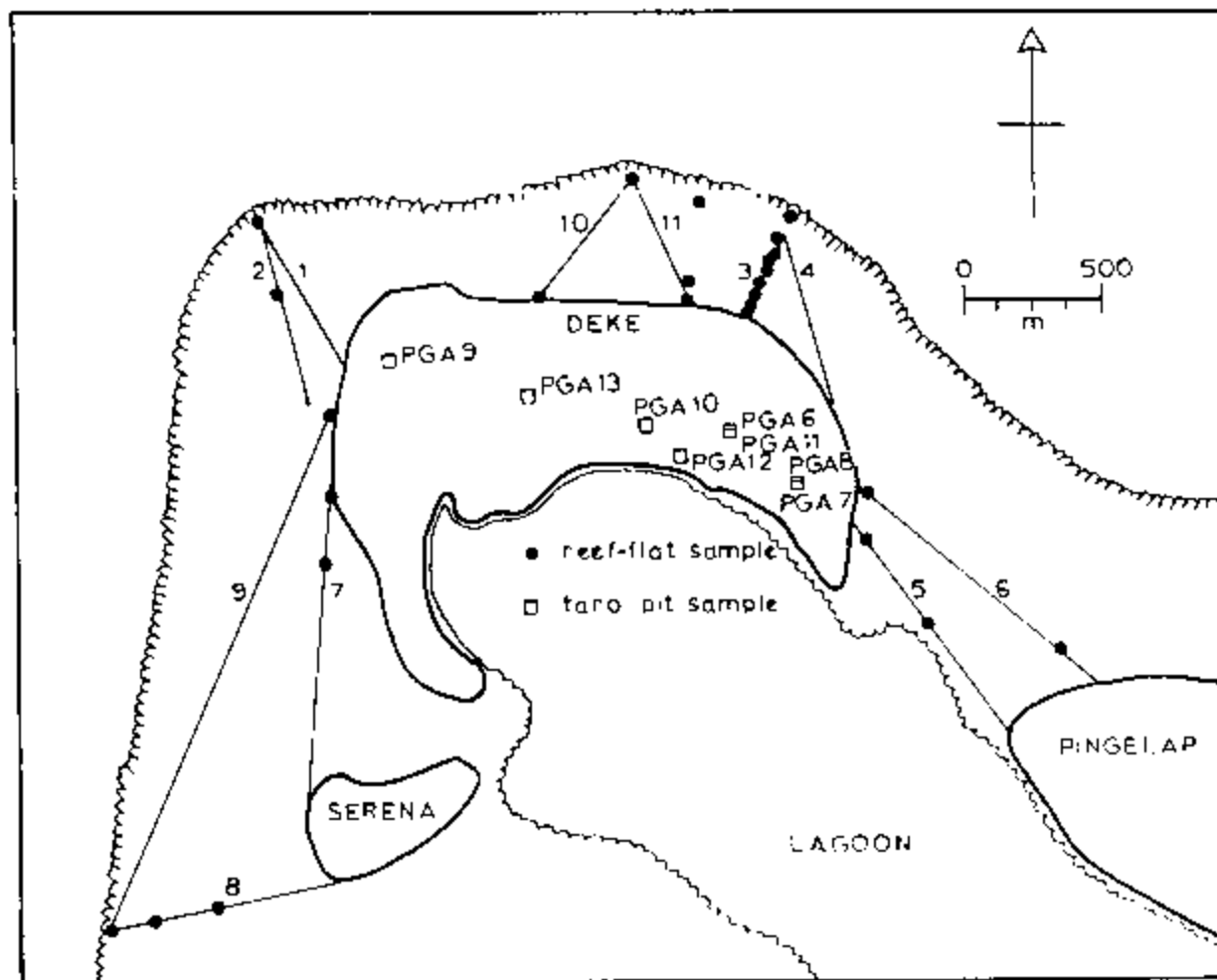


Figure 4. Map of a portion of Pingelap Atoll showing the collection sites for reef-flat and taro-pit rock samples. Numbered lines are traverses used in sampling and describing the reef-flat in the vicinity of Deke Island.



These measurements were taken to the maximum depth of the open hole, which was 32 feet in DS3 and 35 feet in DS4. Twelve profiles were obtained from DS3 and 4 profiles from DS4 for different times and various tidal conditions. Additionally at DS4, specific-conductance measurements were made of water sampled from a fixed depth (17 feet below ground surface) at 1/2 hour intervals for a sampling period of 81 hours.

Estimated chloride-ion concentrations from specific conductance measurements were obtained from graphical data. Standard curves of specific conductance versus chloride ion content of serially diluted seawater were made at the WERI water quality laboratory. Relative-salinity profiles from DS3 were calculated by the following equation (Vacher, 1974):

$$E = 100 \frac{C - C_f}{C_s - C_f}$$

where C is specific conductance and  $C_f$  and  $C_s$  are concentrations in the fresh and salty end-members, respectively. A value of 52,000 was used for  $C_s$ . The value of  $C_f$  was dependent on the specific conductance sequence in each profile. An end-member  $C_f$  value was taken at the point on the profile curve where specific conductance began to constantly increase. Relative salinity is then plotted against depth below the water table on probability paper in order to determine the actual thickness at the transition zone.

#### Surface-Based Geophysical Surveys

Two surfacel-based geophysical methods were employed by the study. Specifically, these methods were (1) seismic-refraction profiling and (2) earth-resistivity soundings. These methods were used in an attempt to determine the subsurface structure and, to a certain extent, the thickness of the fresh-water lens. Several measurement stations were established across the study island; their locations are shown on the map of Figure 5.

#### Seismic-Refraction Profiling

Seismic-refraction methods have been used in a wide variety of investigations involving the determinations of subsurface structure. Among these investigations are numerous applications of the method in groundwater-related studies. The object of refraction seismology is to obtain a time-distance graph from the first arrival of sound waves generated by an energy source. From time-distance graphs, seismic velocities can be calculated and depth determination can be made.

Detection of refracted sound waves generated by controlled energy sources (e.g., hammer striking a steel plate, weight drop, or explosion) usually produces a seismic-record indicating one or more events that are caused by the change in velocity of the wave front. Seismic energy is transmitted through solid material as elastic waves. Abrupt changes in the elastic properties of the medium through which these waves are propagated will cause the waves to be refracted or bent. The degree to which the wave

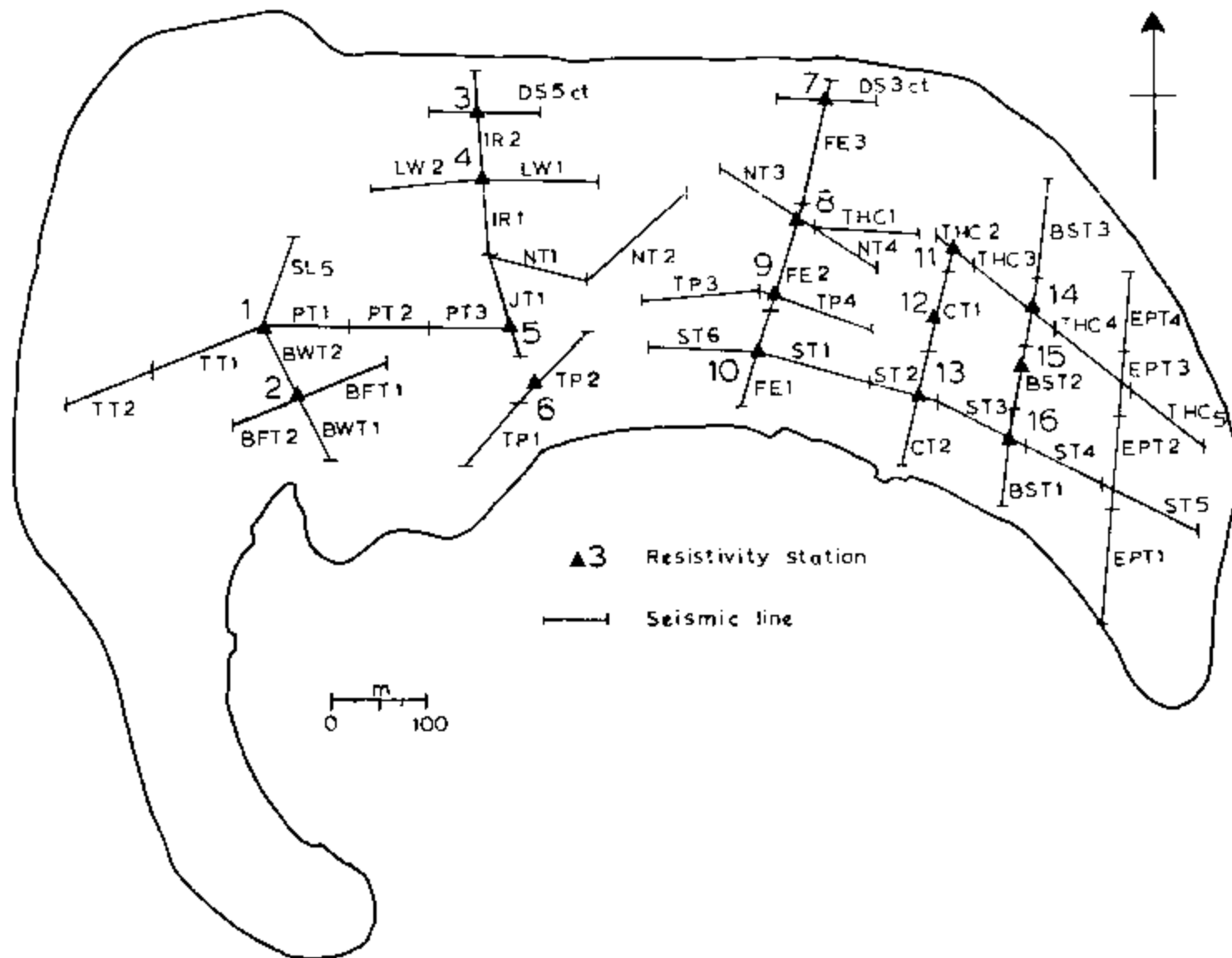


Figure 5. Map of Deke Island showing the locations of seismic-refraction lines and earth-resistivity stations.

paths are refracted is related to Snell's Law, that is, the sine of the angle of incidence is equal to the sine of the angle of refraction. Another way of expressing this law is by the following equation:

$$\frac{\sin i}{\sin r} = \frac{V_1}{V_2}$$

where

$i$  = angle of incidence,

$r$  = angle of refraction

$V_1$  = velocity of transmission of the elastic wave in the incidence medium, and

$V_2$  = velocity of transmission of the elastic wave in the refraction medium.

A primary concept in refraction work is that of the critical angle. Where  $r$  is equal to  $90^\circ$ ,  $\sin i$  is equal to  $V_1/V_2$ . Here, the incident wave path or ray strikes the interface at the critical angle and the refracted wave travels parallel to the interface. A refracted wave front acts as a first arrival when its travel time from the source through the refraction medium to the detector is equal to or greater than the time required for the direct wave to travel from the source to the same detector. The path that first-arrival waves take is dependent upon the depth to the reference interface and the distance between the first detector and the energy source (Telford et al., 1976; Zobdy et al., 1974).

When first-arrival times derived from seismograms are plotted on a time-distance graph, a break in slope of the curve will occur where the time taken for both direct and refracted waves to travel from the energy source to the detector is the same. Seismic velocities are obtained from the slope on the time-distance curve (i.e., velocity is the inverse of the slope).

The most widely used of all field techniques in refraction work is profile shooting. To obtain the necessary time-distance data, shot points and detectors or geophones are laid out on long lines and repeated shots are taken at various positions at the ends and middle of the geophone spread. If successive spreads are necessary, the lines are overlapped by at least one or two geophones.

During field operations, a total of 48 seismic-refraction lines or spreads were established across the study island. Each line was shot in both the forward and reverse order; several lines were shot at the midpoint of the spread. The energy source used in the refraction work was a sledge hammer striking a steel plate. Geophone spread consisted of 12 detectors spaced at 25-foot intervals connected to a McSeis-1300 (model 1191) Signal Enhancement Seismograph. A permanent record was produced on light-sensitive paper.

Although a number of analytical approaches are available (see, for example, Telford et al., 1976; Dobrin, 1976), the least time-consuming method utilizes computer processing of the time-distance data. The computer program used to process the Deka data was first published by the U.S. Bureau of Mines (Scott, 1972). The program generates a two-dimensional model representing a layered-earth depth interpretation. Travel times are picked from the seismogram by the user. These times, together with shot point and geophone locations and refraction layer control information, are used as program input. A first approximation delineation for each refraction interface is obtained by a computer adaptation of the delay-time method. The approximation is then tested and improved by the computer through the use of a ray-tracing procedure in which ray travel times computed for the model are compared to field data. The model is subsequently adjusted in an iterative manner such that the discrepancy between computed and measured travel times is minimized. Seismic velocities and depths to refractor interfaces, among other information, are printed as the final step.

### Earth-Resistivity Sounding

In addition to the application of seismic-refraction profiling in groundwater investigations, earth-resistivity measurements are widely used in the determination of subsurface characteristics and, in many cases, water quality. Essentially, the method involves measuring the electrical resistivity of earth materials by introducing an electrical current into the ground and monitoring the potential field developed by that current. In most earth materials, electricity is conducted electrolytically by the interstitial fluid, and resistivity is controlled more by porosity, water content, and water quality than by the resistivities of the matrix (Zohdy et al., 1974). Clay minerals, however, are capable of conducting a current electronically, and the electrical flow in a clay unit is both electronic and electrolytic.

In conducting earth-resistivity soundings, a commutated direct current or very low frequency (<1 Hz) current is introduced into the ground through two electrodes (Zohdy et al., 1974). The potential difference is measured between a second pair of electrodes; the current and potential measurements are used to calculate apparent resistivity.

The most commonly used electrode configuration for vertical electrical soundings, and the one used in this study, is the Schlumberger array. Four electrodes are placed along a straight line on the ground surface such that the outside current electrode distance ( $AB$ ) is equal to or greater than 5 times the inside potential electrode distance ( $MN$ ). For any linear, symmetric array  $AMNB$  of electrodes, the apparent resistivity is given by (Zohdy et al., 1974):

$$\rho_a = \pi \frac{(AB/2)^2 - (MN/2)^2}{MN} = \frac{\Delta V}{I}$$

where

$\Delta V$  = measured potential difference, and  
 $I$  = electrical current

A Soiltest R-60 resistivity unit was used to conduct the soundings. The unit utilizes dry-cell batteries as a power source with a maximum output of 810 volts and 1.0 amps. Sixteen resistivity stations were established at various sites around Deke (Figure 5). All soundings utilized the Schlumberger configuration with a maximum current electrode ( $\overline{AB}/2$ ) spacing of up to 200 feet.

Resultant data generated during the resistivity survey were analyzed by a trial-and-error procedure of curve matching. The first step was to plot the field data on a graph of apparent resistivity versus electrode spacing ( $\overline{AB}/2$ ) for each station and smooth the vertical electrical sounding (VES) curve to remove the discontinuities produced by the method of measurement (see, for example, Zohdy et al., 1974). Next, an appropriate layer model was selected as a first approximation to the field VES curve. Layer thickness or depth and resistivity values are used as input to a computer program (Zohdy, 1974) which calculates the model VES curve. This model VES curve is then compared to the field VES curve for goodness of fit (usually a qualitative comparison). If necessary, the input values are adjusted and the program rerun. This procedure is continued until a reasonable match is achieved between the model and field curves.

As discussed by Zohdy (1974), for a given earth model composed of horizontally stratified, laterally homogeneous, and isotropic layers, the computer program calculates the Schlumberger apparent resistivity in two parts. First, the total kernel function  $T = f(h, \rho, \lambda)$  is calculated for an n-layer model using Sundi's recurrence formula which is given by

$$T_1 = (h, \rho, \lambda) = [1 - Q_1 e^{-2\lambda h_1}] / [1 + Q_1 e^{-2\lambda h_1}]$$

$$Q_i = [\rho_i - \rho_{i+1} Q_{i+1}] / [\rho_i + \rho_{i+1} Q_{i+1}]$$

$$T_{n-1}(h, \rho, \lambda) = [1 - Q_{n-1} e^{-2\lambda h_{n-1}}] / [1 + Q_{n-1} e^{-2\lambda h_{n-1}}]$$

$$Q_{n-1} = [\rho_{n-1} - \rho_n] / [\rho_{n-1} + \rho_n]$$

where

$\rho_i$  = Resistivity of the  $i^{\text{th}}$  layer, and

$h_i$  = thickness of the  $i^{\text{th}}$  layer.

The second part in the calculation of the Schlumberger apparent resistivity is based on convolving the inverse filter coefficients (Chosh's coefficients) with the computed total kernel function curve. The convolution is made twice and six apparent resistivity values per logarithmic cycle are obtained. The abscissas of the computed points are logarithmically equally spaced, with

$$(\overline{AB}/2)_{i+1} / (\overline{AB}/2)_i = 1.468$$

where  $\overline{AB}/2$  is the Schlumberger electrode spacing.

## RESULTS OF THE INVESTIGATION

Study results are presented in this section. The arrangement is similar to that of the previous section, that is, results from the various components of the investigation are given in the same order as the methods for each study component. Much of the data and analysis are summarized and discussed in the text, however, relevant data collected in the field and data in a reduced form are presented in the appendices. The organization of the appendices is:

Appendix A - Water-Level Data

Appendix B - Geophysical Data

Appendix C - Drilling Logs and Sample Descriptions

Appendix D - Relative-Salinity Data

(See Appendix table of contents for specific data included within the appendices).

## Water-Level Monitoring Program

## Lagoon Tides

Elevation of successive lagoon tide highs and lows are shown in Figure 6. As shown in the figure, the tide is mixed semidiurnal and diurnal. The diurnal component dominates during the quarter moons, when there is a neap range of about 30 cm. At new and full moon, the tide is strongly semidiurnal with a spring range of about 75 cm.

Mean sea level for the 36 days of record is 23.7 cm above the datum which is used throughout this report. This datum, the lagoon low tide of 1337hr of March 6, will continue to be used in order to avoid negative numbers for water-level elevations.

Figure 5 also shows the run of daily mean sea level. As shown in the figure, there is a considerable day-to-day variation in daily mean sea level, with a range of some 25 cm, and a one-day jump of some 22 cm. It is apparent from the figure that this variation in daily mean sea level is a tidal phenomenon. Specifically, daily mean sea level fluctuates with a 14-day period; there is a minimum during the neap, diurnal tides and a maximum during the spring, semidiurnal tides. As shown below, this cycle is the principal control on the variation of ground-water levels in Deke.

A comparison of the daily mean sea level and inverted atmospheric pressure is made in Figure 7. According to the "inverted-barometer effect", sea level should rise 1 cm for each drop in barometric pressure of 1 mb (Wunsch, 1972). As shown in the figure, any sea-level variation due to barometric fluctuations would be completely overwhelmed and masked by the large-scale tidal variations; at best, the pressure-related variations might be responsible for a small-range (some 5 cm or less) sawtooth modulation of the curve of daily mean sea level.

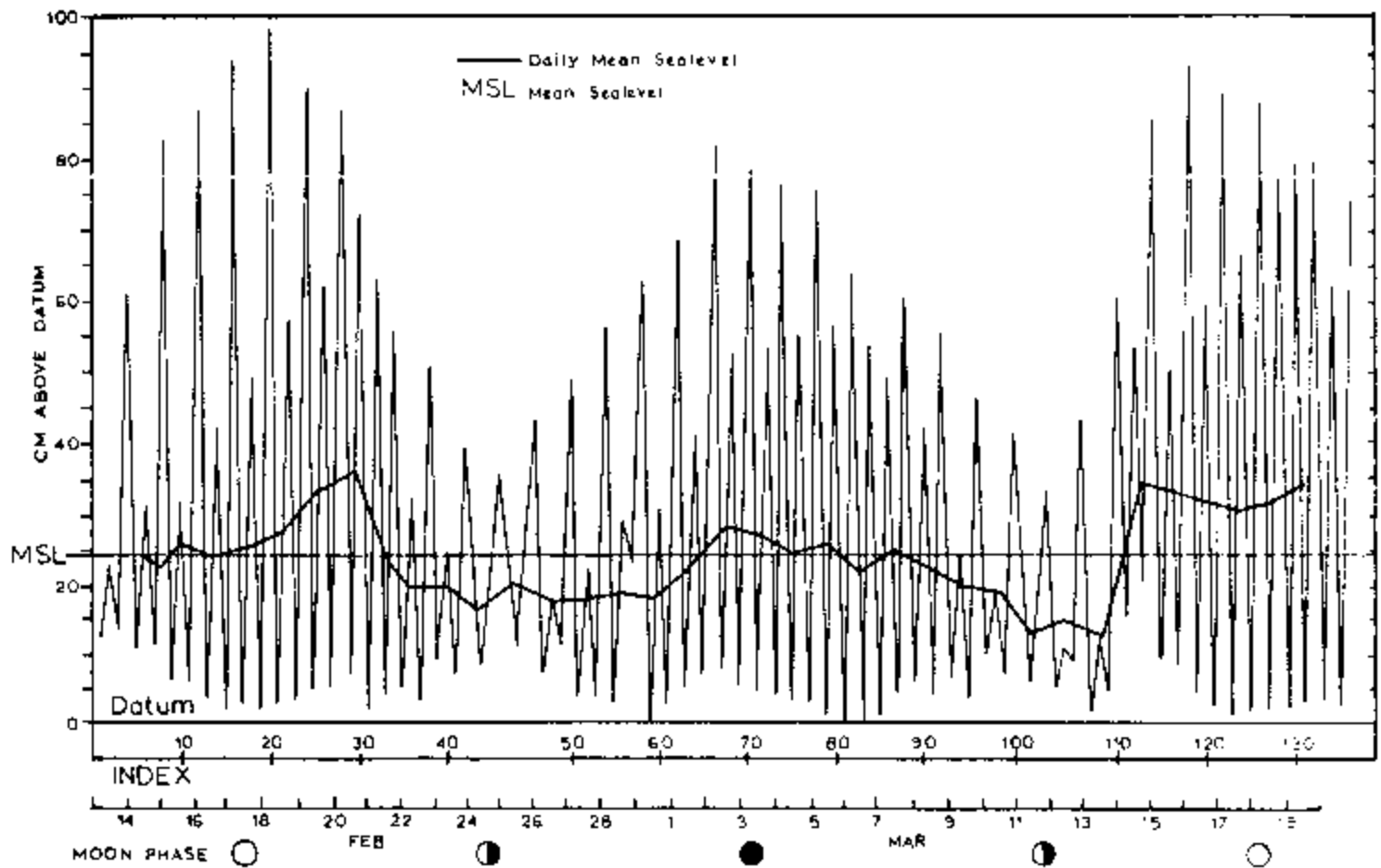


Figure 6. Graphs showing the tidal highs and lows and the daily mean at the lagoon recorder station.

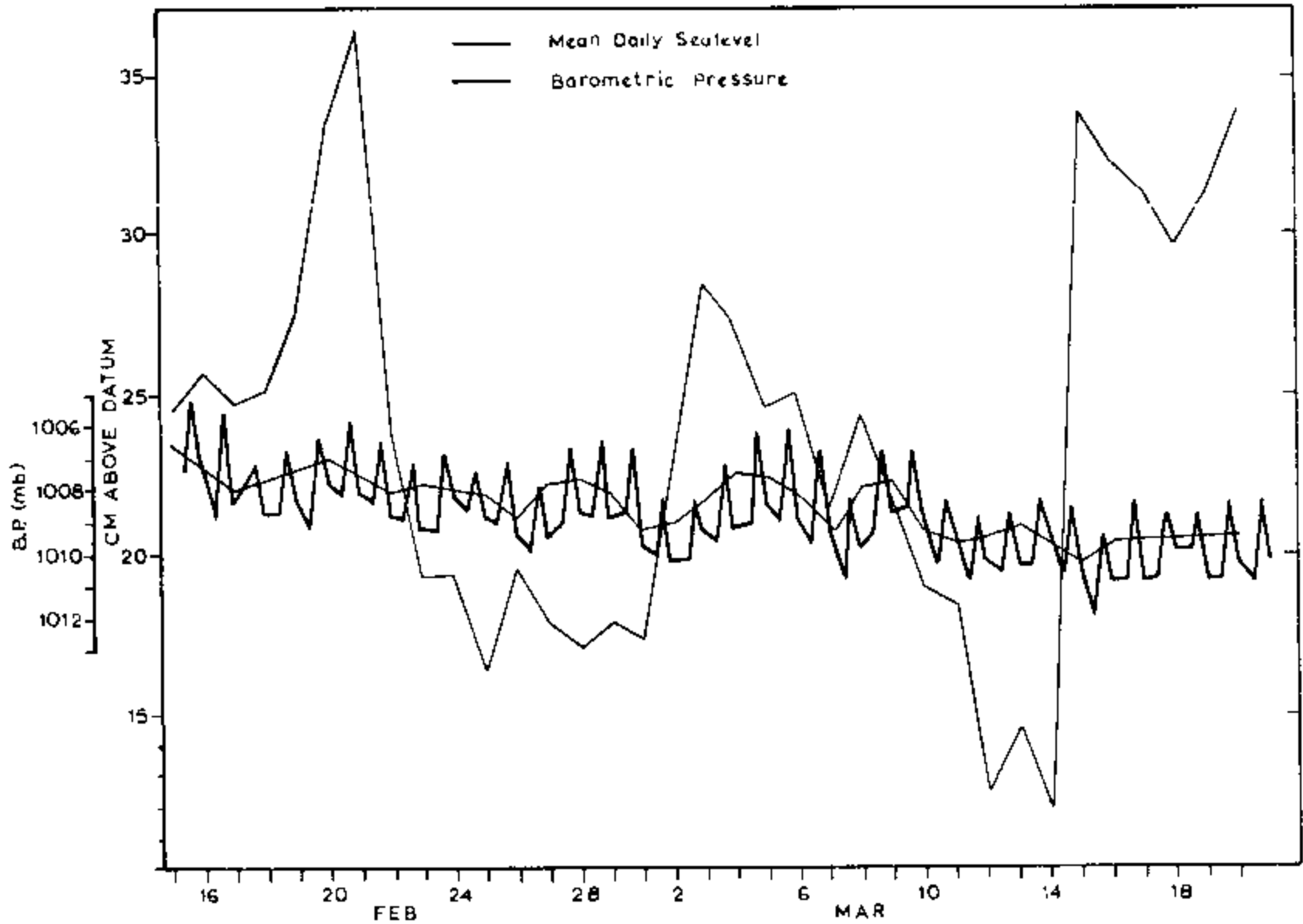


Figure 7. Graphs showing daily mean sea level at the lagoon recorder station and barometric pressure. The larger-amplitude graph of barometric pressure is the plot of the three-times-daily readings; the other is the daily average.



One of the particularly striking features of the tidal variation in the lagoon is that the tidal fluctuation is asymmetric. This can be seen in all of the lagoon recordings. Figure 8 shows an example. As shown in the figure, there is a smaller variation in elevation between successive lows than between successive highs. For lows that are below a depth of about 10 cm (the top of the reef flat), the tracing of the curve for these lows is asymmetric, with a slow approach to the minimum followed by a rapid rise. There are also unequal time differences between the highs and lows: on average (see Table 1), it takes 7hr 48min to go from a maximum to a minimum and 4hr 17min to go from a minimum to a maximum, with an overall period of 12hr 5min (in comparison with a typical semidiurnal period of 12hr 25min and equal times of 6hr 12.5min between the extremes). This striking asymmetry of the lagoon tide obviously reflects the fact that the closed-lagoon configuration impedes the free exchange of water between the open-ocean and the lagoon.

Some of the results of the study of ground-water tides help establish the character of the lagoon tide. These results are summarized in Figure 9, which shows the lagoon tidal curve in comparison with the tidal water-level variations at B5 (DS4), a deep piezometer some 30m inland from the beach along the reef-bordered northern shore. This piezometer gives one of two largest documented tidal ranges in Deke, and these give the closest approach to a measurement of the open-ocean tide. The curve for the lagoon is from a continuous recording and the curve for B5 is for temporally disjunct measurements of depth with a chalked tape.

As shown in Figure 9, the low in the lagoon occurs some 2.5 hours after the low at B5, and, in contrast, there is little time difference in the occurrence of the highs. For the March 18 data, shown in Figure 9, the high in the lagoon is 10 minutes after the high at B5; this lag apparently increases in March 19 and 20 (see Table 2) to 15 and 17 minutes as the height of the maximum decreases from 102 cm on March 18 to 93 and 78 cm on March 19 and 20, respectively.

From Figure 7 and Table 2, the range in the lagoon is about 60% that of B5. However it is quite obvious in Figure 9 that the reduction is taken disproportionately from the low. The water-level average at B5 is 29 cm, with an amplitude of 73 cm. The average lagoon level in the 24 hours preceding the peak shown in the figure is 25.9 cm; so, the "amplitude" of the high is 61 cm and the "amplitude" of the low is 25 cm. Thus, although the overall range in the lagoon is dampened to some 60% relative to B5, the high is dampened to 80% and the low to some 34%.

It should be noted that these figures on dampening and lag of the lagoon tide are both underestimates of the dampening and lag relative to the open ocean, because there is undoubtedly some dampening and lag between the open ocean and B5. This can be seen from the range and time data (Table 2) for B6 (DS5) which is a similarly installed piezometer 12m inland from B5. At B6, the high occurs 5 to 6 minutes later than at B5 and the range has been dampened to 71% of its value at B5.

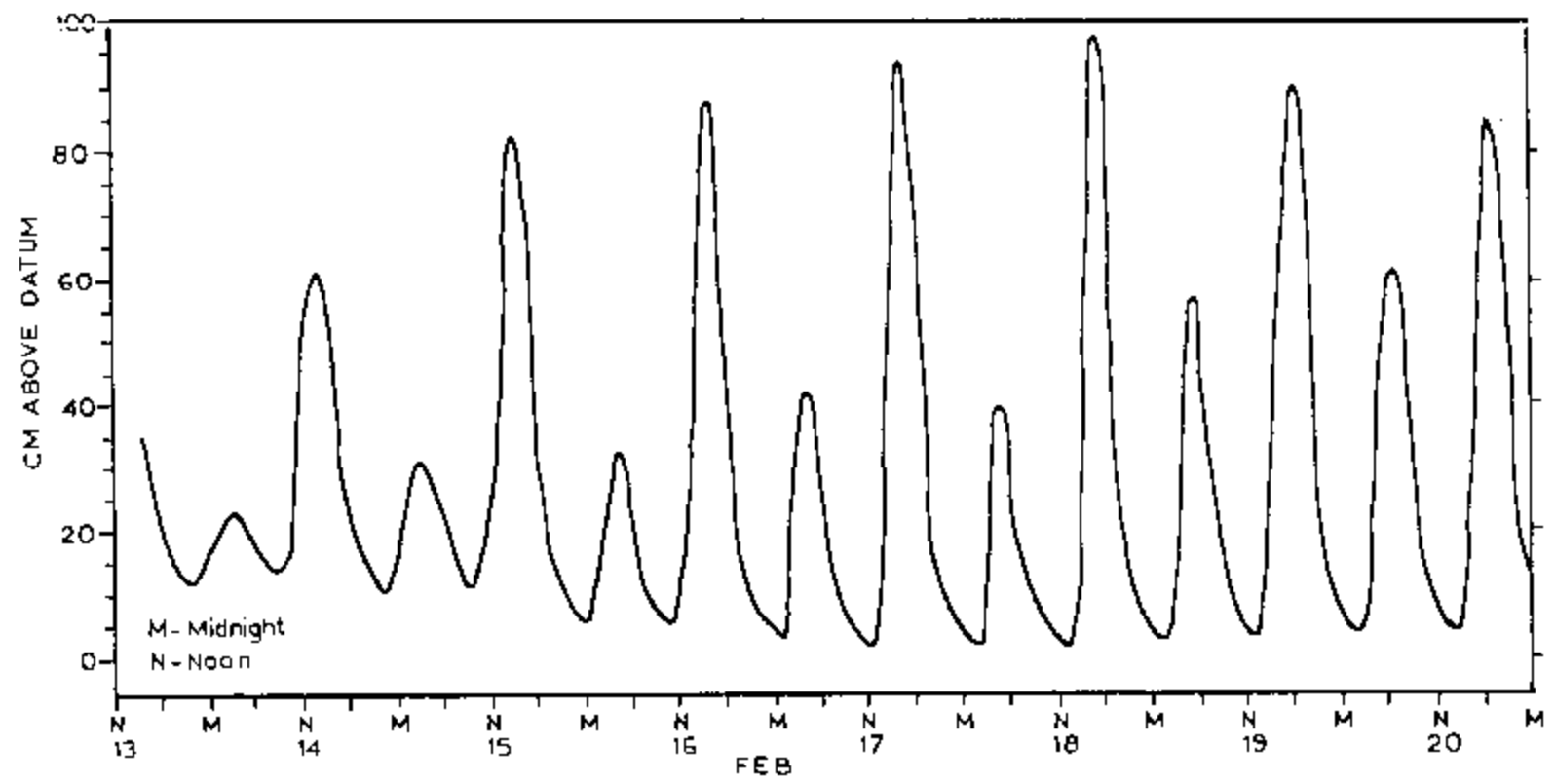


Figure 8. Graph showing a representative week-long recording of the semidiurnal tides in the lagoon.

Table 1. Tidal data from continuous recordings.

A. Ranges (cm)						
Well	Dates	$\underline{n}$ *	$\underline{R}_1$	$\underline{R}_2$	$\underline{R}_1/\underline{R}_2$	
(1) $R_1$ = Range at <u>well</u> ; $R_2$ = Range in <u>lagoon</u> for same period						
B4	2/18 - 3/2	43	11.54	44.5	0.26	
C4	2/18 - 3/9	73	6.81	50.4	0.13	
C5	2/25 - 3/15	67	9.55	42.8	0.22	
D1	3/3 - 3/16	47	21.20	44.2	0.48	
E3	3/9 - 3/21	43	9.97	51.0	0.20	
(2) $R_1$ = Range at <u>E2</u> ; $R_2$ = Range at <u>E3</u> (nearby piezometer)						
E2		19	2.55	12.54	0.20	
(3) Overall lagoon						
Lagoon	2/13 - 3/21	135		50.4		
B. Times						
Well	Date	$\underline{n}$	<u>Lagoon</u>		<u>Time between Extremes</u>	
			High	Low	High to low	Low to high
(1) Lag = time at <u>well</u> after time of corresponding extreme at <u>lagoon</u>						
B4	2/18 - 3/2	22	1:10	-0:32	6:06	5:59
C4	2/18 - 3/9	37	2:53	1:07	6:02	6:03
C5	2/25 - 3/15	34	2:22	0:56	6:22	5:43
D1	3/3 - 3/16	24	0:53	0:56	7:51	4:14
E3	3/9 - 3/21	22	3:00	1:23	6:11	5:54
(2) Lag: Time at <u>well</u> after time of corresponding extreme at E3						
E2		10	1:38	1:10	5:43	6:22
(3) Overall lagoon						
Lagoon	2/13 - 3/21	63			7:48	4:17

\*n = in A refers to number of extremes; in B, refers to number of highs and number of lows.

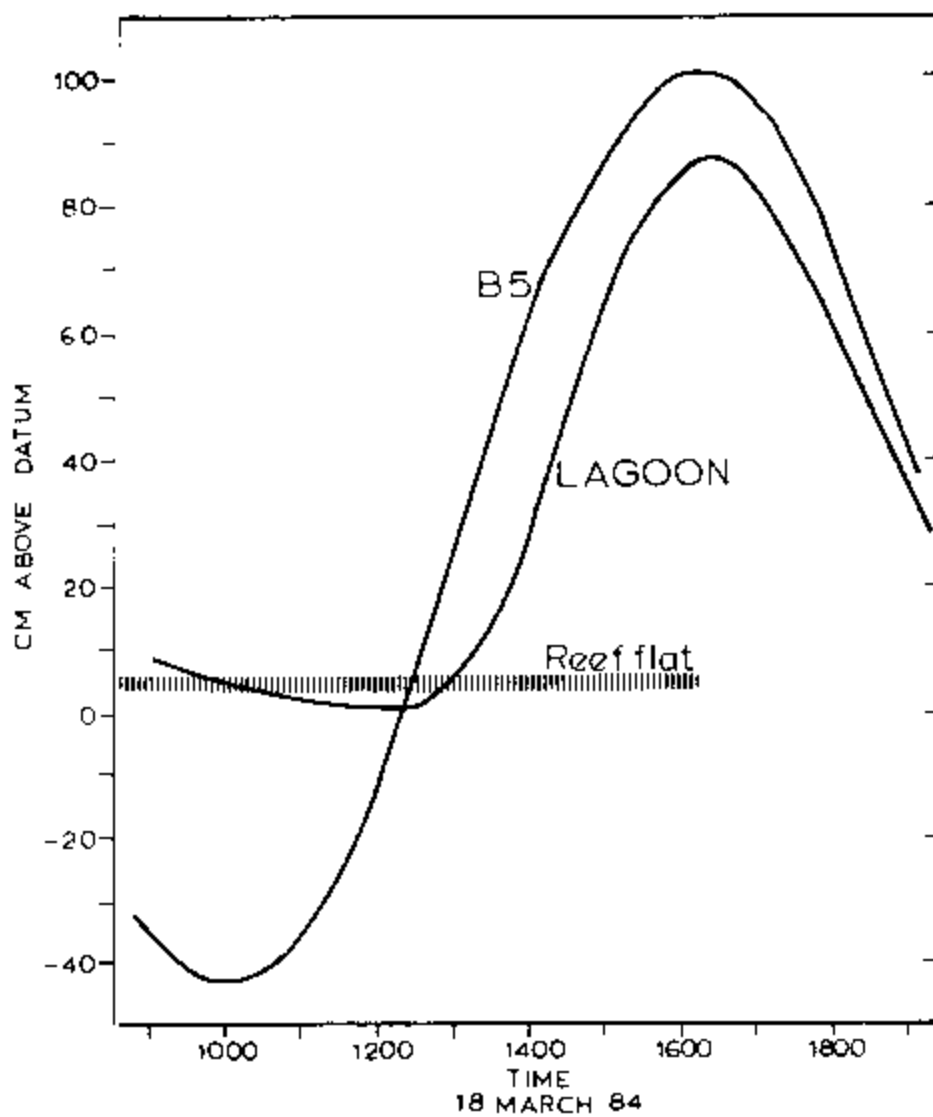


Figure 9. Graphs showing a tidal cycle in the lagoon and at a deep piezometer (B5) located near the ocean shore. Note the relative position of the reef flat.

Table 2. Results of the tide studies of March 18, 19, 20.

	Min		Max		Range	LAG after DS4		StP Lag after Pz
	Time	Elev	Time	Elev		Min	Max	
<u>3/18 Data</u>								
B5 (DS4)	957	-44	1610	102	146	-	-	
D4 (DS3)	1000	-45	1610	106	151	0:00	0:00	
Pz1 Pz	1000	-40	1615	103	143	0:03	0:05	
StP	dry		1615	56				0:00
Pz2 Pz	1110	11	1725	48	57	1:15	1:15	
StP	dry		1905	41				1:40
Pz3 Pz	1220	19	1835	45	26	2:23	2:25	
StP	dry		1850	44				0:15
Lagoon	1221	1.0	1620	88.1	87.1	2:24	0:10	
<u>3/19 Data</u>								
B5 (DS4)			1650	93	(133)**	-	-	
B6 (DS5)			1655	78	(94)	-	0:05	
Tide Pipe			1700	114	-		0:10	
D4 (DS3)			1635	97	-		-0:15	
C1			2055	37.6	(13.4)		4:05	
C2			2005	42.5	(15.8)		3:15	
C3			1957	46.3	(22.6)		3:07	
C4			2013	37.8	(13.0)*		3:23	
Lagoon			1705	79.1	77.1		0:15	
<u>3/20 Data</u>								
B5 (DS4)			1722	77.9	(68?)		-	
B6 (DS5)			1728	66.3	(43?)		0:06	
Tide Pipe			1746	89.0	-		0:24	
E3			1938	36.4	11.3*		2:16	
E2			2026	33.3	3.0*			0:48
Lagoon			1739	61.5	59.1		0:17	

\* Range from continuous recordings and is the average of the adjoining low-high and high-low differences.

\*\* Ranges in parentheses are from extrapolation of a partial cycles; see Appendix A, Table A4.

## Ground-Water Tides

From the tide study data of March 18-20, when discrete-time depth-to-water measurements were made over a few-hour period, the times and elevations of the extremes were determined: a low and succeeding high for March 18, and a high for March 19 and for March 20. These derived data are listed in Table 2 and cover eleven localities including 3 piezometer-standpipe pairs. Also included in Table 2 are the implied ranges and lags relative to B5, the deep piezometer that is close to the ocean shore. Listed ranges include values from the March 19 and 20 data where the estimate is from extrapolation based on fitting a sine curve to the data of the partial cycle.

Results from the continuous recordings and discrete-time sampling are combined, to the extent that this is possible, in Table 3. The tidal efficiency (TE) indicates the range at the site relative to the range at B5. Where the site was covered by the discrete-time sampling, the tidal efficiency was taken from those results; where the site was covered by only the continuous recording, the long-term tidal efficiency relative to the lagoon was multiplied by 0.6, the lagoon-to-B5 range-ratio in order to convert TE relative to lagoon to TE relative to B5. Lags were handled in an analogous manner. For the time difference between successive extremes, the values in Table 1 were used for the continuously recorded wells and, for the others, the lag-of-high data of Table 2 were used with the assumption that the time difference between successive highs is 12hrs 25min.

Because of the various ways the numbers in Table 3 are derived, the compilation gives only an approximation of the between-well differences in TE and lag. Examination of observation well hydrographs, for example, indicates that there can be a sizable disparity in TE or lag from one day to another. However, the results of Table 3 -- even though approximate -- reveal a definite areal pattern in the ground-water tides and this is shown in Figures 10, 11, and 12.

### Areal Patterns

Figure 10 is a map showing how the parameter, time difference between successive extremes, varies geographically. In the lagoon this parameter is 7:48/4:17 meaning that the time between a high and succeeding low is some 2:31 longer than the time interval between a low and succeeding high; the case at D1 is the same. For the wells along the north shore (e.g. B5, Pz1), however, there is no such inequality of the high-to-low and low-to-high time differential, which is the case also in the open ocean. Therefore, as shown on the map, there is a rather broad region in the northern part of the island where the ground-water tides are like the open ocean in terms of equal times between successive extremes, and a comparatively narrow southern fringe where the ground-water tides are like the lagoon in that there is a pronounced inequality of successive time differences between extremes.

As shown in the maps of Figures 10 and 11 there is a very definite pattern of decreasing ranges and increasing lags inland. Highs occur in

Table 3. Combined results of the tidal studies.

	Tidal efficiency relative to B5	Lag of high, after B5	Time difference between extremes (high to low/low to high)
D4	1.03	-0:15	6:10/6:15
B5	1.00	0:00	6:10/6:15
Pz1	0.98	0:05	6:12/6:13
B6	0.71	0:05	
D1	0.28	1:08	7:51/4:14
Pz2	0.25	1:15	6:12/6:13
Pz3	0.18	2:25	6:12/6:13
C3	0.17	3:07	
B4	0.15	1:25	6:06/5:59
C5	0.13	2:37	6:22/5:43
C2	0.12	3:15	
C4	0.10	3:07	6:02/6:03
C1	0.10	4:05	
E3	0.09	3:15	6:11/5:54
Tide Pipe	-	0:17	
Lagoon	0.60	0:15	7:48/4:17

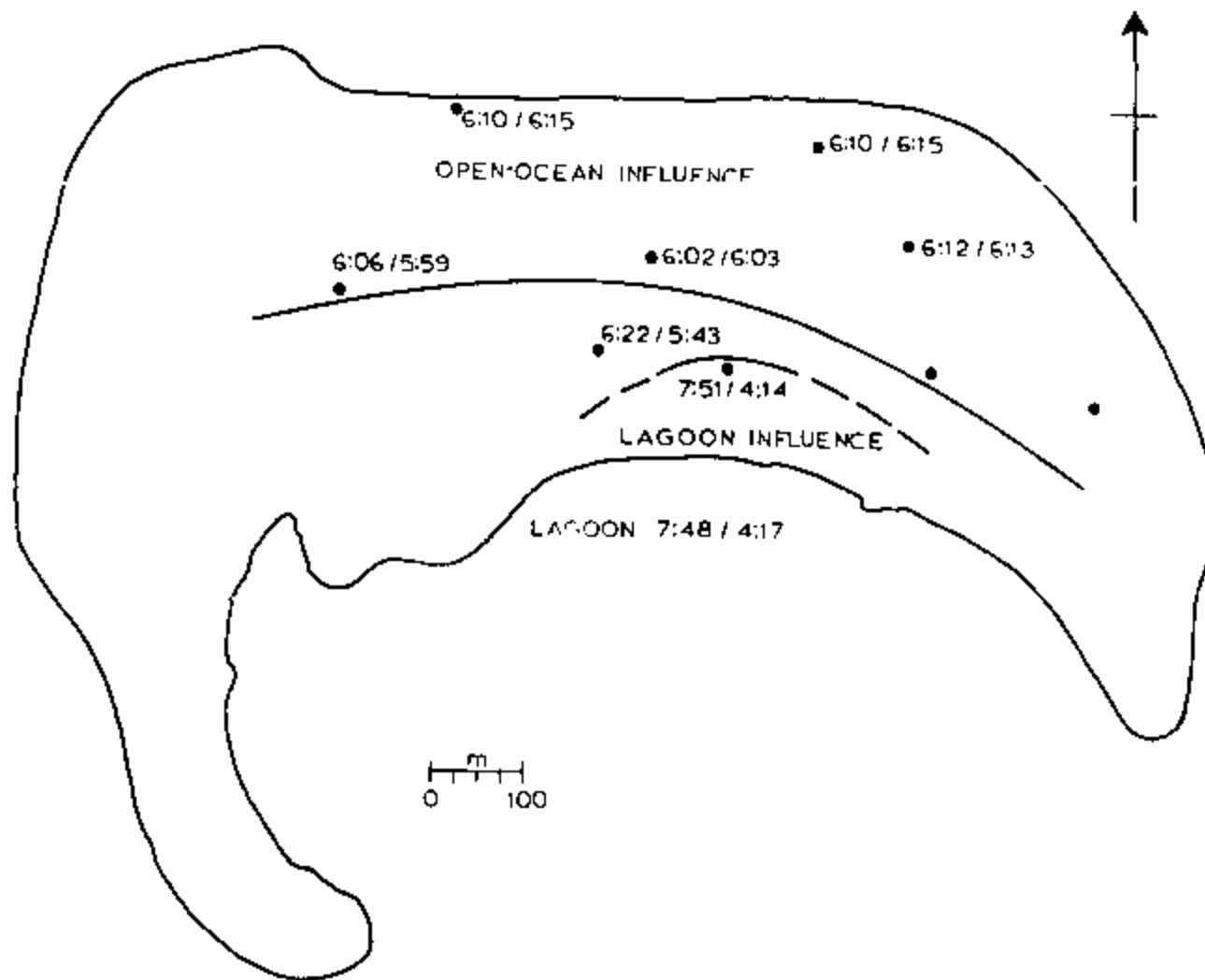


Figure 10. Map of Deke Island showing the geographical variation of high-to-low and low-to-high tidal time differentials. Note the time differential within the lagoon tide.



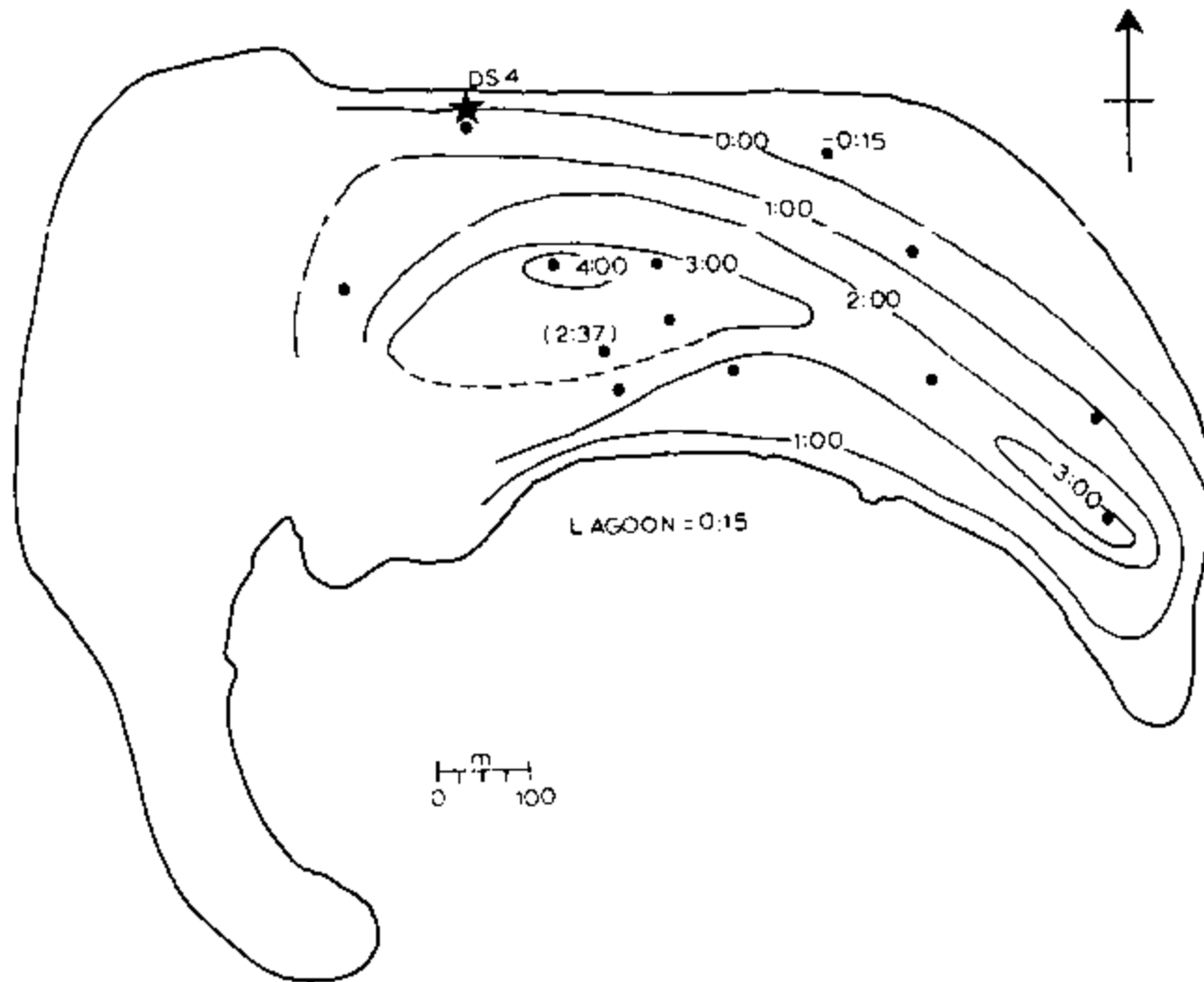


Figure 11. Map of Deke Island showing the time lag of the tidal highs. Lag time is relative to observation well DS4 (starred location). Lag time in hours and minutes.

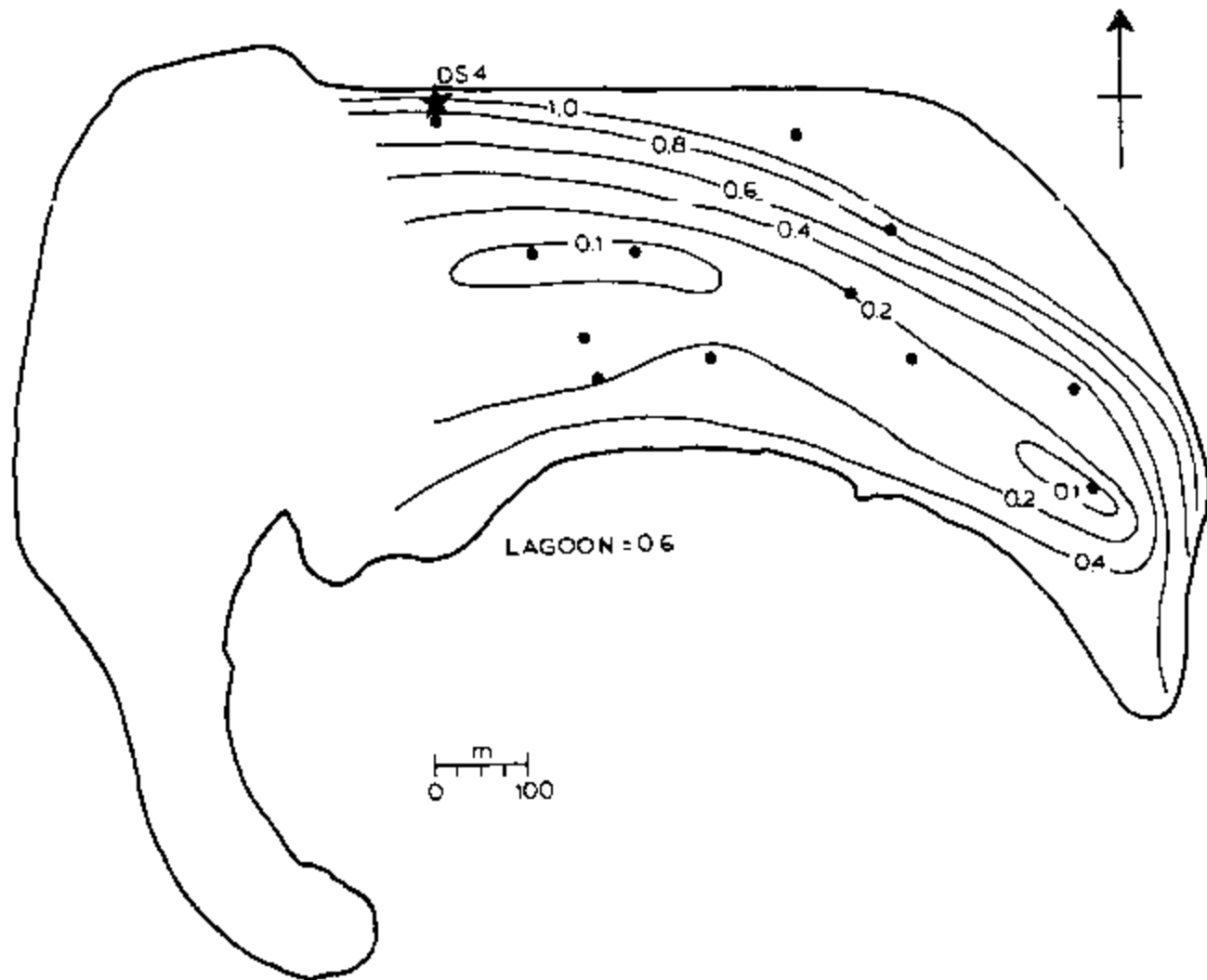


Figure 12. Map of Deke Island showing the geographical distribution of tidal efficiency. Values are relative to the range at observation well DS4 (starred location).

the interior of the island some 3 to 4 hours after they occur at B5 and in the lagoon. Dampening is such that a range of some 7 to 8 cm is a typical average for the interior, in comparison with some 50 cm in the lagoon (Table 3) and, from the TE value of the lagoon, some 83 cm at B5. The range in the open ocean was not measured, but the clear implication of Figure 11 is that it is significantly larger than the range at B5.

#### Standpipe vs. Piezometers

Tidal behavior at the 3 piezometer-standpipe pairs is shown in Figure 13. Piezometer data give the head variation of groundwater below the hard layer. Measurements within standpipes represent the head of the water that rests on the hard layer. As shown in the figure, water is present above the hard layer only at high tide. The tidal fluctuation in head of the unconfined water is considerably dampened relative to that of the underlying confined water.

In 2 of the 3 cases, there is a time lag between the occurrence of the high in the confined aquifer and the (later) high in the unconfined water. The curve for the tidal high in the unconfined water at Pz1 trails off -- very unlike a sine curve -- clearly suggesting retarded drainage back into the confined aquifer once the piezometric surface drops below the top of the confining bed.

Results shown in Figure 13 also indicate a relation between the thickness of the hard layer, on the one hand, and the difference between the standpipe and piezometer curves, on the other. In order of decreasing thickness of the hard layer as found by drilling, the piezometer sites can be ranked Pz1, Pz2, Pz3. Accordingly, from Pz1 to Pz3 there is a progression toward convergence of the two curves. As indicated by the small difference between time and elevation of the high at Pz3, where the hard layer is some 4 to 6 inches thick, if the hard layer pinched out altogether, then the two curves would be identical -- as they should be.

The lower pair of curves in Figure 13 is from E2 and E3 where continuous recorders were installed at the time of the piezometer studies. E2 is a tarp pit which is dug down to the hard layer; E3, which is about 10 m away from E2, is a hand-dug well from World War II, and it penetrates through the hard layer. The standpipe-piezometer pair of E2-E3 differs from those of the Pz1 - Pz3 sites in that the hard layer lies below the low-water level of the standpipe, so the full range of the tidal fluctuations can be measured at both standpipe and piezometer.

As shown in Figure 13, the tidal fluctuation at E2 is dampened and retarded relative to that at E3. The results of the simultaneous recordings at the two localities for a 5-day period are shown in Figure 14. As summarized in Table 1, the range at E2 is dampened to 20% that of E3, and the highs and lows occur 1 to 1.5 hours later. Over the 5-day period, the average level at E2 was slightly (1.1 cm) higher than that at E3.

Figure 13 also shows a considerable difference in the ranges, and the timing of the highs and lows, at the various piezometers. This variation is part of that shown for the entire island in Figures 11 and 12, that is,

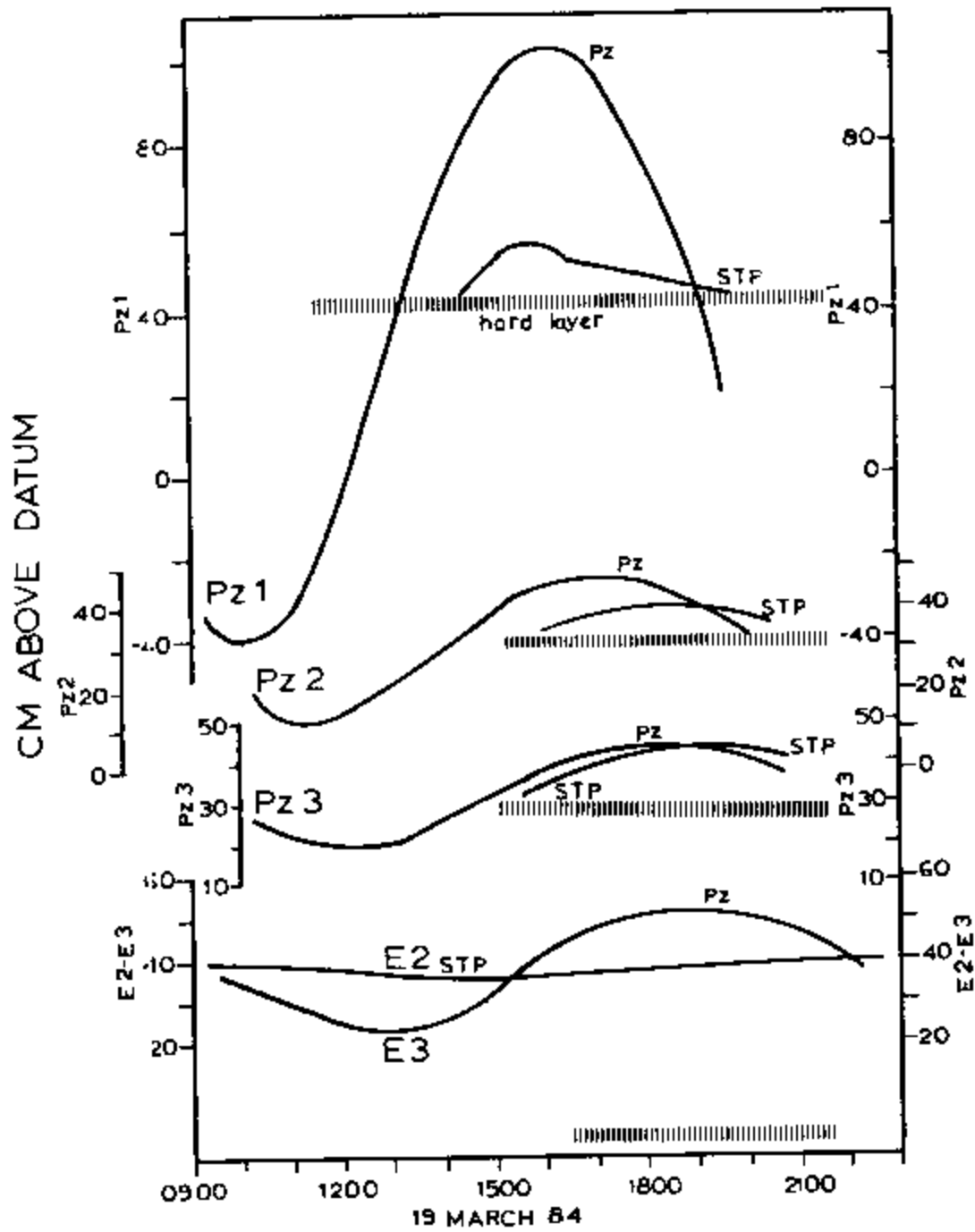


Figure 13. Graphs showing the simultaneous tidal variations at piezometer-standpipe pairs.

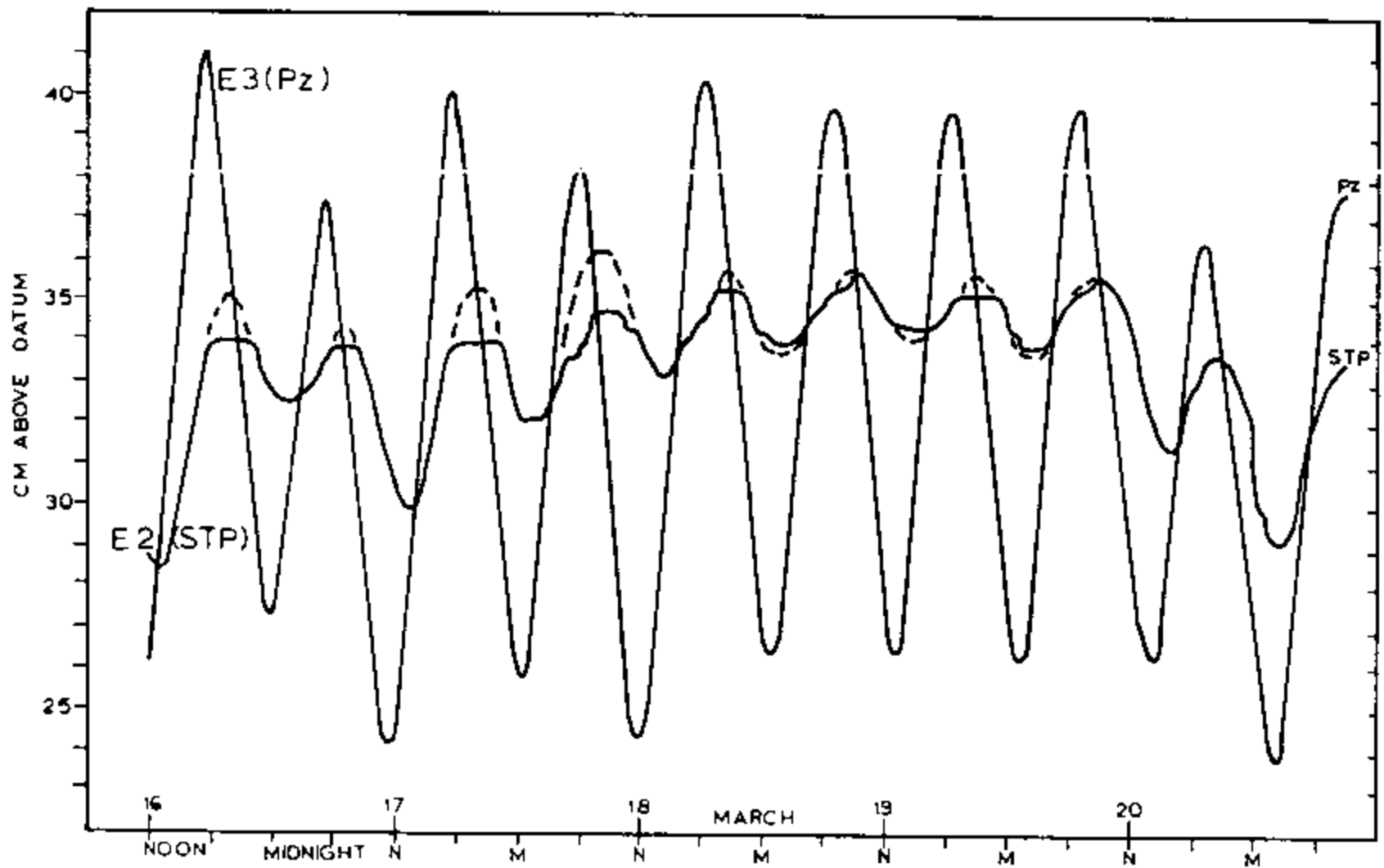


Figure 14. Simultaneous continuous recordings at two observation wells. E2 is a standpipe situated atop the hard layer and E3 is a piezometer installed in a hand-dug well penetrating the hard layer.

Figures 10 and 12 show the range and time-lag at piezometers for (northern) localities where the hard layer is present and for the tidal fluctuation of the water table in standpipes for part of the island south of the pinchout of the hard layer. The validity of combining ranges of a piezometric variation with that of a water-table variation is shown by Figure 13 where it can be seen that the one grades from north to south into the other.

#### Ocean Shore Tide Pipe

Tide studies also included an effort to measure the tidal fluctuation in the beach along the northern, reef-facing shoreline. Results are summarized in Figure 15. As shown in the figure, the high in the tide pipe occurs some 24 minutes after and some 11 cm higher than the corresponding high at the B5 piezometer located 30 m inland of the tide pipe. Thus the beach tide is clearly retarded from that of the open ocean (by the time difference between B5 and the tide pipe plus that between the open ocean and B5, this latter quantity being implied by Figure 11). The range at the beach though is probably larger than at B5 judging from the larger elevation of the high at the tide pipe and its location closer to the shoreline. The attempt in Appendix A to estimate the range at the tide pipe from the partial curve is inconclusive, because the curve departs substantially from a sine curve. The trailing off of the curve is like that at Pz1 and, as at that locality, indicates that downward drainage is impeded by the hard layer.

#### Day-to-Day Variations

Most of the daily water levels are from the average of two depth-to-water measurements taken 6hr to 6hr 15min apart and thus, to the extent possible with daily readings, effects of a semidiurnal tidal variation have been eliminated. Other results listed in the appendix -- those indicated by parentheses -- are from continuous recordings; for these, the daily levels are taken as the average of a morning reading and one 6 hrs later, so that these results would be comparable to the other measurements.

#### 14-Day Time Series

For the purpose of presentation here, the focus will be on a subset of the full set of results listed in the appendix. This subset, which is given in Table 4, consists of the daily levels at 14 wells over a 21-day period, 23 February through 14 March. The wells and time period are selected in order to provide the longest-running time series at the largest number of wells, with all the data being obtained in the same manner. With 2 exceptions, the 14 wells are standpipes in taro pits; the exceptions are E4, which is a hand-dug World War II well, and B3 which is an auger hole. E2 is perched on the hard layer; with the possible exceptions of C1 and B2, which may be punched through the hard layer, all the other wells in the time series are at sites where the hard layer is not present.

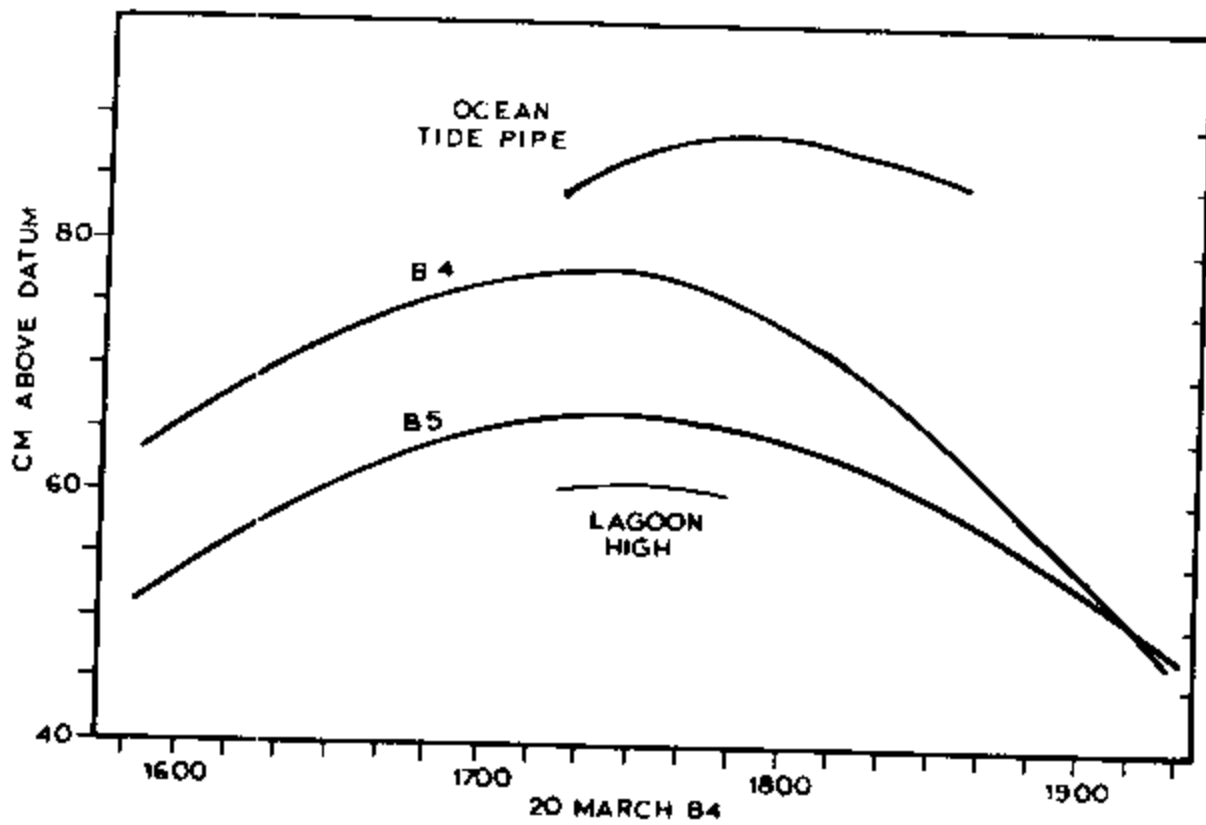


Figure 15. Graph showing the tidal high at two nearshore inland piezometers and at a standpipe installed in an ocean-facing beach.

Table 4. The 14-well time series. Water levels in cm.

	February														March						
	23	24	25	26	27	28	29	1	2	3	4	5	6	7	8	9	10	11	12	13	14
A1	32.8	32.5	31.0	33.7	29.6	27.0	27.8	29.6	34.0	34.8	35.3	33.9	31.9	31.5	31.8	31.8	40.3	35.6	33.7	29.0	27.4
A2	34.3	34.5	33.4	34.3	32.1	29.5	29.2	28.8	33.0	34.0	32.6	33.7	31.8	31.9	32.2	32.7	40.8	37.9	34.2	31.6	28.9
A3	32.1	31.8	31.8	33.4	31.0	28.0	27.7	28.0	30.5	32.0	30.6	32.4	30.3	30.0	30.8	31.0	36.5	34.1	31.5	29.9	26.3
A4		31.0	29.4	30.0	26.8	23.8	24.4	26.3	31.5	32.1	30.9	31.8	30.7	30.4	29.7	29.6	36.9	32.1	29.2	26.7	24.8
B1	33.0	31.4	30.7	31.3	28.2	27.0	27.9	30.7	38.2	42.5	36.5	34.2	31.3	30.2	31.6	30.6	34.5	33.7	28.5	26.3	25.8
B2	33.4	32.4	30.8	31.1	28.9	26.8	27.3	30.1	34.6	35.5	34.0	35.1	33.2	31.9	32.1	31.8	43.5	37.5	31.5	30.2	26.7
B3	29.3	31.4	30.0	32.1	29.5	27.0	29.9	32.3	36.1	40.5	31.5	35.4	29.7	29.5	32.3	31.7	34.8	30.7	26.6	28.3	27.7
C1	34.9	33.1	31.2	30.2	26.3	26.7	26.1	26.8	28.4	31.7	32.2	31.6	32.0	30.9	31.2	30.9	36.1	39.5	33.9	29.1	26.3
C2	33.7	33.6	32.2	32.8	29.8	27.9	28.8	30.0	34.0	35.2	34.8	35.0	32.9	31.6	32.1	31.9	36.5	36.7	32.5	28.8	27.4
C3	32.3	32.3	30.9	31.4	28.5	26.3	27.3	30.3	34.5	36.6	34.4	34.9	32.9	32.2	33.2	32.2	37.4	34.1	29.5	26.6	25.6
D3	31.4	32.7	32.3	31.9	28.4	25.9	26.9	29.3	35.4	36.5	35.7	34.6	29.4	28.4	29.5	28.9	38.2	34.4	31.3	27.0	25.5
E1	32.0	32.1	29.5	30.5	27.8	25.3	27.3	30.5	36.1	37.2	35.0	34.5	30.5	29.7	31.4	31.3	34.0	33.9	28.5	26.0	25.0
E2	36.4	32.8	28.7	28.0	26.8	24.5	23.7	26.6	36.9	35.3	34.7	33.8	32.5	32.8	33.0	30.9	41.1	41.9	34.7	28.7	25.2
E4	30.8	31.8	30.0	31.9	28.4	25.9	29.1	31.9	37.3	39.4	32.7	32.9	30.8	29.9	31.6	31.3	39.2	31.6	27.7	26.1	26.0



The 14 time series are shown in two groups in Figures 16 and 17. Statistics for the 14 wells are listed in Table 5, and statistics for the 21 days are listed in Table 6. The daily statistics are shown as a time series in Figure 18.

Obvious facts of the day-to-day variations are shown by Figures 16, 17, and 18: water levels within the wells rise and fall together, and this variation can be of considerable amplitude. For example, the level at all 14 wells group within a small range -- on average, about 8 cm (Table 6). Over the 21 days, each well varies over a range of 9 to 17 cm, depending on the well. Daily levels can change as much as 8 or 10 cm in a matter of 2 or 3 days or less. As shown in Figure 18 there were two significant rises in the 21 days of the survey. The first was March 3 where the water levels on average were 9 cm higher than they were 4 days earlier. The second was March 10 when the levels, on average were 7 cm higher than they were one day earlier.

The day-to-day variation summarized in Figure 18 can be easily related to daily rainfall and daily lagoon level. Rainfall figures represent the amount of rain collected in the gage at 0700 hrs of the indicated day. Daily lagoon levels are from continuous recordings and represent the average lagoon level over the 24 hours preceding 12 noon of the indicated day. It is obvious from comparison of the two sets of graphs that the first rise (the one of March 3) is due largely to a rise in daily sea level as recorded in the lagoon, and that a 4-cm rainfall probably added to the rise. The second rise (of March 10) is due to the 8-cm 2-day rainfall which more than balanced the effects of a downward trending daily sea level.

Overall, there is a strong correlation between daily ground-water levels and the daily lagoon level. For the 21-day record the correlation coefficient between  $\bar{W}$  (the run of the 14-well mean) and  $L$  (the daily lagoon record) is 0.55. For the shorter period February 23 through March 9 (i.e., before the big rainfall), the correlation coefficient between  $\bar{W}$  and  $L$  is 0.71.

### Reduced Levels

Figures 16 to 18 give water-level elevations relative to a fixed and arbitrary datum, the low tide of March 6 1337 hr. It is customary in reports of island and coastal hydrology to give the elevations, also, relative to mean sea level. Such results, or reduced levels, give the head in the ground-water body relative to the head at the shoreline (which is taken to be zero), or, in another view, the head loss that a water particle experiences in its flow from its inland position to the shoreline.  $\bar{W}-L$ , or the reduced level for the 14-well average, is shown in Figure 19 together with  $L$  and the daily rainfall. The upper curve is by definition a representation of an average daily head for groundwater. From visual comparison of  $\bar{W}-L$  and  $L$ , it is obvious that there is a strong negative correlation between the two; the correlation coefficient is -0.73. Thus, on a daily basis, the reduced levels, or the ground-water heads, are strongly controlled by changing sea level: as sea level rises there is less head differential between inland and shoreward sites.

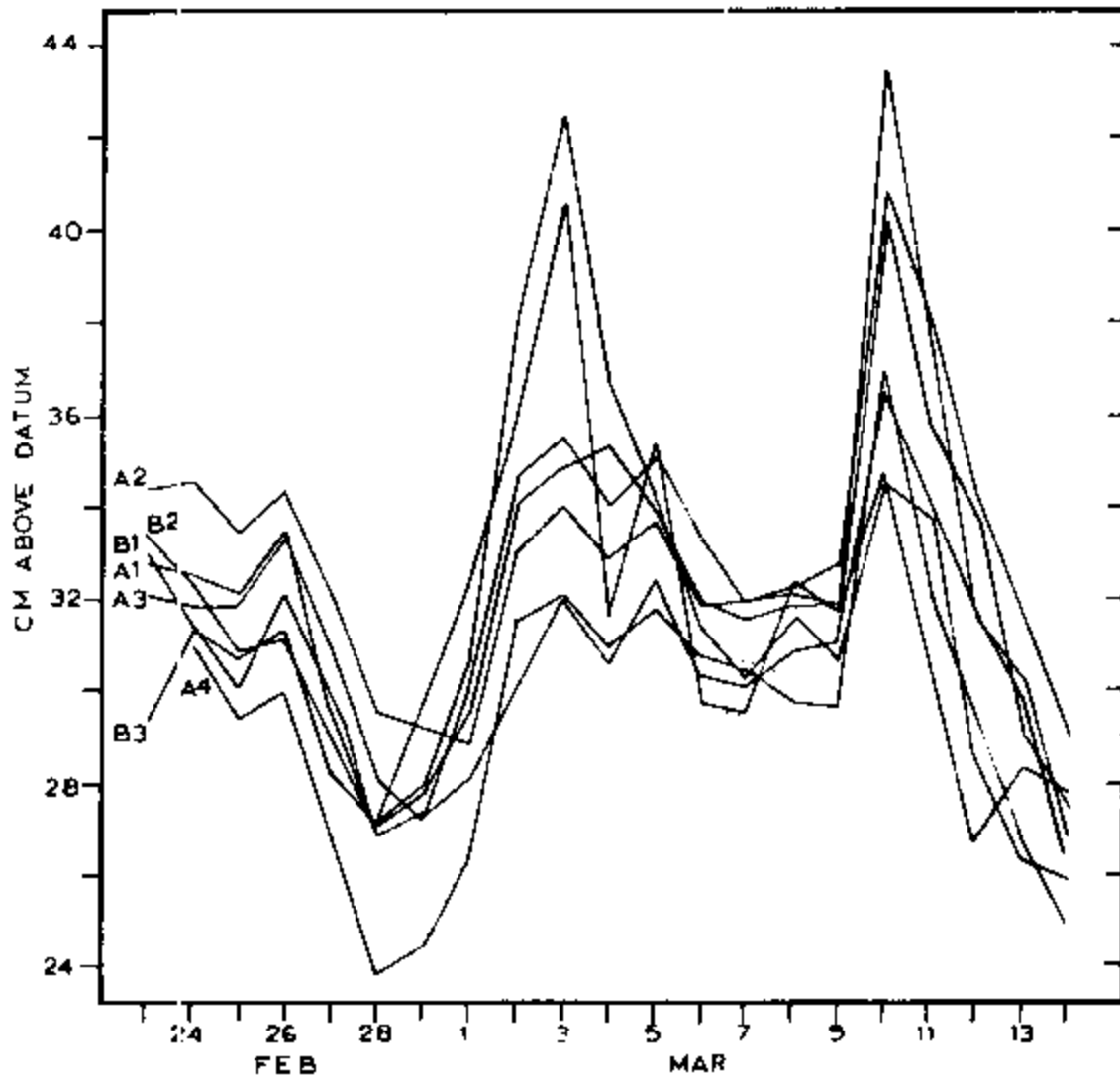


Figure 16. Hydrographs from observation wells located within the western portion of Deke Island.

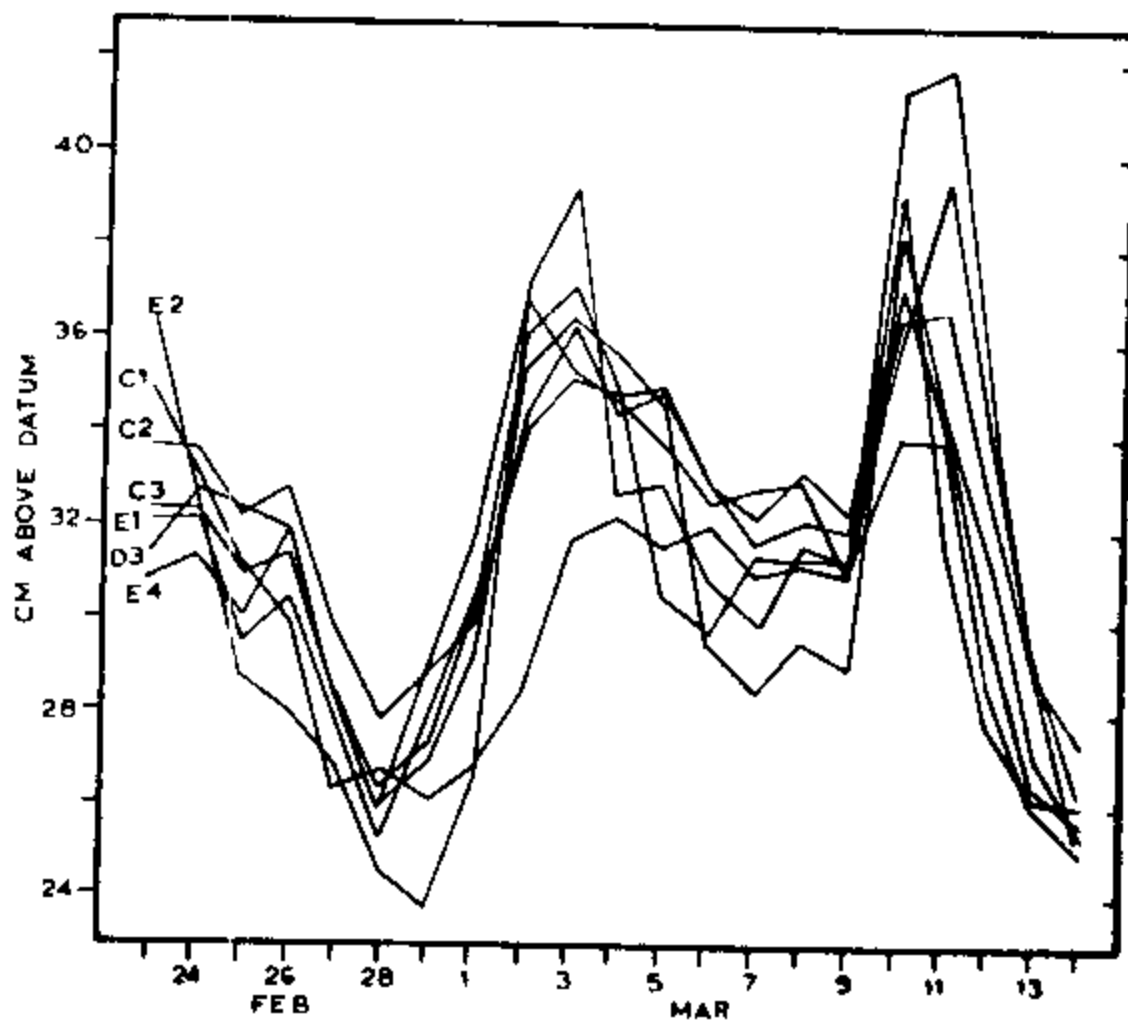


Figure 17. Hydrographs from observation wells located within the eastern portion of Deke Island.

Table 5. 14-Well time series: Well statistics. Water levels in cm.

	<u>Ave</u>	<u>SD</u>	<u>Max</u>	<u>Min</u>	<u>Range</u>
A1	32.1	3.2	40.3 (3/10)	27.0 (2/28)	13.3
A2	32.9	2.8	40.8 (3/10)	28.8 (3/1)	12.0
A3	30.9	2.3	36.5 (3/10)	26.3 (3/14)	10.2
AA	29.4	3.2	36.9 (3/10)	23.8 (2/28)	13.1
B1	31.6	4.1	42.5 (3/3)	25.8 (3/14)	16.7
B2	32.3	3.8	43.5 (3/10)	26.7 (3/14)	16.8
B3	31.3	3.3	40.5 (3/3)	27.0 (2/28)	13.5
C1	30.9	3.5	39.5 (3/11)	26.1 (2/29)	13.4
C2	32.3	2.7	36.7 (3/11)	27.4 (3/14)	9.3
C3	31.6	3.3	37.4 (3/10)	25.6 (3/14)	11.8
D3	31.1	3.7	38.2 (3/10)	25.5 (3/14)	12.7
E1	30.9	3.5	37.2 (3/3)	25.0 (3/14)	12.2
E2	31.9	5.1	41.9 (3/10)	24.5 (2/28)	17.4
E4	31.2	3.8	39.4 (3/3)	25.9 (2/28/)	13.5
Max	32.9	5.1	43.5	28.8	17.4
Min	29.4	2.3	36.5	23.8	9.3
Range	3.5	2.8	7.0	5.0	8.1

Table 6. 14-Well time series: Day statistics. Water levels in cm.

	<u>Ave</u>	<u>SD</u>	<u>Max</u>	<u>Min</u>	<u>Range</u>
2/23	31.80	1.84	36.4 (E2)	29.3 (B3)	7.1
24	31.35	0.97	34.5 (A2)	31.0 (A4)	3.5
25	30.85	1.29	33.4 (A2)	28.7 (E2)	4.7
26	31.61	1.66	34.3 (A2)	28.0 (E2)	6.3
27	28.72	1.61	32.1 (A2)	26.3 (C1)	5.8
28	26.54	1.46	29.5 (A2)	23.8 (A4)	5.7
29	27.39	1.74	29.9 (B3)	23.7 (E2)	6.2
3/1	29.37	1.88	32.3 (B3)	26.3 (A4)	6.0
2	34.32	2.74	38.2 (B1)	28.4 (C1)	9.8
3	35.95	3.19	42.5 (B1)	31.7 (C1)	9.8
4	33.64	1.87	36.5 (B1)	30.6 (A3)	5.9
5	33.84	1.23	35.4 (B3)	31.6 (C1)	3.8
6	31.42	1.22	33.2 (B2)	29.4 (D3)	3.8
7	30.78	1.24	32.8 (E2)	28.4 (D3)	4.4
8	31.61	1.07	33.2 (C3)	29.5 (D3)	3.7
9	31.19	1.01	32.7 (A2)	28.9 (D3)	3.8
10	37.84	2.81	43.5 (B2)	34.0 (E1)	9.5
11	35.26	3.14	41.9 (E2)	30.7 (B3)	11.2
12	30.95	2.64	34.7 (E2)	26.6 (B3)	8.1
13	28.16	1.75	31.6 (A2)	26.0 (E1)	5.6
14	26.33	1.17	28.9 (A2)	24.8 (A4)	4.1

Max	37.8	3.19	43.5	34.0	11.2
Min	26.3	0.97	28.9	24.8	3.5
Range	11.5	2.22	14.6	9.2	7.7

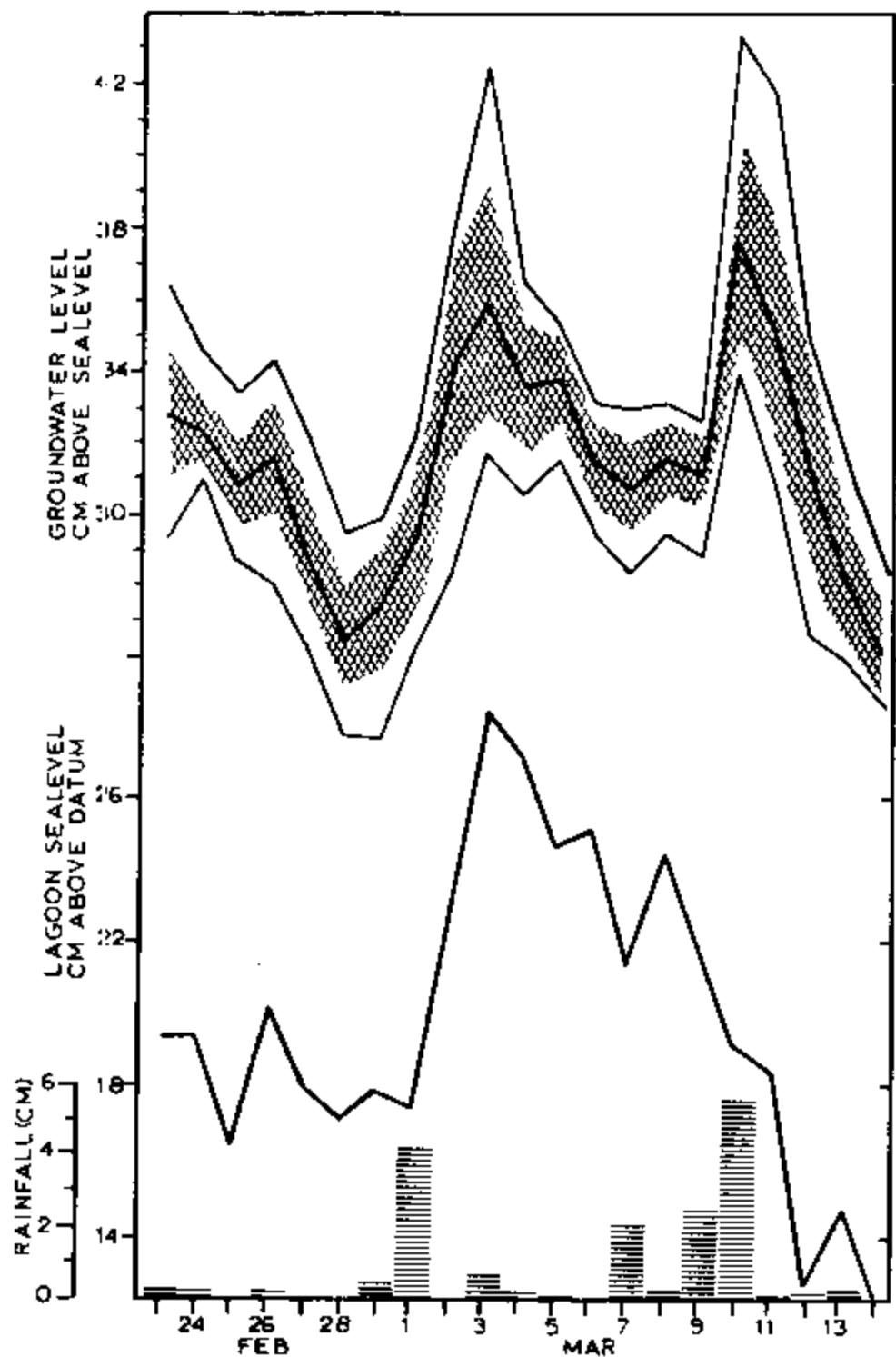


Figure 18. Graphs of ground-water levels, daily lagoon level, and daily rainfall. Ground-water level is the average from 14 wells over a 21-day measurement period. In the upper graph, the heavy line represents the mean, the cross-hatched band represents the  $\pm$  one standard deviation about the mean, and the uppermost and lowermost lines represent the maximum and minimum level respectively.

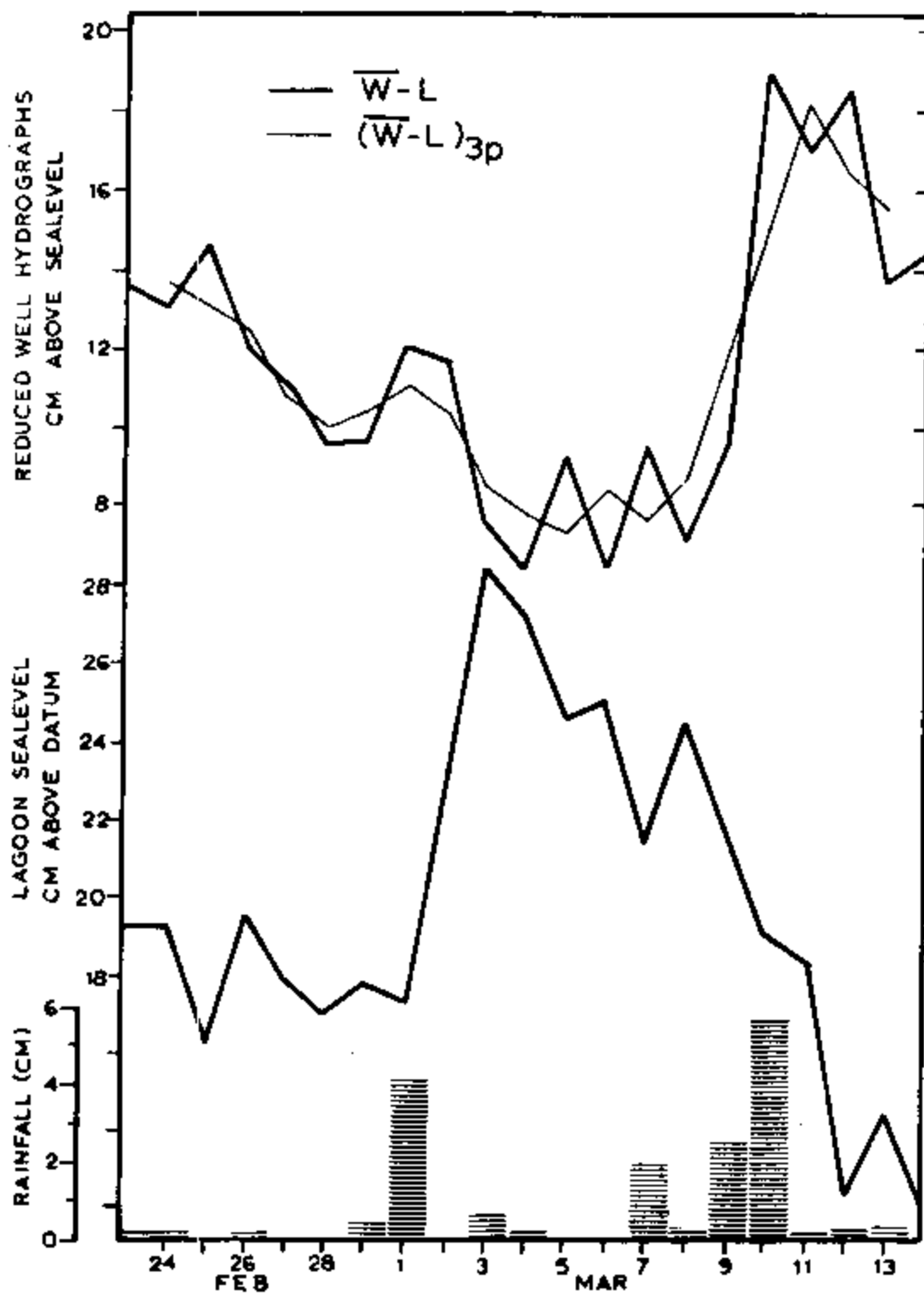


Figure 19. Graphs of reduced well hydrographs, daily mean lagoon level, and daily rainfall. Upper graph shows reduced levels and a 3-point moving average (the lighter line) for the 14 observation wells.

Included in Figure 19 is a 3-point moving average of the run of reduced levels. This curve,  $(\bar{W}-L)_{3P}$ , is merely a smoothed version of  $\bar{W}-L$ ; the strong negative correlation with sea level is the same. However it does make comparison with the rainfall record more clearcut.

Comparison of the rainfall record and the reduced levels in Figure 19 indicates that the ground-water head was increased by rainfall with both the March 2 and March 10-11 events. Because sea level was rising during the March 2 event and falling during the later event, the upswings in reduced levels represent, respectively, an underestimate and an overestimate of the amount of water that was added to fresh ground-water storage by the two rainfalls.

Obviously, then, the reduced levels do not relate directly to changing quantities of fresh groundwater stored in the aquifer. This important implication of Figure 19 will be examined further in the Discussion below.

### Standpipes vs. Piezometers

The run of daily levels at the E2-E3 pair is shown in Figure 20. This period of record is 26 days (in contrast to that of Figures 16-19), and results include readings from continuous recordings.

As shown in the figure, the level at E2 (the perched taro pit) is generally higher than that at E3 (the piezometer), but the difference is slight. Statistics for the 26-day series are: the means of E2, E3, and E2-E3 are 32.2, 31.2, 0.9 cm, respectively; the standard deviations for E2, E3, and E2-E3 are 4.6, 3.7, and 1.6 cm, respectively. Thus, on average, E2 is about 1 cm higher than E3 and, from the standard deviation of the difference, the two levels are within 2.5 and -0.7 cm of each other some 68% of the time. The fact that E2 is consistently higher, albeit slightly, than E3 may reflect recharge by downward drainage through the hard layer in this 26-day rainy period. The fact that the two are consistently as close as they are would seem to suggest that, over the long term heads above and below the hard layer tend to equilibrate.

### Areal Patterns

Although all the wells rise and fall together as indicated in Figures 16 to 19, it is apparent from Table 5 that they rise and fall by different amounts. Day-to-day variability, as measured by either the standard deviation or the range of the 21-day time series, is in general larger at wells closer to the shoreline than at wells located further inland.

In order to better document this geographic variation in the time variability of the daily measurements, the data set is expanded from the 14 wells of Figures 16-19 and Tables 4-6 to cover a total of 21 wells. Well statistics for this expanded set are listed in Table 7 and include the results at 5 recorder sites and the statistics at 3 sites where a partial record was enlarged to cover the full 21-day period so that all the well statistics would cover the same time interval. For the latter, blanks were



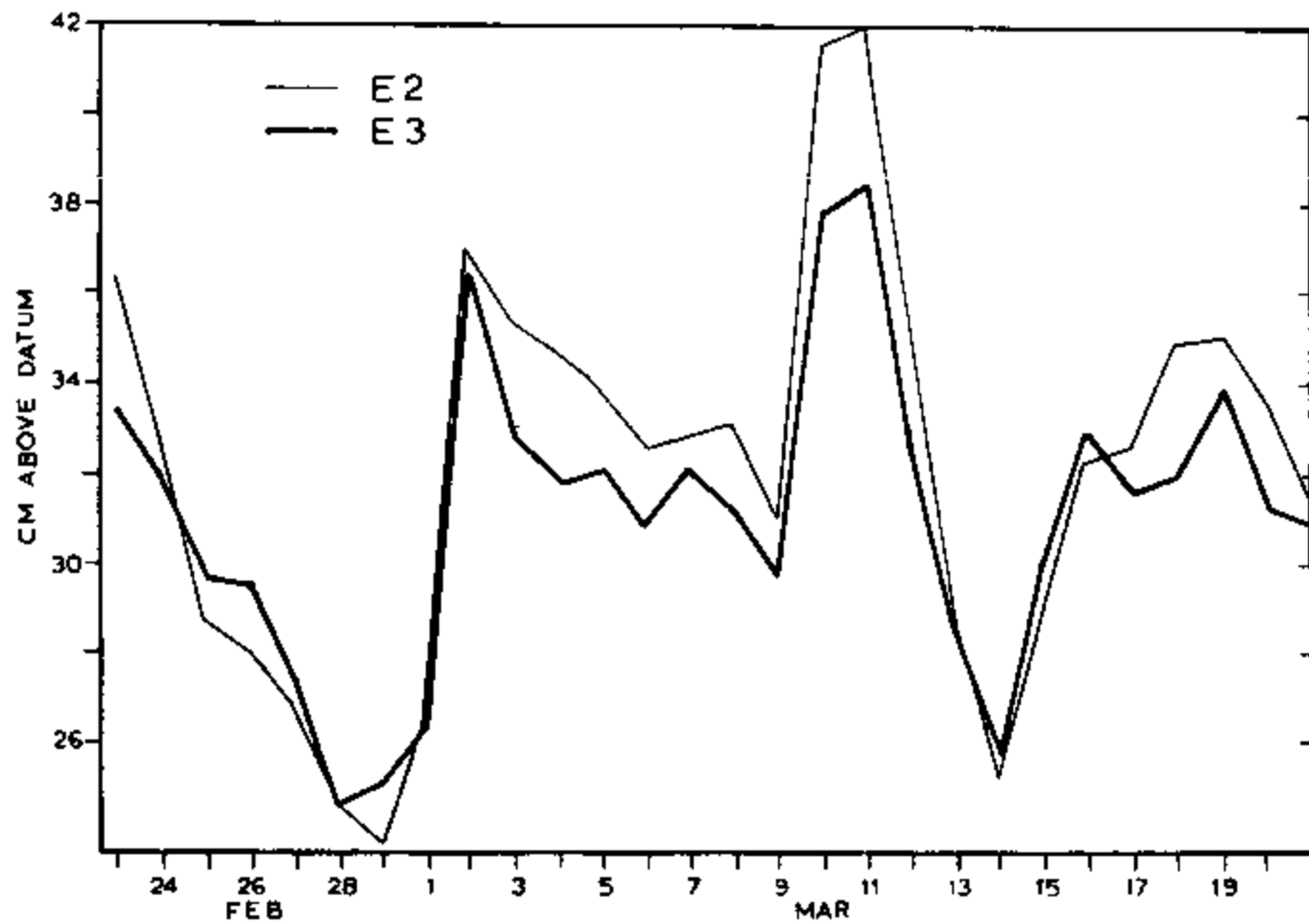


Figure 20. Graph of daily water levels at two observation wells.

Table 7. Expanded time series: Well statistics. Water levels in cm.

	<u>Ave</u>	<u>SD</u>	<u>Range</u>
A1	32.1	3.2	13.3
A2	32.9	2.8	12.0
A3	30.9	2.3	10.2
A4	29.4	3.2	13.1
B1	31.6	4.1	16.7
B2	32.3	2.8	16.8
B3	31.3	3.3	13.5
(B4)*	32.8	3.1	12.0
C1	30.9	3.5	13.4
C2	32.3	2.7	9.3
C3	31.6	3.3	11.8
(C4)	30.4	2.9	9.4
(C5)	31.1	2.6	9.0
(D1)	30.6	4.7	20.7
D2*	30.9	3.3	11.6
D3	31.1	3.7	12.7
E1	30.9	3.5	12.2
(E2)	31.9	5.1	17.4
(E3)	30.8	3.8	13.7
E4*	31.2	3.8	13.5
E5	30.0	3.9	13.6

( ) indicates a well for which the 21-day period includes continuous recording.  
 \* indicates a well for which a partial record was made up to a full 21-day record so that all well statistics would cover the same period. B4 includes 4 days that were filled in from A2. E5 and D2 include 8 days that were filled in from E4 and D3 respectively. All other wells are from Table 5.

filled from measurements at nearby wells that behave similarly over the period of simultaneous measurements.

The standard deviation and range of these 21 21-day time series are shown respectively in Figures 21 and 22. The obvious result is that both measures of the day-to-day variability decrease inland from the lagoon in a systematic (mappable) manner. This is consistent with the fact, evidenced by Figure 18, that the principal control on the daily water levels is the sea-level variation, and this sea-level effect diminishes inland in the same manner as the tides shown in Figure 12.

It can be noted in Figures 21 and 22 that the variability at D1 and E2 is anomalously high for their geographic position. As noted above, the E2 taro pit is perched on the hard layer; the D1 taro pit is in part perched on and in part seemingly dug through the hard layer. The implication would seem to be that where vertical flow is impeded by the presence of a hard layer beneath the taro pit, the water-level response to rainfall, and possibly evapotranspiration, is larger than it otherwise would be.

#### Water-Level Maps

Averages for the 21-day water-level series at the 21 sites are listed in Table 7. These results are shown on a map in Figure 23. There is a water-level ridge that extends the length of the island and curves parallel to the lagoon. The overall configuration is not symmetric; as seen by the 31-cm contour, the ridge occurs preferentially closer to the lagoon, and away from the reef-facing shoreline.

It should be noted that the map represents mixing of results from wells where no hard layer is present with those where the hard layer has probably been punched through (forming a piezometer). As shown on the map, this mixing apparently does not make any difference; the pattern of results is contourable, at least to the accuracy of the data which, as indicated by the asterisks and parentheses, are derived in a number of different ways. This result is consistent with the finding in the study of day-to-day variations that, over a period of some time, there is little, if any, difference in level between piezometer and adjacent standpipe.

The map of Figure 23 is especially significant, because it shows the average water level over the longest period of time that is possible for this study. Thus it gives the best approximation of the long-term heads with sea level removed. As shown on the figure the axis of the ridge is defined by the 31-cm contour. Average for the lagoon level for the same period is 20 cm. Thus over the 21-day period, the head in the heart of the lens is on average 11 cm above sea level. Using the standard Ghyben-Herzberg ratio (see for example Todd, 1959 or other texts on ground-water hydrogeology), this result translates to a depth-to-interface of some 4.5 m (or 15 ft.)

The map of Figure 23 shows the water-level configuration over only a limited part of the island -- the lagoon side. The reason is that wells (piezometers) were not available in the northern part of the island until the last few days of the study, and these days were spent in documenting

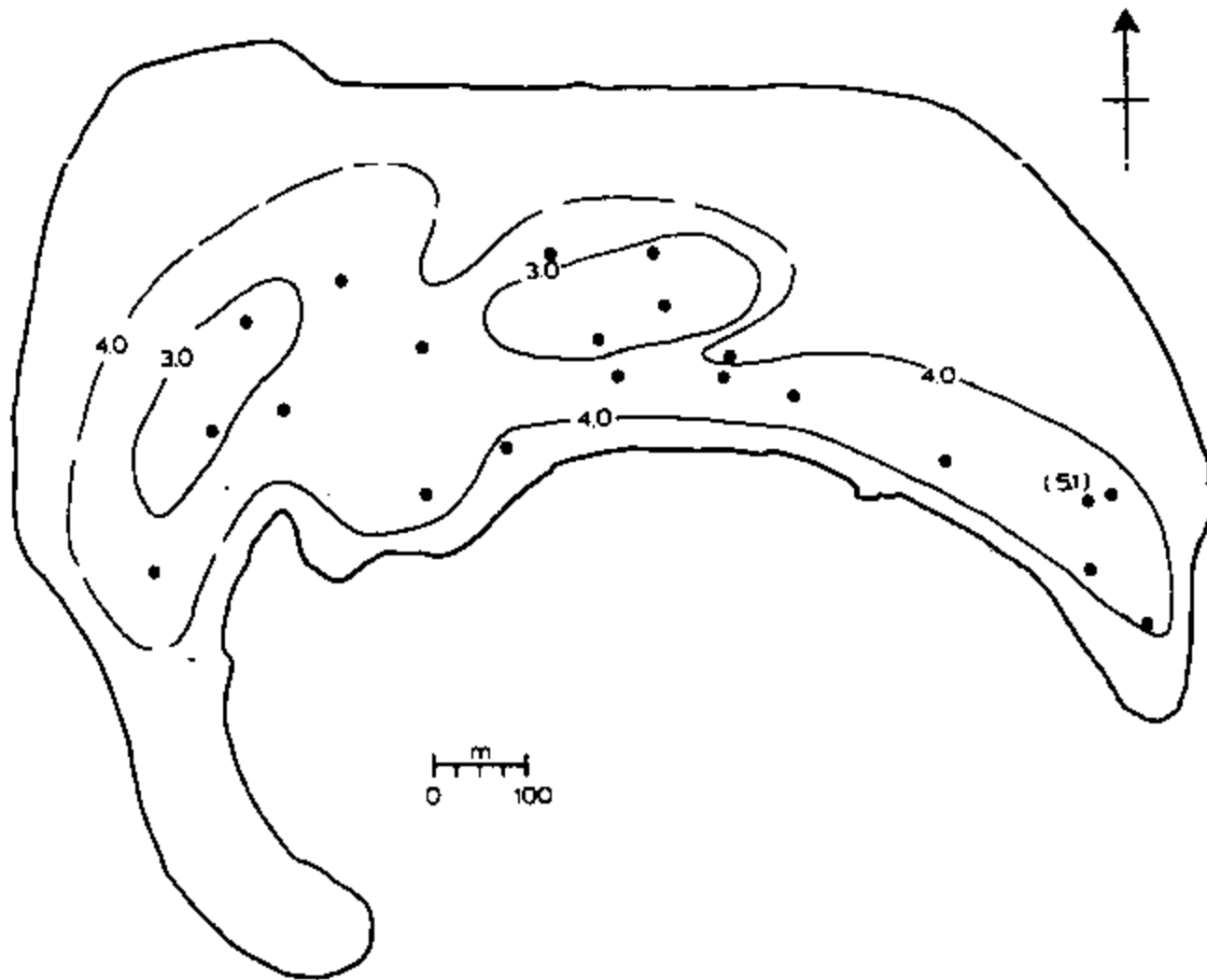


Figure 21. Map of Deke Island showing the geographic distribution of standard deviation for a 21-day series of water levels.

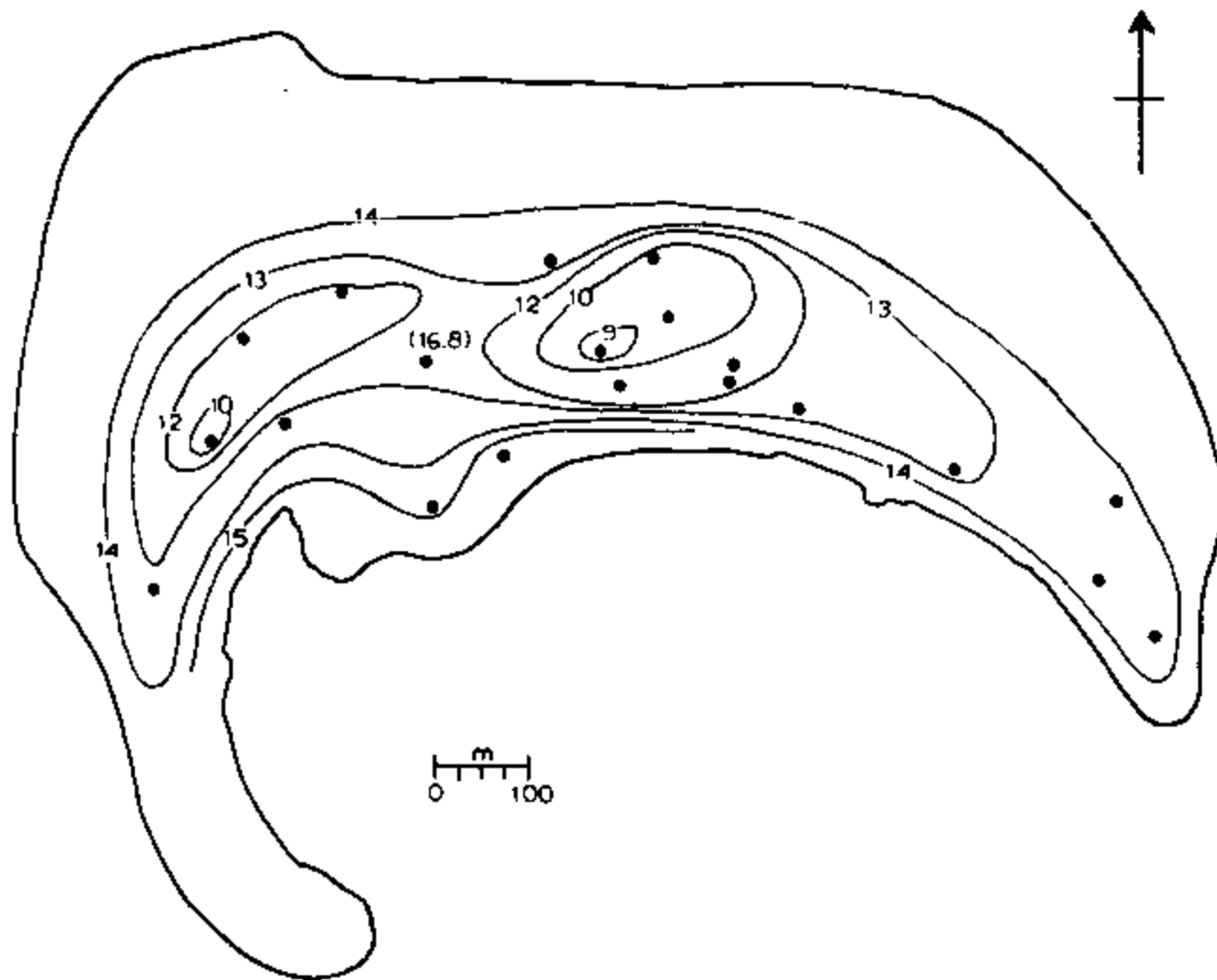


Figure 22. Map of Deke Island showing the geographic distribution of the range of the 21-day series of water levels.

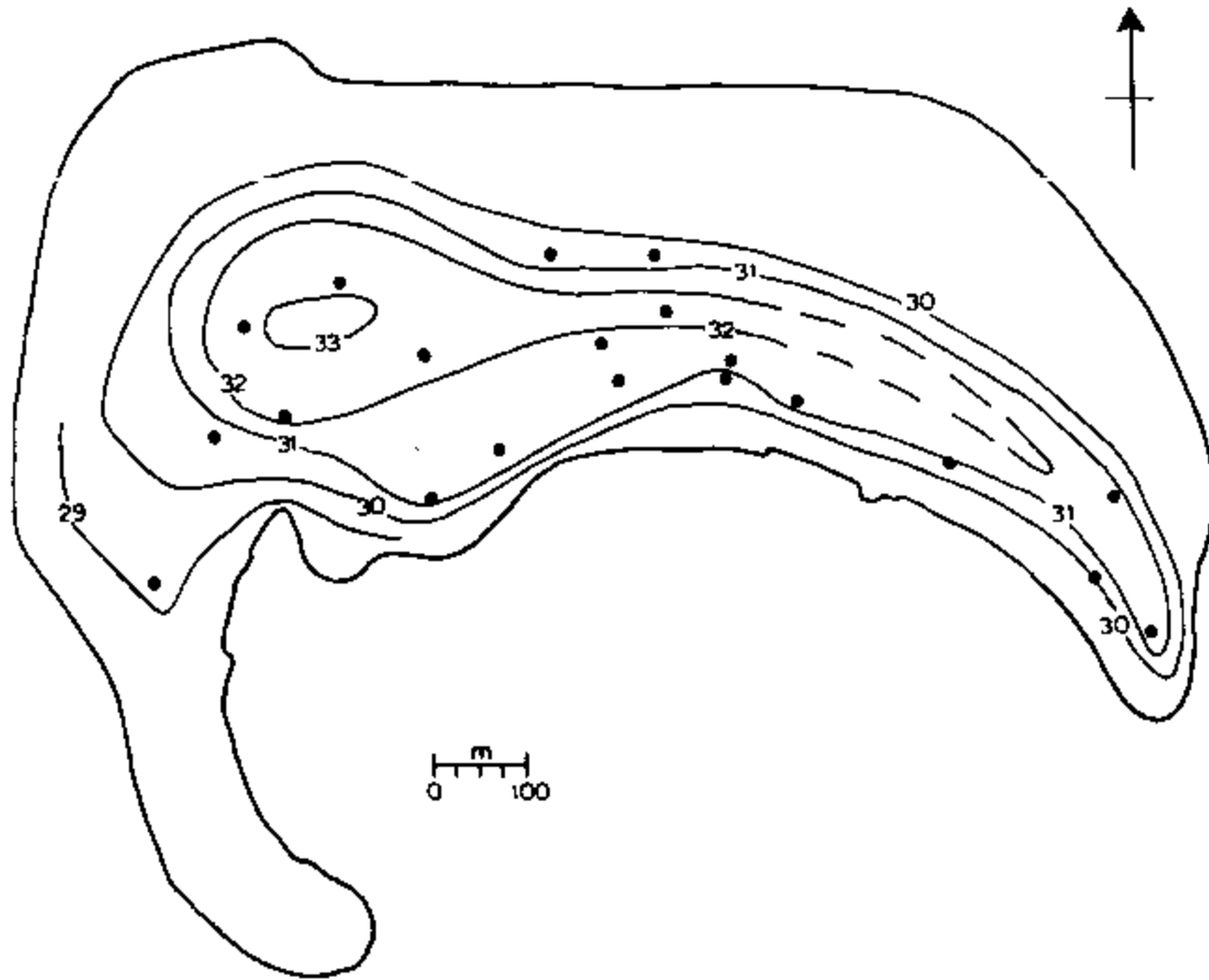


Figure 23. Map of Deke Island showing the geographical distribution of the average water level measured in observation wells. Water levels represent the 21-well average for a 21-day measurement series.

the difference in standpipes and piezometers. However results at D4 are of sufficient duration to allow the map to be extended northward to better define the asymmetry. This is done in Figure 24.

Figure 24 shows a water-level map of the average of 2 measurement days, March 13 and March 19. These two dates are selected because March 13 was a low-sea-level day and March 19 was high-sea-level day. The intention is to average out, to the extent possible, the effects due to daily variations in sea level such as the abnormally high ground-water levels close to the shoreline when daily sea level is on a high (as documented in Figures 16 and 17).

As shown on the map, the asymmetry of the island water levels is well defined. The level at D4 is lower than at any other site on the island. The axis occurs in the southern half of the island, and, accordingly, the surface defined by the water levels slopes more steeply toward the lagoon than toward the northern reef-facing shoreline.

In addition, the map shows the southern limit of the hard layer with the relative position of the axial mound to the south of the layer boundary. Thus the area on the lagoon side where the hard layer is not present serves as the recharge area for groundwater beneath the hard layer that borders the reef-facing shoreline. Overall, the hydrogeology is that of a confined aquifer that occurs in the north and crops out in the south. The confining bed is the hard layer, and it occurs at about mean sea level.

## Geomorphology and Surface Geology of Deke

### Geomorphology

The topographic map of Deke is shown in Figure 25. Examination of the map reveals the presence of four physiographic regions: (1) a high ridge on the northern and western margin of the island; (2) a gently sloping central platform; (3) a small depression in the south-central portion of the island; and (4) a low ridge on the southern (lagoon) margin of the island.

Along the northern and western margin of the island is a prominent ridge delimited by the dashed 7-ft. contour on the map of Figure 25. This ridge has an average width of 300 feet with extreme widths of 100 and 600 feet. The top rarely exceeds 10 feet in elevation.

A small elongated northeast-southwest trending depression characterizes the topography of south-central portion of the island. This depression is outlined by the hatched 4-ft and dashed 3-ft contours and appears to be a low between two wash-over fans.

A poorly defined, narrow ridge is along the lagoon margin of the island. In general, the crest of this ridge is situated approximately 100 feet inland from the lagoon shoreline and at an average elevation of 4.5 feet.

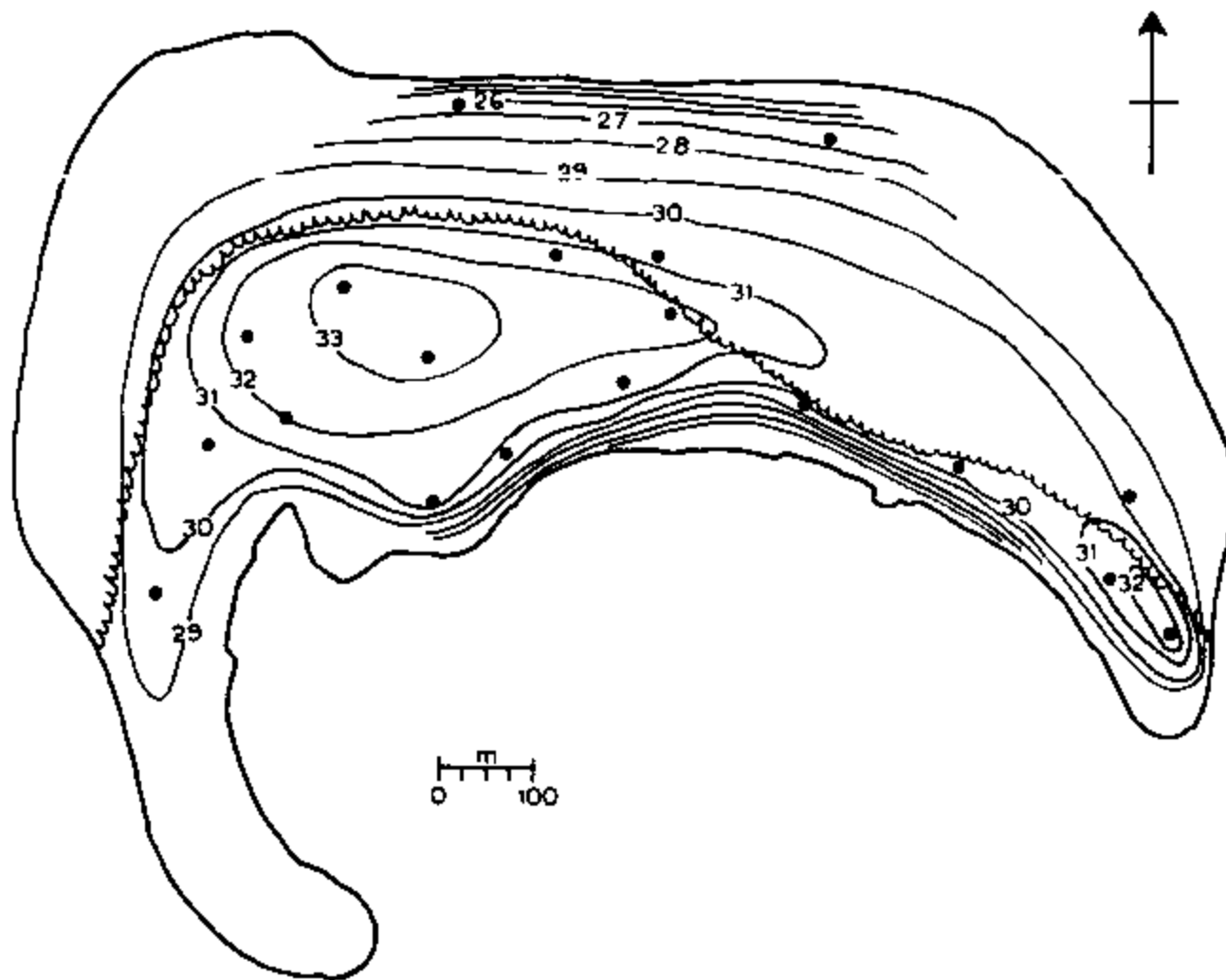


Figure 24. Map of Deke Island showing the geographic distribution on ground-water levels for two measurement days. Water-level data are based on the average from two measurement days. The map represents the across-the-island pattern of the groundwater level surface: a piezometric surface where the hard layer is present and a water-table surface elsewhere.



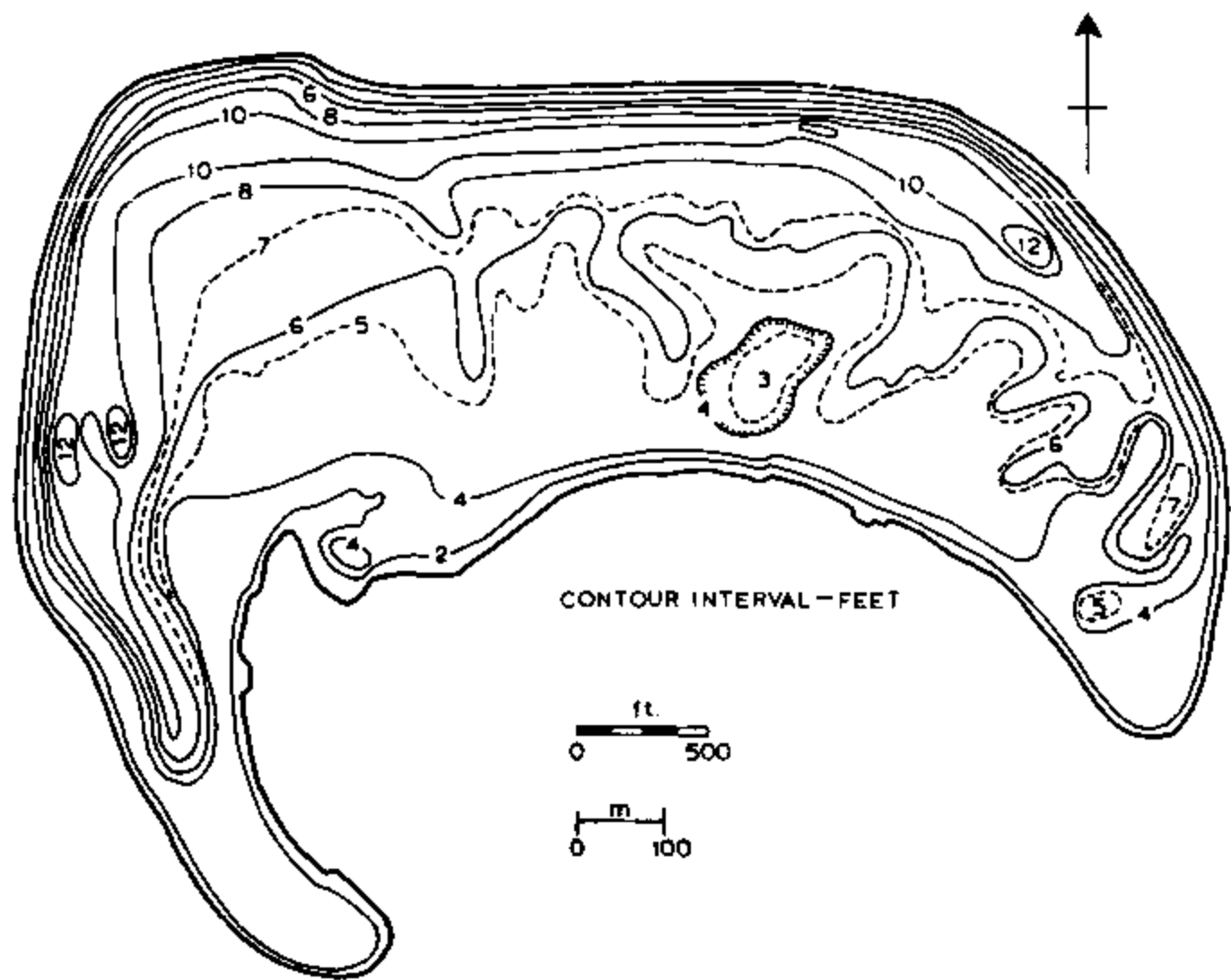


Figure 25. Topographic map of Deke Island. Contour interval in feet.

## Grain-Size Distribution

Figure 26 shows a map of mean grain size (in Phi units) for coarse-grained surface material. As inferred from the map, there are three grain-size zones: (1) a northern and western cobble (-6.50 to -7.50) zone; (2) a central coarse-pebble (-4.50 to -6.00) zone; and (3) a southern medium-pebble (-3.00 to -4.00) zone. It is obvious that the mean grain size of the gravel fraction decreases lagoonward. Example distribution curves for each of these zones are given by the graphs of Figure 27.

The zone along the northern and western margin of the island is composed primarily of angular cobble-size coral rubble and boulder-size (larger than -8.00) coral heads. The distribution curve is flattened and skewed to the right which indicates the sediments are poorly sorted and there is an excess of finer grained material.

The coarse-pebble zone corresponds to wash-over fans of the central platform. Sediments from these wash-over fans closely approximate a normal distribution.

The medium-pebble zone on the lagoon margin differs from the other zones in that the sediment-size curve of the gravel fraction is narrow, indicating a comparatively well-sorted distribution. Also, the distribution is strongly skewed to the right indicating a large excess of finer-grained material.

Statistical parameters calculated from the grain-size distribution of sieved sand samples are listed in Table 8 and graphs of the size distribution are shown in Figure 28. Obviously, the sand is polymodal; examples of 3-, 4-, and 5-mode distributions are indicated. It is clear that the polymodality is due to the presence of certain constituent particles. Results of an examination of the constituent particles found in each mode show that: (1) mode-1 at -4.220 and mode-2 at -3.170 are composed of angular coral fragments; (2) mode-3 at -0.420 is composed of the foraminifera Calcarina sp.; (3) mode-4 at 0.250 is composed of the foraminifera Baculogypsina sp.; and (4) mode-5 at 2.040 is composed of rounded fragments of coral and various small foraminifera.

Vertical profiles of mean grain size, sorting, skewness, and sand and gravel percentages for the three measured sections are shown in Figure 29. At D4 (DS3), the sand percentage increases with depth, and the mean grain size decreases with depth. At B5 (DS4), the mean grain size and sand percentage are quite variable. At P2, there is only a slight increase in sand percentages and mean grain size with depth.

## Surface Geology

The surface geological map of Deke (Figure 30) is a combination of the topographic map and the mean-grain-size map; supplemental data are from a series of tape-and-compass traverses. As shown by the map, there are four zones: a ridge composed of cobbles and boulders; a series of coalescing wash-over fans consisting of coarse pebbles and cobbles; a narrow band of coarse to medium pebbles and sand; and, a lagoon berm composed of sand with

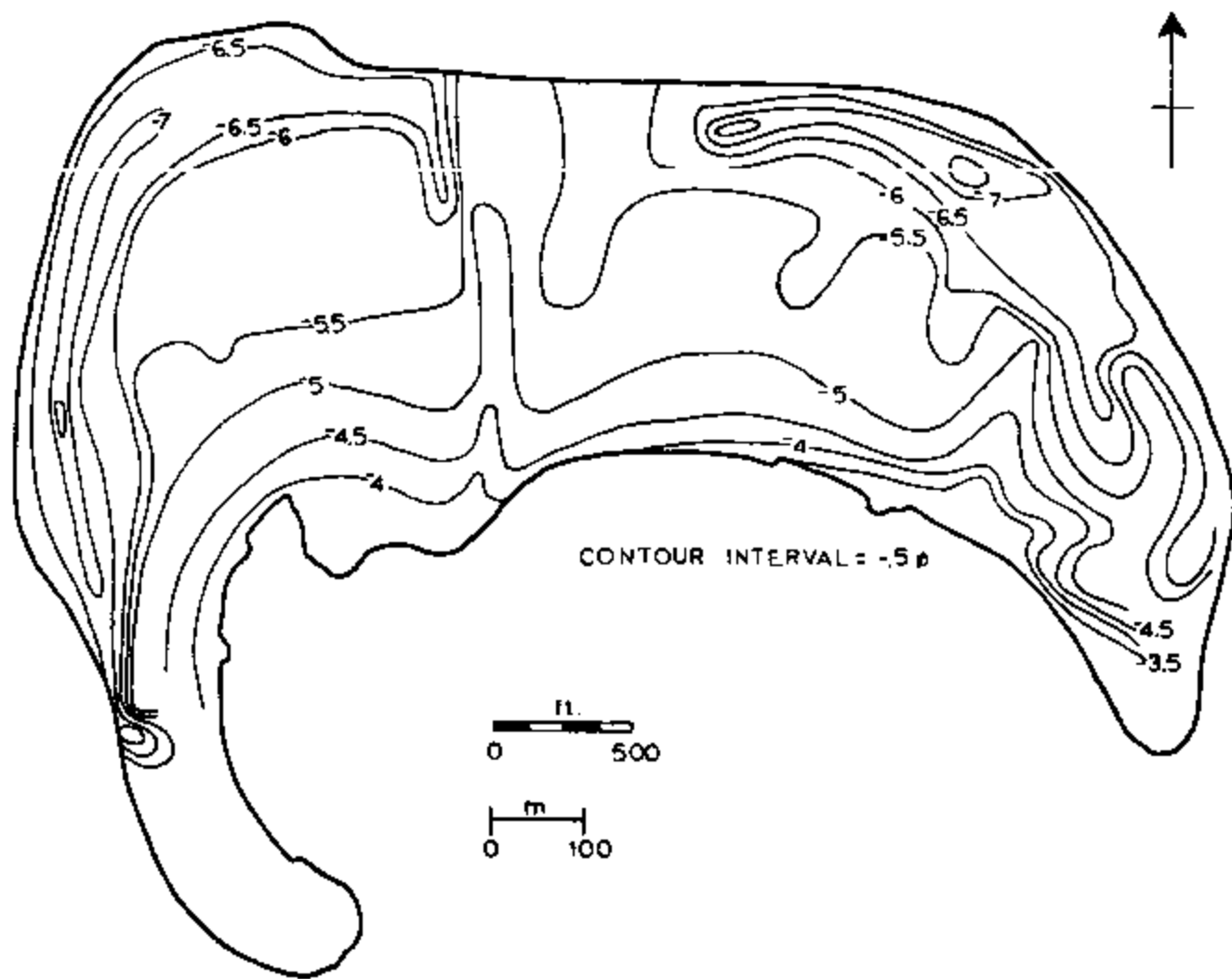


Figure 26. Contour map of the sediment distribution at the surface of Deke Island. Distribution is given in Phi units.

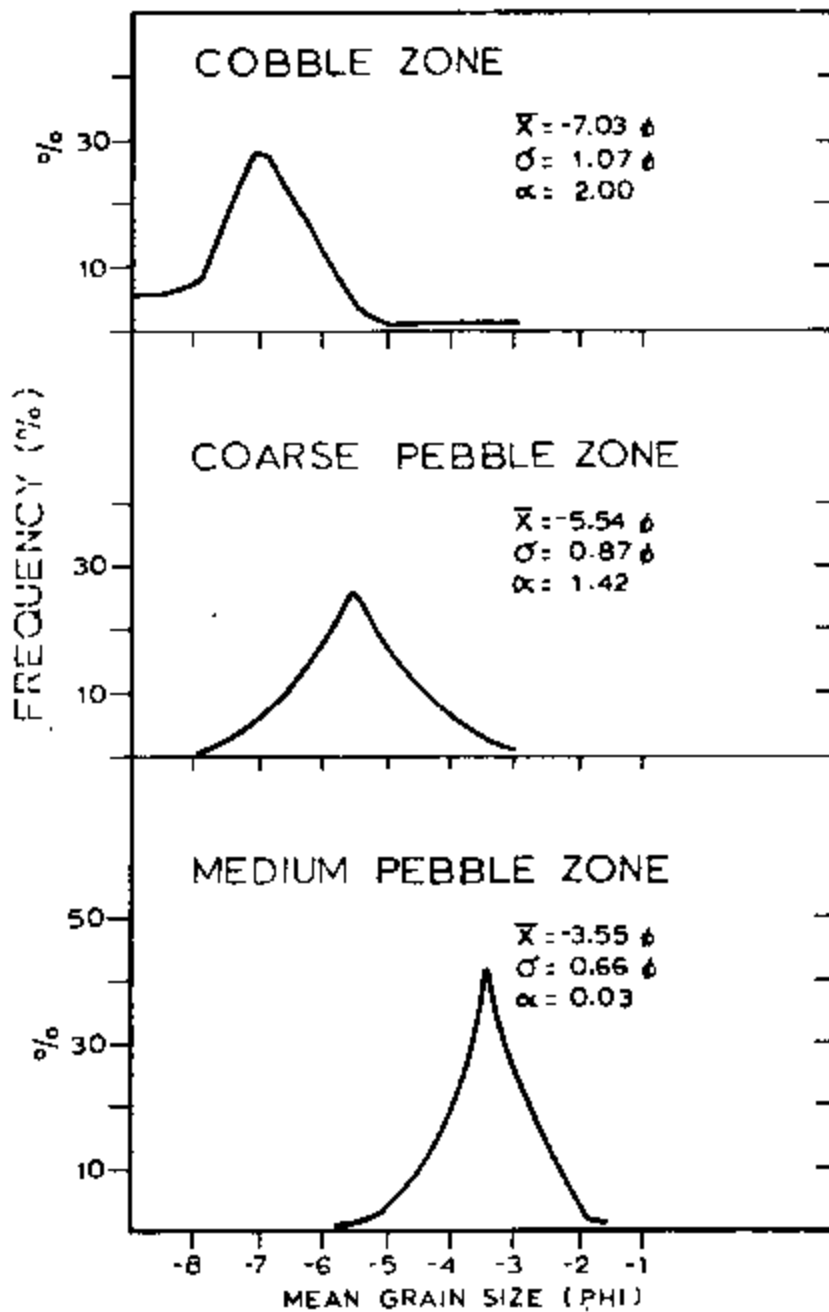


Figure 27. Grain-size distribution of surface sediment samples within three mapped zones.

Table 8. Statistical parameters calculated from sieved samples. Grain size in phi units.

Sample number	mean ( $\bar{x}$ )	Standard deviation ( $\sigma$ )	Skewnes ( $\alpha$ )	Percent gravel	Percent sand
1	-1.25	2.46	+0.03	49.78	48.45
2	-0.33	2.18	+0.79	27.76	71.93
3	-1.04	2.36	+0.08	43.49	55.58
4	-1.67	2.39	-0.46	57.65	41.75
5	-1.92	2.60	-0.62	62.25	37.35
6	-0.24	2.37	+0.36	35.32	63.81
7	0.53	2.05	+0.81	20.28	79.20
8	-1.62	2.75	-0.11	56.41	43.26
9	0.06	1.36	+0.87	9.61	90.16
10	-1.24	2.32	+0.13	46.85	52.93
11	-3.16	2.00	-0.81	84.37	15.50
12	-2.41	1.92	-0.71	70.91	28.80
13	-2.02	1.99	-0.63	72.18	26.96
14	-1.10	2.23	-0.05	53.88	46.00
15	-1.50	2.43	-0.17	59.71	40.00
16	-1.46	2.42	-0.29	62.95	36.67
17	-0.56	1.69	-0.07	52.11	47.58
18	-1.76	2.24	-0.04	57.25	42.51
19	-1.69	2.58	-0.02	54.77	44.97
20	-0.98	2.05	+0.40	35.70	64.19
21	-0.13	0.92	+0.89	9.15	90.62
22	-2.84	1.88	-0.53	74.63	25.05
23	-0.09	2.24	+0.47	31.15	68.73
24	-3.06	1.97	-0.73	86.69	18.26
25	-0.26	0.96	+0.89	5.27	94.47
26	-1.59	2.36	-0.06	59.48	40.30
27	-2.30	1.94	-0.36	66.91	33.01
28	-2.64	1.79	-0.26	60.67	39.13

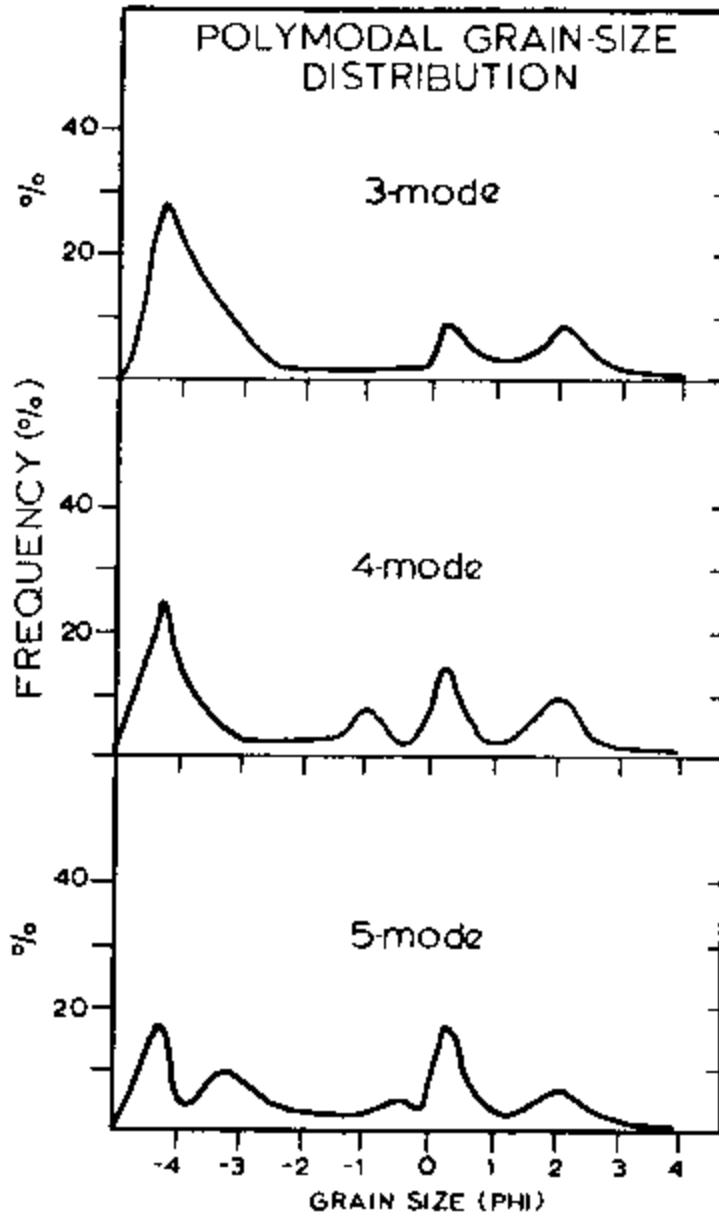


Figure 28. Example graphs of polymodal grain-size distribution for sieved samples.

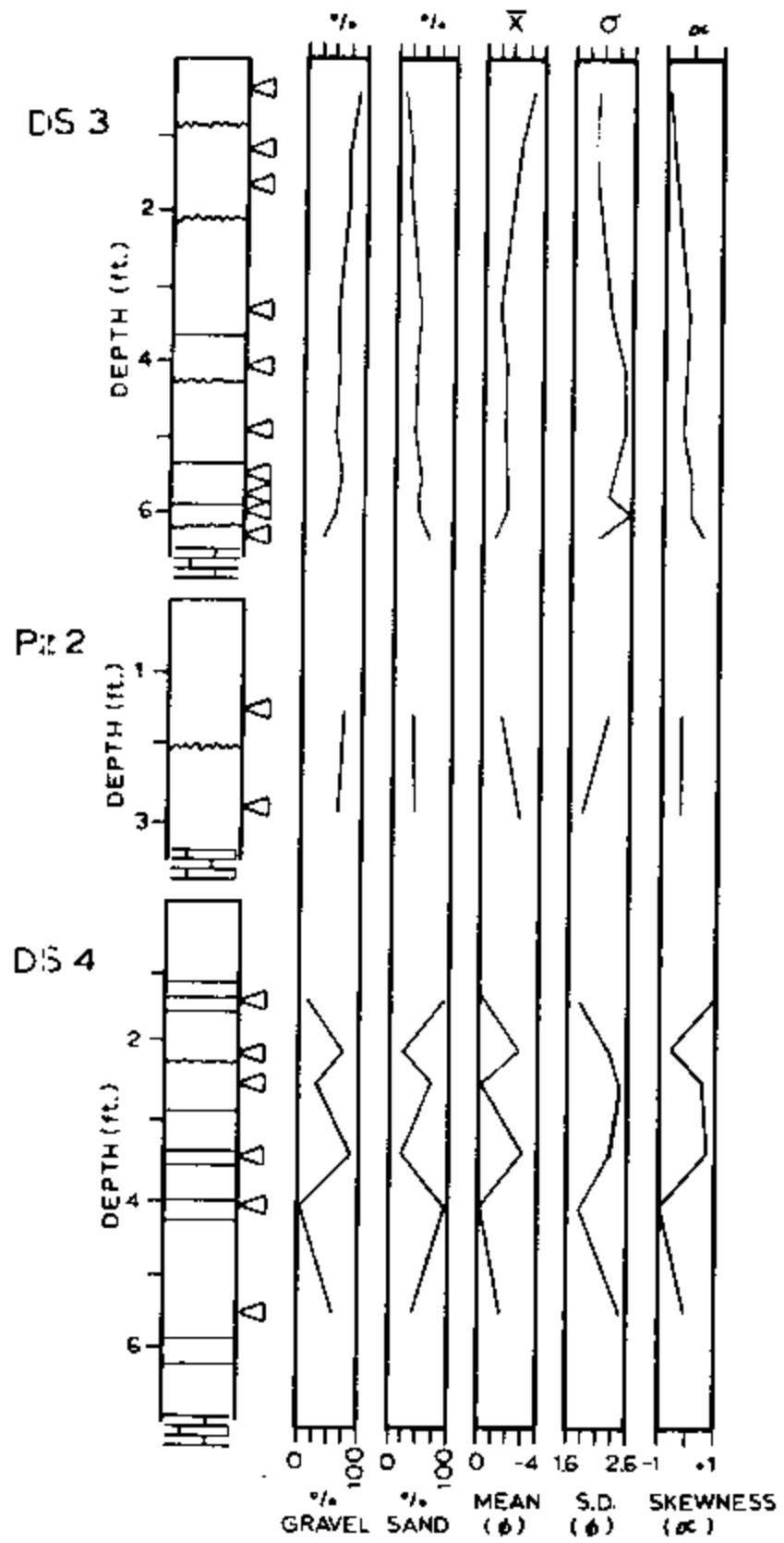


Figure 29. Results of sieve analyses on samples collected from stratigraphic test pits.

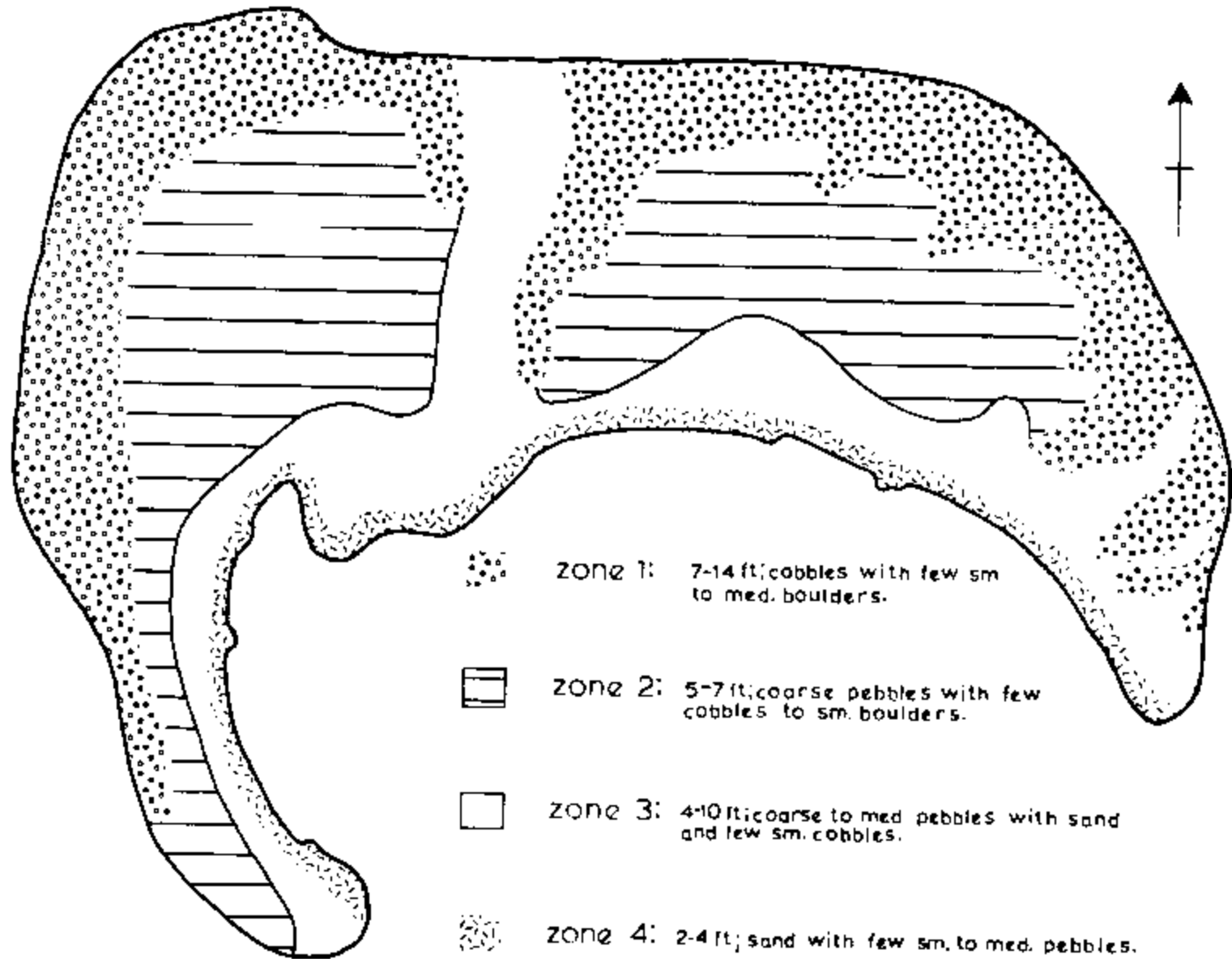


Figure 30. Map of Deke Island showing the distribution of surface sediments. Elevation datum is lower low tide in the lagoon.



scattered medium pebbles. In addition to these shore-parallel zones, there is a zone composed of sand with coarse to medium pebbles that cuts across the island. This zone probably represents a now filled tidal pass that separated two smaller islands that merged to become Deke.

Seven profiles across the island (location shown by the map of Figure 31 and profile shown in Figure 32) show a strong correlation between grain size and elevation. In general, the coarsest grains are found at higher elevations close to the ocean side of the island and the finer-grained sediments are found at lower elevations along the lagoon margin.

### Stratigraphic Sections

Two types of sedimentary deposits are recognized in measured sections within stratigraphic test pits. The first type is characterized by a sharp lower boundary, a large mean grain size, and a small sand percentage. The second type is a layer of sediments which is finer grained and better sorted; its lower boundary is gradational and the upper boundary is a truncation surface on which sediments of the first type are deposited. The thickness of these units varies from 1 to 3 feet. It is thought that the first type of sediments represents the deposits of large waves that washed over the island during intense storms; the second type, on the other hand, is a more normal sequence of beach sediments deposited between major storms.

A total of five stratigraphic sections were measured on Deke Island. Two of these Pz1 and Pz2, are uniform through the section: each records a single wash-over event that deposited cobbles, coarse pebbles, and sand. At B5, and the stratigraphic test pit at A6, there is evidence of an alternation of three wash-over events with three periods of normal beach development. The section measured at B6 shows two coarse pebble and sand wash-over events and three periods of beach development. Graphic logs and detailed descriptions are presented in the Appendix.

### Subsurface Geologic Investigation

Results of the core drilling operations and the reef flat hard layer sampling program are presented below. As noted in the Appendix table of contents, detailed descriptions of both core samples and slab sections are listed in the Appendix; general descriptions are given in this section.

### Core Drilling

Drilling into Deke and the reef complex upon which it sits was not an easy task. Severe caving and hole collapse slowed the operation to the point that more time was consumed to prepare a site and complete the borehole than was initially anticipated. Therefore, only three deep drill sites were successful using the pipe-mounted drill rig. Each of these sites required considerable effort to prepare. First, a pit was hand dug to the hard layer. Next, a PVC pipe was cemented to the hard layer to prevent leakage. The hole was then partially backfilled and a length of

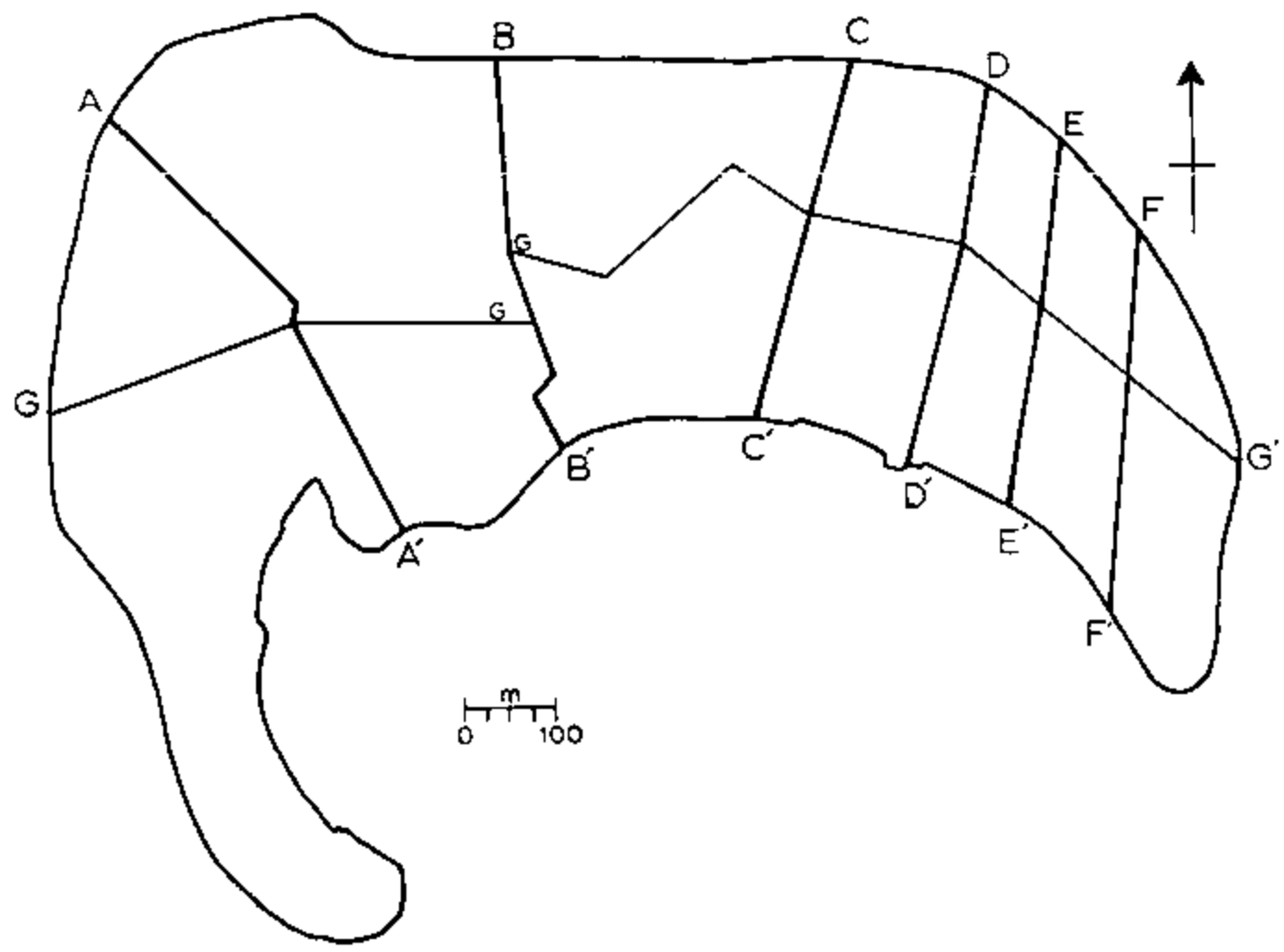


Figure 31. Map of Deke Island showing the traverses used in topographic profiling and surface sediment sampling. Figure 32 shows the results of the mapping exercise.

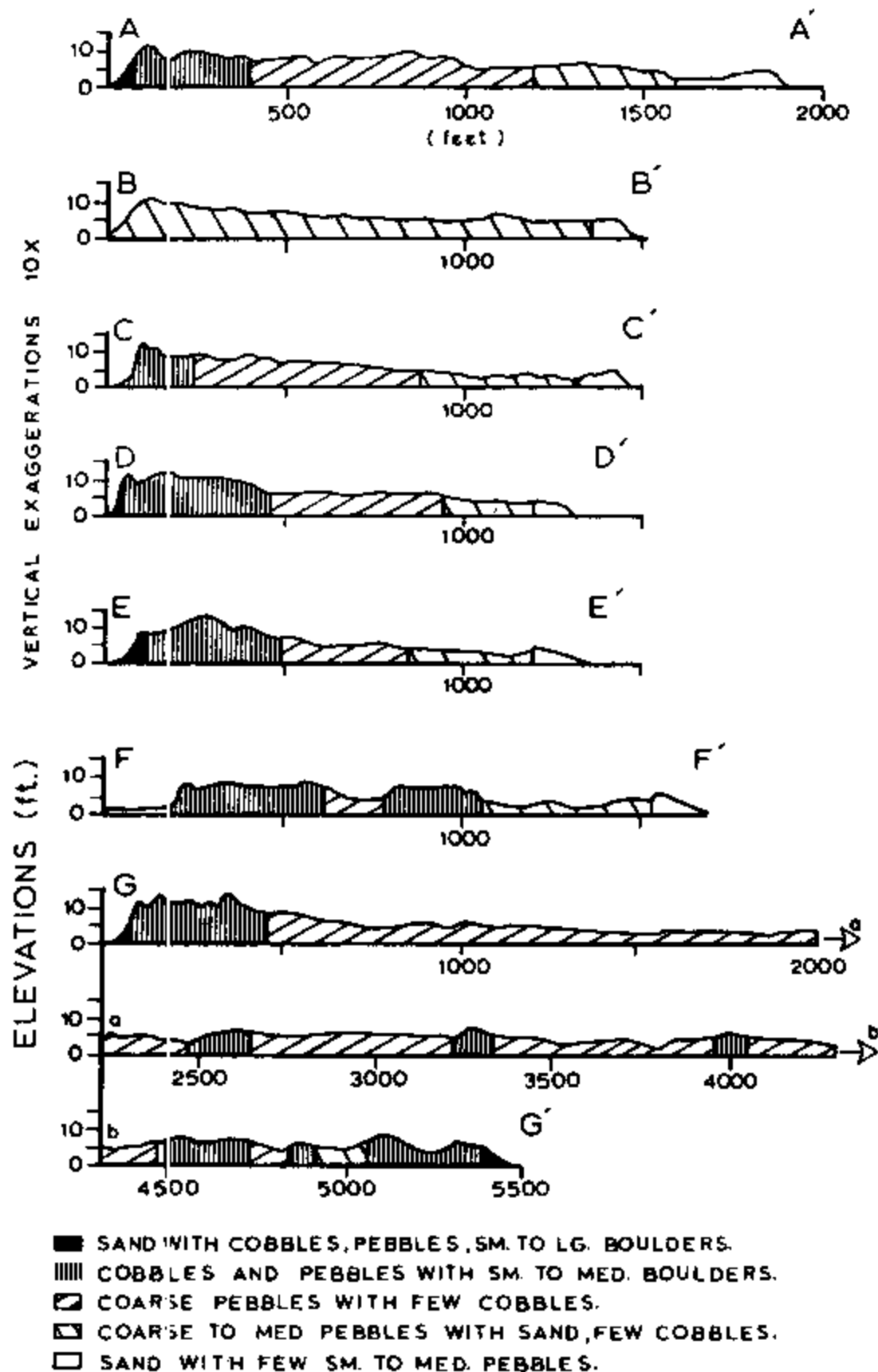


Figure 32. Profiles showing topographic cross sections and sediment-size zones. Refer to Figure 31 for cross-section locations.

steel pipe (threaded at the top end) was connected to the plastic casing. Portland-type cement was used to seal the joint between the two lengths of pipe and the remainder of the hole. After allowing the cement to cure, the site was finally ready for drill installation. About three days were necessary to complete the preparations of a single site.

Drilling time at each site was about 1.5 working days. This included shut-down time necessary for the replenishment of the water supply (usually supplied by filling drums at the shoreline and rolling them to the drill site). Core recovery was about 25% at site DS3 and about 22% at the others. Most of this percentage of recovery is attributable to excellent recovery from the hard layer; corad returns below the hard layer were generally poor to occasionally nonexistent. Total hole depths are 70 feet, 80 feet, and 25 feet at DS3, DS4, and DS5, respectively.

Summary logs including drilling characteristics are shown in Figure 33. In general, the same subsurface lithology was encountered at each of the three sites. About 3 to 5 feet of the hard layer was drilled, beneath which the units seemed to be unconsolidated to poorly consolidated foraminiferal sand and gravel-sized reef-derived rubble with occasional coral heads in probable growth position. Drilling characteristics within certain intervals suggest the presence of alternating hard and soft zones. These zones, from what core was retrieved, appear to be associated with layers of coralline algae and encrusting coral types and layers of unconsolidated sand or gravel. Lithology and composition of the hard layer appears to be the same at all three sites and also is similar in character to samples from the reef flat (described below). In general, the hard layer is composed of reef-derived coral and coralline algal rubble, foraminifera tests and fragments, mollusk shell fragments, and echinoid spines. There is an abundance of encrusting Gypsina vesicularis on coral fragments. Associated with Gypsina is a ramose form of Homotrema rubrum, which is characteristic of reef flat environments. Also, there is an abundance of Calcarina spengelri, the tests of which tend to be loosely packed and crudely bedded. Mixed with Calcarina, but to a lesser extent, is Baculogypsina sphaerulata. Baculogypsina disappears about 10m below the hard layer, which suggests that it is a more recent reef component. Calcarina and Baculogypsina are characteristic of reef-flat environments with densest growth in the outer reef-flat subzone. Other uncommon foraminifera associated with the hard layer are Sporadotrema cylindricum, Heterostegina depressa, Miniacina miniacina, Robulus sp. and Amphistegina lessonii. These foraminifera are common in shallow-water environments, either reef-flat or reef-margin subzones. Another conspicuous component of the hard layer assemblage is the calcareous alga Porolithon onokae. This species is very common along the reef margin, but can have a wider depth distribution. The various constituent particles of the hard layer are well cemented forming a relatively dense unit with little apparent effective porosity and presumably very low permeability. The abundance of cement within the fabric of the hard layer tends to rapidly decrease with depth, particularly within the foraminiferal sand below the hard layer of typical composition (readily seen in the core of DS5).

At depths below the land surface of about 55 feet in DS3 and 48 feet in DS4 a distinct change in particle constituents occurs. Plates of the green algae Falimeda become very abundant and make up a large percentage of

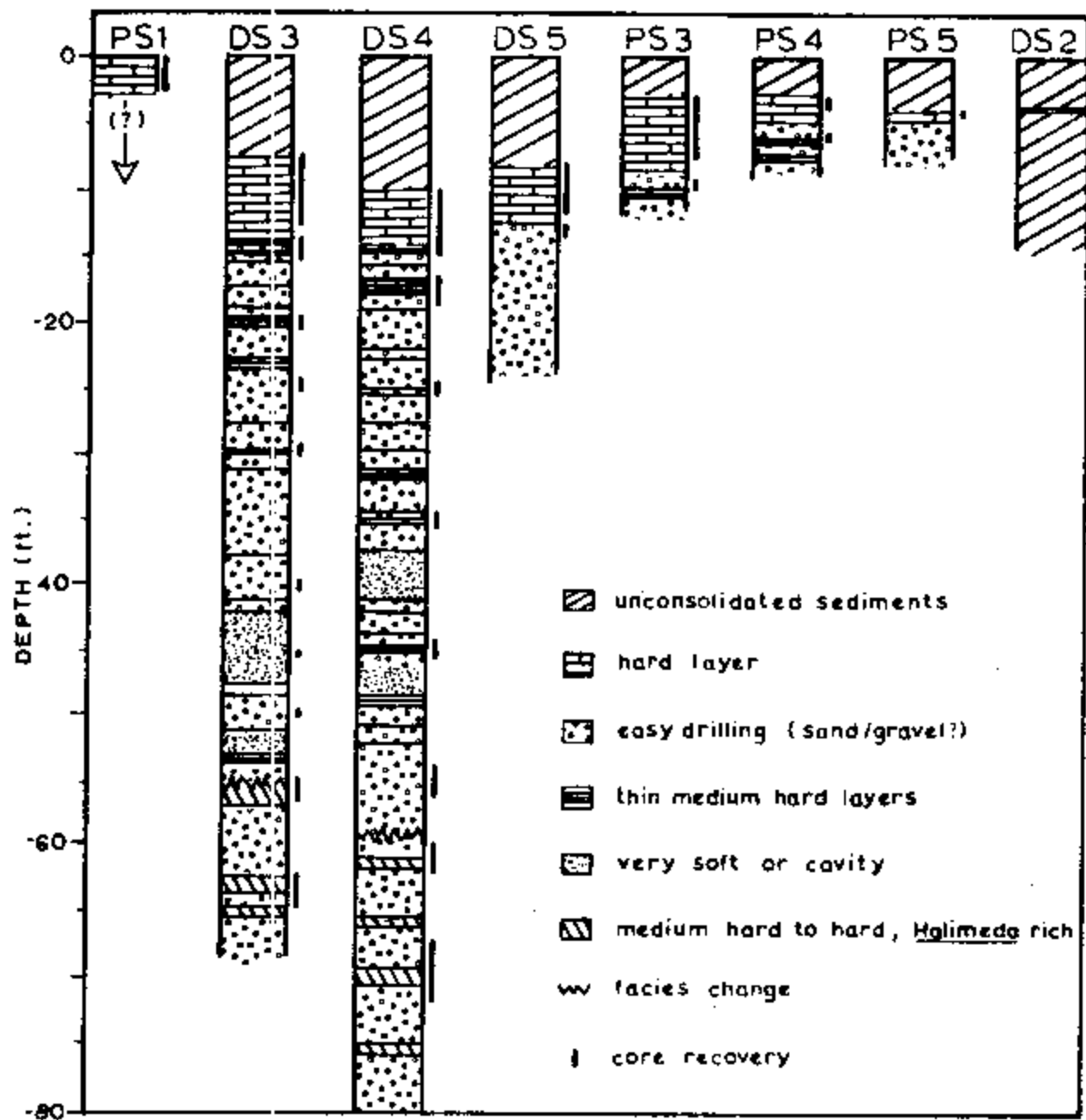


Figure 33. Geological and drilling logs for all cored boreholes across Deke Island. All depths are relative to ground surface.

the sediment. This unit, or, as it is named here, Halimeda facies, extends past the bottom of the two deeper boreholes. It is interesting to note that a similar facies was encountered during the drilling operation on Bikini Atoll (Emery et al., 1954) at depths ranging from 32 to 53 feet. In fact, other units sampled during the Bikini work are remarkably similar in character and vertical position to those described by this study.

The Halimeda facies is composed of biota components which suggest deposition in quieter waters (either lagoon or reef-flat terrace) compared with the hard-layer assemblage. Gypsina is very common and has a "leafy" or layered growth pattern with fine "mud" deposition between layers. This growth form is characteristically found below wave base. There is a large amount of fragmented Homotrema and encrusting Miniacina. Halimeda plates have thin encrustations of Gypsina. This foraminiferal distribution also occurs in lagoon environments or on terraces below wave base (20-30m). Other uncommon foraminifera found in the Halimeda facies are Sporadotrema, Sorties, Quirqueloculina, Carpenteria utricularis and few relict planktonic foraminifera. There are a few ostracod shells and fragments of Porolithon. Unfortunately there are insufficient foraminiferal or other diagnostic biotic components in the Halimeda facies to determine the original environment of deposition.

A number of short cores were obtained through the use of the Packsack drill. This rig required far less effort in terms of site preparation and thus less time was involved in its application. Cores were taken from the hard layer with one exception; one site (PS1) was located near DS3 on the reef flat. Depths ranged from a few inches to about 6 feet with relatively good core recovery. Little difference was observed between Packsack cores and those recovered from the hard layer at the deep-drill sites.

From results of the core drilling in general, it appears that the hard layer thins from the ocean shoreline toward the lagoon (Figure 34). At DS3 the hard layer is 5.5 feet thick; however at Pz3, near the lagoon shore, the thickness is only a few inches. Intermediate thickness values for Pz1 and Pz3 are 3.2 feet and 1.5 feet respectively. Presumably, the hard layer disappears or laterally grades into a unit with a less indurated character.

#### Reef-Flat and Hard-Layer Samples

Reef-flat and hard layer samples are described in detail in the Appendix. A comparison of reef-flat and hard-layer sample descriptions indicates a similar if not same origin for both sample sets. An additional comparison between surface and cored material indicates deposition within the same environment. The primary conclusion to be drawn is that Deke Island was depositively constructed upon the hard substrate of the reef flat.

#### Geophysical Surveys

Results from the application of two surface-based geophysical methods (seismic refraction and earth resistivity) are presented below. In general, the application of these methods produced information related to

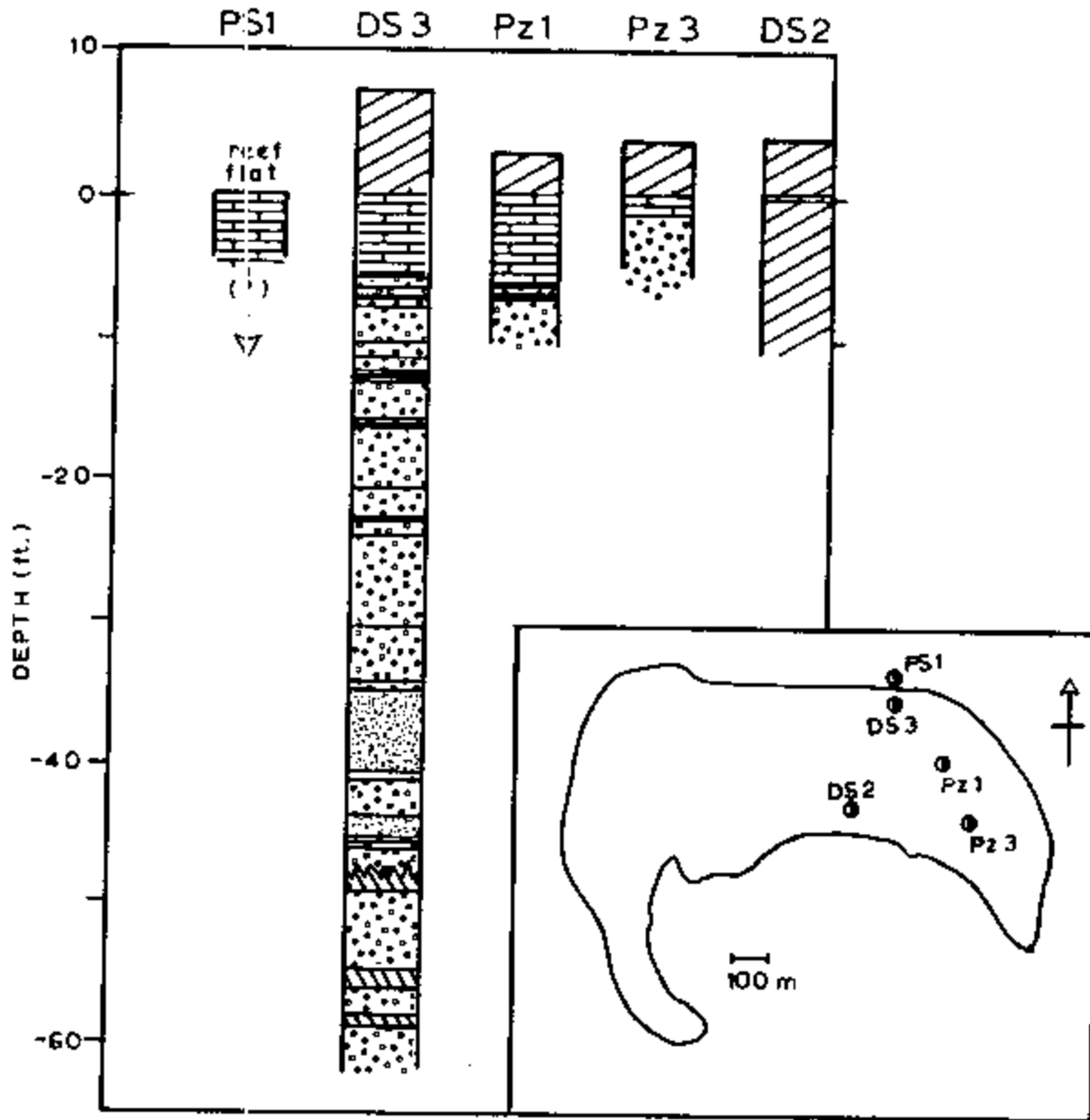


Figure 34. Geologic logs of selected cored boreholes across Deke Island. Note the lagoonward thinning of the hard layer.

the physical properties of the aquifer and quality of the groundwater within the upper 100 feet of the atoll complex. Where possible the results of the surveys were calibrated with ground-truth data obtained from core drilling operations and from field observations.

### Seismic-Refraction Profiling

Some 48 seismic lines were established across the island. Results, in the form of refractor depths and layer velocities, are presented in Tables 9 and 10. Table 9 lists values for those lines which indicated a two-layer subsurface system. These seismic layers correspond to the sediment comprising the island and to the underlying back-reef associated depositional environment of the atoll complex. Table 10 lists analytical results for those lines which exhibited the presence of a third layer at depth. Again the uppermost refractor unit corresponds to the actual sediment zone of the island and the second seismic unit represents the upper portion of the back-reef environment including the hard layer. The third refractor unit is also part of the reef complex; however, it appears that this unit possesses somewhat different properties than the overlying layer. Seismic velocities are quite variable in distributions and refractor surfaces are highly irregular in topographic relief. Table 11 lists summary statistics for seismic velocities determined by the computer analysis of the various seismograms.

Seismic velocities measured for the top layer averaged 1372 ft/sec (standard deviation of 209 ft/sec) and are typical of relatively dry unconsolidated sediments. This material, of course, is readily observed on the ground surface and in the side walls of test pits.

Of greater interest are the velocities measured in the underlying layers. The average velocity for layer 2 is 5178 ft/sec and the range is from 4692 to 6033 ft/sec. However, the standard deviation of 313 ft/sec indicates a relatively small spread of values suggesting fairly uniform density characteristics across the areal extent of the unit. From velocity information, it appears that this unit on the whole is composed of unconsolidated to possibly very weakly cemented carbonate sediments. There is an exception; the top portion of layer 2 over much of the island is occupied by the hard layer. Although relatively thin, as compared to the back-reef complex, the hard layer is a well indurated zone situated at about sea level or just beneath the sediment comprising the island and probably has an affect on seismic velocity measurements. However, at this point in the investigation, little information is available to adequately evaluate these affects.

Results from 35 of the 48 seismic lines indicated the presence of a 3-layer subsurface system, particularly beneath the northern half of the island. The average velocity for this third refractor unit is 7719 ft/sec with a standard deviation of 1850 ft/sec. As indicated by the standard deviation, velocity values range over a considerable interval, specifically from 5128 ft/sec (similar to layer 2 values) to 12361 ft/sec (4 velocity values in excess of 10000 ft/sec). This velocity spread indicates that layer 3 may be composed of material similar to layer 2 in places while other areas may be composed of relatively dense well-cemented material



Table 9. Seismic velocities determined from the computer analysis of first arrival times for 2-layer seismograms. Velocities are in feet/second.

Seismic-Line Designation	Layer 1	Layer 2
BFT-1	1457	5167
BFT-2	1438	5378
BWT-2	1847	4966
CT-1	1538	5122
CT-2	1479	5275
FE-1	1500	5213
FE-1A	1774	4995
FE-2A	1307	5271
JT-1	1522	4997
TPT-1	1310	4967
TPT-2	1363	4930
TPT-3	1266	5088
TPT-4	1398	5867
TT-1	1431	4962
TT-2	1131	5550

Table 10. Seismic velocities determined from the computer analysis of first arrival times for 3-layer seismograms. Velocities are in feet/second.

Seismic-Line Designation	Layer 1	Layer 2	Layer 3
BST-1	1497	5110	6343
BST-2	1443	4936	12074
BST-3	1486	5530	7432
BWT-1	2043	4913	6013
CL-1	1848	5210	9338
DS3CT	1273	5439	8720
DS5CT	1228	5096	7146
EPT-1	1435	4906	6852
EPT-2	1558	5190	7274
EPT-3	1484	4954	9536
EPT-4	1281	4734	6654
FE-2	920	5335	6874
FE-3	887	5176	8125
IR-1	1335	5066	9299
IR-2	1163	5239	8213
LW-1	1358	4692	6827
LW-2	1343	4847	10259
NT-1	1320	4922	7155
NT-2	1331	5343	6927
NT-3	1428	5881	8453
NT-4	1303	6033	9810
PT-1	1218	4908	5373
PT-3	1208	4846	5837
ST-1	1329	5111	5938
ST-2	1119	4743	5802
ST-3	1341	5437	7106
ST-4	1232	5665	6254
ST-5	1243	4924	5434
ST-6	1359	5048	5973
THC-1	1621	5857	10250
THC-2	1616	5124	8538
THC-3	1259	5107	7108
THC-4	1379	5227	9743
THC-5	1096	5633	12361

Table II. Summary statistics for seismic velocities determined by computer analysis of 2- and 3-layer seismograms. Dimensional parameters are in feet/second. Forty-nine seismic refraction lines were run across Deke.

Parameter	Layer 1	Layer 2	Layer 3
mean	1372	5178	7719
standard deviation	209	313	1850
minimum	887	4692	5128
maximum	2043	6033	12361*

\* 4 velocities for layer 3 are in excess of 10,000 ft/s.

(i.e., limestone). Core drilling in an area where the seismic record indicated the presence of a third layer at velocities somewhat higher than the average retrieved samples of poorly consolidated reef-derived sediments, not unlike layer 2 in physical make up. Thus, it is difficult to say with certainty the real nature of layer 3, particularly in areas where seismic velocities exceed those typical of poorly indurated material.

Because the top of layer 2 is located at about sea level, the thickness of layer 1 is given by the ground-surface elevation. Thickness values for layer 2, however, are not as easily determined. Where present, the top of the third refractor appears to be highly variable in elevation ranging from a few feet to as much as 100 feet or more below sea level. Therefore the thickness of layer 2 is equally variable.

An advantage to applying computer analysis to seismic-refraction data is the ability to easily process field information obtained from overlapped or coupled lines. In addition to smoothing the input data and calculating averages or characteristic layer velocities, a continuous profile of depths to the refractors is provided for the length of the coupled lines. Thus, by plotting these various refractor depths on distance - elevation graphs a pictorial representation of the subsurface seismic structures can be obtained. Figure 35 shows five seismic profiles across Deke, three are in a more or less north-south direction and the remaining two run the length of the island.

From the profiles of Figure 35, the highly irregular topograph of the top of layer 3 is readily apparent. Profiles D and E show a discontinuity in the third layer refractor near the lagoon shoreline. Seismograms for lines run within the western sector of Deke, for the most part, did not indicate the presence of a third layer. Although there is no data available, it is possible that either the third layer grades into sediments of the second layer or the third layer disappears at a depth beyond the detection limits of the seismograph using the hammer and steel plate as the energy source.

Additional points that are emphasized by the profiles of Figure 35 are (1) the variability of layer 3 velocities and (2) the uniformity of layer 2 velocities. From the areal distribution of third-layer velocities (Table 10) it appears that higher values tend to be associated with the ocean side beneath the island. A number of reasons are possible to explain the apparent velocity distribution; however, the most likely is a change in facies (depositional environment) from the ocean side toward the lagoon. Although the field evidence is slim, this contention is partly validated by the seismic behavior of the layer 3 refractor along longitudinal profiles, that is, the disappearance of the third layer. The uniform velocity distribution within layer 2 suggests that the lithology of the second layer changes very little across the island. However, based on data from drilling sites along the ocean shore and from stratigraphic test pits close to the lagoon, there does appear to be some component difference between samples, especially those below the hard layer and those where the hard layer is absent.

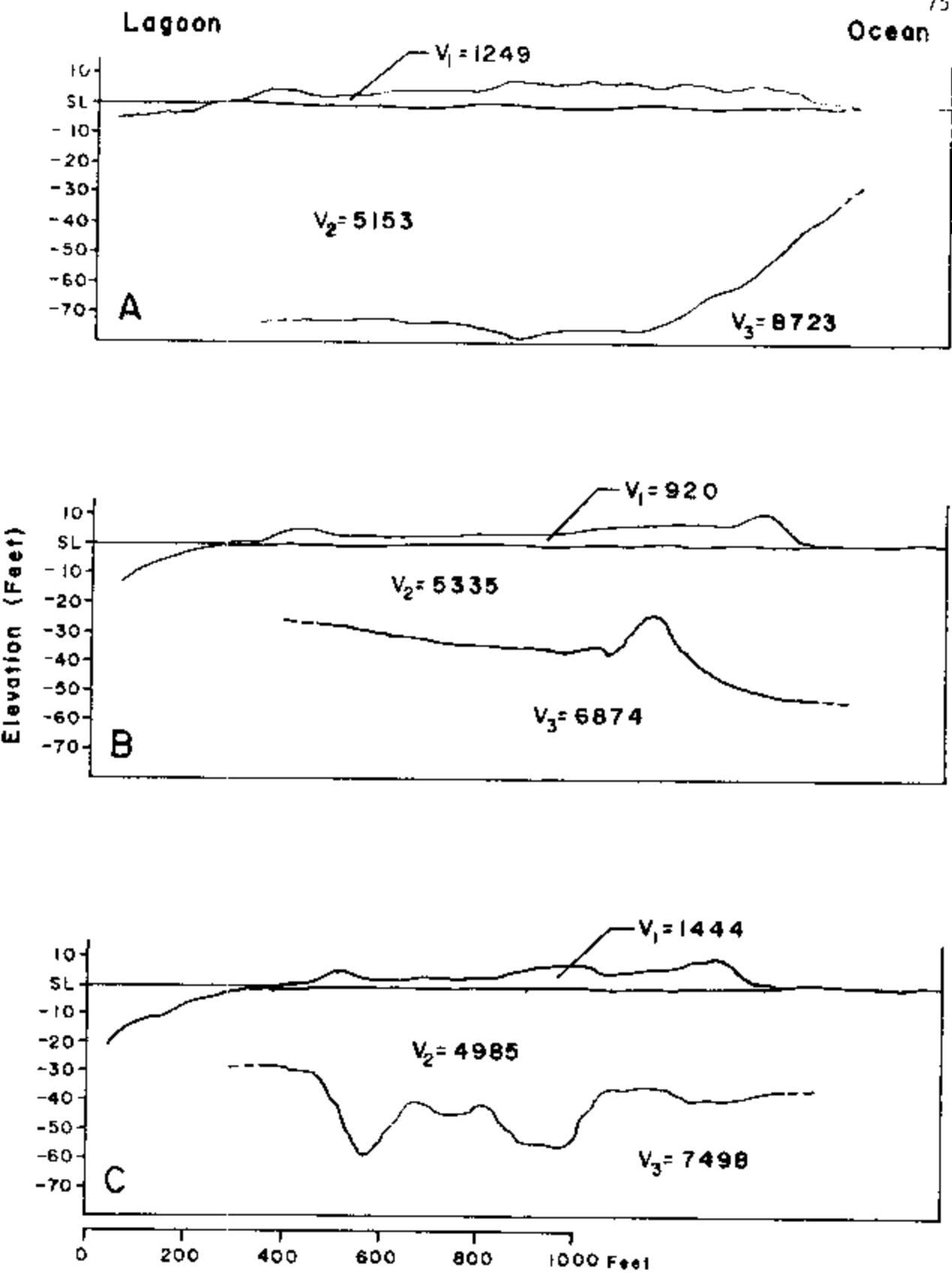


Figure 35. Seismic profiles across Deke Island. Profiles constructed from layer-velocity and depth-to-refractor determinations for coupled seismic lines. Insert map shows the locations of the various profile lines.

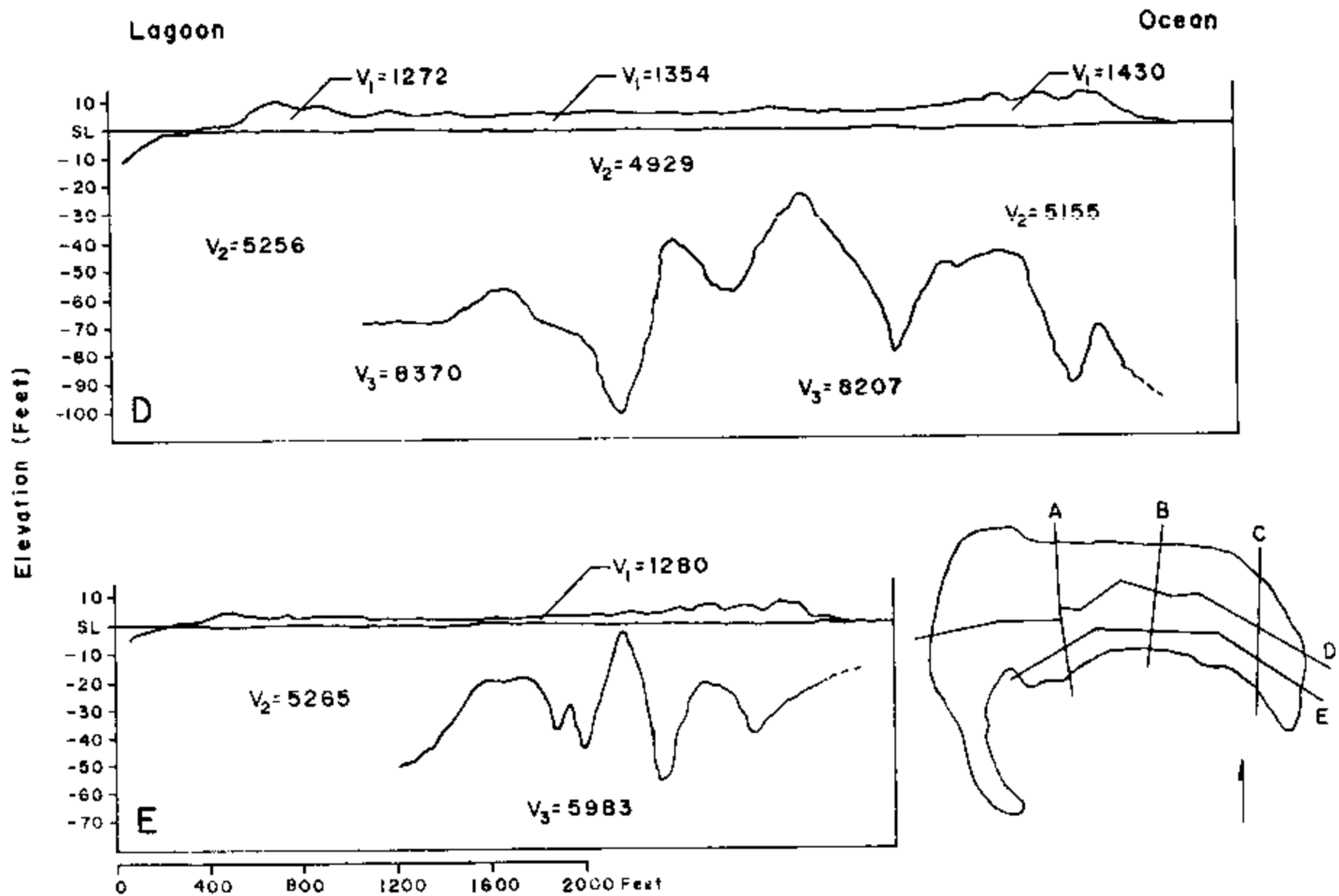


Figure 35. Continued.

## Earth-Resistivity Soundings

Results from the trial-and-error curve matching of computed vertical electrical sounding (VES) curves with field VES curves are listed in Table 12. These results indicate the presence of four distinct layers of differing electrical properties. Layer 1 corresponds in areal distribution and thickness to the uppermost seismic refractor (and the sediment mosaic of the island). However, the remaining layers do not correlate with those defined by seismic shooting. The reason is, of course, the methods are measuring different physical properties of the earth medium. Resistivity layers 2, 3, and 4 represent respectively, the freshwater portion of the lens, the zone of mixing between fresh and underlying saltwater, and the salt water beneath the lens.

From the resistivity results, it appears that the freshest portion of the lens is about 8 to 11 feet thick but may be as much as 15 feet in certain areas. A cored borehole, located along the north shoreline, penetrated the lens and bottomed in the salt-water region. Conductivity profiles obtained from this borehole indicate a fresh-water thickness of some 14 feet and a mixing zone (resistivity layer 3) of comparable thickness. Therefore, it appears that a significant quantity of freshwater is available from the lens flow system of Deke.

## Water Quality

Limited surveys of ground-water quality were made at a number of wells. Specific conductance was the primary water quality parameter used to characterize groundwater. Additionally, estimated chloride-ion content of discrete water samples and relative salinity profiles from deeper observation wells were calculated from specific conductance data. Other water-quality parameters measured on a more limited basis were temperature, chloride ion (probe), pH, alkalinity, calcium hardness (as mgCa/l and mgCaCO<sub>3</sub>/l) and total hardness. These water-quality parameters were measured in surface groundwater at various sites between March 17 to 20, 1984 (Table 13). There were 12 specific conductance profiles taken in DS3 from March 6 to 18 (Table 14) and 4 profiles taken in DS4 from March 15 to 18, (Table 15). Relative salinities of groundwater at depths below the water table were calculated from DS3 specific conductance profile data (Table 16).

A contour map of groundwater chloride-ion concentration was generated from the March 17 specific conductance and estimated chloride data (Table 13). The map shows chloride distribution in groundwater which overlies the hard layer (Figure 36). There are three areas of freshwater distributed along the lagoon side of the island. These areas are approximately located along the edge of the hard layer. A contour map of total hardness (Figure 37) show a similar pattern as seen for chloride concentrations. Specific conductance readings taken on March 18 were measured at an extreme high tide. These measurements were distinctly higher when compared to March 17 readings, which were taken on a rising tide (Table 13). However, a contour map of these higher conductance readings shows a similar pattern as seen in the chloride map (Figure 36).

Table 12. Layer thickness and resistance determined from matching field vertical electrical sounding (VES) curves with computer-generated VES curves. Computer program by Zohdy (1974).

Station No.	Elev (ft)	Layer 1		Layer 2		Layer 3	
		Thickness (ft)	ohm-ft	Thickness (ft)	ohm-ft	Thickness (ft)	ohm-ft
1	5.0	6.0	1415	11.0	500	8.0	20
2	5.5	2.3	1683	7.0	650	11.0	25
3	8.6	9.0	1667	*25.0	800	15.0	10
4	7.1	6.0	1567	*20.0	800	10.0	10
5	4.1	4.0	1550	6.0	700	25.0	40
6	4.7	3.0	1016	7.0	300	12.0	30
7	8.5	7.0	925	14.0	2000	7.0	10
8	6.0	5.5	2383	16.0	2100	25.0	60
9	3.7	5.5	967	8.0	300	15.0	20
10	2.8	2.0	765	11.5	425	7.0	9
11	7.0	6.5	2567	10.0	2500	20.0	60
12	6.5	6.0	2675	8.0	3100	25.0	4
13	4.5	3.5	900	8.0	350	10.0	30
14	5.2	5.0	1450	10.0	2400	5.0	10
15	6.3	5.3	1400	10.0	900	20.0	20
16	4.7	4.0	600	7.0	400	8.0	20

Layer 1 - Dry unconsolidated sediment comprising Deke.

Layer 2 - Fresh-water lens.

Layer 3 - Transition zone.

\* Results are of suspect.



Table 13. Water quality data for samples collected from observation wells.

Site	Time	March 17, 1984			March 18, 1984							March 20, 1984		
		Temp (c°)	S. Cond. ( $\mu$ mhos/cm)	Chloride* (mg/l)	Time	Temp (c°)	S. Cond. ( $\mu$ mhos/cm)	pH	Alkalinity (MgCaCO <sub>3</sub> /L)	Chloride** (mg/l)	Ca Hardness (mgCaCO <sub>3</sub> /L)	Ca Hardness (mgCaCO <sub>3</sub> /L)	T. Hardness (mgCaCO <sub>3</sub> /L)	Chloride** (mg/l)
A 1	1645	27.3	1200	320										6.4
A 2	1642	27.3	1750	305										9.5
A 3	1650	27.3	1275	335	1745	25.8	2150	7.30	390	17.8	141	320	412	10.0
A 4	1657	26.4	1100	290	1740	26.4	1600	7.69	250	14.0	98	244	304	9.8
A 5	1625	26.5	1000	260	1710	26.4	1600	7.52	280	13.3	101	252	316	
B 1	1350	26.8	1125	300										6.4
B 2	1630	26.8	1350	360										310
B 3	1330	28.0	1280	335	1755	27.3	1700	7.45	370	14.2	106	264	392	8.0
B 4	1636	26.8	900	235	1720	26.4	1500	8.25	210	13.5	55	136	180	6.2
F 1	1625	26.5	1000	260	1710	26.8	1750	7.85	290	17.2	69	172	240	
C 1	1618	27.4	1850	500										36.5
C 2	1535	26.8	1100	290										5.8
C 3	1358	26.8	1100	290										5.6
C 4	1610	27.6	1200	320										6.8
D 2	1413	27.5	1125	300	1703	27.8	2750	7.40	310	32.1	106	264	348	29.0
D 3	1420	27.0	480	<100	1700	26.2	1900	7.88	250	11.6	85	212	280	
D 4	0800	-	1350	360	1515	28.3	3550	7.32	250	230.	112	280	424	
E 1	1426	26.5	1150	305										9.7
E 2	1432	27.0	925	240	1622	26.8	2250	7.70	250	27.5	90	224	292	22.2
E 3	1436	27.5	1000	260	1620	26.4	2250	7.60	220	16.5	77	192	216	7.2
E 4	1443	26.8	1300	350	1630	26.3	2550	7.28	300	25.0	133	332	460	34.1
E 5	1449	27.5	1275	335	1635	27.0	21800	7.40	340	17.8	104	260	348	7.1
Pz1p <sup>1</sup>	1511	28.0	2650	750	1600	26.8	4550	7.25	250	370.	98	244	432	
Pz1s <sup>2</sup>	1511	-	1850	500	1600	27.1	3650	-	-					
Pz2 <sup>3</sup>	1455	28.5	6500 <sup>4</sup>	1900	1615	28.0	2150	10.40 <sup>3</sup>	-	44.9	32	80	104	26.2
Pz3c <sup>4</sup>	1520	-	34500 <sup>4</sup>	11500	1650	27.2	7500	-	-					460
Pz3s <sup>4</sup>	1520	-	2150	595	1650	27.2	3380	7.52	280	10.5	96	244	352	

\* Cl<sup>-</sup> concentration determined by graphical method (conductance vs. Cl<sup>-</sup> graph).

\*\* Cl<sup>-</sup> concentration determined by specific-ion electrode method; samples taken from water surface.

1 - from hard layer

2 - on top of hard layer

3 - probably caused by cementing stands pipe in previous 48 hours.

4 - seawater introduced from drilling.

Table 14. Depth related specific-conductance and estimated chloride-ion data for DS3.

Depth below max water table (ft)	Profile 1 Date: 3-6-84 Time: 0900		Profile 2 Date: 3-7-84 Time: 1330		Profile 3 Date: 3-9-84 Time: 0930		Profile 4 Date: 3-13-84 Time: 0830		Profile 5 Date: 3-14-84 Time: 0810		Profile 6 Date: 3-14-84 Time: 1730	
	S.Cond.	Chl**	S.Cond.	Chl	S.Cond.	Chl	S.Cond.	Chl	S.Cond.	Chl	S.Cond.	Chl
1												
2												
3												
4	2725	705	120	>100	1800	385	6500	2005	3900	1110	2050	470
5			3400	935					6500	2005	2050	470
6	2725	705	3425	945	1950	435	5250	1575	6500	2005	2025	460
7			3425	955					6250	1920	2025	460
8	2750	710	3050	955	2000	455	2450	610	3200	865	2025	460
9			2450	610					2450	610	2100	490
10	2400	590	2275	550	2100	490						
11									2300	555	2200	520
12	2300	555	2275	550	2200	540	2350	575	2250	575	2250	540
13							2350	575				
14	2600	660	2350	575	3000	800	2450	610	2400	590	2600	660
15							2500	625				
16	2950	780	2650	675	2550	645	2500	625	3100	830		
17			3050	815			2650	675				
18	5500	1660	3650	1020	1000	2175	3500	970	3000	830	6500	2005
19							4500	1315	3600	1005	7500	2350
20	7050	2195	6060	1835	13000	4245	8250	2610	8000	2520	12000	4245
21			9050	2885			10300	3315	12500	4075	17000	5625
22	16000	5280			20000	6660	18000	5970	17000	5625	20000	6660
23	16500	6835					20000	6660	19500	6490	22500	7325
24	25000	8535			26250	8515	25500	8560	25000	8365	26750	8990
25							29000	9765	27500	9745	32500	9935
26					30000	10110	30250	10195	29250	9850	30250	10195
27							31250	10540	30250	10195	30500	10280
28					31000	10455	32000	10800	31750	10540	30750	10370

\* S. Cond. = Specific conductance, umhos/cm.  
 \*\* Chl. = Estimated chloride (mg/l), based on specific conduct.

Table 14. Continued

Depth below max water table (ft)	Profile 7 Date: 3-15-84 Time: 0830		Profile 8 Date: 3-16-84 Time: 0830		Profile 9 Date: 3-17-84 Time: 0800		Profile 10 Date: 3-17-84 Time: 1545		Profile 11 Date: 3-18-84 Time: 1115		Profile 12 Date: 3-18-84 Time: 1515	
	S. Cond.	chl	S. Cond.	chl	S. Cond.	chl	S. Cond.	chl	S. Cond.	chl	S. Cond.	chl
1											3500	970
2							2175	515			3500	970
3							2225	530			3550	990
4	185	<100	400	<100	dry		2350	575	305	<100	3550	990
5	2860	730	1500	280	1350	230	2375	580	1300	<100	3575	995
6	2975	790	2400	590	2300	555	2375	580	2300	555	3575	995
7	3175	860	2550	645	2300	555	2400	590	2375	580	3575	995
8	2750	710	2575	650	2325	565	2400	590	2375	580	3600	1005
9	2450	610	2475	615	2450	610	2375	580	2450	610	3600	1005
10	2400	590	2475	615	2475	615	2400	590	2475	615	3600	1005
11	2375	580	2500	625	2500	625	2425	600	2500	625	3650	1020
12	2400	590	2525	635	2600	660	2475	615	2525	635	3700	1040
13	2400	590	2600	660	2875	755	3250	885	2700	695	4400	1175
14	2400	590	2600	660	2875	755	3250	885	2700	695	4400	1180
15	2450	610	2725	705	3000	800	3500	970	2800	730	4500	1315
16	2500	625	2750	710	3250	885	3575	995	2850	745	4550	1330
17	3000	800	3000	800	3100	830	5500	1660	3000	800	5000	1490
18	3500	970	3600	1005	4700	1385	8000	2520	3400	935	7800	2455
19	6000	1835	8000	2520	6250	1920	8750	2780	4050	1160	8500	2695
20	800	2520	10000	3210	11750	3820	13000	4245	8250	2610	13500	4420
21	12500	4075	14000	4590	15750	5195	17000	5625	12250	3990	18000	5970
22	17000	5625	18000	5970	19000	6315	19750	6570	17000	5625	20000	6660
23	19500	6490	20000	6660	20750	6920	23000	7695	19250	6400	23250	7955
24	24750	8300	26000	9730	27000	9075	28000	9420	24500	8215	28000	9420
25	27500	9245	28000	9420	29000	9765	30000	10110	27750	9335	31000	10455
26	29500	9935	29000	9765	30750	10377	31300	10455	30000	10110	32000	10800
27	30000	10110	30000	10110	31250	10540	31500	10625	30750	10370	32500	10970
28	3025	10280	32000	10800	31500	10625	31500	10625	3100	10455	32500	10970

\* S. Cond. = Specific conductance,  $\mu\text{mhos}/\text{cm}$ .\*\* chl = estimated chloride ( $\text{mg}/\text{l}$ ), based on graphical data.

Table 15. Depth related specific-conductance and estimated chloride-ion data for DS4.

Depth below max water table (ft)	Profile 1 Date: 3-15-84 Time: 0845		Profile 2 Date: 3-16-84 Time: 0805		Profile 3 Date: 3-17-84 Time: 0740		Profile 4 Date: 3-18-84 Time: 0912	
	S.Cond.	Chl	S.Cond.	Chl	S.Cond.	Chl	S.Cond.	Chl
1	205	<100	118	<100	dry		dry	
2	2075	480	2000	455	190	<100	145	<100
3	2050	470	2150	505	1900	420	1800	385
4	2125	495	2375	580	2450	610	2300	555
5	6500	2005	6900	2145	8800	2800	7500	2350
6	12000	3900	13750	4505	16000	5280	15750	5195
7	12750	4160	14000	4590	16250	5365	16500	5455
8	12750	4160	14000	4590	16250	5365	16500	5455
9	12750	4160	13750	4505	16250	5365	16500	5280
10	13250	4335	14000	4590	16750	5540	16250	5365
11	15250	5025	16000	5280	18000	5970	17000	5625
12	17500	5800	16250	5365	18000	5970	17750	5885
13	19250	6400	17000	5625	20000	6660	18000	5970
14	21000	7005	19000	6315	24000	8040	18500	6145
15	21250	7090	20000	6660	24500	8215	19000	6315
16	22000	7350	20750	6920	25000	8385	19250	6400
17	22000	7350	21250	7180	25500	8560	20000	6660
18	22000	7350	21250	7180	25500	8560	20000	6660
19	22250	7435	21500	7265	25500	8560	20000	6660
20	22250	7435	21750	7265	25500	8560	20250	6745
21	22250	7435	22000	7350	25750	8645	20750	6875
22	22250	7435	22000	7350	25750	8645	20500	6835
23	22250	7435	22000	7350	26000	8730	20500	6835
24	22250	7435	22000	7350	26000	8730	20500	6835

\* S. Cond. - Specific conductance,  $\mu\text{mhos/cm}$ .

\*\* Chl. - estimated chlorine ( $\text{mg/l}$ ), based on graphical data.

Table 16. Relative-salinity profile data for DS3. See Appendix for individual profile plots.

Profile	Number of Points	Slope of line	* 1% Relative Salinity Depth (ft)	** 50% Relative Salinity Depth (ft)	Correlation Coefficient
1	6	0.1512	13.3	21.3	0.9568
2	4	0.3167	13.5	29.0	0.9617
3	6	0.1609	13.0	20.8	0.9729
4	9	0.1237	14.6	20.6	0.9877
5	10	0.1300	14.5	20.8	0.9941
6	10	0.1539	12.8	20.3	0.9895
7	10	0.1487	13.9	21.1	0.9905
8	10	0.1462	13.7	20.8	0.9929
9	11	0.1581	13.0	20.7	0.9759
10	12	0.1778	12.7	21.4	0.9746
11	10	0.1430	14.1	21.1	0.9798
12	13	0.1824	14.5	23.5	0.9515

\* depth below the water table of groundwater at 1% relative salinity

\*\* depth below the water table of groundwater at 50% relative salinity

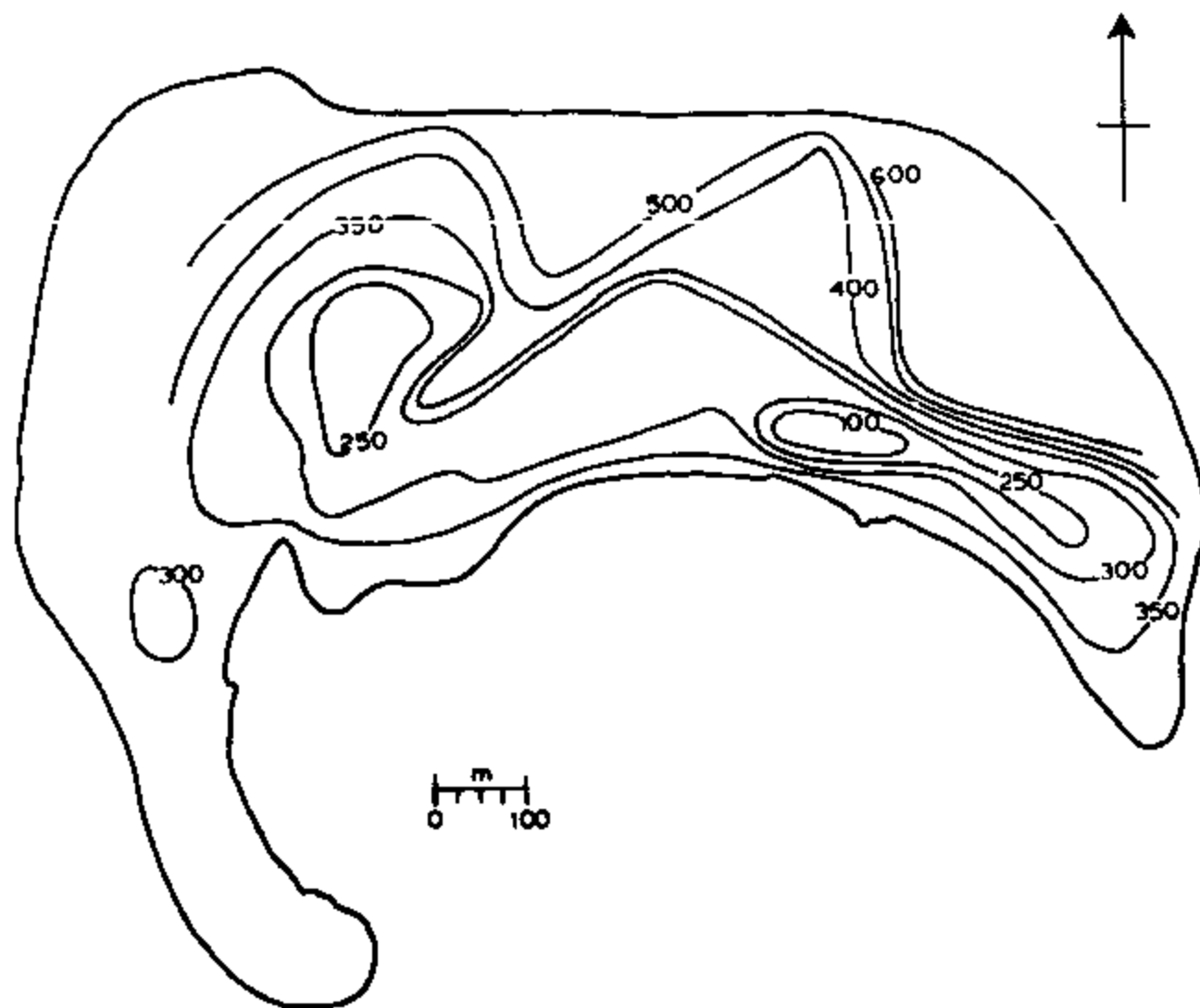


Figure 36. Map of Deke Island showing the geographic distribution of chloride-ion concentration in observation wells. Data derived from the analyses of water samples collected from observation wells on March 17, 1984.

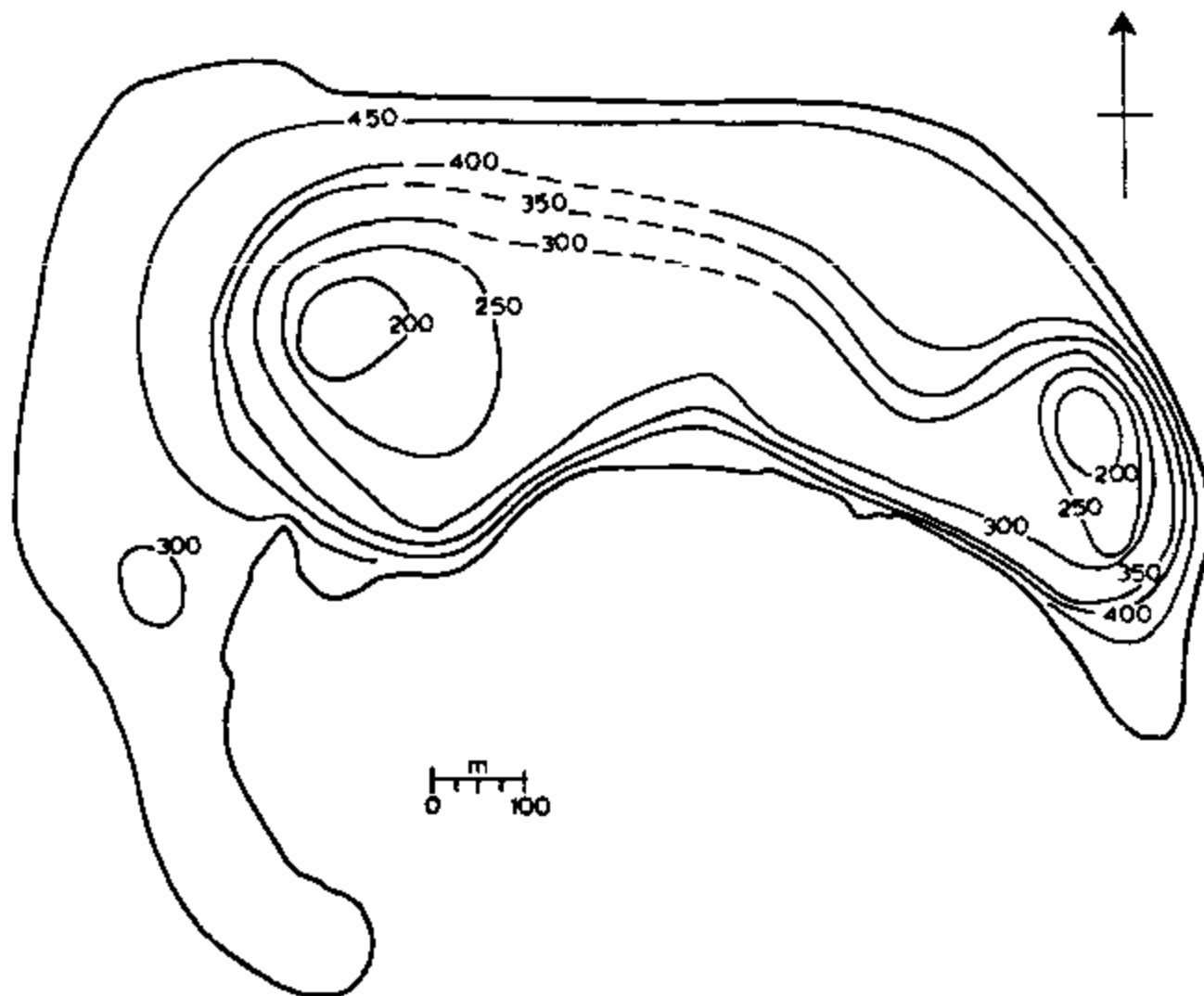


Figure 37. Map of the Deke Island showing the geographical distribution of total hardness measured in observation wells. Data derived from the analyses of water samples collected from observation wells on March 18, 1984.

Water samples were collected from a fixed depth of 2 m below the water level in DS4 at 1/2 hour intervals for over 40 hours. These samples were analyzed for specific conductance and selected samples were returned to the WERI water laboratory for chloride-ion determination by titration. The specific conductance curve with time for DS4 shows sharp increases and decreases that generally correspond with tidal change (Figure 38). The graph of Figure 38 shows four major peaks, 4, 7, 10 and 12. Time intervals between the major peaks are 11 hrs, 11 hrs, and 6.5 hrs respectively. There is an average of 6 hours between major and minor peaks (the latter are numbered 1, 6, and 9). This indicates that another factor besides tidal change is influencing the specific conductance fluctuations in DS4.

Relative-salinity regression lines were generated from DS3 specific conductance profiles in order to determine the 1% and 50% relative salinity depths below the water table. Representative relative-salinity regressions are presented in Figure 39; the individual regression lines for each profile are presented in Appendix D.



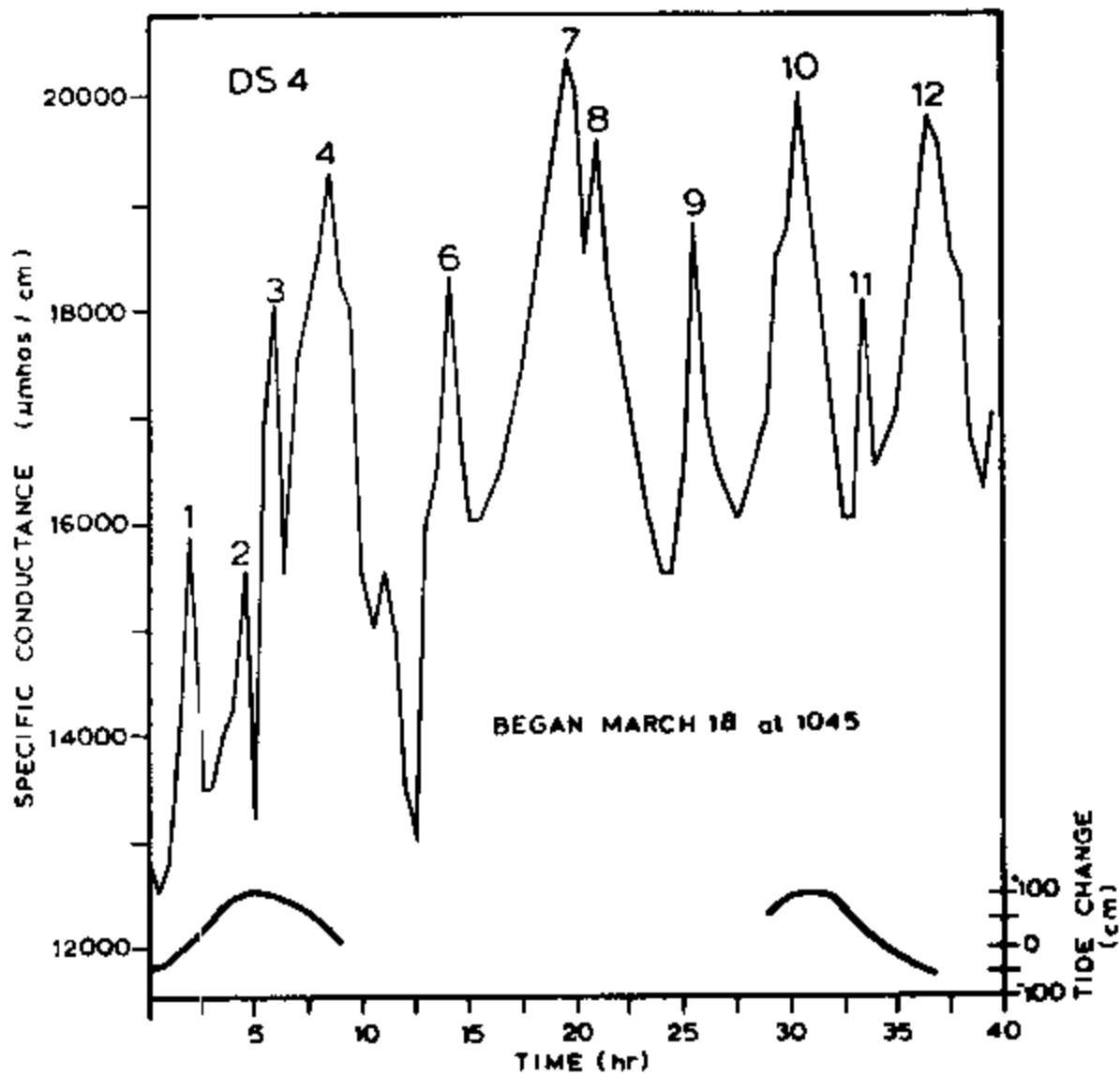


Figure 38. Graph of specific conductance versus time at observation well DS4. The lowermost curve shows measured tidal fluctuations in the well for the same period.

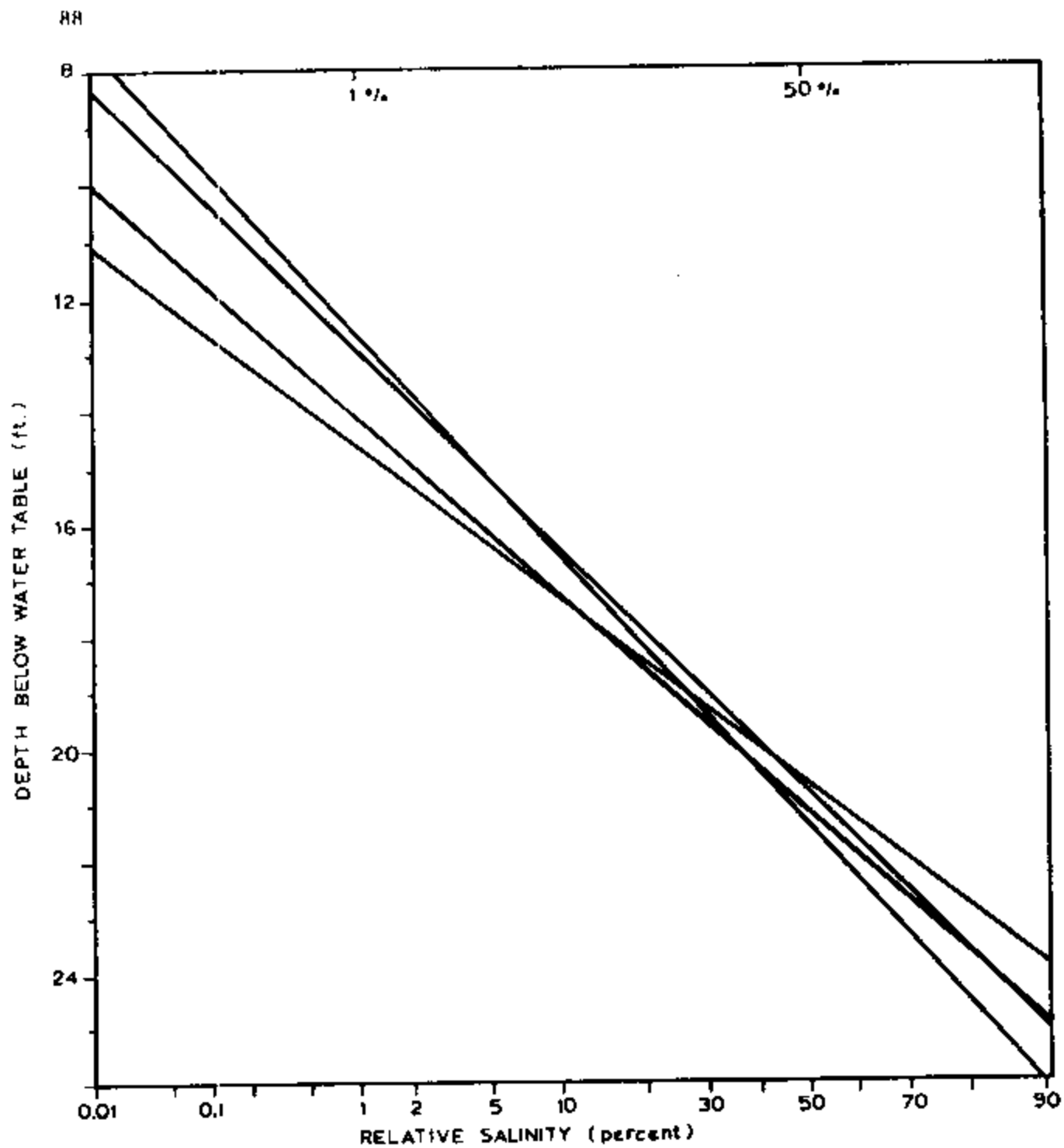


Figure 39. Probability plot of relative salinity measurements from observation well D4.

## DISCUSSION

A number of new and relevant aspects of atoll island hydrogeology have surfaced as a result of the work conducted on Deke Island. Interpretation of field data collected during the course of the study has led to a better understanding of the physical make-up of an atoll island and the role played by the various geologic components in the occurrence of groundwater and its dynamics of flow. Availability of detailed water-level information has provided the necessary foundation to logically interpret hydrographs from wells located in the fresh-water lens and, therefore, separate the effects of sea-level fluctuations and rainfall events. These topics, in addition to the practical implications of the study findings, are presented in the discussion that follows.

### Interpretation of Water-Level Data

In the presentation of results it was noted that a customary practice in studies of coastal and island hydrology is to convert observed water-level elevations, which are relative to some fixed datum, to "reduced levels" which give the head relative to sea level. Results from Deke indicate that, for reduced levels computed from daily data, there is a strong negative correlation with sea level. Thus, these daily heads do not in themselves relate directly to the quantity of fresh groundwater in storage. The purpose of this discussion is to examine this proposition further.

By way of introduction it should be pointed out that two facts of Ghyben-Herzberg systems motivate the conversion of actual (observed) water-level elevations to reduced levels. First, the shoreline is the peripheral drain for the fresh groundwater of the island. Models that treat the circulation of recharge-derived fresh groundwater consider a static sea level and set the head at the shoreline equal to zero. Thus by subtracting sea level from the measured elevations, the intention is to recast the inland elevations so they give the difference in head between the inland sites and the point of outflow, which changes as sea level changes.

The second motivation is the Ghyben-Herzberg Principle, which stipulates that, ignoring mixing, the thickness of the fresh-water column is some 41 times the elevation of the water table above sea level. Thus changes in the elevation of the water table relative to sea level signify changes in the fresh-water storage. In subtracting sea level from the observed elevation the idea is to obtain a set of numbers that reflects the quantity of fresh groundwater beneath the island. As indicated by the data shown in Figure .9, this idea is misguided and the problem is not that simple.

This problem of converting actual water-level elevations to a derived set that reflects changes in fresh-water storage is a real, practical problem. The principal reason for monitoring water levels in the first place is to get an idea of the changes in storage. Models are available that give water-table variations in response to a recharge schedule (e.g., Ayers, 1980; Ayers and Vacher, 1983). For these models to be applied to an

inland, they must be fit to a set of data that shows how the elevation of the water table varies with time at a number of localities; either these data must have the effects of sea level removed or the models need to be reformulated to take account of the changing position of sea level. The point of this discussion is that the reduced levels do not constitute an appropriate set of data for such interpretation of volume changes and that a more labored technique is required to remove the effects of sea level. An example of such a procedure is presented later in this discussion.

### Reduced Levels

A look at the results at individual wells sheds light on why there is a problem with the reduced levels. In Figure 20, the 21-day run of observed water levels (W) is shown for three selected wells: A2, which from its inland location should have comparatively little sea-level influence; E4, which is located very close to the shoreline in a narrow peninsula and, therefore, should have a very strong sea-level effect; and C2, which is in an intermediate position but closer to an A2-type setting than an E4-type setting.

The graphs of Figure 40 show the expected pattern. The variability is largest, by far, at E4. This is particularly evident in the water-level response to the prominent sea-level rise of March 2-3. The same pattern is reflected in the well statistics listed in Table 17. The standard deviation of the 21-day variation at E4 (3.8 cm) is much larger than it is at the inland wells (2.7 and 2.8 cm). At the higher-variability nearshore well, E4, the correlation of the time series with the lagoon sea-level record (L) is stronger (correlation coefficient,  $r = 0.65$ ) than it is for the lower-variability inland wells (e.g., for A2 vs. L,  $r = 0.16$ ).

Reduced levels (W-L) for the same 3 wells are shown in Figure 41. Smoothed versions, from a 3-point moving average, are shown in Figure 42 in combination with the lagoon sea-level record and rainfall. From inspection of these figures it is obvious that, by subtracting the sea-level record from the less-variable inland water-level records, the variability is increased in the reduced levels. In the process, the subtraction imposes a strong negative correlation on the result. This is shown also in Table 17. A2, which is the least variable of the three in its measured levels (SD = 2.8 cm), has the most variable reduced levels (SD = 5.0 cm), and, in the transformation from observed to reduced levels, the correlation with lagoon record has been altered from that of a poor positive correlation ( $r = 0.16$ ) for the observed levels to a strong negative correlation ( $r = -0.82$ ) for the reduced levels.

Thus, the problem with reduced levels is rather straightforward. Day-to-day variation in sea level exerts a major control on the day-to-day variation in water levels, which is why there is a positive correlation between ground-water levels and the lagoon record. The sea-level effect diminishes inland because waves generated by the sea-level variation are attenuated as they advance laterally -- as is the case also for the higher-frequency tides; the dampening, however, is less than for the tides because the dampening rate varies inversely with period of the wave. The attenuation is sufficient, however, to be reflected in a smaller

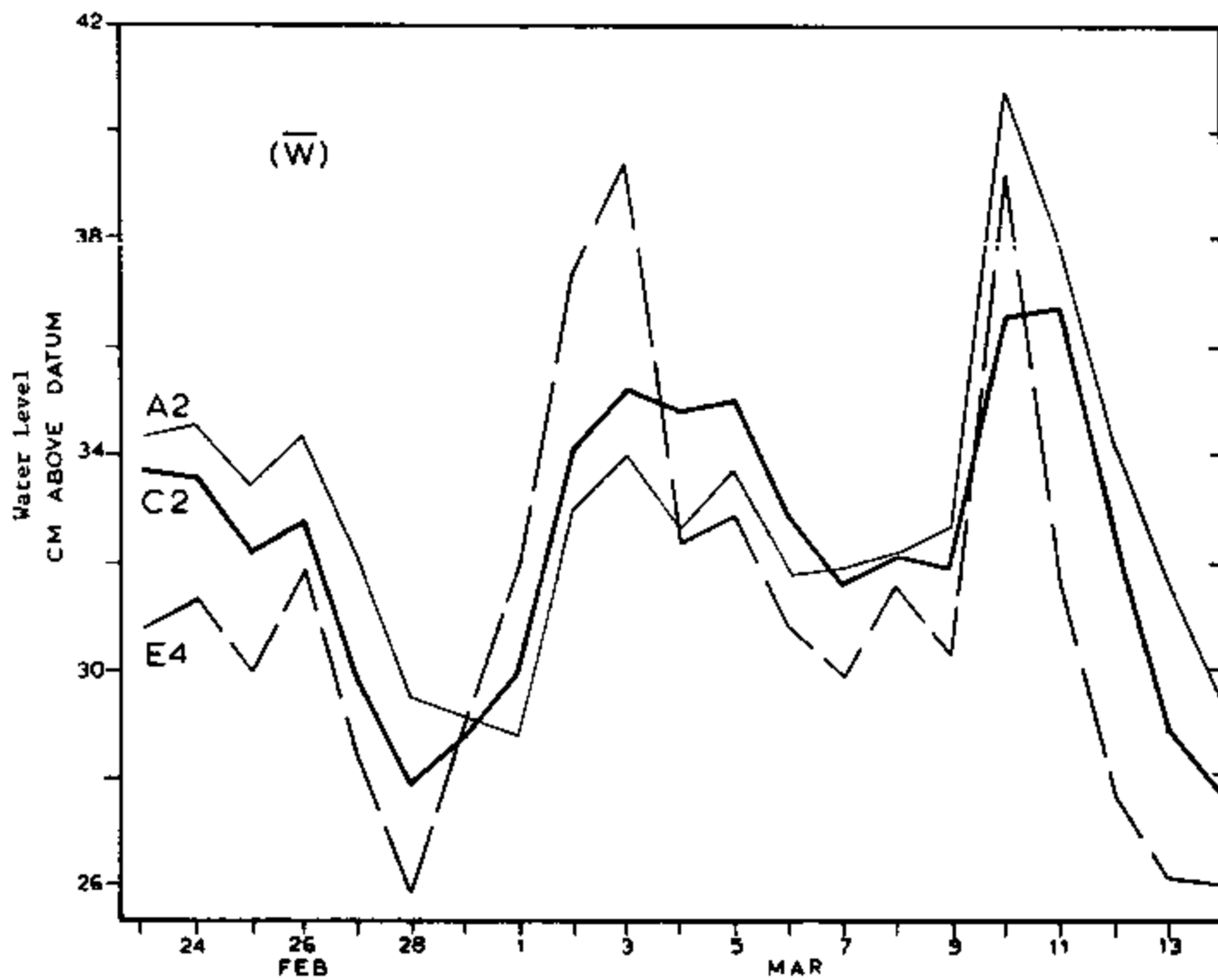


Figure 40. Hydrographs of three observation wells on Deke Island. Water levels ( $w$ ) are daily values over a 21-day measurement period.

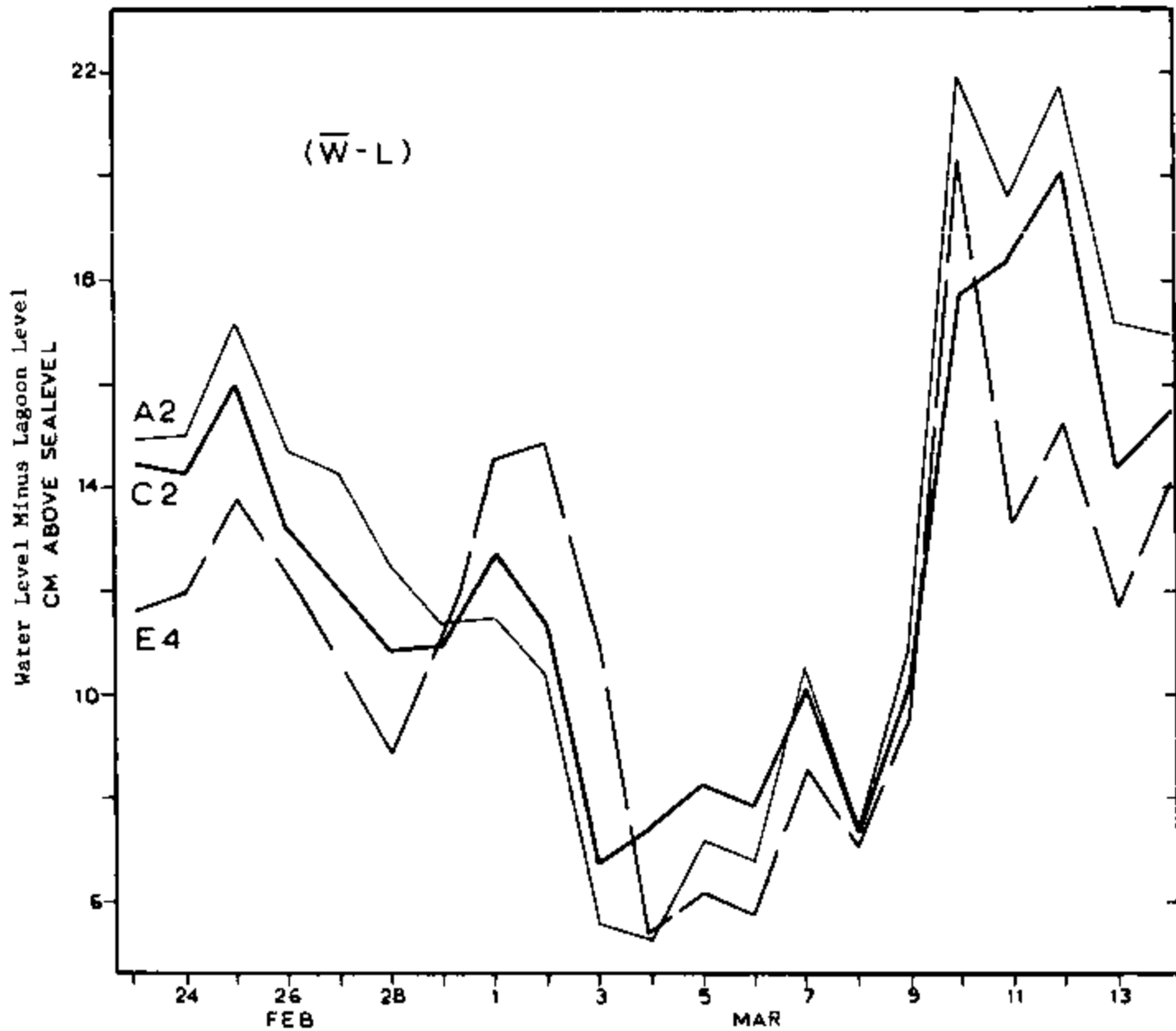


Figure 41. Graphs of reduced hydrographs at three observations wells. Reduction by subtracting the lagoon (L) from the observed level (W).

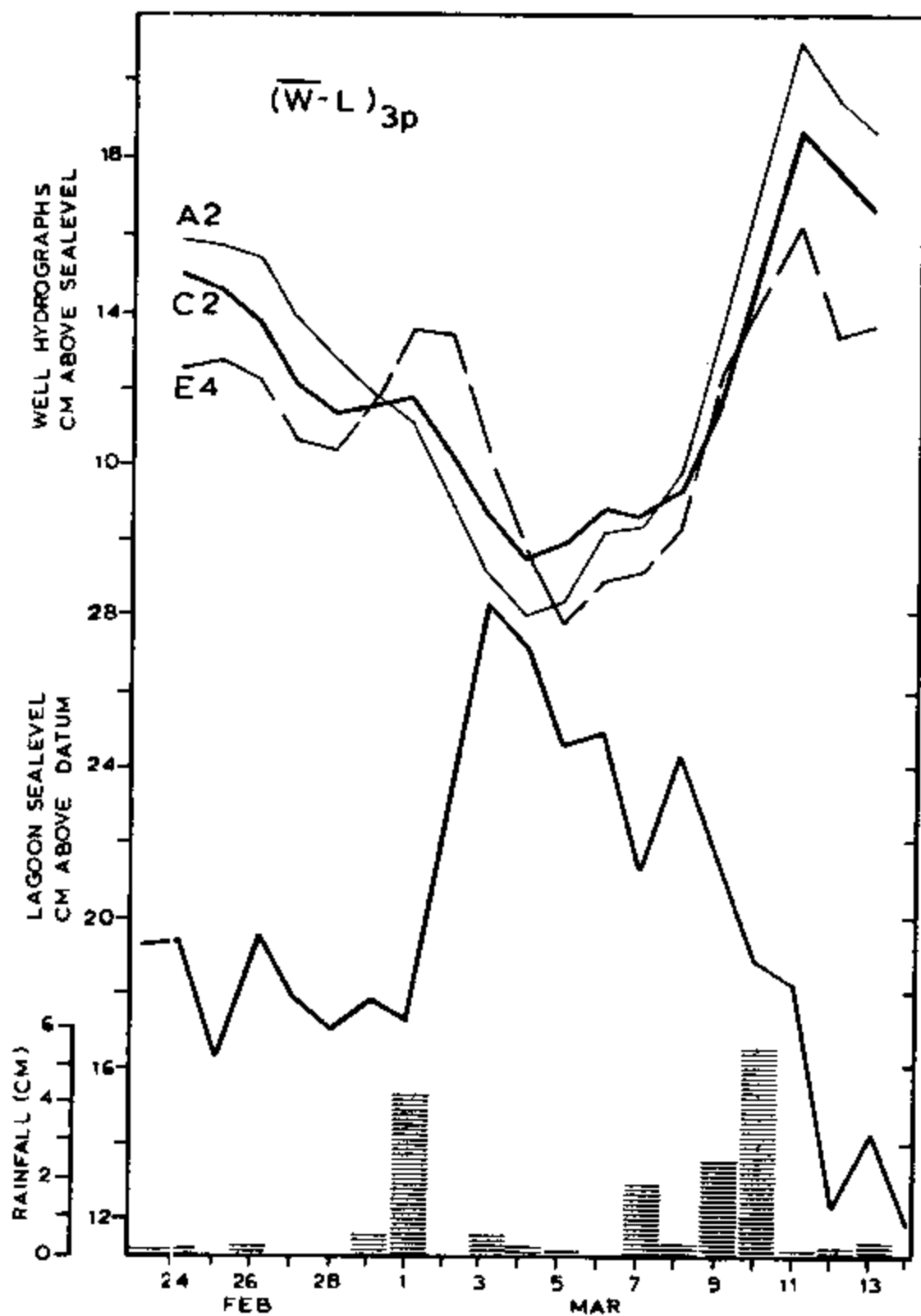


Figure 42. Graphs of smoothed reduced water levels at three observation wells, daily mean lagoon level, and daily rainfall. Water levels smoothed by a three-point moving average.

Table 17. Correlation of measured water levels, reduced water levels, and "constant-sea-level hydrographs" with the lagoon record.

	$s_x^2$	$s_x$	$s_y^2$	$s_y$	$s_{xy}$	$r_{xy}$
L	20.06	4.48				
$\bar{W}$			9.38	3.06	7.84	0.57
W for A2			8.04	2.84	1.99	0.16
W C2			7.31	2.70	6.82	0.56
W E4			14.20	3.77	10.95	0.65
W-L for $\bar{W}$			13.82	3.72	-12.23	-0.73
W-L A2			25.14	5.01	-18.50	-0.82
W-L C2			14.44	3.80	-13.75	-0.81
W-L E4			13.31	3.65	-9.62	-0.59
CSL for $\bar{W}$			6.83	2.61	3.03	0.26
CSL A2			9.26	3.04	-3.55	-0.26
CSL C2			4.37	2.09	0.18	0.02
CSL E4			9.09	3.01	2.61	0.19

$s_x$ ,  $s_x^2$ ,  $s_y$  and  $s_y^2$  refer to standard deviation and variance of the indicated variable;  $s_{xy}$  and  $r_{xy}$  are the covariance and correlation coefficient of the indicated variable with  $x$ , the lagoon sea-level record.



variability (e.g., standard deviation) of the daily water levels at A), for example, compared to E4. Also, as the sea-level effect diminishes inland, the daily variation at the wells becomes less like that in the lagoon; the result is that at inland sites other factors which are masked at nearshore sites become relatively more important and the record at these inland sites is less correlated with the sea-level record. In converting these measured water levels to reduced levels, the full variability of sea level is subtracted, equally, from each of the wells. Thus there is "overcompensation" for sea level and this overcompensation is largest at inland wells where the sea-level effect is least due to the lateral dampening. Thus the reduced levels correlate negatively with sea level, and the correlation is strongest inland.

To put the matter more succinctly, consider an island which is recharged in such a way that there is no water-table variation other than that due to sea-level variations (i.e., the textbook steady-state lens). Consider also that the island is sufficiently large that all sea-level variations are dampened out at some point inland. Observed water levels then at this point would be constant with respect to time. Reduced levels, found by subtracting the daily (or monthly) sea-level variation from the daily (or monthly) water-level records would graph as the mirror image of the sea-level records; there would be a correlation coefficient of  $-1.00$ ; and it would be quite a mistake to interpret that graph of reduced levels in terms of changes in fresh-water storage. This example is an exaggeration of the case made by the results from Deke.

#### Constant-Sea-Level Water-Level Hydrographs

A constant-sea-level (CSL) water-level hydrograph is an abstraction from the water-level data to show the water-level variations that would be present if there were no variations due to sea level. Thus if the effects of sea level could be removed from the water-level data, the remaining run of numbers (the CSL hydrograph) would record the phenomena related to changes in fresh-water storage such as recharge events, drainage to sea, evapotranspiration from the lens, and hydrostatic adjustments of the interface.

It is apparent from the above discussion that the reduced levels at a well do not constitute a CSL hydrograph. It is also apparent from the discussion that, in order to correctly remove the sea-level variations from records for a number of wells, a different correction factor must be applied at each locality, because the sea-level effect differs from place to place due to the lateral dampening. The important consequence of this fact is that the correct removal of sea level -- by the application of different correction factors at different localities -- would change, and in some cases might even reverse, the difference in head between particular wells. Thus the map of these "heads with sea level removed" could be quite different from that of the reduced levels for any given day. Reduced levels correctly represent heads relative to sea level on any particular day. Heads with sea level removed portray an imaginary surface, which when superimposed on the surface reflecting the waves crossing the island that day from the sea-level variations, gives the observed configuration.

Despite the fact that they are imaginary, these heads are of critical importance because they isolate variables related to the volume of fresh groundwater.

An attempt to remove the sea-level effect at C2 and hence derive a CSL hydrograph for that well is shown in Table 18. In the calculation scheme shown in the table, the CSL hydrograph is derived from the run of reduced levels (Col 3). The strategy is to reduce the day-to-day change in the reduced levels (Col 4) by an amount (Col 5) which is thought to be attributable to the sea-level variation. This amount is taken to be a fraction (a, in the table) of the sea-level change. The fraction is determined by matching  $\Delta(W-L)$  and  $\Delta L$  at three conspicuous sea-level-related sawtooth excursions in the curve of W-L. By subtracting the head changes which are attributed to sea-level changes from the changes in reduced levels, the result is a succession of head changes which are thought to be due to factors other than sea level. These numbers (Col 6) are then converted to a CSL hydrograph by first cumulating the changes (resulting in Col 7) and then adjusting that run of numbers by assuming that the mean of the CSL hydrograph is equal to the mean of the reduced levels over the period of measurement.

Results of the calculation for C2 are shown in Figure 43A; also shown are the results for A2 and E4. These three graphs in Figure 43A represent the daily CSL hydrographs at the three selected wells and are to be compared with Figure 41 which shows the three runs of reduced levels at the three wells. In Figure 43B the comparison between CSL hydrograph and reduced level is made directly for C2. In Figure 44, the CSL hydrograph for the 14-well average,  $\bar{W}$ , is shown in comparison with (a) the analogous reduced levels and their three-point moving average in the upper part of the figure, and (b) the rainfall and the lagoon record in the lower part of the figure.

Comparison of CSL hydrographs to the analogous runs of reduced levels shows that the attempt to remove the sea-level variation does in fact greatly reduce the variability of the time series and eliminate at least the obvious correlation with the sea-level record. These improvements are reflected in the statistics listed in Table 17. The removal of the sea-level effect from the reduced levels reduces the variance by 65% to 70% for the two inland cases (A2 and C2) and 50% for the 14-well average. At the same time, the resultant run of numbers -- the CSL hydrographs -- correlate poorly, if at all, with the lagoon record: correlation coefficients range from -0.26 to +0.26, with that for C2 being 0.02.

In comparing the graphs of reduced levels and the CSL results, it is worth noting how the shapes of the curves have been altered in removing the sea-level effect. There have been two important changes. First, the downward trend and low (between March 1 and 8) that dominate the reduced levels in all the graphs are largely removed and, by their loss, are shown to be an artifact of the arithmetic leading to the reduced levels; conclusions based on the reduced levels would incorrectly exaggerate the amount of recession between rainfalls. The second change is that the response to rainfall of March 2 is brought out. From reduced levels, it would appear that the 4-cm rainfall event had little effect on the water level as seen by the 14-well average, and, at best, had only decreased the

Table 18. Calculation of CSL hydrograph at C2.

Columns	(5)	(6)	(7)	(8)
(1) L	(5) $-a\Delta L$	(6) Col (4) - Col (5)	(7) Running Sum of Col 6	(8) Col 6 + difference in Average of Cols 3 and 7 (CSL Hydrograph)
(2) $\Delta L$				
(3) W-L (Reduced levels)				
(4) $\Delta(W-L)$				

	(1)	(2)	(3)	(4)	(5)	(6)	(7)	(8)
2/23	19.2		14.5				0	13.8
24	19.3	+0.1	14.3	-0.2	-0.1	-0.1	-0.1	13.7
25	16.2	-3.1	16.0	+1.7	+2.5	-0.8	-0.9	12.9
26	19.6	+3.4	13.2	-2.8	-2.7	-0.1	-1.0	12.8
27	17.8	-1.8	12.0	-1.2	+1.4	-2.6	-3.6	10.2
28	17.0	-0.8	10.9	-1.1	+0.6	-1.7	-5.3	8.5
29	17.8	+0.8	11.0	+0.1	-0.6	+0.7	-4.6	9.2
3/1	17.3	-0.5	12.7	+1.7	+0.4	+1.3	-3.3	10.5
2	22.6	+5.3	11.4	-1.3	-4.2	+2.9	-0.4	13.4
3	28.4	+5.8	6.8	-4.6	-4.6	0	-0.4	13.4
4	27.3	-1.1	7.5	+0.7	+0.9	-0.2	-0.6	13.2
5	24.6	-2.7	8.3	+0.8	+2.2	-1.4	-2.0	11.8
6	25.0	+0.4	7.9	-0.4	-0.3	-0.1	-2.1	11.7
7	21.3	-3.7	10.3	+2.4	+3.0	-0.6	-2.7	11.1
8	24.5	+3.2	7.6	-2.7	-2.6	-0.1	-2.8	11.0
9	21.7	-2.8	10.2	+2.6	+2.2	+0.4	-2.4	11.4
10	18.9	-2.8	17.7	+7.5	+2.2	+5.3	+2.9	16.7
11	18.3	-0.6	18.4	+0.7	+0.5	+0.2	+3.1	16.9
12	12.4	-5.9	20.1	+1.7	+4.7	-3.0	+0.1	13.9
13	14.4	+2.0	14.4	-5.7	-4.6	-1.1	-1.0	12.8
14	11.9	-2.5	15.5	+1.1	+2.0	-0.9	-1.9	11.9
Ave.			12.4				-1.4	12.4

Calculation of  $\epsilon$ , the correction factor.

2/25	$\Delta(W-L)$	$\Delta L$		
26	1.7 } 4.5	-3.1 } 6.5	$4.5/6.5 = 0.69$	
	-2.8 }	+3.4 }		
3/7	2.4 } 5.5	-3.7 } 6.9	$5.3/6.9 = 0.77$	ave
8	2.9 }	3.2 }		0.80
3/12	1.7 } 7.4	-5.9 } 7.9	$7.4/7.9 = 0.94$	
13	-5.7 }	2.0 }		

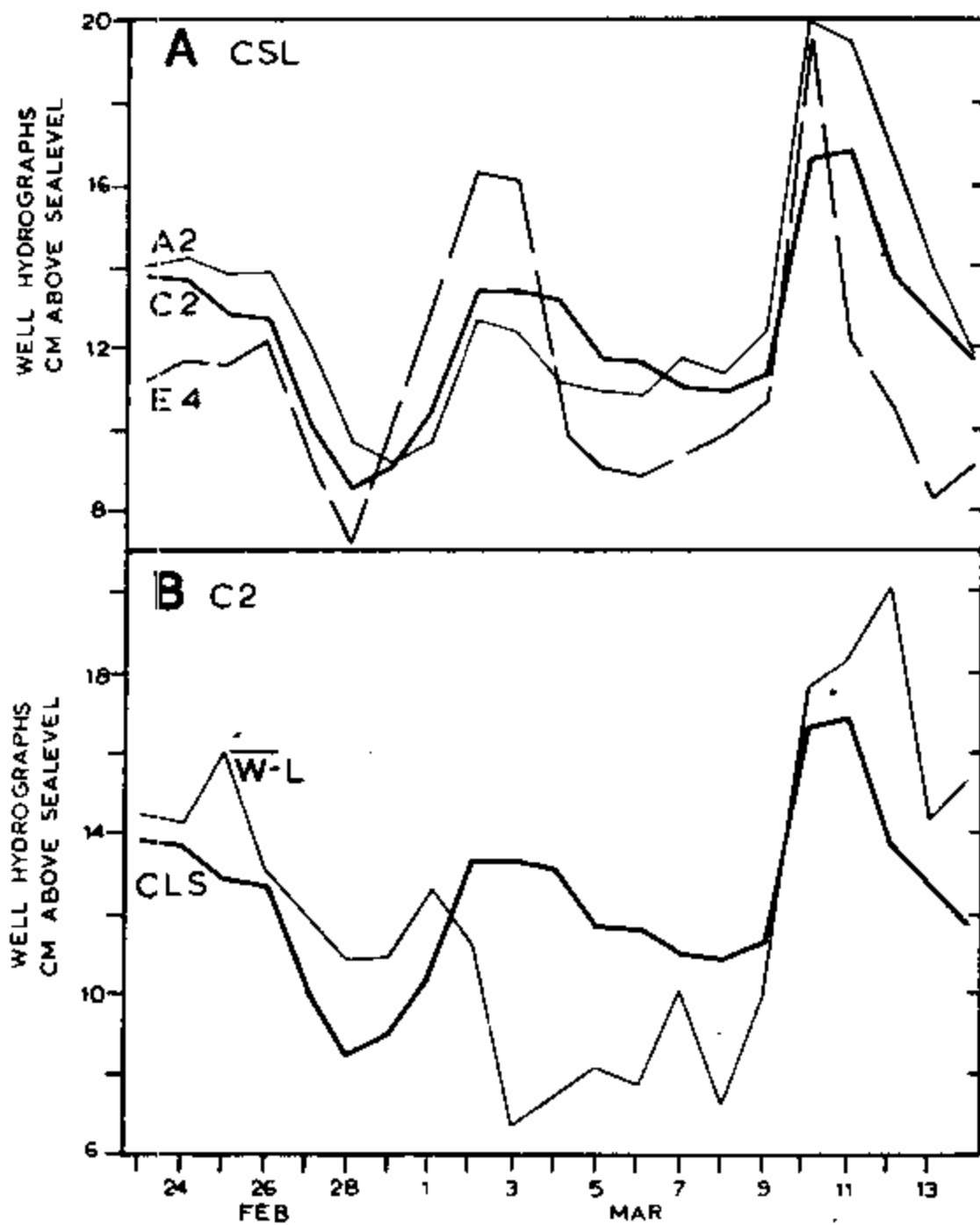


Figure 43. Comparison of constant sea-level hydrographs and reduced hydrographs at three observation wells.

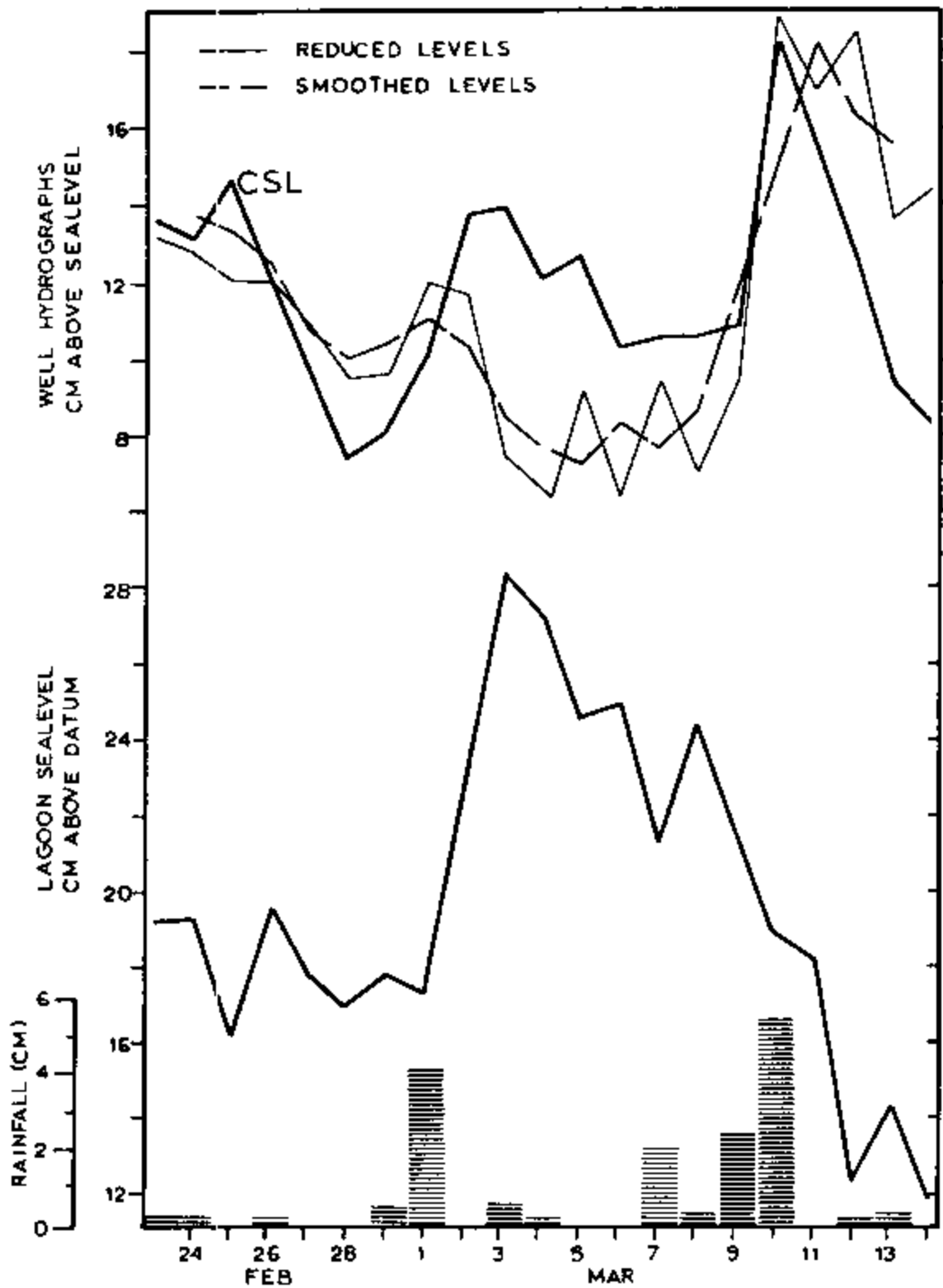


Figure 44. Graphs of reduced ground-water levels, daily lagoon level, and rainfall for a 21-day measurement period. Water levels are averaged for 14 wells and are relative to the constant-sea-level datum.

rate of descent at the A2 (see Figure 41). However, again, this would be a misinterpretation; as shown by the CSL hydrograph there was an important recharge event resulting from the March 2 rainfall, but it was obscured in the reduced levels because water levels were also rising in association with the 14-day tidal variation.

In order to further clarify the correlation with rainfall, the CSL hydrograph for the 14-well average is generalized in Figure 45, by subjectively smoothing out the irregularities. The overall shape of the resultant curve is like that of successive peaks and recessions of a surface-water flood hydrograph that is, there is a rapid rise with rainfall, and an exponential-decay shape to the recession. It is clear from this graph that once sea level is removed, the main water-level story consists of rainfalls which increase water-level elevations and post-rainfall equilibrations that are seen as recessions. These equilibrations would be due to accelerated flow to sea (because of the increased heads and their gradients) and subsidence of the interface (because of the accretion of water at the top of the lens).

It is worth noting where the 21-day average, 11.7 cm, falls on Figure 45. This level represents the 21-day, 14-well average ( $\bar{W}_w$  of 31.5 cm above datum) less the 21-day lagoon average (19.8 cm). In contrast to this average level, there is a much lower level that is reached in the recessions between rain-correlated peaks. The low on Feb 28, for example, is about 8 cm above sea level. To the extent that these recessions would taper off to some near-level asymptote (in geometry analagous to a base flow-level in flood hydrographs), this asymptote would appear to lie at about 5 to 6 cm above sea level, or about 50% of the 21-day average; it appears that this level could be reached (by extrapolating the curves) in a matter of 10 days to 2 weeks without recharge. The point is that while there may be some 15 ft of fresh groundwater (ignoring mixing), it appears that it is extremely vulnerable to droughts with -- if these CSL levels can be translated to volumes without consideration of lagging-interface effects -- as much as half of the lens being lost in a 2-wk period of no rain.

#### Hydrogeological Framework of Deke

The hydrogeological framework of Deke Island can be deduced, at least in general terms, from drilling information, geophysical data, geological mapping, and direct observations. Several lithologically distinct units comprise the geology of Deke and the reef complex upon which it sits. These units, in some cases, produce rather pronounced hydraulic effects on the groundwater-flow system and exhibit some unique water bearing properties. Except for the reef-flat plate or hard layer, all units can be classified as excellent aquifers.

Various geological components of the reef complex are shown diagrammatically by the cross sections of Figures 46 and 47 (the legend is given by Table 19). These sections are drawn along two seismic profiles (A and C) shown on the location map of Figure 35. The greatest amount of field data (acquired by several independent methods) was collected along these two lines and therefore it is appropriate to utilize the composite information in the construction of the sectional views.

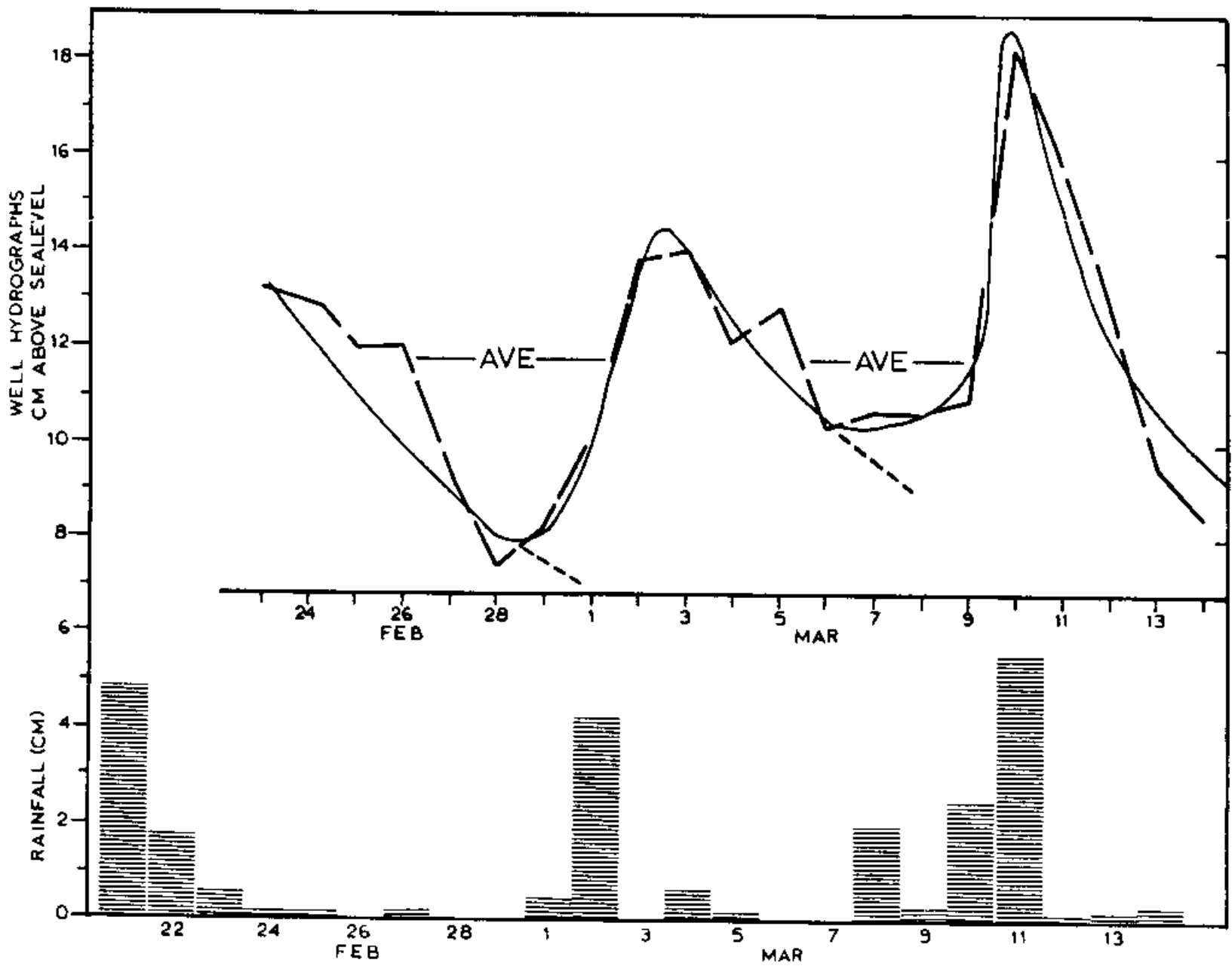


Figure 45. Generalized observation well hydrograph and rainfall. The well hydrograph represents the 14-well average relative to constant sea level.

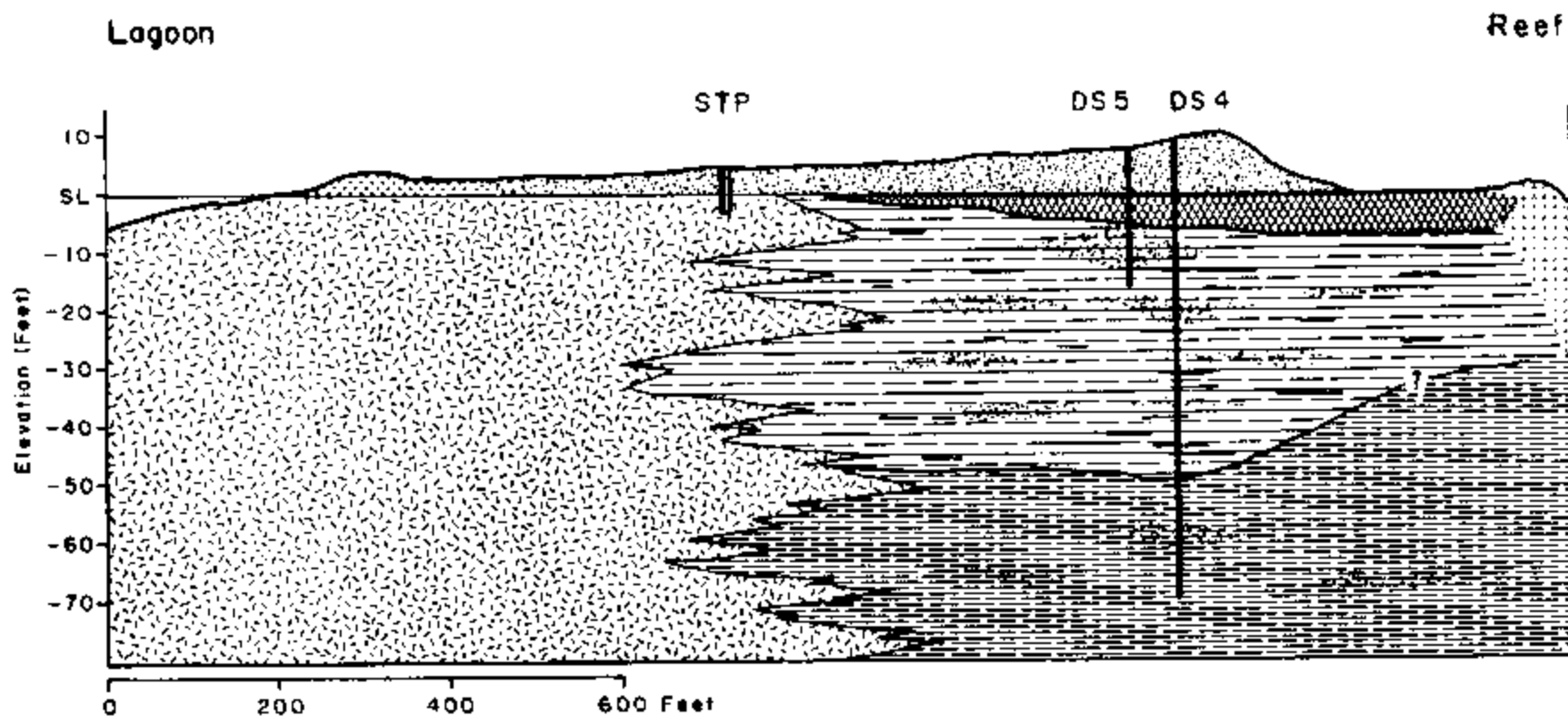


Figure 46. Hydrogeologic cross section along seismic profile A. Cross section, along profile A of Figure 35, is constructed from composite data. In addition to drill site and stratigraphic test pit (STP) information, seismic lines designated by JT, IR, LWT, PT, and TP were used in the construction. Refer to Table 16 for unit symbol and description.



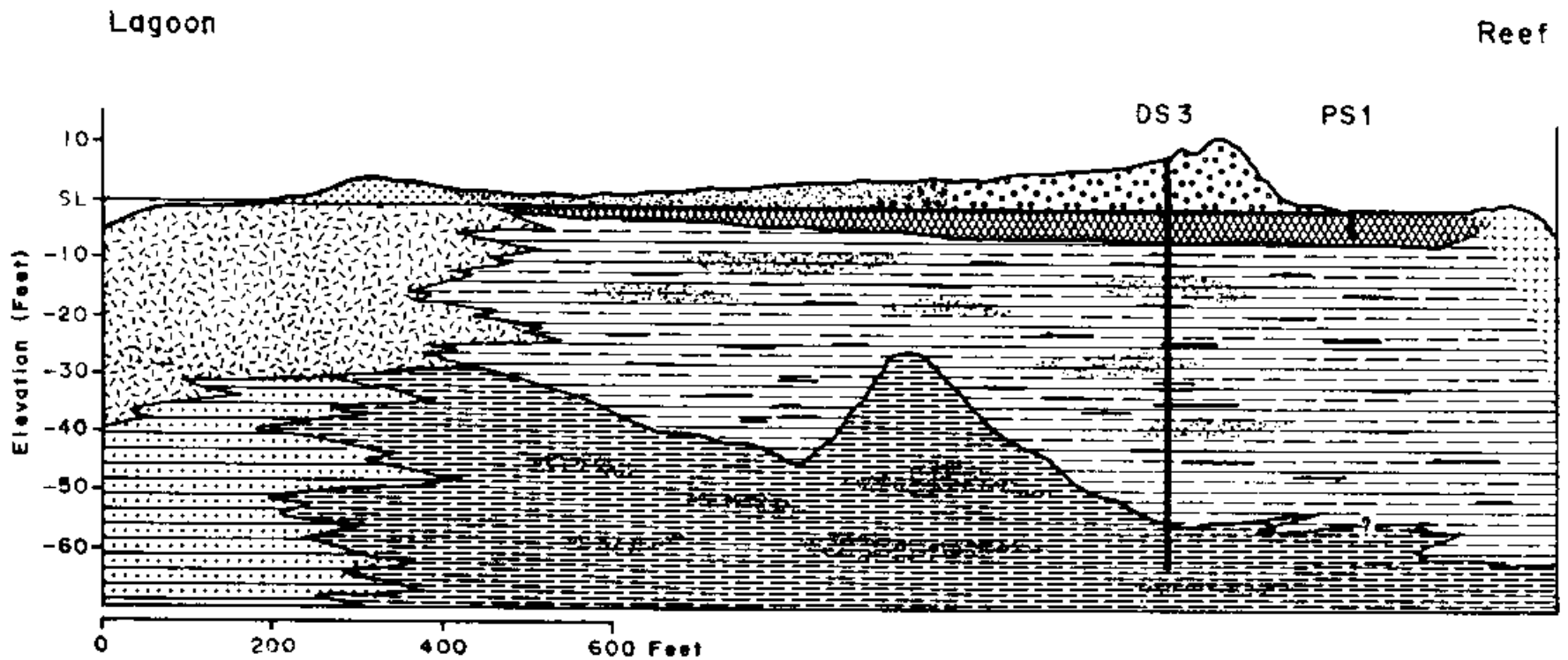


Figure 47. Hydrogeologic cross section along seismic profile C. Cross section, along profile C of Figure 35, is constructed from composite data. In addition to drill site information, seismic lines designated by FE, NT, TP, and ST were used in the construction. Refer to Table 16 for unit symbol and description.

Table 19. Legend to Figures 46 and 47.

Unit No.	Symbol	Description
1		Unconsolidated sediment comprising Deke Island.
2		Reef structure.
3		Well indurated sediments of the hard layer (reef flat); Permeability is very low.
4		Unconsolidated to poorly consolidated sediments probably associated with back-reef deposition; Permeability is very high.
5		Mostly unconsolidated sand-size sediments probably deposited in the sand apron behind the reef flat; Permeability is high.
6		<u>Halimeda</u> facies composed of poorly consolidated sand- and gravel-sized reef rubble; Permeability is very high.
7		Unit composition is unknown, may be associated with lagoon deposition; Permeability is probably similar to that of unit 5.
		Unit contact established by measurement.
		Hypothetical unit contact; represents a gradation between units.

As depicted in the diagrams, the island unit rests partly upon the reef flat (hard layer) and partly upon sands deposited lagoonward of the reef flat. The latter appear to be fairly uniform in character, mostly unconsolidated, and form a relatively thick unit. The reef flat extends beneath the island at variable distances but forming a continuous plate from the reef margin to wherever it grades into sediments of the sand apron. Beneath the reef flat, and apparently associated with it, are sand and gravel-size sediments derived from the reef environment. A notable characteristic within this unit (observed drilling response) is alternating hard and soft zones. Based on the analysis of cores, these zones are associated with well-cemented sections and with probable unconsolidated layers. This alternation of cemented and non-cemented zones would certainly produce a strong horizontal component to the groundwater - flow regime (anisotropy). Another point that is noteworthy is the close affiliation between the reef-flat (hard layer) and this unit. Constituent particles comprising both units are the same; the difference is the abundance of cement. As readily observed in core samples, the amount of cement binding the sediment decreases with increasing depth. The reef flat forms a wedge shape plate with the thickest portion toward the reef. Where the plate grades into the lagoonward unit (sand apron) the lithologic character of the unit beneath the plate changes and there is a lack of matrix cement. All of this seems to indicate that the process of cementation is somehow linked to sea-water circulation along the ocean shoreline. Further, since the unit below the reef flat is similar in particle composition but lacks thick zones of well cemented sediment, the process of reef-flat cementation is probably controlled by the percent day sea-level stand. Hopefully, as more field data become available, the origins of the reef flat will be explained. Because of the important role it plays in the ground-water hydrogeology of atolls, the endeavor is an important one.

The presence of a Halimeda facies underlying the units discussed above was confirmed by drilling and its contact was mapped by seismic shooting. Based on seismic-velocity data there seems to be a transverse change in either density or composition from the ocean shoreline toward the lagoon. Velocities tend to be somewhat less adjacent to the lagoon. It seems that the best explanation would be a change in composition associated with disparate depositional environments. That is, the Halimeda facies probably grades into an environment more closely related to lagoon deposition. Whatever the depositional configuration might be, these deeper units do not play as an important role in the hydrogeology as the overlying units.

Of the many units that comprise the reef complex, four are of direct hydrogeological importance. Specifically, these units are (1) the island itself, (2) the reef-flat plate or hard layer, (3) the unit beneath the reef-flat, and (4) the unit behind the reef flat. Each unit directly affects the occurrence and behavior of the fresh ground-water resource.

The main hydrological function of the island unit is simply to catch rainwater and transfer it to the subsurface units. Numerous processes are involved with the transmittal of water, however. Rainfall is first intercepted by plants and water is returned to the atmosphere by direct evaporation. After rainwater reaches the ground surface, some of it is used by the plants and transpired back to the atmosphere, some of it is

retained in the soil and sediments of the unsaturated zone, some of it evaporates directly, and the remainder eventually percolates downward into the saturated zone. All of these processes, of course, are part of the hydrological cycle and are important factors to be considered when dealing with the overall water budget.

As documented by water-level observation in standpipe-piezometer pairs, the reef-flat plate or hard layer functions as a confining bed beneath which fresh groundwater is under hydraulic pressure. The presence of the plate greatly affects the configuration and behavior of the fresh-water lens as well as previously held views of how groundwater occurs beneath atoll islands. A simple Chyben-Heizberg lens model does not apply to the flow system of Deke. The picture is greatly complicated by (1) partial confinement of the flow system, (2) leaky behavior of the reef-flat plate, (3) impendence of direct recharge to the subsurface, and (4) extension of the discharge area past the ocean shoreline. Some of these points will be discussed later; however, the second point is worth pursuing since it reflects the hydrogeologic properties of the unit. As documented during the water-level investigation, the reef-flat plate is not totally impermeable. On the rising tide, groundwater is pumped upward through the plate. The process, of course, is delayed and its magnitude is dampened compared to the same action without the presence of the plate (refer back to Figure 13). On the falling tide, infiltrating rainwater and the residual groundwater (i.e., that left standing above the hard layer due to the rising tide) tend to drain by gravity downward into the lens system. Thus, there is some degree of vertical permeability. Although the unit is relatively dense and well cemented, there are numerous voids that appear in slabbed cores and hand samples. Groundwater may move along routes within a poorly developed network of interconnected voids. Another possible route for water movement is along fracture traces. Numerous fractures were observed and many mapped on the exposed reef flat. Most of these fractures were relatively long and continuous and appeared to be open. If these fractures exist beneath Deke within the reef-flat plate (and probably do), then they may provide a possible avenue for water movement.

There is a sharp contrast in permeability between the reef-flat plate and the underlying unit. Low abundance of fabric cement and numerous unconsolidated zones, in addition to the wide sediment size range, contribute to a relatively high permeability. Although no direct measurement of permeability was made, it can be roughly estimated. If it is assumed that the permeability of this unit is similar to an equivalent sand and fine gravel aquifer, then an order of magnitude estimate would be 1500 ft/day. This high value is validated by a somewhat fortuitous experience after completion of drilling at DS3. Seawater was used as the drilling fluid. After drilling was completed, a salinity profile was measured in the borehole and for several days thereafter. Measurements indicated that the borehole had cleared well within a 24-hour period, no doubt a testament to very high permeability. Because of the apparent anisotropic nature of the unit, vertical permeability would probably be considerably less. Considering the areal extent of this unit, it would be reasonable to say that the greatest volume of freshwater within the lens is stored in unit 4.

The last hydrogeologically important unit to be discussed is unit 5. From available information, this unit is composed of unconsolidated sand derived from both the lagoon and the reef environments. The portion of the unit of interest underlies the island between the reef-flat plate and the lagoon shoreline. Because the plate is missing, recharge water infiltrating island sediments enters the flow system unimpeded. Of greater interest is the apparent disparate permeability between this unit and unit 4. Again no direct measurement of permeability was made; however, from the type of sediment comprising unit 5 and its more uniform size distribution (observation from stratigraphic test pits) and from the greater dampening of the tidal signal (refer back to Figure 10), it can be deduced that the permeability of unit 5 is probably an order of magnitude less than that of its neighbor. Generally, clean sands in the size of that for unit 5 have a measured permeability of around 150 ft/day.

In the discussion above concerning the various units significant in the hydrogeology of Deke, some values of permeability have been estimated. These estimates may not be valid because no direct measurements were obtained from the field. At this stage in the investigation of atoll hydrology it is relatively unimportant to attach a permeability figure to any particular unit. What is important is the recognition of units with disparate permeability and their relative position within the hydrogeologic framework of an atoll island complex. The fine tuning and attachment of numbers will come at a later stage in atoll studies.

#### The Fresh-Water Lens System

Under ideal conditions where the aquifer is homogeneous and isotropic, the system is recharged uniformly, and there are no outside influential factors (eg. sea-level variations), a symmetric Ghyben-Herzberg lens would be maintained. This, however, is not the case for the Deke system. The fresh-water lens is partially confined, is maintained within complex geologic units possessing disparate water-bearing properties, is subjected to non-uniform recharge events of variable magnitude, and is greatly effected by sea-level variations due to tidal frequencies, barometric pressure changes, and long-term steric effects. All of these factors, and a few more, contribute to the complexity of the flow system beneath Deke.

To simplify matters, the following discussion will be centered around the presentation of a conceptual model of the fresh-water lens system beneath Deke. This model has been generalized by utilizing the results from water-level reduction calculations, specific-conductance measurements in boreholes, water-quality analyses, and resistivity work. The model is presented in Figure 48. It should be noted that, for clarity, the vertical deminsions have been greatly exaggerated. In reality, at true scale, representation of the lens thickness would be little more than the width of a single line.

A number of important points concerning the subsurface flow system of Deke are illustrated by the diagram of Figure 48. Among these points are (1) the asymmetry of the lens configuration, (2) the relative position of the reef-flat plate and the primary recharge area, (3) the ground-water

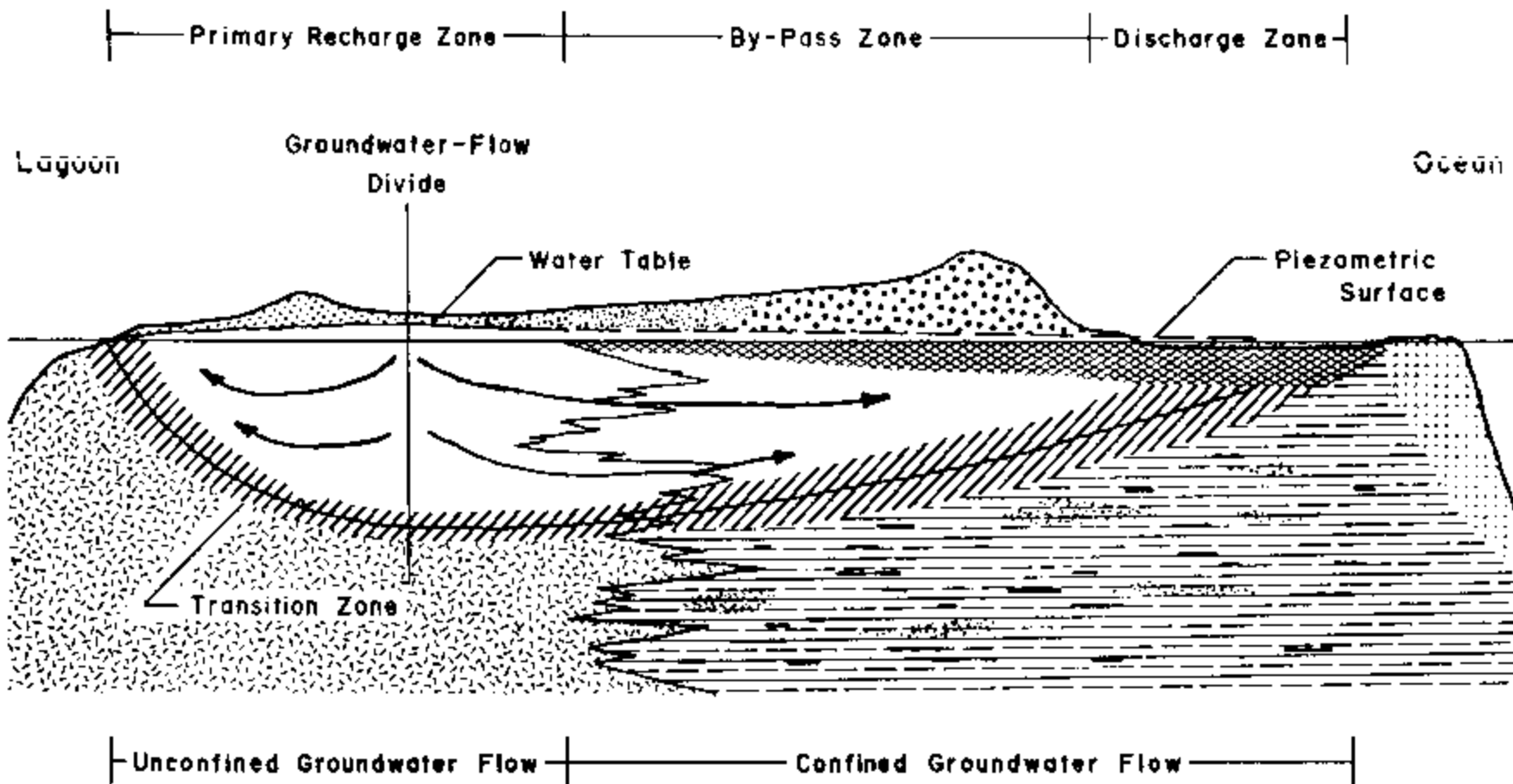


Figure 48. Generalized conceptual model of the Deke Island groundwater-flow system.

flow pattern, (4) the zones of ground-water discharge, and finally, (5) the thickness variability of the transition zone.

One of the most obvious features of the model is the asymmetric configuration of the lens. Fresh groundwater is stored within two hydrogeologic units (units 4 and 5 of Figures 46 and 47) as pointed out earlier in the discussion. It was also pointed out that there is a distinct permeability contrast between the two units: the lower permeable unit located along the lagoon side of the reef complex and the higher permeable unit located along the ocean side. The thickest portion of the lens occurs within lower permeable unit. Resistance to flow due to low permeability tends to maintain higher heads which in turn depresses the position of the transition zone thus producing a thicker lens.

Direct recharge occurs over that portion of the lens where the reef-flat plate is not present. Infiltrating rainwater enters the system under unconfined or water-table conditions. This direct influx of water may be an additional factor which contributes to the asymmetry of the lens. Incoming water produces local changes in storage which in turn produces a thicker lens.

The combination of asymmetric head distribution and localized ground-water recharge, in addition to the hydraulic effects of the reef-flat plate, produce an unusual subsurface flow pattern. Two flow paths are possible. If a particle of water enters the system on the lagoon side of the flow divide, the path taken is relatively short and flow is directly into the lagoon. The point of exit is in the vicinity of the beach face. If, however, a particle of water enters the system on the ocean side of the divide, the path taken is much longer. The water particle will travel under confined conditions beneath the reef-flat plate and exit the system somewhere near the reef. Because of the presence of the confining bed, it is not appropriate to assume that the ocean shoreline of the island is the discharge zone. At this point the island unit is not a factor in the control ground-water movement. What does control flow is the hydrogeology of the reef complex, the island merely plays the role of a rainwater catchment. Misinterpretation of atoll island systems can arise if this concept is overlooked.

Specific characteristics of the zone of mixing or transition zone between fresh groundwater and the underlying salty water were not well documented during the field work. However, from conductance profiles and indirect evidence some general features can be deduced. Sea level fluctuations, in particular tidal responses, are factors mainly responsible for creating and maintaining transition zones in island systems. As the level of the sea oscillates, the lens must also move in concert with the change because the flow system is in hydraulic link with the sea. With the rise and fall of the fresh-water body, mixing between fresh and salty water occurs at the lower boundary of the lens. The thickness of the transition zone or the degree to which this mixing occurs is dependent on (1) the frequency and amplitude of the sea-level oscillation and (2) the permeability of the aquifer. In units of low permeability, the transition zone is normally thin due to a greater attenuation of the landward propagating wave signal generated at the shoreline by a given sea-level oscillation, such as a tidal signal. In units of higher permeability, the

opposite is the usually case, that is, a thicker transition zone develops. We know that there is permeability contrast between the two units within which the lens system occurs. This is reflected in the head distribution and location of the thickest part of the lens along the lagoon side of the island. Therefore, it can be concluded that the thinnest transition zone will occur where the lens is the thickest and the thickest transition zone will occur in the unit of higher permeability nearer the ocean shoreline. Further, since we know the geographical distribution of the tidal efficiency, which reflects the inland attenuation rate, then we can conclude that the transition zone thins inland but at two different rates corresponding to the disparate permeability across the reef complex. The greatest rate of thinning is associated with the lagoon shoreline and landward to the groundwater-flow divide.

Relative-salinity profiles obtained from DS3, shown in Figure 49, have been extracted from the Appendix to illustrate a point related to the behavior of the transition zone during tidal fluctuations. The three pairs of profiles shown in the probability plots represent the conditions within the transition zone at low and high tides for three measurement days. Line A in each of the diagrams represents the profile at low tide and line B represents the condition at high tide. One would expect the transition zone to move vertically in concert with the tides with little change in thickness. From the profile information, it seems that the transition zone, rather than move up and down, thickens and thins according to the tidal highs and lows, respectively. The degree of change is reflected by the change in slope of the profile regression line. The expected displacement upward of iso-salinity lines with a rising tide does not appear in the profile data: in fact, it seems that the opposite occurs (in two of the profiles). This, in part, may be due to the non-homogeneous and anisotropic nature of the aquifer, in part, to flow dynamics close to the boundary discharge zone or, in part, due to mixing in an open borehole. If the measured profiles reflect the actual conditions within the lens, then the interpretation of the data leads to the conclusion that the transition zone increases in thickness with a rising tide and decreases in thickness with a falling tide. More detailed studies of the dynamics of the transition zone are needed to fully comprehend the processes at work.

#### Practical Implications of the Study Results

Results from the hydrogeologic investigation of Deke Island have led to a better understanding of the geological construction of an atoll platform and how fresh groundwater occurs within this framework. Of equal importance is the recognition of the various factors that control the behavior of the fresh-water lens and its associated transition zone. All of these general aspects are important components of the overall picture of atoll island hydrology.

A number of the study findings explain why certain water-related problems are experienced by atoll island communities. Among the major problems are salt-water intrusion, contaminated wells, and seasonal water shortages. By applying what is known of the flow system, many of these problems can be avoided or their effects greatly reduced.



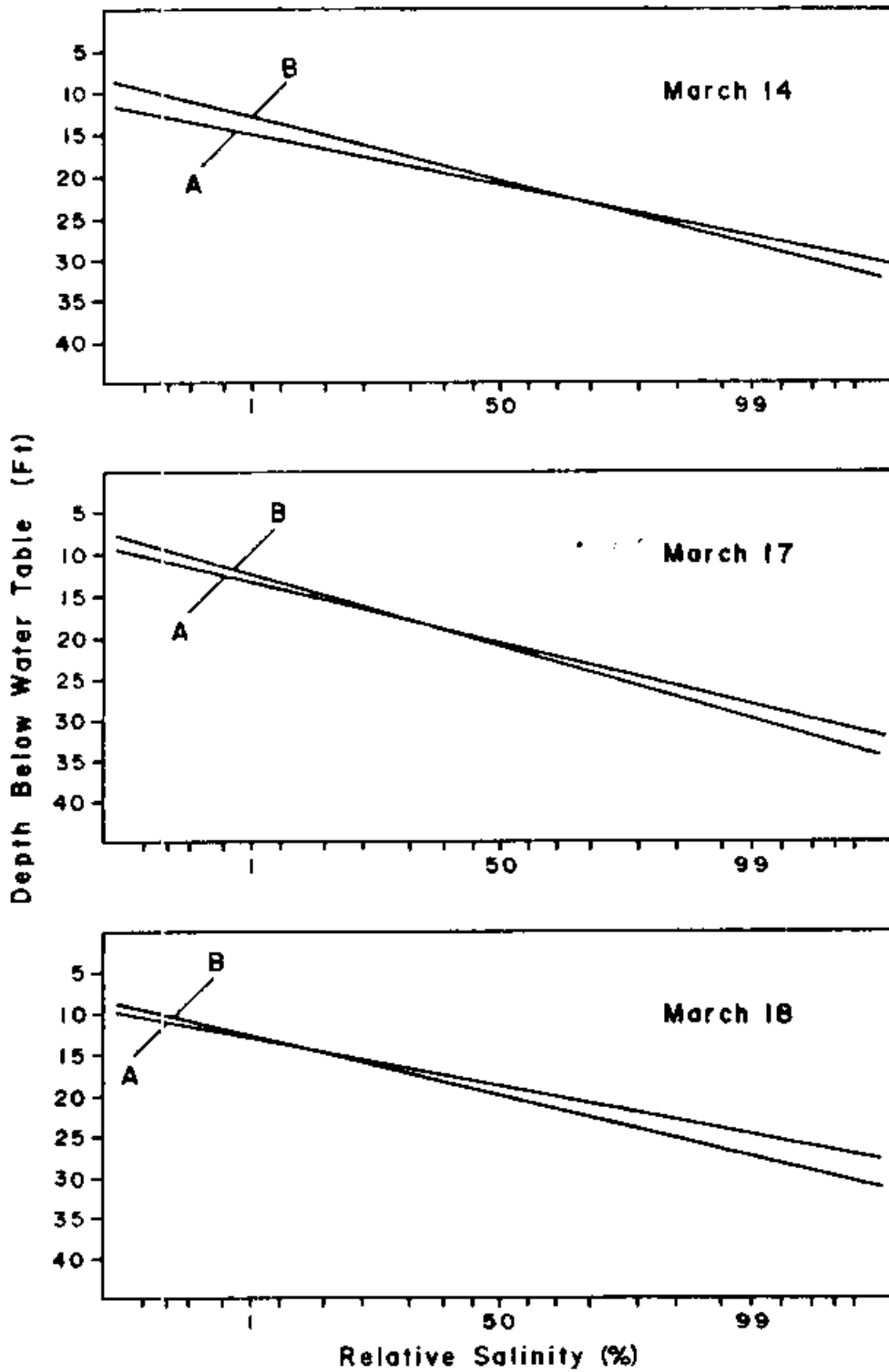


Figure 49. Probability plots of relative-salinity profiles at DS3. Each pair of profiles represents measurements at low tide (A) and high tide (B).

It is now readily apparent why, on some islands similar to Deke, salt-water intrusion into cultivated areas occurs. From first-hand observations, the favored area for growing food plants, taro in particular, is within the central depression. The usual practice is to remove the original sediments down to about the ground-water level and refill with organic matter until a relatively thick humus soil is produced; planting takes place within this new soil. As time passes and the demand increases for additional food to support the community, the area of cultivation is gradually enlarged. Enlargement usually is toward the ocean shoreline. It was long ago realized by islanders that the freshest groundwater was available near the lagoon and this was the logical place upon which to settle. For many islands the expansion was extended over the reef-flat plate and the highly-permeable unit beneath. During the dry season when there is little recharge available to maintain the lens configuration, the greatest reduction in fresh-water storage occurs within the highly-permeable units. The fresh-water column decreases and the transition-zone thickness increases resulting in a well-mixed brackish-water zone underlying the food crop. With the strong tidal pumping action through the reef-flat plate, very saline water enters the root zone of the cultivated taro. Thus, enlargement of taro patches toward the ocean shoreline should be avoided and the thickness of the soil layer in the taro patch should be maintained by constant filling with organic material.

Groundwater beneath atoll islands is subject to contamination by the day-to-day activities of the inhabitants. Nitrate, phosphate, and microbial contamination are the most common. Control of this situation could be gained by properly designing and locating washing and toilet facilities and, in some cases, livestock impoundments taking into account the following: (1) the ability of the unsaturated zone to filter organic substance; (2) the pattern of ground-water flow; (3) the hydraulic constraints of the system; (4) the location of discharge zones; and (5) the resident time of water within the flow system. As an example, for lens systems similar to Deke, water-sealed toilets or pit latrines and washing facilities should be located very near the shoreline to avoid contamination of wells up gradient. The best location is on the ocean-facing shore, but in most cases this is the furthest distance from the village and thus is not preferable by the community. A second location is the outskirts of the occupation area and along the shoreline. Toilet facilities should be engineered such that a sufficient unsaturated zone beneath the unit is available for filtration of the waste material. If sanitary facilities must be located within the village area, then they must be located sufficiently down gradient from potable water wells such that seasonal changes in the flow pattern will not cause contamination of ground-water sources. However, a very detailed on-site study may be necessary to properly site the facility.

A potentially dangerous problem for the atoll situation is the use of fertilizers and pesticides. If the groundwater is consumed, under no circumstances should these agricultural products be used. Toxic chemicals are easily leached from the soil and enter the flow system directly. These compounds are not absorbed by the carbonate sediments of the aquifer nor are they broken down by the groundwater.

Water shortages experienced by island inhabitants during the annual dry season or during droughts, for the most part, could be avoided with proper well design and appropriate location. Most lens systems are fairly stable even during extended times of little or no rainfall. With accurate mapping of the fresh-water lens, the resource could be sensibly developed to meet the needs of the community. In general, the best area to place potable-water wells is half way between the lagoon shoreline and the edge of the reef-flat plate. This locality should be situated over the thickest part of the fresh-water lens provided that the area is of a sufficient width that will allow enough recharge in order to maintain the system. Field measurements may be necessary to determine what the "sufficient width" will be. All wells used for potable water should be located up gradient from sanitary facilities.

#### Guidelines for Further Study

If sensible decisions are to be made related to the practical solutions to water-related problems on atoll islands, then the effort of acquiring new information must be continued because the picture is by no means complete at this time. The work on Deke has produced a foundation upon which to build. We have acquired a great amount of information about the system, however, we do not know many important factors or understand all the processes that govern the dynamics of the atoll-island system.

We know the general characteristics of the various hydrogeologic components and their respective influence on the groundwater-flow system of Deke. We do not know if these same hydrogeologic units are common to atoll island systems elsewhere. If they are common and a general model of atoll geology can be formulated, then the extent of the fresh-water resource beneath any given island can be estimated involving minimal field work and costs.

We know that there is a contrast in permeability across the island and also with depth. We do not know the value of permeability for each hydrogeologic unit. It is important to acquire this information because estimates of safe yield for any groundwater-flow system are based on calculations where the central parameter of the equations is permeability. On a smaller scale, permeability is an important factor in the determination of well yields and safe pumping rates (in order to avoid salt-water upconing).

We know the short-term behavior of the lens system in response to sea-level fluctuations and rainfall events. We do not know the seasonal or long-term behavior of the fresh-water lens. Tidal oscillations recorded in the lagoon of Pingelap Atoll represent particular conditions within a closed lagoon. Because of the pronounced tidal effects in the lens it is important to know how the tides differ in open lagoons and if the size, depth, and configuration of the lagoon contribute to these differences. In terms of lens response to recharge or rainfall events, it is of particular interest to know the behavior of the system under conditions of extended dry periods or drought. Many inland communities across the Pacific region suffered severe water shortages due to the drought produced by the 1983 El Niño. In many instances, the lens became the only source of fresh-water.

The main question to be addressed is: How long can a lens system maintain itself under conditions of little or no rainfall?

We know the general pattern of flow within the lens system of the uninhabited island of Deke. We do not know the flow pattern that may exist given the same hydrogeology but with the influence of human occupation. Taro cultivation is one of the main sources of food production and the practice usually involves a significant portion of an island. Because of the method of cultivation, mentioned above, the planted area has the potential of exchanging large volumes of water between the atmosphere and the lens system. The main processes are evapotranspiration (dominate during dry periods) and recharge by direct rainfall. There is no doubt that these processes will produce a flow pattern different than that of Deke. The question is: How much different will the flow pattern be and what seasonal effects will be produced? Also, the question arises: How will the water quality be affected by seasonal changes in flow patterns?

It is often said that scientific investigations produce more questions than answers. This is partially true for the Deke study. Because of the discoveries made during the course of the investigation, a new set of questions must be addressed. The hydrogeology and groundwater-flow system of Deke is probably not unique. Numerous atoll islands in the Western Pacific exhibit similar characteristics. An example is Nukuoro Island located on Nukuoro Atoll some 300 miles southwest of Ponape (see Ayers and Clayshulte, 1983). Because of the potential for the existence of similar systems as that of Deke and because a firm foundation has been laid by the results of the Deke study, it is extremely important that this work be extended to other areas.

As an aid to future investigative activities related to atoll island hydrogeology, the following set of guidelines and suggestions are presented.

1. Identification of major hydrogeologic components. Two general methods are used to obtain subsurface information; these methods are drilling and geophysical surveys. Drilling strategies may include hand or power augering where sediments are non-indurated, core drilling where sediments are well cemented, and bailer sampling (sampler is driven into the ground and a sediment sample is retrieved) where sediments are poorly consolidated. Core drilling is best suited for the reef-flat plate and the associated underlying units. The driller should be prepared to use foam or mud as a circulating fluid and to case the borehole to prevent caving. The geophysical technique best suited for the determination of subsurface strata is seismic refraction. Although experience is necessary for both the field operation and the data analysis, the technique is an extremely valuable information-gathering tool. Best results are obtained by running as many lines as field conditions will allow. It is suggested that a stronger energy source other than the hammer system be used in order to obtain a clear record that reflects the subsurface structure.

2. Determination of the hydraulic properties of the major hydrogeologic units. The properties of porosity and permeability are the most important and are determined by a variety of methods; several should be attempted in order to establish a confirmed set of values. Among the methods best suited for the small island setting are (1) small-scale pumping tests, (2) tracer studies, (3) tidal responses, (4) laboratory measurements, and, if sufficient information is available, (5) analytical numerical model studies.
3. Determination of the configuration of the fresh-water lens and its associated transition zone. Numerous methods can be employed to obtain information related to this topic. First, a network of observation wells should be established. This networks must be accurately surveyed such that precise elevations are known at each observation site. If a hard substrate is encountered, then peizometer pairs should be installed (ideally, nested peizometers should be installed). Once established, measurements should be taken on a periodic basis, preferably daily. Observation wells are established by drilling, augering, or driving in well points depending on the subsurface conditions. Several observation wells should penetrate the fresh-water column and transition zone. Salinity profiles can be measured in these wells. A second method is the utilization of earth-resistivity measurements. Although this techniques should be verified by measurements in observation wells, it can be used where observations wells are not present or difficult to install or when reconnaissance information is needed. Results from verified soundings can be extrapolated to unknown areas.
4. Determination of the response of the groundwater-flow system to external factors. Of importance is the behavior of the flow system to sea-level oscillations and rainfall events. Tide gages with continuous recorders should be established in the lagoon as well as in the ocean. As exemplified by the Deke study, the lagoon tide may be very different from that of the ocean and may produce a very pronounced effect on the groundwater levels observed in wells. At least one rainfall gage should be established on the study island and readings taken each day. Depending on the detail to which water-budget calculations are to be made, other relevant weather information should be collected. In addition, several observation wells should be equipped with continuous water-level recorders. If few recorders are available (and this is the usual case), then a schedule of recorder rotation between sites should be established.
5. Establishment of flow directions in the subsurface. This topic is an important one in that the pattern of ground-water flow will determine where the best locations are for wells, sanitary facilities, livestock confinements, and other features that may affect the quantity and quality of the fresh-water resource. Flow patterns are determined by direct measurement methods such as artificial tracer studies and by numerous indirect techniques.

Among the latter are (1) construction of flow nets from head distribution data, (2) flow directions based on water-quality patterns, and, again, if sufficient data are available, (3) application of models.

6. Determination of water quality. The importance of this topic is obvious; groundwater must be fit to drink. Water samples should be collected on a periodic basis and as many constituents as possible should be measured in the field. This process should include the analysis necessary to determine the presence of certain bacteria and viruses. If a particular constituent can not be measured in the field, then necessary steps should be taken to prepare the water sample for later shipment to the laboratory.

## SUMMARY

## Water-Level Monitoring Program

1. Ground-water tides in the northern part of the island are like those in the open ocean in that the time between highs and lows is the same for both locations. Wells close to the lagoon have the lagoon-type inequality of high-to-low and low-to-high time intervals. The lagoon tide is mixed semidiurnal.

2. The range of the tidal fluctuation diminishes inland and there is an inland-increasing time lag for the occurrence of the highs and lows. Close to the shoreline, the tidal range is considerably larger in the north than in the south in part because the range in the lagoon is considerably less than in the open ocean. Overall, the lateral attenuation of the tidal signal is such as to dampen a 1.5 m fluctuation in the north and one of 0.9 m in the lagoon to less than 15 cm in the interior of the 300 m-wide island. It takes 3 to 4 hours for the tide signal to reach the interior.

3. Where the hard layer is present, the tidal fluctuation is larger and generally occurs earlier in the ground-water body beneath the hard layer than in the water that rests on the layer. This difference is clear proof that the hard layer acts as a confining bed. As the confining bed pinches out to the south, the tidal fluctuation in the confined aquifer becomes less different than and eventually becomes identical with the fluctuation in the unconfined layer. In the northern part of the island, the top of the hard layer lies within the range swept out by the piezometric tidal fluctuation, and the rocks above the hard layer are, as a result, dry during part of the tide cycle. In at least one area (E2, E3), the hard layer lies below the ground-water low-tide level, and there is a seemingly permanent unconfined aquifer at that locality.

4. There is a pronounced asymmetry of the lagoon tidal variation due to the impeded exchange between the open ocean and the lagoon. The lows are truncated. The lows lag some 2hr 20min more than the highs so that, on the average, the time between a high and a low is 7hr 48min and that between a low and high is 4hr 17min.

5. There is a substantial day-to-day variation in the water levels at all the wells. The principal control is the variation in daily sea level as measured in the lagoon. Rainfall also causes obvious increases.

6. Water-level fluctuations that are related to sea-level variation reflect the 14-day tide characteristics. This sea-level variation is dampened out laterally as it progresses inland through the island. As a result, the day-to-day variability is largest in wells close to the shoreline, although all the wells in the island are affected, and the overall pattern is that all the wells rise and fall in unison.

7. The day-to-day water-level variability in the unconfined water above the hard layer is larger than that measured in drilled or dug-through piezometers. This is probably a rainwater-catchment effect. It appears also that, during wet periods, the level in the unconfined layer is slightly higher than the piezometric surface. However, the difference is

might: the first-order result is that, over a period of some weeks, the average at a piezometer is about the same as that at an adjacent standpipe.

8. Water levels averaged over the 21-day period define a water-level ridge that occurs on the lagoon side of the island, south of the hard layer. This ridge marks the region where the system is under water-table conditions and is the recharge area for the confined aquifer that underlies the hard layer to the north.

### Geomorphology and Geology

1. Deke is characteristic of small islands composed of coarse coral detritus that occupy the reef flats of many atoll platforms. This coral rubble is swept from the reef front by large storm waves and spread across the reef flat and low-lying islands. Horizontal sheets of water from waves breaking on the reef front transport and accumulate sand and gravels as ridges and aprons behind these ridges.

2. Initially, Deke appears to have formed as two small separate islands. Each of these small islands was surrounded on three sides by well-developed ridges of coarse coral gravel. The former tidal pass between the two islands is represented by a north-south zone of sandy coarse pebbles that cuts through the center of the island.

3. Currently, the island is prograding lagoonward as evidenced by the reef-derived sediments accumulating on the lagoon beach and ridge and the angle-of-repose slope just offshore in the lagoon. Further evidence is provided by extensive development of flood tidal deltas and spits along the southeastern and southwestern margins of the island (which gives Deke a concave shape to the south).

4. The surface geology is composed of four main components: a ridge composed of cobbles and boulders adjacent the ocean shoreline; a series of coalescing wash-over fans consisting of coarse pebbles and cobbles behind the boulder ridge; a narrow band of coarse to medium pebbles and sand more or less centrally located; and a low berm composed of sand with scattered medium pebbles along the lagoon shoreline.

5. The subsurface geology beneath Deke is comprised of several distinct units. Underlying part of the island unit is the reef-flat plate (hard layer). This unit is well indurated and wedge shaped, thinning lagoonward and grading into partially unconsolidated sediments of the sand apron unit. Partially consolidated and unconsolidated sediments underly the reef-flat plate. Thickness of this sediment package varies considerably across the island. Similar to the reef-flat plate, this unit appears to grade lagoonward into unconsolidated sediments of the sand apron. A Halimeda-rich unit underlies these sediments to an unknown depth. Physical properties of the Halimeda facies appear to be similar to the overlying material but may differ locally to a great extent as the variability of seismic velocities suggests. The Halimeda facies appears to grade into less indurated sediments toward the lagoon.



## Hydrogeology and Groundwater Occurrence

1. There are four main components comprising the hydrogeology of the study area: the sediments comprising the island; the reef-flat plate; the sand apron behind the plate; and the partly consolidated, partly unconsolidated sediments beneath the reef flat. Each of these units plays a unique role in the hydrology of Deke island.

2. The main function of the island unit is to catch rainwater and transmit it to the subsurface flow system. Numerous aspects of the hydrologic cycle such as plant interception and evapotranspiration are involved in the transmittal process.

3. A significant component of the hydrogeology is the reef-flat plate or hard layer. The plate acts as a leaky confining bed and extends over a large portion of the flow system.

4. Fresh groundwater is stored within the two remaining units. It appears that the sand-apron unit has a lower permeability than the sediments beneath the reef-flat plate. The latter unit seems to be associated with the plate and may be a non-indurated equivalent.

5. Fresh groundwater occurs as a complex lens displacing sea water. The configuration of the lens is asymmetric with the thickest part located within the less permeable unit adjacent the lagoon shoreline.

6. Where the reef-flat plate is present the system is under confined conditions; elsewhere, the system is under water-table conditions. Primary recharge to the system takes place over the area not underlain by the plate.

7. Flow directions follow two routes, one from the groundwater divide directly to the lagoon beach face and the other toward the ocean beneath the reef-flat plate exiting the system somewhere between the island shoreline and the reef.

8. The transition zone between fresh and salty groundwater is created and maintained by sea-level fluctuations, particularly the tides. Its thickness is dependent on the frequency of the sea-level oscillation and on the permeability of the aquifer. The thinnest transition zone is associated with the less permeable unit adjacent the lagoon shoreline.

9. An unexpected behavior of the transition zone in response to tidal fluctuations is to thicken and thin with rising and falling sea level, respectively. This response is apparently a more efficient means of conserving energy or mass than vertical displacement as a unit.

## ACKNOWLEDGMENT

The hydrogeologic investigation of Deke Island, Pingelap Atoll was a major undertaking by the Water and Energy Research Institute (WERI). A year of planning was necessary to ensure that the field work would be completed and reasonable results would be obtained. Because of the remoteness of the study area there was little room for planning error and logistical mistakes. The successful and timely completion of the project required cooperation between the WERI, the Ponape State Government and certain key members of the Pingelap Community Council. It also required a tremendous effort on the part of the research team working long hard days and living under adverse conditions.

Because the following report is the result of a team effort, it is appropriate to identify the members and their respective areas of responsibility. The initial team consisted of two members from the WERI and three members from the Department of Geology, University of South Florida. While in the field, during the later two weeks, the team was joined by two members from the Department of Geology, University of Kansas.

The principal investigator for the project and research team leader was Jerry F. Ayers, Assistant Professor, WERI. His area of responsibility included preparation of the initial project proposal, planning and organization of the field activities, overseeing the purchase of supplies and equipment, coordinating activities related to personnel and equipment transport, coordinating activities associated with the field work and data analysis, conducting geophysical surveys and drilling operations in the field and, finally, preparation of the final report.

A second team member from the WERI, Russell N. Clayshulte, Research Associate, was responsible for the liaison between the WERI and the community of Pingelap Atoll through a pre-project visit to the island. Also associated with the visit was the finalization of transport plans with the Ponape State Government. Additional areas of responsibility included assistance with the project planning stage and other pre-project activities, conducting water-quality surveys in the field, assistance in conducting geophysical surveys and in the drilling operations, general assistance to other field activities, and preparation of appropriate sections of the final report.

Special consultant to the project was H. Leonard Vacher, Associate Professor, Dept. of Geology, University of South Florida. His main areas of responsibility were the supervision of the water-level investigation and the supervision of the superficial geologic mapping program. Various tasks associated with these activities included conducting topographic and elevation surveys, collecting and analyzing water-level data, and overseeing the collection and analysis of geologic information. An additional responsibility was reporting the results and interpreting the data from the water-level investigation sector of the project.

The project was aided by two field assistants David Strout and Richard Stebnisky, Graduate Student, Dept. of Geology, University of South Florida. Both assisted in all aspects of the field work. On an individual basis, David's main responsibilities were the collection and analysis of surface

geological and stratigraphic information and the subsequent reporting of that information and Richard's main tasks were the installation of observation wells and collection and analysis of water-level data.

The project was later joined by Paul Enos, Associate Professor and Michael May, Graduate Student, Dept. of Geology, University of Kansas. Although not part of the research team as originally proposed, their involvement in the project was greatly appreciated. When it was discovered that the hard layer was a major component of the hydrogeology of Deke and that its extent must be known, Paul and Mike took on the responsibility of mapping the hard layer. This task also involved the collection of samples, which was not a simple matter.

The research team members extend their appreciation to the numerous individuals that made the project a success. In particular we thank Mr. Kikuo Apis (Director) and members of his staff, Division of Conservation and Natural Resource Surveillance, Ponape State Government, for their logistical support and coordinating activities without which the project probably would not have gotten to the field work stage. In addition, we extend a well-deserved thanks to Mr. Ihoud Amos for his tireless assistance in all aspects of our field work. Without his invaluable help field work certainly would not have progressed to the stage that it did. Finally, we thank the people of Pingelap Atoll for allowing us to conduct our study on their island and we appreciate the help contributed by the concerned citizens.

## REFERENCES CITED

- American Public Health Association, 1980. Standard methods for the examination of water and wastewater. 15th ed. American Public Health Association, Washington D.C., 1193 pp.
- Ayers, J. F., 1980. Unsteady behavior of fresh-water lenses in Bermuda with applications of a numerical model. Ph.D. Dissertation, Washington State Univ., Pullman, Washington, 300 pp.
- Ayers, J. F., and R. N. Clayshulte, 1983. A preliminary investigation of salt-water intrusion on Nukuoro Island, Nukuoro Atoll, Ponape State. Univ. of Guam, WERI Technical Report No. 42, 90 pp.
- Ayers, J. F. and H. L. Vacher, 1983. A numerical model describing unsteady flow in a fresh water lens. Water Res. Bull. v. 19, no. 5, p. 785-792.
- Dobrin, M. B., 1976. Introduction to geophysical prospecting. McGraw Hill, Inc., 630 pp.
- Emery, K. O., J. I. Tracey, and H. S. Ladd, 1954. Geology of Bikini and nearby atolls. U.S. Geol. Surv. Prof. Pap. 260-A, 265 p.
- Scott, J. H., E. L. Tibbetti, and R. G. Burdich, 1972. Computer analysis of seismic refraction data. U. S. Dept. of Interior, Bureau of Mines Report of Investigation RI-7595, 95 pp.
- Telford, W. M., L. P. Geldart, R. E. Sheriff, and D. A. Keys, 1976. Applied geophysics. Cambridge University Press, New York, 860 pp.
- Todd, D. K., 1959. Ground water hydrology. John Wiley and Sons, New York, 336 pp.
- Vacher, H. L., 1974. Groundwater hydrology of Bermuda, Gov. Bermuda, Public Works Dept., Hamilton, 87 pp.
- Wunsch, C., 1972. Bermuda sea level in relation to tides, weather and baroclinic fluctuations. Rev. of Geophys. and Space Phys., v. 10, 1-49.
- Zohdy, A. A. R., 1974. A computer program for the calculation of Schlumberger sounding curves by convolution. U. S. Geol. Surv. Open File.
- Zohdy, A. A. R., G. P. Eaton, and D. R. Mabey, 1974. Application of surface geophysics to ground-water investigations. U. S. Geol. Surv. Techniques of Water-Resources Investigation, Book 2, Chapter D1, 116 pp.

## APPENDIX A

## CONTENTS

## Page

## Tables -- Water-Level Data

A1. Water levels at observation wells.....	124
A2. Reduced water levels at observation wells.....	127
A3. Tidal highs and lows in lagoon and at observation wells (from continuous recordings).....	130
A4. Tidal data from the study of March 18, 19, 20.....	134
A5. Mean daily sea level from lagoon recorder station.....	138

## Figures -- Continuous Recordings

A1. Lagoon recorder station, February 13 to March 21.....	139
A2. Well B4 recorder station, February 18 to March 2.....	144
A3. Well C4 recorder station, February 18 to March 9.....	146
A4. Well C5 recorder station, February 25 to March 15.....	149
A5. Well D1 recorder station, March 3 to March 16.....	152
A6. Well E2 recorder station, March 16 to March 21.....	154
A7. Well E3 recorder station, March 9 to March 21.....	155

## Tables -- Weather Data

A6. Rainfall and atmospheric pressure.....	157
A7. Other weather observations.....	162



Table A1. continued

Well	2/29	3/1	3/2	3/3	3/4	3/5	3/6	3/7	3/8	3/9	3/10
A1	27.8	29.6	34.0	34.8	35.3	33.9	31.9	31.5	31.8	31.8	40.3
A2	29.2	28.8	33.0	34.0	32.6	33.7	31.8	31.9	32.2	32.7	40.8
A3	27.7	28.0	30.5	32.0	30.6	32.4	30.3	30.0	30.8	31.0	36.5
A4	24.4	26.3	31.5	32.1	30.9	31.8	30.7	30.4	29.7	29.6	36.9
B1	27.9	30.7	38.2	42.5	36.5	34.2	31.3	30.2	31.6	30.6	34.5
B2	27.3	30.1	34.6	35.5	34.0	35.1	33.2	31.9	32.1	31.8	43.5
B3	29.9	32.3	36.1	40.5	31.5	35.4	29.7	29.5	32.3	31.7	34.8
B4(R)	(29.4)	(28.6)	(30.5)					32.4	29.9	32.7	41.4
C1	26.1	26.8	28.4	31.7	32.2	31.6	32.0	30.9	31.2	30.9	36.1
C2	28.8	30.0	34.0	35.2	34.8	35.0	32.9	31.6	32.1	31.9	36.5
C3	27.3	30.3	34.5	36.6	34.4	34.9	32.9	32.2	33.2	32.2	37.4
C4(R)	(26.5)	(27.2)	(30.4)	(31.4)	(30.8)	(31.2)	(30.0)	(29.2)	(29.6)	(27.8)	35.9
C5(R)	(27.9)	(28.0)	(33.8)	(34.6)	(33.0)	(33.9)	(31.7)	(31.2)	(30.6)	(30.7)	(35.8)
D1(R)	28.7	26.4		(47.1)	(37.8)	(34.8)	(30.6)	(29.5)	(28.7)	(26.7)	(30.7)
D2			36.5	37.3	35.0	35.6	27.5	26.6	29.2	29.3	31.7
D3	26.9	29.3	35.4	36.5	35.7	34.6	29.4	28.4	29.5	28.9	38.2
D4											25.9
E1	27.3	30.5	36.1	37.2	35.0	34.5	30.5	29.7	31.4	31.3	34.0
E2	23.7	26.6	36.9	35.3	34.7	33.8	32.5	32.8	33.0	30.9	41.4
E2R											
E3(R)	25.0	26.2	36.4	32.7	31.7	32.0	30.7	32.0	31.1	(29.6)	(37.7)
E4	29.1	31.9	37.3	39.4	32.7	32.9	30.8	29.9	31.6	31.3	39.2
E5			37.5	28.1	26.2	35.9	31.6	30.6	31.2	31.2	37.8

Well	3/11	3/12	3/13	3/14	3/15	3/16	3/17	3/18	3/19	3/20	3/21
A1	35.6	33.7	29.0	27.4						34.9	
A2	37.9	34.2	31.6	28.9						33.6	
A3	34.1	31.5	29.9	26.3						30.9	
A4	32.1	29.2	26.7	24.8						32.9	
B1	33.7	28.5	26.3	25.8						34.6	
B2	37.5	31.5	30.2	26.7						36.5	
B3	30.7	26.6	28.3	27.7						34.0	
B4 (R)	39.2	34.8	32.9	29.5						33.6	
C1	39.5	33.9	29.1	26.3						32.9	
C2	36.7	32.5	28.8	27.4						35.4	
C3	34.1	29.5	26.6	25.6						36.0	
C4 (R)	37.4	32.7	28.8	26.5						32.0	
C5 (R)	(34.6)	(30.1)	(27.8)	(28.5)	(35.5)						
D1 (R)	(31.7)	(29.6)	(27.9)	(30.3)	(46.8)	(33.2)					
D2	31.9	33.0	28.9	29.4						30.6	
D3	34.4	31.3	27.0	25.5						32.9	
D4	46.2	31.9	33.0	38.3						20.5	
E1	33.9	28.5	26.0	25.0						34.6	
E2	41.9	34.7	28.7	25.2						34.3	
E2 (R)						(32.1)	(32.5)	(34.8)	(34.9)	(33.4)	(31.2)
E3 (R)	(38.3)	(32.5)	(28.5)	(25.6)	(29.9)	(32.7)	(31.4)	(31.8)	(33.7)	(31.1)	(30.7)
E4	31.6	27.7	26.1	26.0						39.4	
E5	33.7	28.9	26.7	26.0						36.1	
B5										18.9	
B6										24.0	
Pz1										21.9	
Pz2										26.5	
Pz3										15.4	





Table A2. continued

Well	2/29	3/1	3/2	3/3	3/4	3/5	3/6	3/7	3/8	3/9	3/10
A1	10.0	12.3	11.4	6.4	8.0	7.3	6.9	10.2	7.3	10.1	21.5
A2	11.4	11.5	10.4	5.6	5.3	7.2	6.8	10.6	7.7	11.0	22.0
A3	9.9	10.7	7.9	3.6	3.3	5.7	5.3	8.7	6.3	9.3	17.7
A4	6.6	9.0	8.9	3.7	3.6	6.1	5.7	9.1	5.2	7.9	18.1
B1	10.1	13.4	15.6	14.1	9.2	6.7	6.3	8.9	7.1	8.9	15.7
B2	9.5	12.8	12.0	7.1	6.7	8.6	8.2	10.6	7.6	10.1	24.7
B3	12.1	15.0	13.5	12.1	4.2	5.1	4.7	8.2	7.8	10.0	16.0
B4(R)	(11.6)	(11.3)	(7.9)					11.1	5.4	11.0	22.5
C1	8.3	9.5	5.8	3.3	4.9	7.4	7.0	9.6	6.7	9.2	17.3
C2	11.0	12.7	11.4	6.8	7.5	8.3	7.9	10.3	7.6	10.2	17.7
C3	9.5	13.0	11.9	8.2	7.1	8.3	7.9	11.0	8.7	10.5	18.6
C4(R)	(8.7)	(9.5)	(7.8)	(3.0)	(3.5)	(6.60)	(4.6)	(7.9)	(5.1)	(6.1)	17.0
C5(R)	(10.1)	(10.7)	(11.2)	(6.2)	(5.8)	(9.3)	(6.7)	(9.9)	(6.1)	(9.0)	(16.9)
D1(R)	10.9	9.1		(18.7)	(10.5)	(10.2)	(5.6)	(8.2)	(4.20)	(5.00)	(11.8)
D2			13.9	8.9	7.7	11.0	2.5	5.3	4.7	7.6	12.8
D3	9.1	12.0	12.8	8.1	8.4	4.8	4.4	7.1	5.0	7.2	19.4
D4											7.0
E1	9.5	13.2	13.5	8.8	7.7	5.9	5.5	8.4	6.9	9.6	15.2
E2	5.9	9.3	14.3	6.9	7.4	7.9	7.5	11.5	8.5	9.2	22.3
E2(R)											
F3(R)	7.2	8.9	13.8	4.3	4.4	7.4	5.7	10.7	6.6	(7.9)	(18.8)
F4	11.3	14.6	14.7	11.0	5.4	6.2	5.8	8.6	7.1	9.6	20.4
F5			14.9	-0.3	-1.1	11.3	6.6	9.3	6.7	9.5	18.9

Well	3/11	3/12	3/13	3/14	3/15	3/16	3/17	3/18	3/19	3/20	3/2
A1	17.3	21.3	14.6	15.5							
A2	19.6	21.8	17.2	17.0							
A3	15.8	19.1	15.5	14.4							
A4	13.8	16.8	12.3	12.9							
B1	15.4	16.1	11.9	13.9							
B2	19.2	19.1	15.8	14.8							
B3	12.4	14.2	13.9	15.8							
B4(R)	20.9	22.4	18.5	17.6							
C1	21.2	21.5	14.7	14.4							
C2	18.4	20.1	14.4	15.5							
C3	15.8	17.1	12.2	13.7							
C4(R)	19.1	20.3	14.4	14.6							
C5(R)	(16.3)	(17.7)	(13.4)	(16.6)	(1.6)						
D1(R)	(13.4)	(17.7)	(13.5)	(18.4)	(12.9)	(0.9)					
D2	13.6	20.6	14.5	17.5							
D3	16.1	18.9	12.6	13.6							
D4	27.9	19.5	18.6	26.4							
E1	15.6	16.1	11.6	13.1							
E2	23.6	22.3	14.3	13.3							
E2(R)						(-0.2)	(1.2)	(5.3)	(3.7)	(-0.5)	
F3(R)	(20.0)	(20.1)	(14.1)	(13.7)	(4.1)	(0.1)	*2.3)	(2.5)	(-2.8)		
F4	13.3	15.3	11.7	14.1							
E5	15.4	16.5	12.3	14.1							

Table A3. Tidal highs and lows in lagoon and at observation wells (from continuous recordings).

Date	No.	Lagoon		B4		C4		C5	
		Time	Elev.	Time	Elev	Time	Elev	Time	Elev
2/13	1	2133	12.0						
2/14	2	0329	23.5						
	3	0823	13.5						
	4	1340	61.5						
	5	2225	10.5						
	6	0249	31.0						
2/15	7	0916	11.5						
	8	1500	82.5						
	9	0005	5.7						
2/16	10	0416	32.8						
	11	1054	5.8						
	12	1547	7.3						
	13	0106	3.6						
2/17	14	0411	42.3						
	15	1211	2.0						
	16	1604	94.0						
	17	0157	2.5						
	18	0439	49.4						
2/18	19	1301	2.0			1340	29.0		
	20	1636	97.5	1900	44.7	2035	40.2		
	21	0116	3.2	2352	26.2	0225	31.6		
	22	0500	57.6	0654	39.8	0810	37.0		
	23	1240	3.1	1114	23.4	1412	28.7		
	24	1736	90.0	1942	43.5	2108	39.0		
	25	0130	4.5	0013	25.9	0311	29.2		
2/20	26	0556	61.4	0803	39.8	0905	37.0		
	27	1418	5.0	1202	25.4	0316	29.6		
	28	1754	86.4	2028	42.8	2117	(38.2)		
	29	0054	6.5	0008	29.2	0316	32.7		
2/21	30	0700	72.5	0843	44.1	0919	(40.0)		
	31	1400	1.3	1354	33.3	1520	35.0		
	32	1838	63.3	2057	45.8	2150	41.6		
	33	0333	3.7	0231	32.3	0442	34.5		
2/22	34	0705	55.5	0932	43.6	1025	40.2		
	35	1511	4.9	1508	32.7	1657	34.5		
	36	1907	34.5	2103	39.0	2145	37.2		
	37	0336	3.2	0257	26.6	0445	29.7		
2/23	38	0758	50.5	0957	37.9	1126	35.4		

Date	No.	Lagoon		B4		C4		C5	
		Time	Elev.	Time	Elev	Time	Elev	Time	Elev
	39	1:38	8.9	1529	30.7	1748	31.9		
	40	1:23	24.6	1921	33.8	2052	32.7		
2/24	41	0:34	7.2	0227	25.6	0458	27.8		
	42	0:24	39.1	1111	35.1	1245	33.9		
2/25	43	0:36	8.0	0307	25.5	0459	25.9	0400	24.0
	44	1:29	35.3	1329	34.9	1538	32.1	1549	32.1
	45	2:08	10.7	2326	26.1	0351	26.3	(0314)	(25.1)
2/26	46	14:15	43.2	1329	36.8	1642	33.4	1608	34.7
	47	2:35	6.8	2233	25.7	0113	26.7	0123	24.8
2/27	48	0:22	17.0	0238	28.2	0403	27.3	0414	(25.6)
	49	0:02	10.8	0727	25.8	0925	25.5	0900	23.6
	50	14:09	49.0	1438	36.7	1718	32.8	1638	33.8
	51	2:22	3.6	2219	23.1	0101	24.8	0024	22.7
2/28	52	0:19	22.0	0303	28.8	0512	26.9	0417	25.7
	53	0:53	4.4	0836	21.6	1038	22.7	1002	20.7
	54	14:41	56.4	none	none	(1832)	(32.8)	1713	33.5
2/29	55	0:20	3.0	2240	21.6	2143	(24.8)	0036	22.2
	56	(0430)	29.5	0339	30.0	(0338)	(28.4)	0451	26.9
	57	1:35	22.9	0923	20.8	1105	21.9	0958	20.6
	58	1:22	63.6	1643	38.2	1815	32.9	1729	36.2
	59	2:52	-0.8	2341	22.6	0045	24.8	0012	25.1
3/1	60	0:47	30.5	0458	32.4	(0536)	(30.5)	0451	30.2
	61	1:29	2.4	1001	20.6	1150	22.8	1038	23.0
	62	1:16	68.8	1713	38.9	1846	33.7	1917	37.1
3/2	63	0:40	4.4	2350	26.2	0109	28.4	0159	29.6
	64	0443	40.5	0454	37.2	0636	32.9	0542	34.4
	65	11:01	6.5	1111	24.5	1206	26.6	1112	27.6
	66	1:17	81.4			1903	36.3	1852	41.1
	67	2:56	7.5			0110	29.3	0204	32.8
3/3	68	0443	52.1			0629	34.5	0706	38.1

Table A3. continued

Date	No	Lagoon		D1		C4		C5	
		Time	Elev.	Time	Elev.	Time	Elev.	Time	Elev.
3/3	69	1138	5.0			1227	27.5	1308	29.2
	70	1653	78.0	1625	55.8	1913	37.7	2012	41.3
3/4	71	0100	4.4	0121	27.1	0132	29.4	0220	31.8
	72	0520	53.5	0438	44.4	0647	34.9	0730	37.8
	73	1249	3.6	1253	20.8	1312	26.8	1343	28.1
	74	(1720)	(76.9)	1742	53.6	1942	35.9	2014	40.1
3/5	75	0110	3.0	0232	23.4	0202	28.3	0216	30.2
	76	(0510)	(55.0)	0609	47.4	0731	34.8	0810	38.2
	77	1248	3.0	1415	21.5	1337	27.5	1350	28.6
	78	1632	75.7	1806	53.0	1951	36.1	2022	40.0
3/6	79	0150	1.1	0301	19.7	0217	28.2	0236	29.4
	80	0530	55.7	0632	45.2	0751	34.2	0821	36.7
	81	1337	0	1501	17.4	1422	26.4	1410	26.5
	82	1748	64.5	1740	47.4	1952	33.4	2028	36.6
3/7	83	0218	0.1	0246	17.0	0236	25.1	0237	26.0
	84	0623	54.6	0616	43.7	0826	32.4	0828	35.6
	85	1443	0.5	1447	17.1	1426	25.6	1430	25.6
	86	1820	49.5	1827	40.7	1950	32.0	2020	34.3
3/8	87	0210	4.0	0300	15.2	0229	23.8	0228	23.9
	88	0559	60.7	0659	44.6	0916	32.6	0929	35.8
	89	1421	5.5	1455	17.5	1521	26.5	(1500)	(25.5)
	90	1800	42.8	1826	37.6	2016	31.0	2104	32.4
3/9	91	0218	3.5	0247	13.9	0246	23.4	0320	22.8
	92	0603	55.5	0722	42.3	0930	32.1	0955	34.4
		Lagoon		D1		E3		C5	
3/10	93	1453	6.4	1533	17.8	1539	27.0	1634	26.6
	94	1830	27.3	1838	30.1	2028	31.0	2056	29.6
	95	0246	3.5	0244	12.5	0240	21.8	0340	21.3
	96	0703	46.0	0812	40.2	1215	45.8	1301	37.0
	97	1524	9.6	1605	24.5	1646	41.8		
	98	2003	18.6	1950	26.7	1831	45.0		

Date	No	Lagoon		D1		E3R		C5	
		Time	Elev.	Time	Elev	Time	Elev	Time	Elev
3/11	99	(0:39)	(6.5)	0323	17.2	0504	36.3	0415	30.4
	100	0:26	40.9	0927	38.2	1246	41.3	1123	37.3
3/12	101	0:46	5.4	(0100)	15.0	0535	28.0	0338	23.1
	102	(1040)	(33.5)	(1100)	36.5	1437	34.3	1327	32.1
	103	2:02	4.9	0013	15.0	0159	24.1	0005	21.3
3/13	104	0:31	10.6	0508	17.9	0402	24.4	0256	21.4
	105	0:24	8.1	0800	17.5	0835	23.4	0746	21.1
	106	1:19	43.2	1354	38.3	1648	32.7	1459	32.0
	107	2:06	1.4	0046	12.9	2339	20.4	2313	20.3
3/14	108	0:02	12.2	0417	19.4	0453	23.8	0243	21.3
	109	0:49	3.7	0951	14.2	0915	19.0	0757	17.7
	110	1:31	60.1	1524	47.0	1753	33.0	1557	34.4
	111	2:28	15.0	2301	29.5	2322	21.8	2154	27.6
3/15	112	0:12	54.0	0411	43.8	0620	30.7	0419	34.8
	113	0:21	19.6	1104	32.5	1106	24.3	1006	30.6
	114	1:43	84.7	1555	60.1	1852	38.9		
	115	2:31	9.0	0058	28.6	0035	26.7		
3/16	116	0:13	50.3	0424	43.5	0646	35.1		
		Lagoon		D1		E3R		E2	
	117	1027	7.4	1206	22.9	1215	24.2	1311	28.4
	118	1:32	92.9			1745	41.0	1956	34.0
	119	2:34	3.7			0008	27.4	0154	32.5
3/17	120	0:50	59.5			0545	37.3	0702	33.9
	121	1:19	2.4			1204	24.3	1350	29.6
	122	1:23	89.2			1811	40.0	1948	34.0
3/18	123	0:42	0.6			0050	25.8	0142	32.1
	124	0:03	66.0			0626	38.1	0846	34.7
	125	1:21	1.0			1257	24.9	1406	33.1
	126	1:20	88.1			1832	40.4	2054	35.3
3/19	127	0:01	1.5			0122	26.4	0254	33.9
	128	0:37	77.0			0704	39.7	0912	35.7
	129	1:29	1.5			1328	26.5	1439	34.3
	130	1:05	79.1			1858	39.5	2106	35.2
3/20	131	0:29	2.5			0156	26.3	0300	33.9
	132	0:12	79.6			0728	39.7	0900	35.5
	133	1:41	2.8			1435	26.2	1548	31.5
	134	1:39	61.5			1938	36.4	2026	33.3
3/21	135	0:15	2.0			0238	23.9	0250	29.1
	136	0:01	73.9			0850	37.6	0847	33.6

Table A4. Tidal data from the study of March 18, 19, 20.

Part A. Times and elevations. All elevations are in cm above the lagoon low tide of 3/6.

(1) March 18

B5 (DS4)			D4 (DS-3)		
Time	Elev		Time	Elev	
902	-36.6		918	-40.0	
937	-41.9		950	-44.4	
1027	-41.6		1038	-41.2	
1114	-38.8		1125	0.3	
1231	9.2		1243	17.4	
1430	79.5		1442	88.0	
1551	100.4		1600	105.8	
1643	98.6		1652	101.4	
1730	85.6		1742	83.4	
1902	36.9		1912	33.1	

Pz1			Pz2		
Time	Elev		Time	Elev	
	Pz	StP		Pz	StP
951	-39.8	dry	1010	19.8	dry
1045	-35.8	dry	1046	12.6	dry
1104	-32.0	dry	1144	13.1	dry
1137	-17.7	dry	1209	15.1	dry
1200	-5.2	dry	1258	21.5	dry
1508	94.8	53.4	1525	43.3	dry
1540	101.2	56.2	1611	46.3	34.7
1630	102.5	52.1	1707	47.8	38.1
1658	96.8	50.3	1757	46.1	39.7
1749	79.8	49.4	1823	44.1	40.1
1937	19.9	dry	1950	34.3	39.1

Pz3		
Time	Elev	
	Pz	StP
1018	24.9	dry
1058	22.1	dry
1158	19.5	dry
1217	19.1	dry
1251	20.1	dry
1309	20.9	dry
1535	35.5	33.2
1621	38.9	36.3
1715	42.5	40.6
1805	44.5	43.6
1836	44.7	44.2
1924	43.6	43.8
1959	41.7	42.6



(2) March 19

B5 (DS4)		B6 (DS5)		Tide Pipe	
Time	Elev	Time	Elev	Time	Elev
1523	78.9	1527	66.3	1520	dry
1558	88.8	1554	73.2	1602	90.5
1638	92.1	1641	77.3	1636	112.1
1722	91.4	1726	76.7	1718	113.6
1736	86.4	1734	75.5	1730	114.4
1746	83.4	1743	74.0	1741	108.7
1849	57.7	1852	55.5	1748	106.9
2300	-42.2	2304	-20.9	1845	95.3
				2256	dry

D4 (DS3)		C1		C2	
Time	Elev	Time	Elev	Time	Elev
1537	89.0	1548	30.7	1627	34.7
1611	95.5	1712	32.4	1811	38.6
1702	96.0	1819	34.5	1911	41.5
1800	82.2	1926	36.2	2025	42.4
1834	67.7	2007	37.1	2125	40.9
		2043	37.2	2214	39.2
		2104	37.5	2235	38.2
		2157	36.3		
		2225	35.7		
		2246	35.2		

C3		C4	
Time	Elev	Time	Elev
1622	33.0	1542	31.2
1807	41.4	1707	33.9
1902	45.0	1827	36.1
1935	46.0	1920	37.1
2016	46.1	1959	37.7
2050	45.2	2035	37.5
2138	43.2	2113	36.7
2206	41.7	2149	35.5

Table A4. continued

(3) March 20

DS4 (I-IN)		DS-5 (I-2S)		Tide Pipe	
Time	Elev	Time	Elev	Time	Elev
1606	67.4	1603	54.7	1610	dry
1618	69.8	1613	56.6		
1623	71.3	1620	59.3	1625	dry
1630	72.2	1628	60.5		
1639	72.9	1637	62.1		
1723	77.6	1720	65.5	1725	86.3
1731	77.4	1729	66.0		
1735	77.0	1733	66.3	1738	87.8
1740	76.2				
1745	76.5	1743	65.7	1748	88.9
1752	75.1	1754	64.3	1757	88.3
1801	74.1	1759	64.1	1804	88.0
1809	70.1	1807	63.8	1812	87.1
1817	70.2	1814	62.4	1820	86.7
1822	67.8	1824	60.9	1827	86.1
1845	59.6	1851	54.9		
1917	47.0	1919	47.5		

Part B. Estimate of tidal range from times and elevations that bracket the high.

The following table gives the results of an attempt to extrapolate the range of the tide cycle from the data of 3/19 and 3/20 when measurements were taken from only a few-hour period bracketing the maximum. Assuming that the tide follows a perfect sine curve

$$h = a \cos (2\pi t/t_0),$$

where  $t$  is minutes before or after the peak,  $t_0$  is 745 min, and  $a$  is amplitude, then

$$h_0 - h_1 = h_0 - h_{-1} = 0.126a$$

and

$$h_0 - h_2 = h_0 - h_{-2} = 0.471a,$$

where  $h_0$ ,  $h_1$ ,  $h_{-1}$ ,  $h_2$ , and  $h_{-2}$  are the elevation at  $t-t_{\max}$ , and at  $t_{\max} +1$ ,  $-1$ ,  $+2$ ,  $-2$  hours. The  $h$ 's are read from smooth graphs drawn from available data of  $h$  vs. time (Part A).

The upper set of figures in the following table show the result from the data of March 18 when the range was measured. The lower set of figures gives the results from March 19 and 20, when the range is an unknown. The

first set is included to give an indication of how well the estimates approximate the real amplitude.

The columns labeled +1, -1 give the calculated amplitudes from the points at respectively +1 and -1 hour from the peak, and  $\bar{a}_1$ , gives their average. The +2, -2,  $\bar{a}_2$  columns are analogous for the 2-hour values. The final column,  $\bar{a}$ , gives the average of  $\bar{a}_1$  and  $\bar{a}_2$ , and is taken as the answer. All figures are included in the table in order to give an indication of the quality of the final estimate. If the various estimates diverge widely, probably because the tidal fluctuation is not a perfect sine curve, the answer is rejected.

Date	Well	+1	-1	$\bar{a}_1$	+2	-2	$\bar{a}_2$	$\bar{a}$	meas.
3/18	B5	79.4	79.4	79.4	80.7	67.9	74.3	77	(73)
	D4	87	63	75	76	74	75	75	(75)
	Pz2	31.8	7.9	19.8	21.2	10.6	15.9	17.9	(18.5)
	Pz3	15.9	11.9	13.9	14.9	10.6	12.8	13.4	(13)
3/19	B5	79.4	43.7	61.6	76.4	65.8	71.1	66.4	
	B6	55.6	39.7	47.7	48.8	44.6	46.7	47.2	
	Tide Pipe	103	175	139	55	114(?)	85	reject	
	D4	71	142	106	64	79	72	reject	
	C1	9.5	7.1	8.3	5.7	4.5	5.1	6.7	
	C2	7.9	9.5	8.7	6.4	7.6	7.0	7.9	
	C3	11.1	12.7	11.9	8.9	12.3	10.6	11.3	
C4	8.7	5.6	7.2	6.6	4.7	5.7	6.5		
3/20	B5	79	56	68	70	?		68?	
	B6	47	39	43	45	?		43?	

Table A5. Mean daily sea level from lagoon recorder station.

Average of 12 2-hourly levels ending at 1200 hr. on indicated day.  
Elevation in cm above lagoon low tide of 3/6 1337 hr.

<u>Date</u>	<u>Elav</u>
2/15	24.5
16	25.8
17	24.8
18	25.1
19	27.5
20	33.6
21	36.4
22	23.9
23	19.2
24	19.3
25	16.2
26	19.6
27	17.8
28	17.0
29	17.8
3/1	17.3
2	22.7
3	28.4
4	27.3
5	24.6
6	25.0
7	21.3
8	24.5
9	21.7
10	18.9
11	18.3
12	12.4
13	14.4
14	11.9
15	34.0
16	32.3
17	31.3
18	29.5
19	31.2
20	33.9
21	27.7

Overall Ave. 23.7 (mean daily sea level)  
 Max 36.4  
 Min 11.9  
 Range 24.5

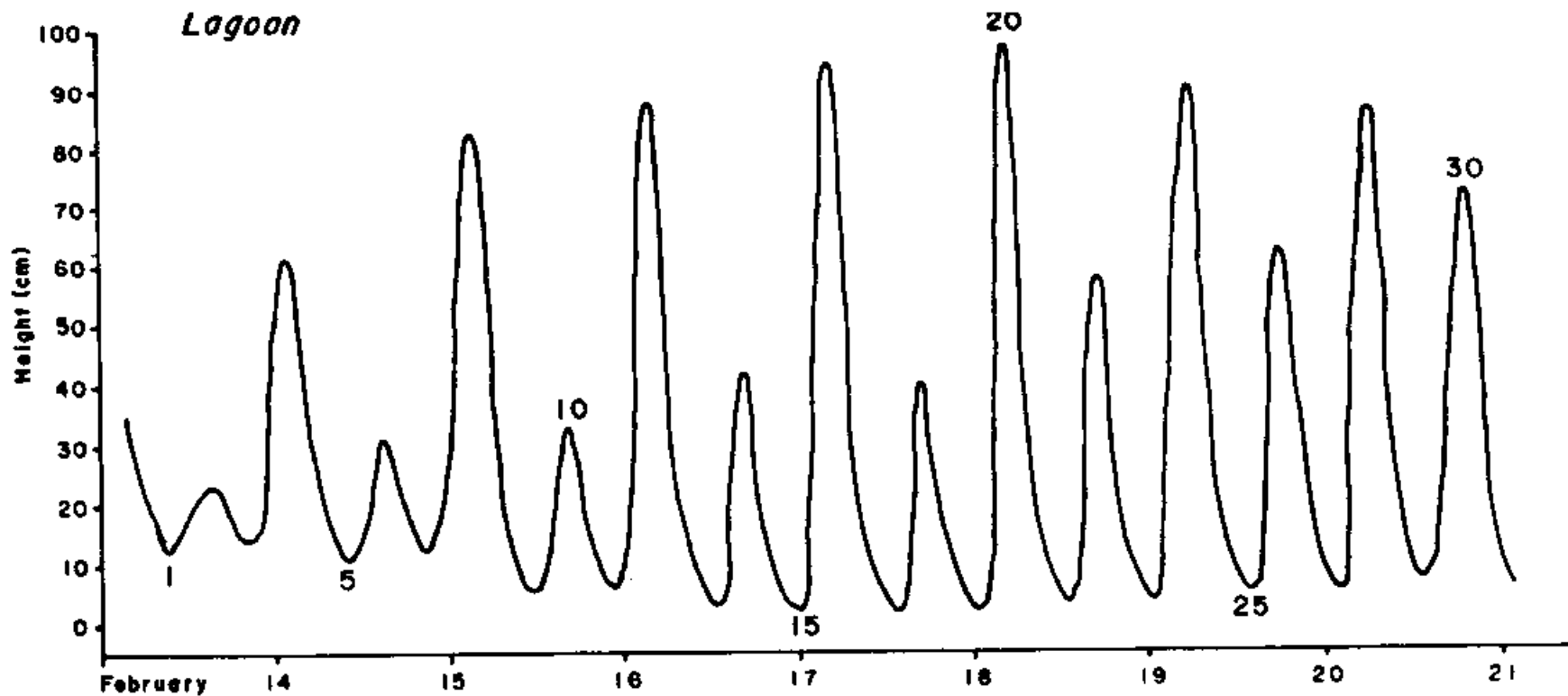


Figure A1. Lagoon recorder station, February 13 to March 21. Tidal extremes are numbered for purpose of correlating tidal record with continuous water-level recorders from selected observation wells.

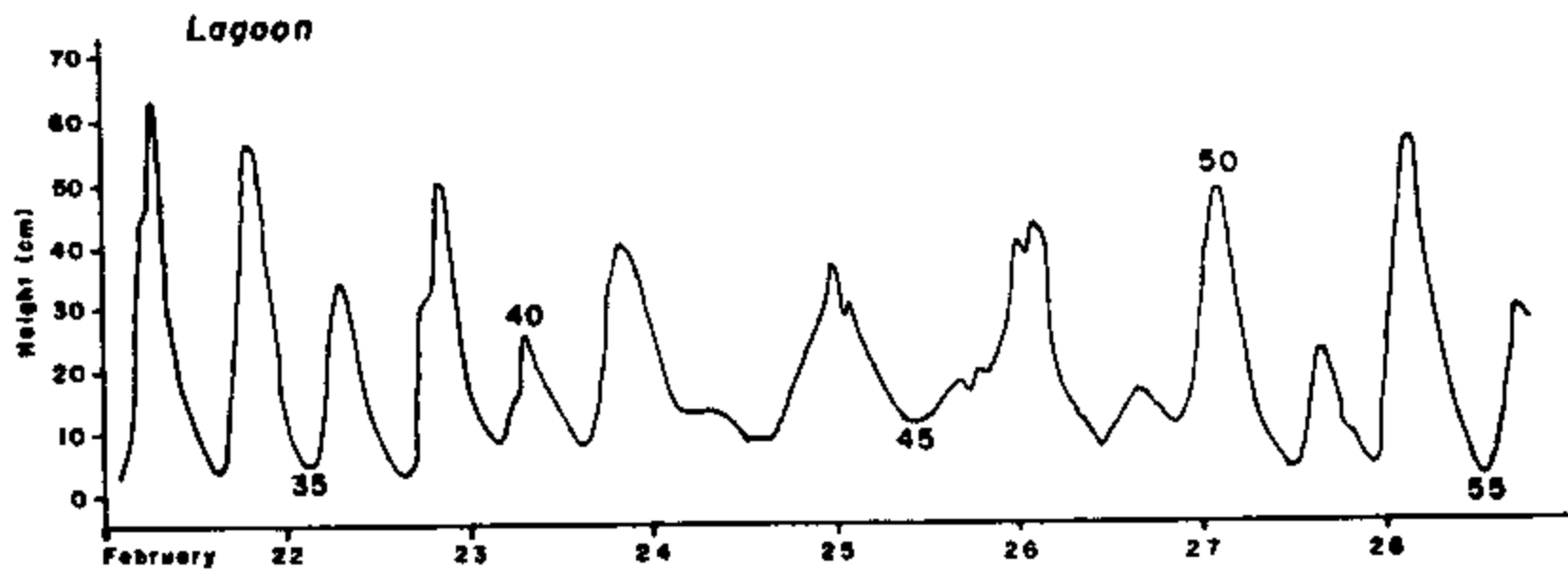


Figure A1. Continued.

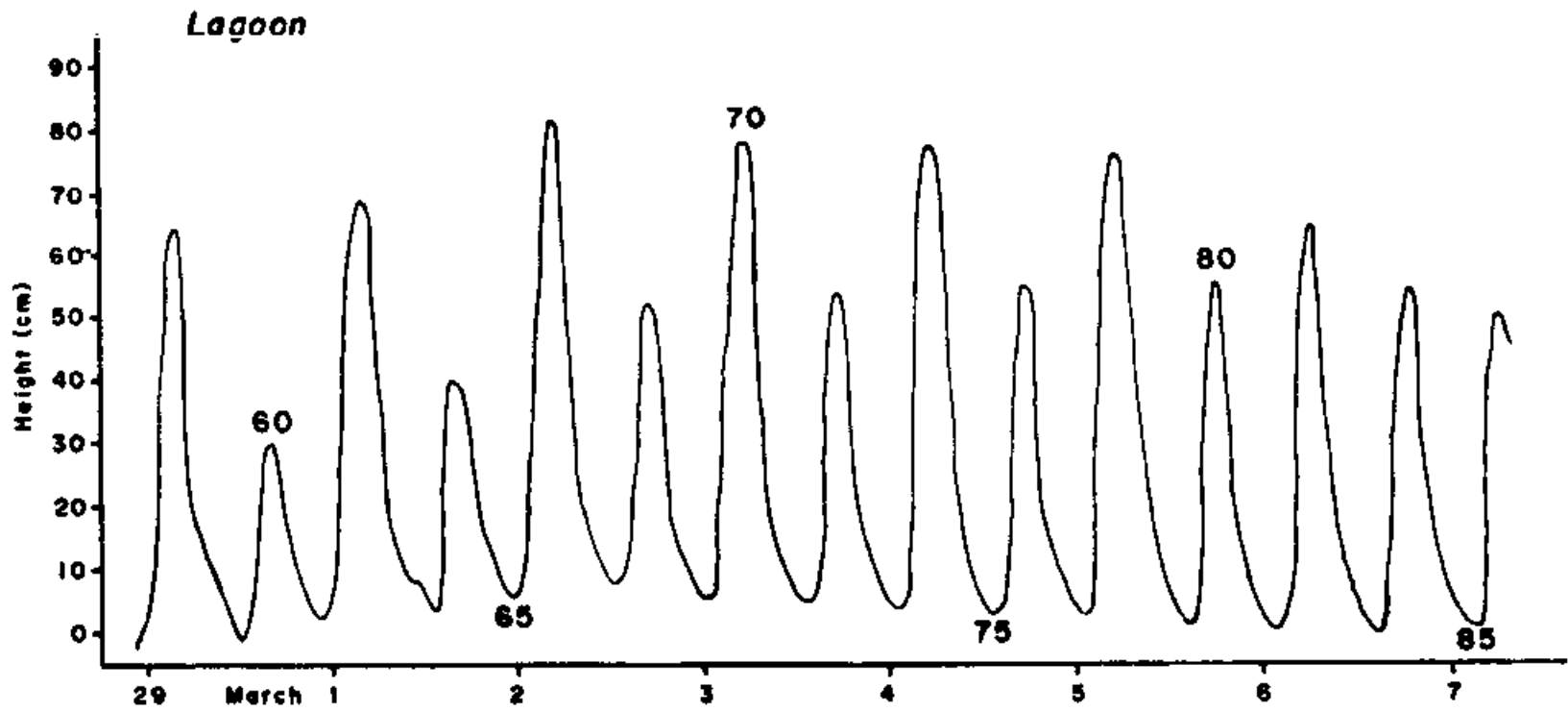


Figure A1. Continued.

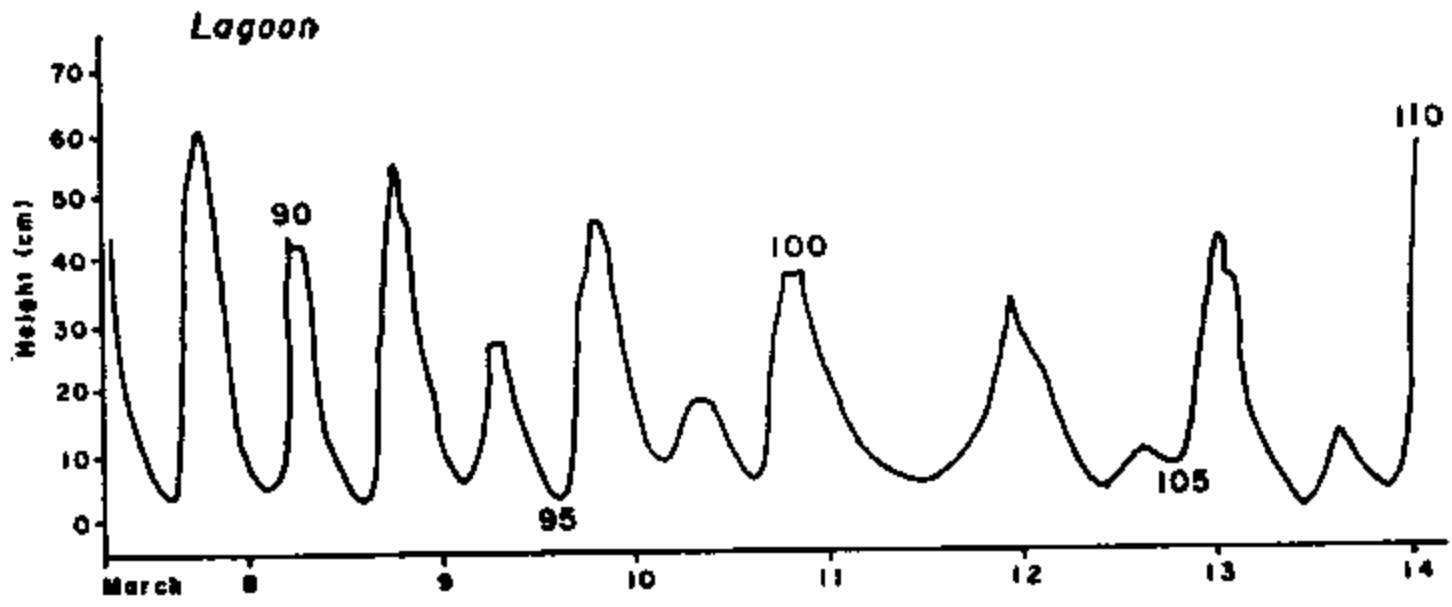


Figure A1. Continued.



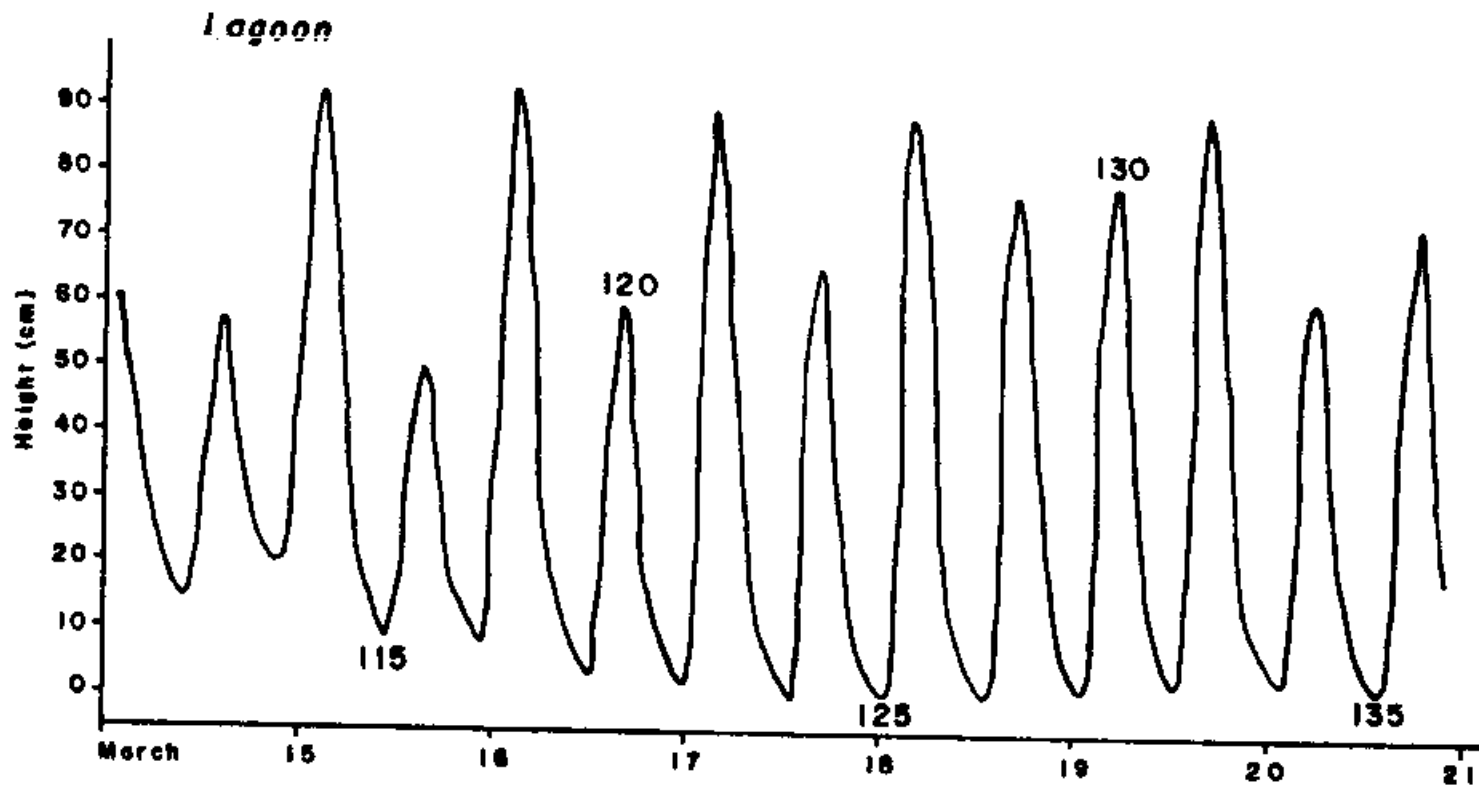


Figure A1. Continued.

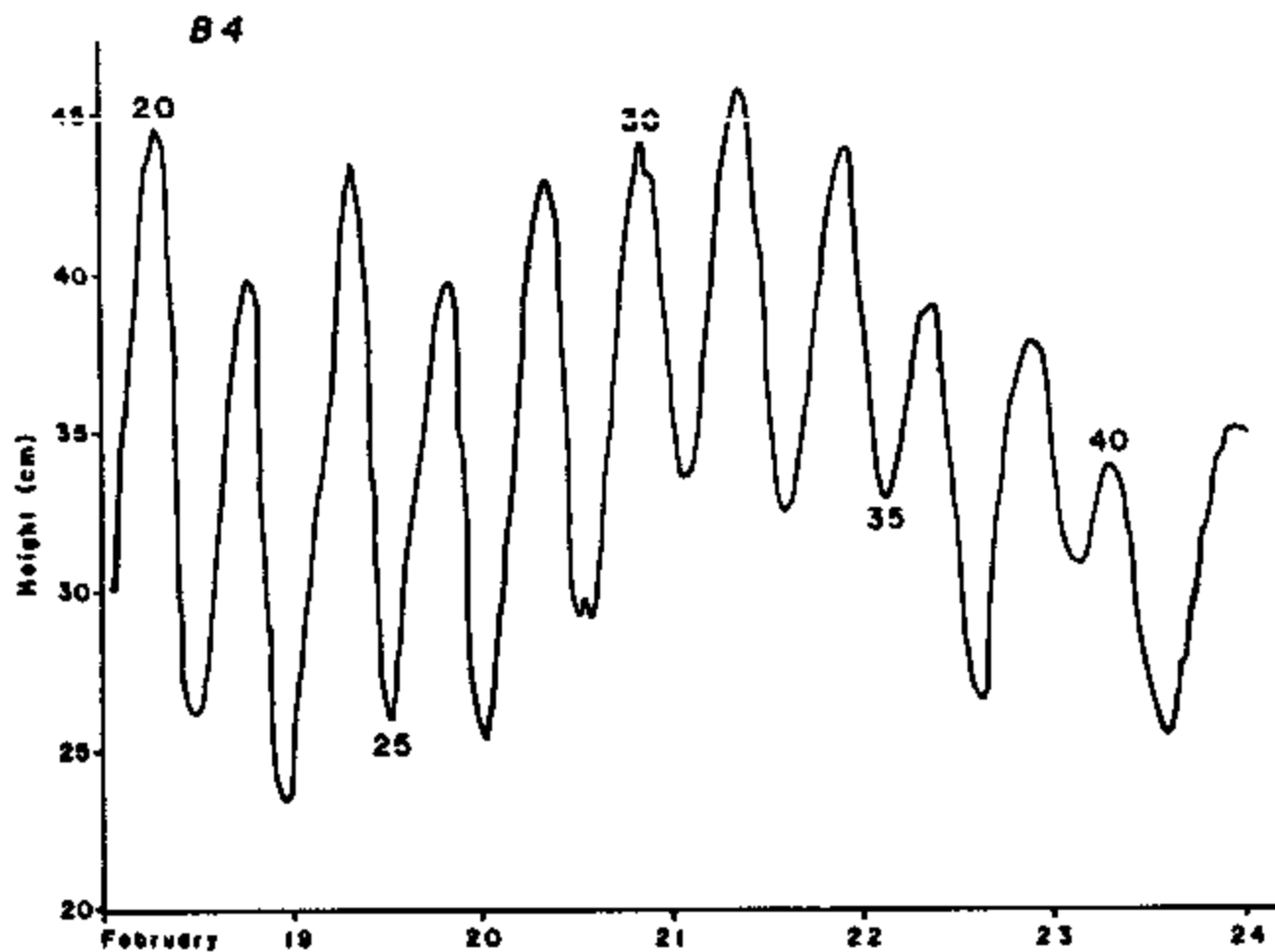


Figure A2. Well B4 recorder station, February 18 to March 2. Numbered high and low extremes correspond to numbered extremes on the lagoon tidal record of Figure A1.

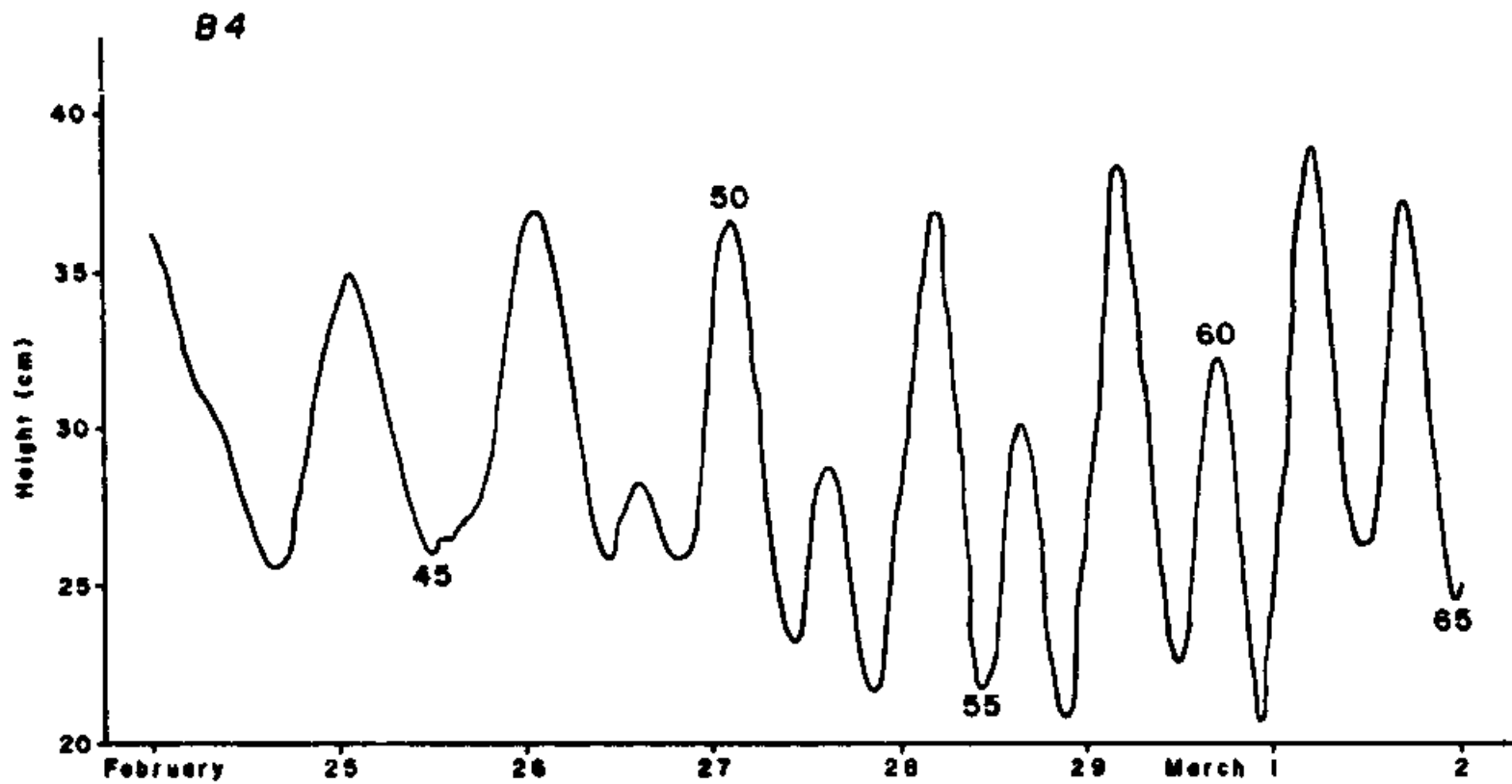


Figure A2. Continued.

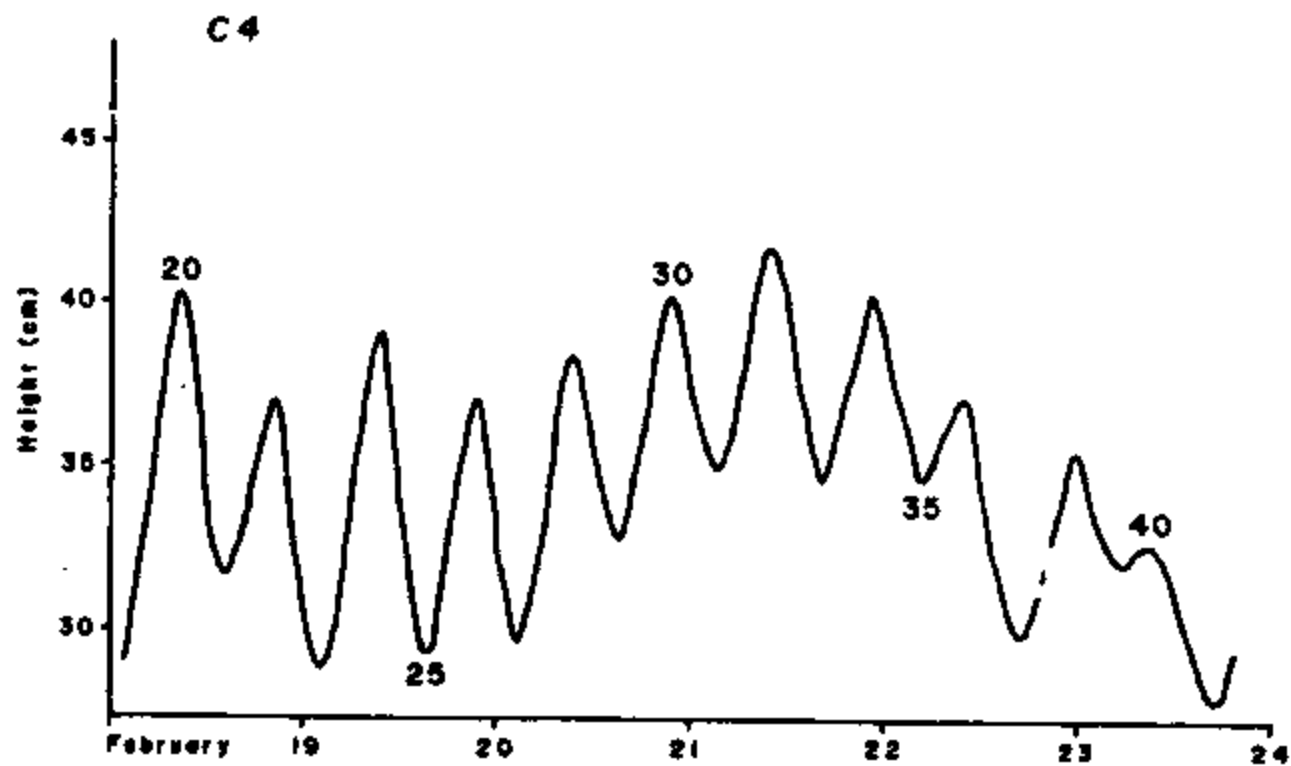


Figure A3. Well C4 recorder station, February 18 to March 9. Numbered high and low extremes correspond to numbered extremes on the lagoon tidal record of Figure A1.

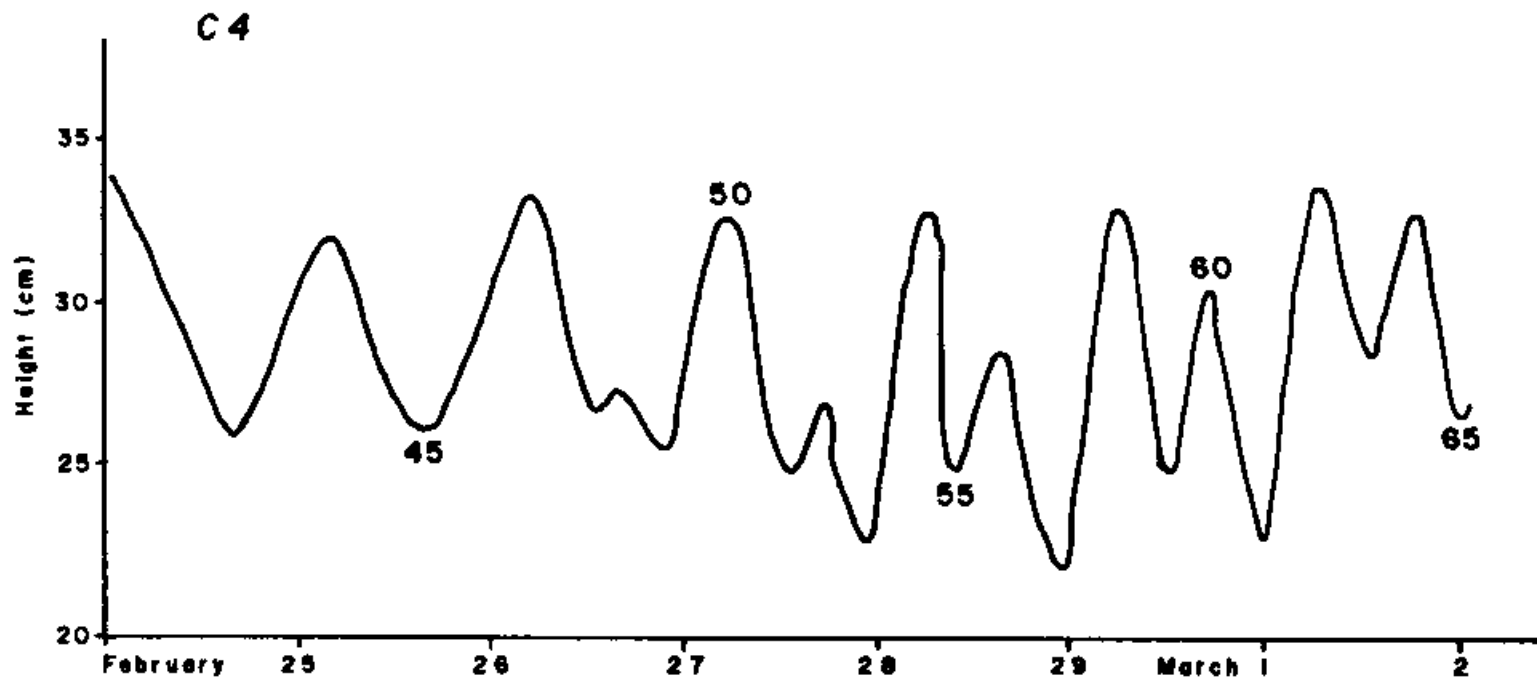


Figure A3. Continued.

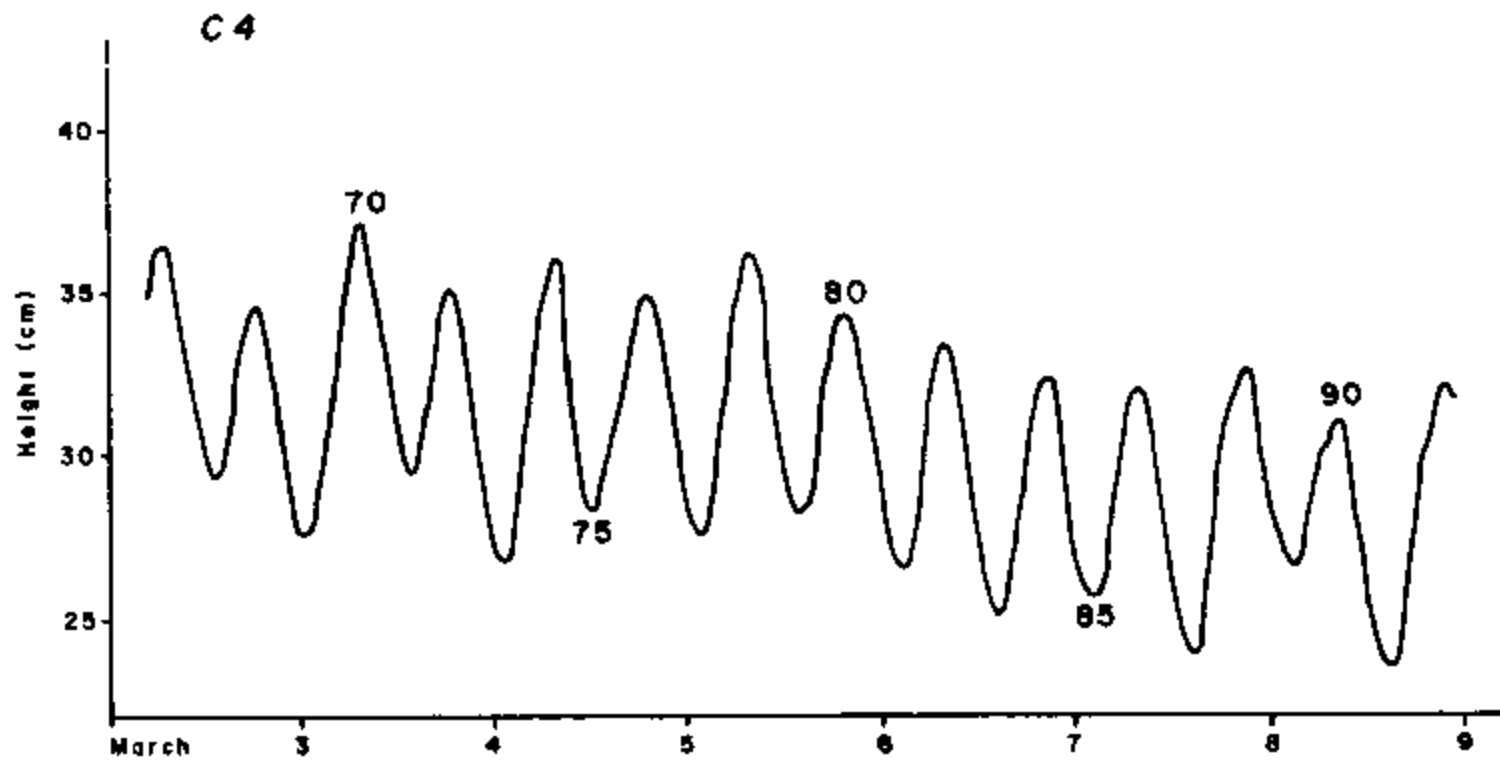


Figure A3. Continued.

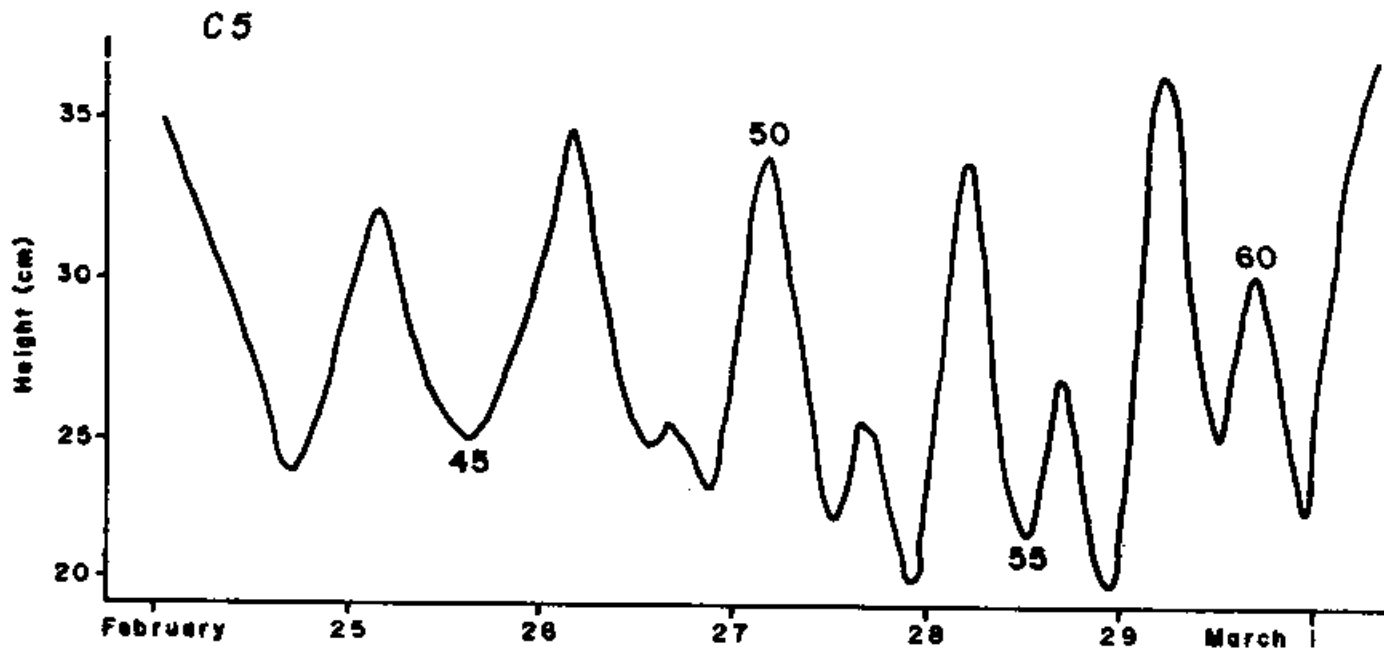


Figure A4. Well C5 recorder station, February 25 to March 15. Numbered high and low extremes correspond to numbered extremes on the lagoon tidal record of Figure A1.

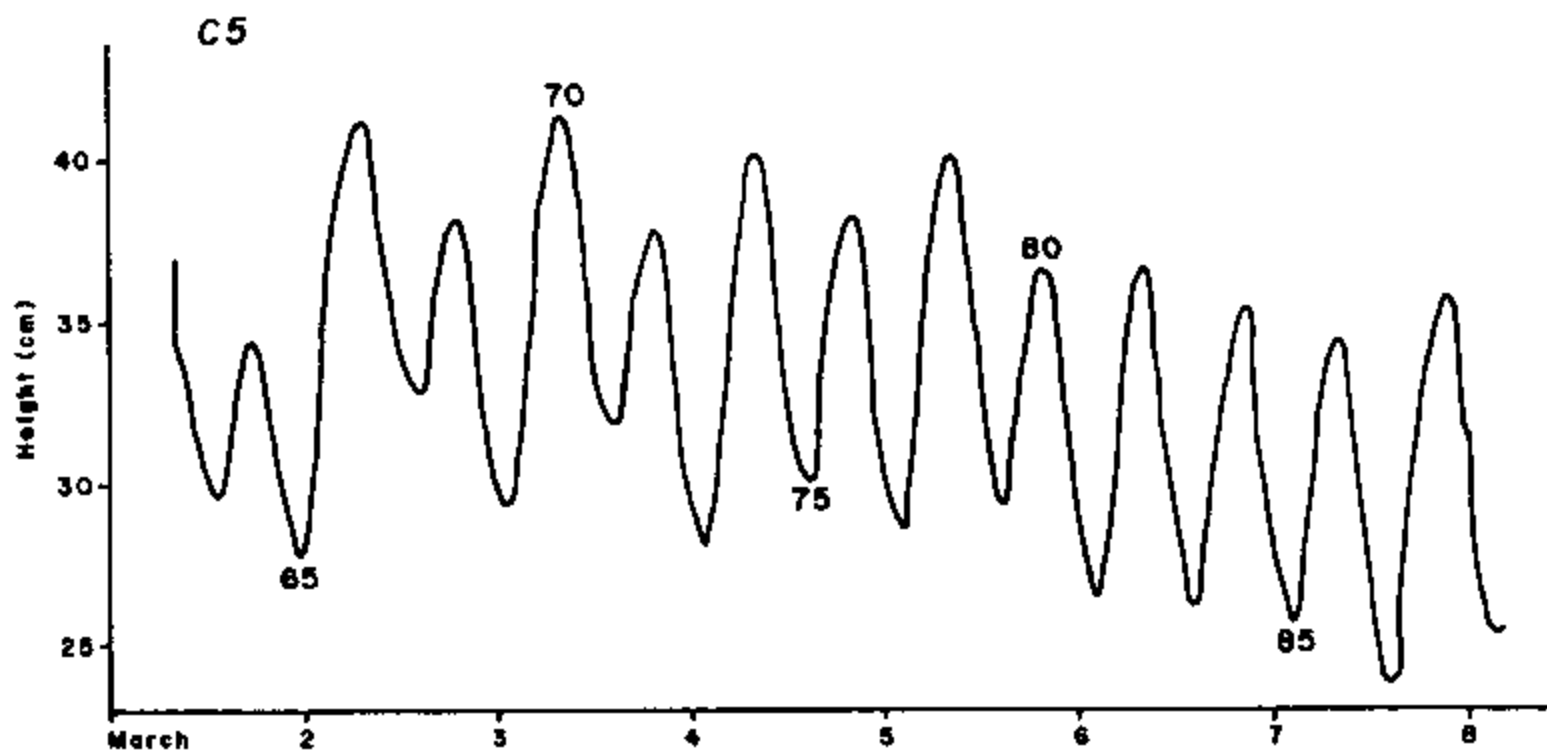


Figure A4. Continued.



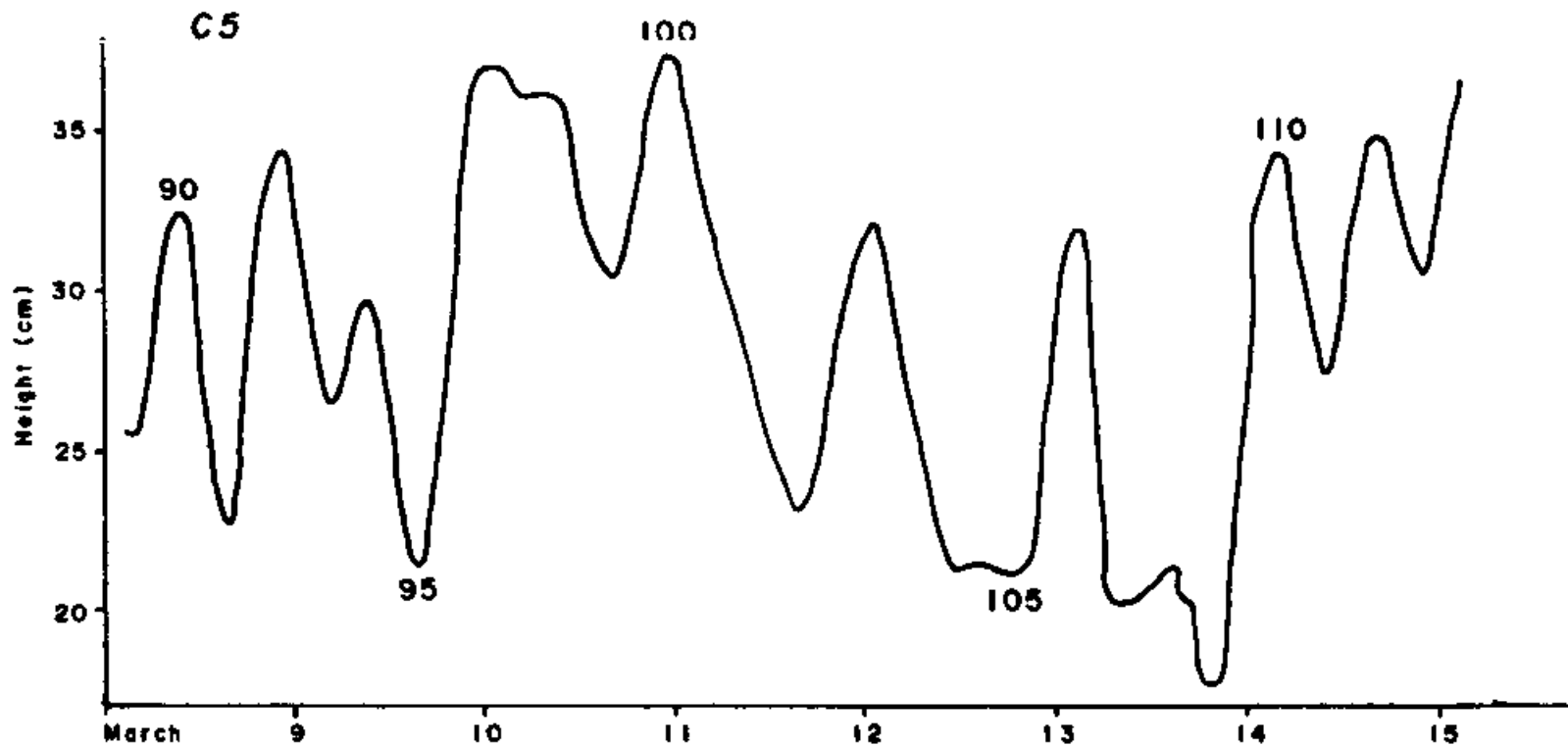


Figure A4. Continued.

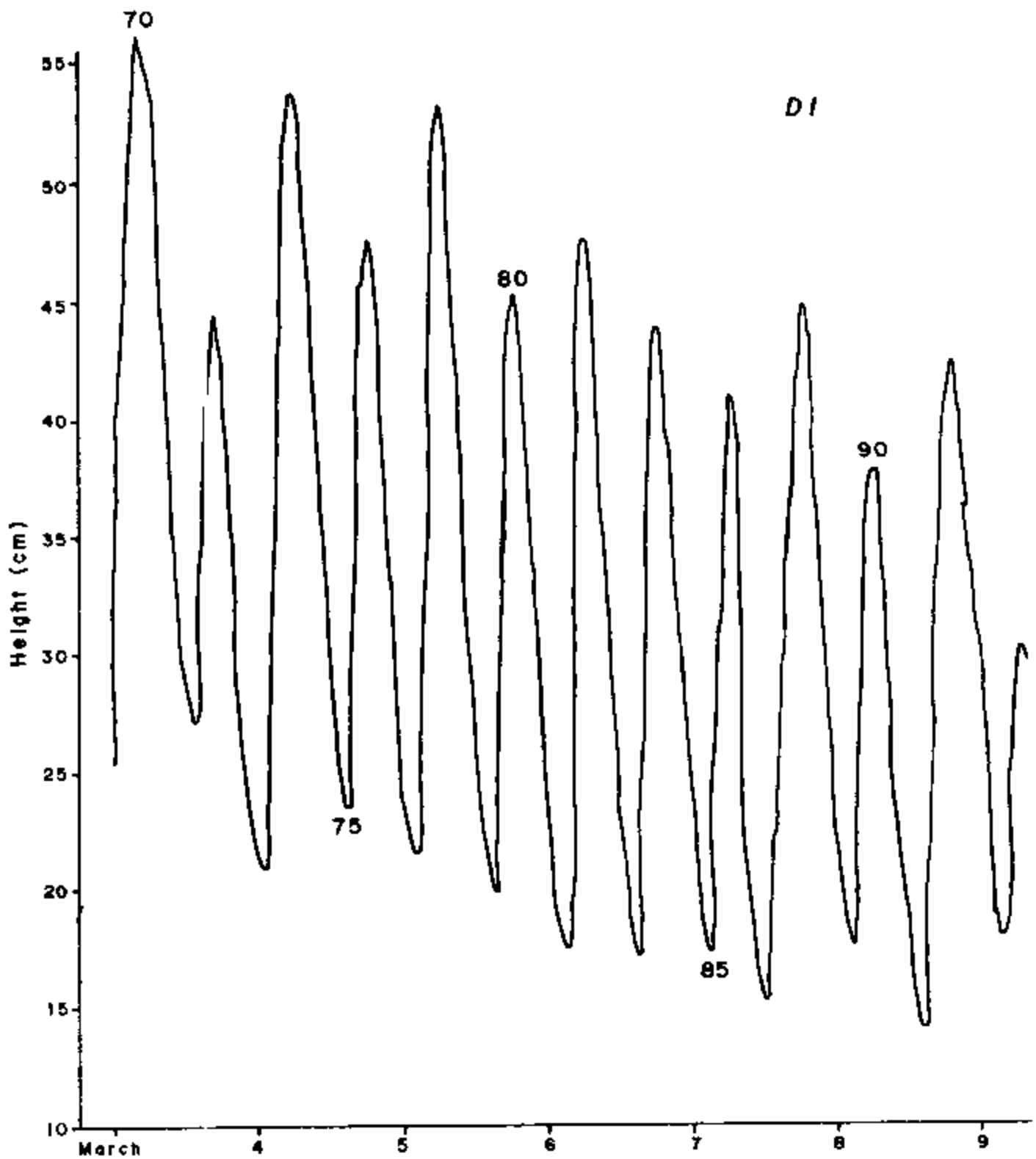


Figure A5. Well D1 recorder station, March 3 and March 16. Numbered high and low extremes correspond to numbered extremes on the lagoon tidal record of Figure A1.

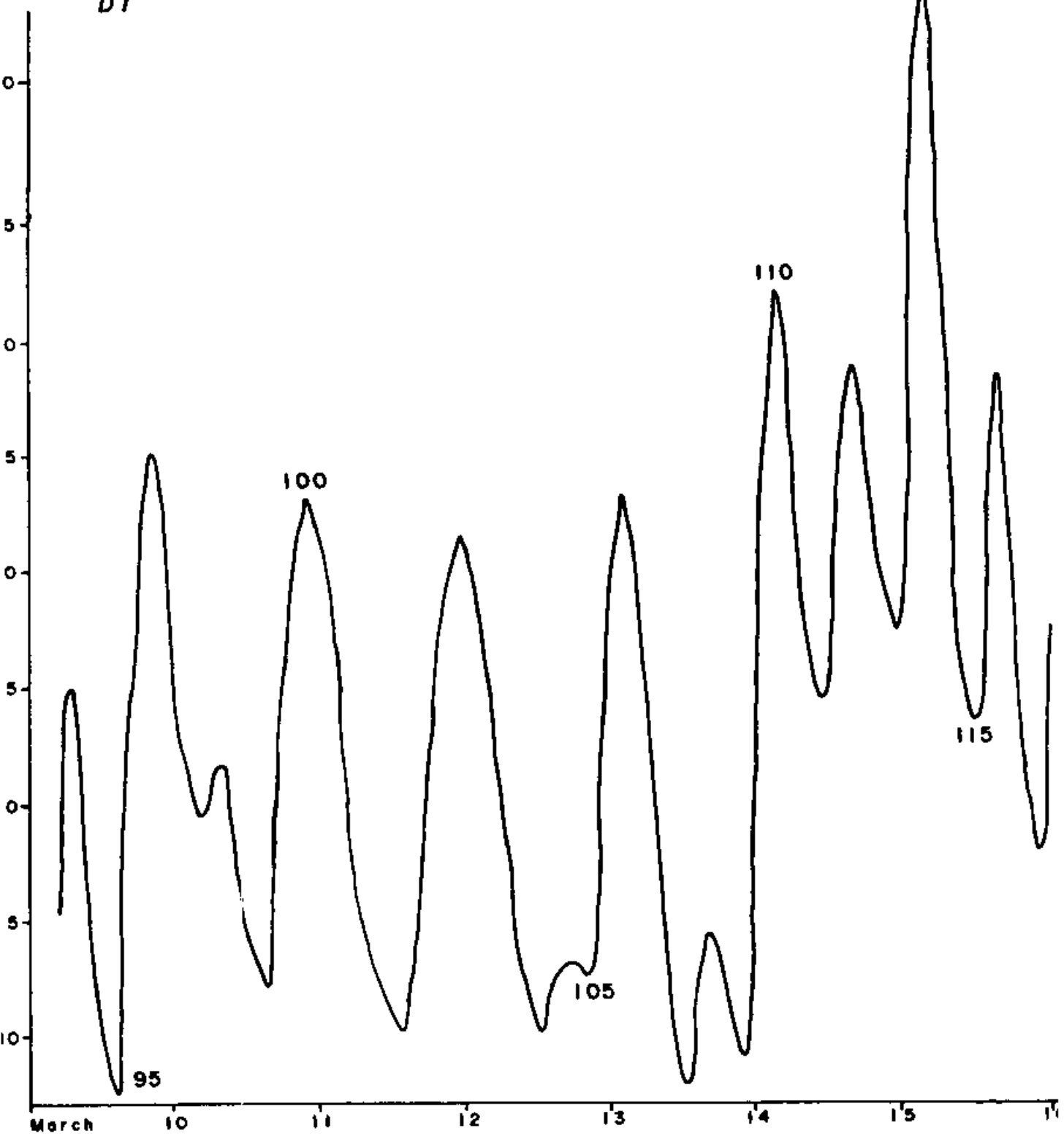
*DI*

Figure A5. Continued.

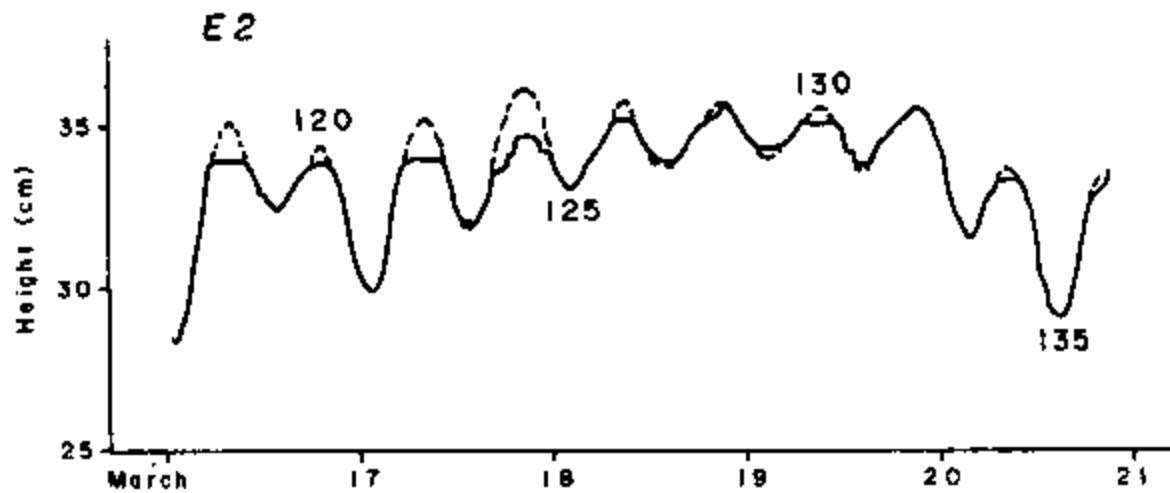


Figure A6. Well E2 recorder station, March 16 to March 21. Numbered high and low extremes correspond to numbered extremes on the lagoon tidal record of Figure A1.

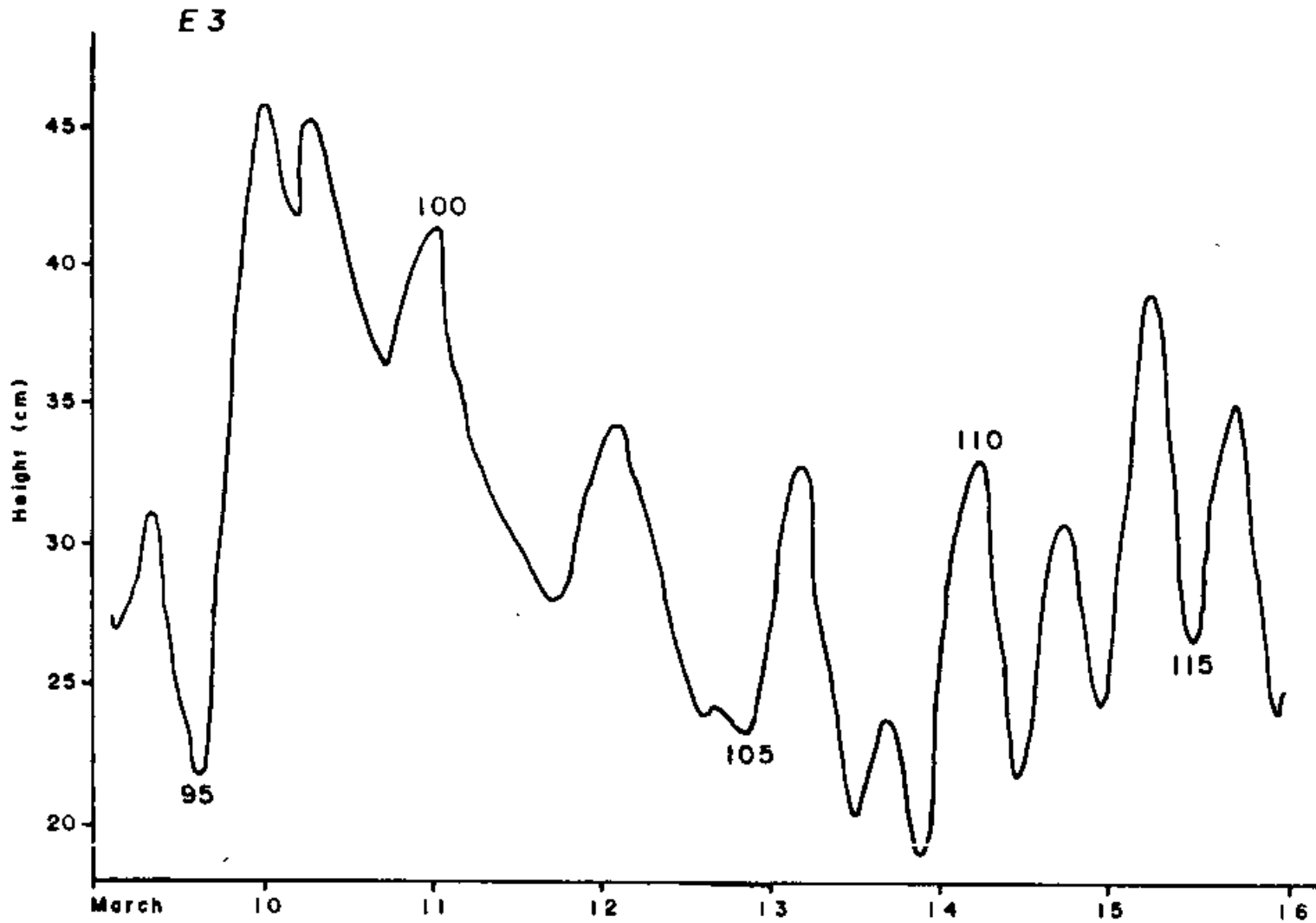


Figure A7. Well E3 recorder station, March 9 to March 21. Numbered high and low extremes correspond to numbered extremes on the lagoon tidal record of Figure A1.

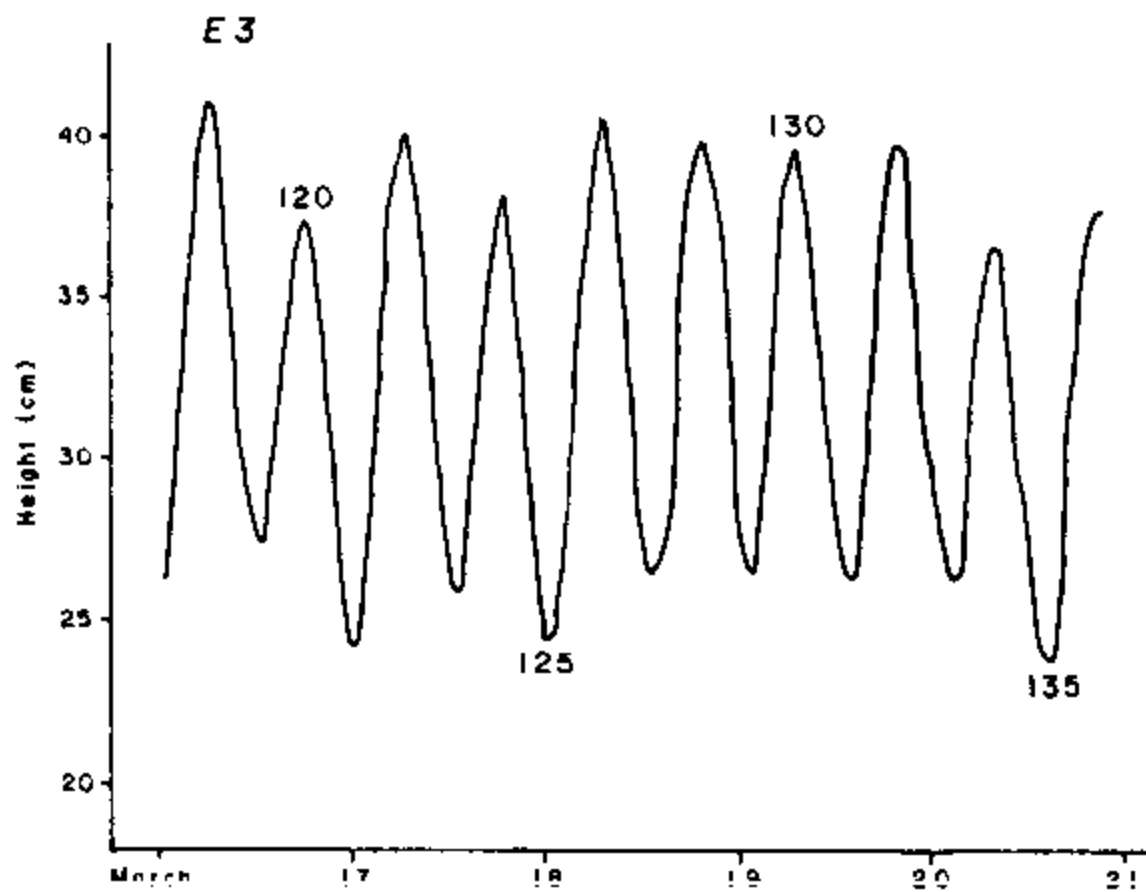


Figure A7. Continued.

Table A6. Rainfall and atmospheric pressure.

Date	Deke		Pingelap		
	Time <sup>*</sup>	Rainfall (cm) <sup>*</sup>	Time <sup>*</sup>	Rainfall (cm)	Pressure
2/13	0700	3.3	1100	2.1	1009.4
			1700	0.3	1006.8
			2300	0	1008.1
2/14	0700	1.1	1052	0.3	1008.5
			1655	0	1005.8
			2253	0	1007.7
2/15	0700	0.3	1053	2.4	1008.6
			1655	1.0	1005.1
			2254	0	1007.4
2/16	0700	6.1	1057	4.7	1009.0
			1655	2.2	1005.6
			2255	0	1008.5
2/17	0700	2.0	1700	0	1007.2
			2300	0	1008.8
2/18	0700	0.2	1100	0.6	1008.8
			1700	0	1006.8
			2300	0	1008.3
2/19	0700	0.3	1100	0.6	1009.3
			1700	0.2	1006.3
			2300	0	1007.8
2/20	0700	0.2	1053	2.3	1008.2
			1655	0	1005.8
			2253	0	1008.1

Table A6. continued

Date	Deke		Fingelap		Pressure
	Time*	Rainfall (cm)	Time*	Rainfall (cm)	
2/21	0700	4.8	1055	4.7	1008.5
			1655	3.1	1006.4
			2257	0	1008.9
2/22	0700	1.7	1055	5.1	1009.0
			1652	0	1007.1
			2250	0	1009.3
2/23	0700	0.6	1100	2.1	1009.4
			1700	0.3	1006.8
			2300	0	1008.3
2/24	0700	0.2	1100	.3	1008.8
	1130	0	1700	0	1007.3
	1730	0	2300	0	1008.9
2/25	0700	0.2	1100	0	1009.2
	1100	0	1700	0	1006.9
	1650	0	2300	0	1009.3
2/26	0700	0	1056	0	1010.0
	1008	0	1652	0	1007.9
	1611	0	2252	0	1009.6
2/27	0700	0.2	1058	0	1009.1
	1025	0	1652	0	1006.6
	1625	0	2252	0	1008.8
2/28	0700	0	1053	0	1008.9
	1045	0	1655	0	1006.4
	1650	0	2253	0	1009.0
2/29	0700	0	1100	0	1008.8
	1025	0	1700	0	1006.8



Date	Deke		Pingelap		Pressure
	Time*	Rainfall (cm)	Time*	Rainfall (cm)	
	1750	0	2300	0	1009.8
3/1	0700	0.5	1100	0	1010.2
	1100	0.3	1700	0	1008.3
	1700	0.3	2300	4.3	1010.3
3/2	0700	4.2	1100	5.1	1010.3
	1040	0	1700	0	1008.3
	1645	0.1	2300	0	1009.3
3/3	0700	0	1055	0	1009.8
	1200	0	1650	0	1007.2
	1800	0	2255	0	1009.2
3/4	0700	0.6	1053	0	1009.1
	1045	0.1	1653	0	1006.2
	1652	0.2	2257	0	1008.4
3/5	0700	0.2	1054	0	1009.1
	1035	0	1657	0	1006.1
	1640	0	2253	0	1009.6
3/6	0700	0.1	1100	0	1009.8
	1100	0	1700	0	1006.8
	1600	0	2300	0	1009.4
3/7	0700	0	1100	1.2	1010.8
	1340	1.3	1700	0.2	1008.3
	1722	1.7	2300	0.1	1009.9
3/8	0700	2.0	1100	2.4	1009.3
	1102	0.2	1700	0	1006.8
	1702	0.2	2300	0	1008.8
3/9	0700	0.3	1100	0	1008.6

Table A6. continued

Date	Deke		Pingelap		Pressure
	Time *	Rainfall (cm)	Time *	Rainfall (cm)	
	1010	0	1700	0	1006.8
	1605	0.2	2300	0	1008.8
3/10	0700	2.5	1100	3.8	1010.3
	1125	4.2	1700	2.9	1008.3
	1715	5.5			
3/11	0700	5.6	1100	2.9	1010.8
	1035	0	1700	0	1008.8
	1640	0	2300	0	1010.3
3/12	0700	0.1	1100	0	1010.7
	1102	0	1700	0	1008.7
	1720	0	2300	0	1010.3
3/13	0700	0.2	1100	0.7	1010.4
	1032	0	1700	0.1	1008.3
	1634	0	2300	0	1009.9
3/14	0700	0.3	1100	0.1	1010.8
	1040	0	1700	0	1008.6
	1638	0	2300	0	1010.7
3/15	0700	0	1100	0	1012.1
			1700	0	1009.3
			2300	0	1010.9
3/16	0700	0	1100	0	1010.9
			1700	0	1008.4
			2300	0	1010.9
3/17	0700	0	1100	0	1010.8
			1700	0	1008.8
			2300	0	1008.8

Date	Deke		Pingelap		
	Time *	Rainfall (cm)	Time *	Rainfall (cm)	Pressure
3/18	0700	0.6	1100	1.4	1009.9
			1700	1.1	1008.8
			2300	0	1010.9
3/19	0700	0.8	1100	0.8	1010.9
			1700	0	1008.4
			2300	0	1010.3
3/20	0700	0.9	1100	0	1010.9
			1700	0	1008.4
			2300	0	1010.3
3/21	0700	0			
3/22	0700	0.2	1100	0.5	1010.3
			1700	0	1008.2
			2300	0	1009.3

\*Time is the time the gage was read, so the corresponding amount is the rain that fell since the previous measurement time, except for rainfalls opposite 0700h on Deke, where the entered rainfall is the total since the previous 0700 reading.

Table A/. Other weather observations.

Date	Time	Wind		% Cloud		Lagoon
		Direction	Intensity	Cover		
2/28	1045	NE	light	15		small wind ripples
	1650	E	calm	40		very small wind ripples
2/29	1050	E	light	25		ripples
	1650	E	light	25		large ripples
3/1	1105	E	moderate			
	1545	E-NE	calm/mod			pulsating wind, wind tide
3/2	1045	E	moderate	30		small waves
	1650	E-NE	light/heavy	60		pulsating wind, wind tide
3/3	1200	E-NE	moderate	10		very small waves
	1800	E	light	45		very small waves
3/4	1050	E	light/mod	90		V. small waves, sprinkling
3/5	1045	E	heavy	75		up to 12" waves
	1645	E-SE	mod/heavy	15		8" waves
3/6	1100	E	light	5		slightly choppy
	1700	E	light	10		4" waves
3/7	1340	E-NE	calm	100		calm, drizzling rain
	1800	E	calm	90		calm
3/8	1058	E	light	50		5" waves
	1712	E	light	50		4" waves
3/9	1010	E	heavy	100		9" waves, heavy rain
	1020	E	light	50		sunny
	1605	E	heavy	90		8-10" waves, light rain
3/10	1130	E-NE	heavy	100		raining heavily, constantly
	1800	E-NE	heavy	100		raining heavily

Date	Time	Wind		% Cloud Cover	Lagoon
		Direction	Intensity		
3/11	1040	NE	calm	5	v. small ripples
	1638	E-NE	calm	10	v. small ripples
3/12	1100	NE	calm	40	small ripples
	1715	E	calm	15	small ripples
3/13	1050	E-NE	calm	90	ripples
	1640	E-NE	light	95	6" waves
3/14	1100	E-NE	calm	10	ripples (large)
	1638	NE	light	10	4" waves
3/20	1220	NE	calm	30	3" waves
	1810	E-NE	clam	10	calm

\*For wind intensity: calm, 0-2 knots; light, 3-6; mod. 7-10, heavy, more than 10. All windspeed are estimates.

## APPENDIX B

## CONTENTS

	Page
Figure -- Introduction	
B1. Location map of seismic-refraction lines and earth-resistivity stations.....	171
Tables -- Seismic-Refraction Data (2-layer)	
B1. HFT-1: Shotpoint information, geophone data, and arrival times.....	172
B2. HFT-1: Smoothed position of layers beneath shotpoints and geophones.....	173
B3. HFT-2: Shotpoint information, geophone data, and arrival times.....	174
B4. HFT-2: Smoothed position of layers beneath shotpoints and geophones.....	175
B5. HWT-2: Shotpoint information, geophone data, and arrival times.....	176
B6. HWT-2: Smoothed position of layers beneath shotpoints and geophones.....	177
B7. CT-1: Shotpoint information, geophone data, and arrival times.....	178
B8. CT-1: Smoothed position of layers beneath shotpoints and geophones.....	179
B9. CT-2: Shotpoint information, geophone data, and arrival times.....	180
B10. CT-2: Smoothed position of layers beneath shotpoints and geophones.....	181
B11. FE-1: Shotpoint information, geophone data, and arrival times.....	182
B12. FE-1: Smoothed position of layers beneath shotpoints and geophones.....	183
B13. FE-1A: Shotpoint information, geophone data, and arrival times.....	184
B14. FE-1A: Smoothed position of layers beneath shotpoints and geophones.....	185

B15.	FE-2A: Shotpoint information, geophone data, and arrival times.....	186
B16.	FE-2A: Smoothed position of layers beneath shotpoints and geophones.....	187
B17.	JT-1: Shotpoint information, geophone data, and arrival times.....	188
B18.	JT-1: Smoothed position of layers beneath shotpoints and geophones.....	189
B19.	TPT-1: Shotpoint information, geophone data, and arrival times.....	190
B20.	TPT-1: Smoothed position of layers beneath shotpoints and geophones.....	191
B21.	TPT-2: Shotpoint information, geophone data, and arrival times.....	192
B22.	TPT-2: Smoothed position of layers beneath shotpoints and geophones.....	193
B23.	TPT-3: Shotpoint information, geophone data, and arrival times.....	194
B24.	TPT-3: Smoothed position of layers beneath shotpoints and geophones.....	195
B25.	TPT-4: Shotpoint information, geophone data, and arrival times.....	196
B26.	TPT-4: Smoothed position of layers beneath shotpoints and geophones.....	197
B27.	TT-1: Shotpoint information, geophone data, and arrival times.....	198
B28.	TT-1: Smoothed position of layers beneath shotpoints and geophones.....	199
B29.	TT-2: Shotpoint information, geophone data, and arrival times.....	200
B30.	TT-2: Smoothed position of layers beneath shotpoints and geophones.....	201

Tables -- Seismic-Refraction Data (3-layer)

B31.	BSF-1: Shotpoint information, geophone data, and arrival times.....	202
------	---	-----

B32.	BST-1: Smoothed position of layers beneath shotpoints and geophones.....	203
B33.	BST-2: Shotpoint information, geophone data, and arrival times.....	204
B34.	BST-2: Smoothed position of layers beneath shotpoints and geophones.....	205
B35.	BST-3: Shotpoint information, geophone data, and arrival times.....	206
B36.	BST-3: Smoothed position of layers beneath shotpoints and geophones.....	207
B37.	BWT-1: Shotpoint information, geophone data, and arrival times.....	208
B38.	BWT-1: Smoothed position of layers beneath shotpoints and geophones.....	209
B39.	CL-1: Shotpoint information, geophone data, and arrival times.....	210
B40.	CL-1: Smoothed position of layers beneath shotpoints and geophones.....	211
B41.	DS3CT: Shotpoint information, geophone data, and arrival times.....	212
B42.	DS3CT: Smoothed position of layers beneath shotpoints and geophones.....	213
B43.	DS5CT: Shotpoint information, geophone data, and arrival times.....	214
B44.	DS5CT: Smoothed position of layers beneath shotpoints and geophones.....	215
B45.	EPT-1: Shotpoint information, geophone data, and arrival times.....	216
B46.	EPT-1: Smoothed position of layers beneath shotpoints and geophones.....	217
B47.	EPT-2: Shotpoint information, geophone data, and arrival times.....	218
B48.	EPT-2: Smoothed position of layers beneath shotpoints and geophones.....	219
B49.	EPT-3: Shotpoint information, geophone data, and arrival times.....	220



B50.	EPT-3: Smoothed position of layers beneath shotpoints and geophones.....	221
B51.	EPT-4: Shotpoint information, geophone data, and arrival times.....	222
B52.	EPT-4: Smoothed position of layers beneath shotpoints and geophones.....	223
B53.	FE-2: Shotpoint information, geophone data, and arrival times.....	224
B54.	FE-2: Smoothed position of layers beneath shotpoints and geophones.....	225
B55.	FE-3: Shotpoint information, geophone data, and arrival times.....	226
B56.	FE-3: Smoothed position of layers beneath shotpoints and geophones.....	227
B57.	IR-1: Shotpoint information, geophone data, and arrival times.....	228
B58.	IR-1: Smoothed position of layers beneath shotpoints and geophones.....	229
B59.	IR-2: Shotpoint information, geophone data, and arrival times.....	230
B60.	IR-2: Smoothed position of layers beneath shotpoints and geophones.....	231
B61.	LWT-1: Shotpoint information, geophone data, and arrival times.....	232
B62.	LWT-1: Smoothed position of layers beneath shotpoints and geophones.....	233
B63.	LWT-2: Shotpoint information, geophone data, and arrival times.....	234
B64.	LWT-2: Smoothed position of layers beneath shotpoints and geophones.....	235
B65.	NT-1: Shotpoint information, geophone data, and arrival times.....	236
B66.	NT-1: Smoothed position of layers beneath shotpoints and geophones.....	237
B67.	NT-2: Shotpoint information, geophone data, and arrival times.....	238

B68.	NT-2: Smoothed position of layers beneath shotpoints and geophones.....	239
B69.	NT-3: Shotpoint information, geophone data, and arrival times.....	240
B70.	NT-3: Smoothed position of layers beneath shotpoints and geophones.....	241
B71.	NT-4: Shotpoint information, geophone data, and arrival times.....	242
B72.	NT-4: Smoothed position of layers beneath shotpoints and geophones.....	243
B73.	PT-1: Shotpoint information, geophone data, and arrival times.....	244
B74.	PT-1: Smoothed position of layers beneath shotpoints and geophones.....	245
B75.	PT-2: Shotpoint information, geophone data, and arrival times.....	246
B76.	PT-2: Smoothed position of layers beneath shotpoints and geophones.....	247
B77.	PT-3: Shotpoint information, geophone data, and arrival times.....	248
B78.	PT-3: Smoothed position of layers beneath shotpoints and geophones.....	249
B79.	ST-1: Shotpoint information, geophone data, and arrival times.....	250
B80.	ST-1: Smoothed position of layers beneath shotpoints and geophones.....	251
B81.	ST-2: Shotpoint information, geophone data, and arrival times.....	252
B82.	ST-2: Smoothed position of layers beneath shotpoints and geophones.....	253
B83.	ST-3: Shotpoint information, geophone data, and arrival times.....	254
B84.	ST-3: Smoothed position of layers beneath shotpoints and geophones.....	255
B85.	ST-4: Shotpoint information, geophone data, and arrival times.....	256

B86.	ST-4: Smoothed position of layers beneath shotpoints and geophones.....	257
B87.	ST-5: Shotpoint information, geophone data, and arrival times.....	258
B88.	ST-5: Smoothed position of layers beneath shotpoints and geophones.....	259
B89.	ST-6: Shotpoint information, geophone data, and arrival times.....	260
B90.	ST-5: Smoothed position of layers beneath shotpoints and geophones.....	261
B91.	THC-1: Shotpoint information, geophone data, and arrival times.....	262
B92.	THC-1: Smoothed position of layers beneath shotpoints and geophones.....	263
B93.	THC-2: Shotpoint information, geophone data, and arrival times.....	264
B94.	THC-2: Smoothed position of layers beneath shotpoints and geophones.....	265
B95.	THC-3: Shotpoint information, geophone data, and arrival times.....	266
B96.	THC-3: Smoothed position of layers beneath shotpoints and geophones.....	267
B97.	THC-4: Shotpoint information, geophone data, and arrival times.....	268
B98.	THC-4: Smoothed position of layers beneath shotpoints and geophones.....	269
B99.	THC-5: Shotpoint information, geophone data, and arrival times.....	270
B100.	THC-5: Smoothed position of layers beneath shotpoints and geophones.....	271

#### Figures -- Earth-Resistivity Results

B2.	Station 1: Field VES curve and computed VES curve.....	272
B3.	Station 2: Field VES curve and computed VES curve.....	273
B4.	Station 3: Field VES curve and computed VES curve.....	274
B3.	Station 4: Field VES curve and computed VES curve.....	275

B6.	Station 5:	Field VES curve and computed VES curve.....	276
B7.	Station 6:	Field VES curve and computed VES curve.....	277
B8.	Station 7:	Field VES curve and computed VES curve.....	278
B9.	Station 8:	Field VES curve and computed VES curve.....	279
B10.	Station 9:	Field VES curve and computed VES curve.....	280
B11.	Station 10:	Field VES curve and computed VES curve.....	281
B12.	Station 11:	Field VES curve and computed VES curve.....	282
B13.	Station 12:	Field VES curve and computed VES curve.....	283
B14.	Station 13:	Field VES curve and computed VES curve.....	284
B15.	Station 14:	Field VES curve and computed VES curve.....	285
B16.	Station 15:	Field VES curve and computed VES curve.....	286
B17.	Station 16:	Field VES curve and computed VES curve.....	287

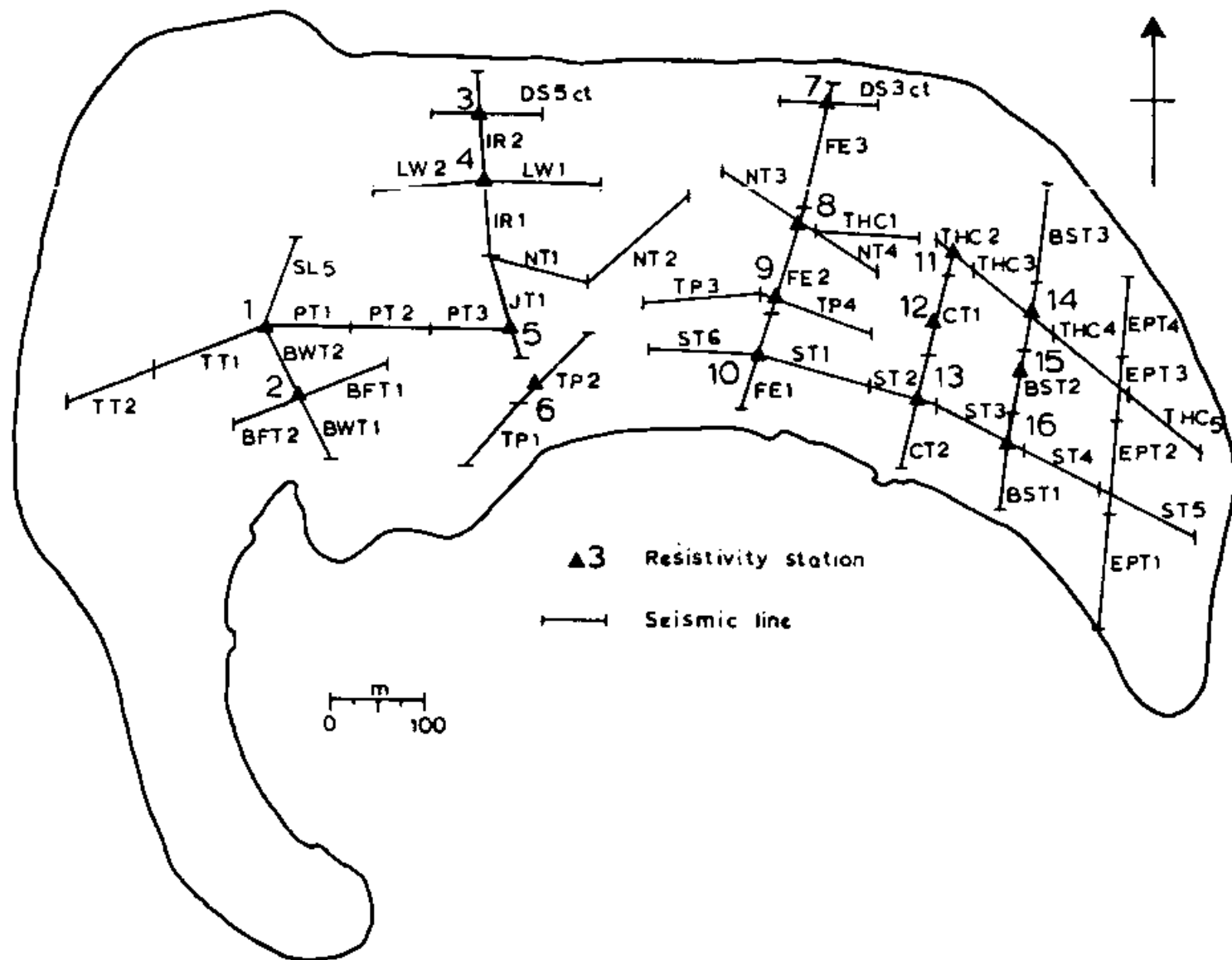


Figure B1. Location map of seismic-refraction lines and earth-resistivity stations.

Table B1. BFT-1: Shotpoint information, geophone data, and arrival times. Times are in msec.

	SP	Elev (ft)	X Loc (ft)	Y Loc (ft)	Depth (ft)					
	F	5.5	-25.0	0.0	0.0					
	M	5.5	140.0	15.0	0.0					
	R	5.5	300.0	0.0	0.0					

Geo	Elev (ft)	X Loc (ft)	Y Loc (ft)	SP	F	SP	M	SP	R
1	5.5	0.0	0.0	12.8	1	37.5	2	68.4	2
2	5.5	25.0	0.0	20.4	2	33.9	2	63.9	2
3	5.5	50.0	0.0	25.2	2	30.4	2	59.0	2
4	5.5	75.0	0.0	32.5	2	27.1	2	56.0	2
5	5.5	100.0	0.0	35.6	2	21.8	2	50.2	2
6	5.5	125.0	0.0	41.4	2	17.1	1	45.8	2
7	5.5	150.0	0.0	45.5	2	15.5	1	39.0	2
8	5.5	175.0	0.0	49.3	2	20.0	2	33.9	2
9	5.5	200.0	0.0	56.2	2	23.3	2	29.0	2
10	5.5	225.0	0.0	61.5	2	29.0	2	24.5	2
11	5.5	250.0	0.0	66.3	2	32.3	2	18.0	2
12	5.5	275.0	0.0	73.2	2	35.0	2	17.0	1

Table B2. BFT-1: Smoothed position of layers beneath shotpoints and geophones.

SP	Position	Surface Elev (ft)	Layer 2	
			Depth (ft)	Elev (ft)
F	-25.0	5.5	5.7	-0.2
M	140.0	5.5	9.9	-4.4
R	300.0	5.5	8.7	-3.2
<b>Geophone</b>				
1	0.0	5.5	6.5	-1.0
2	25.0	5.5	7.7	-2.2
3	50.0	5.5	8.6	-3.1
4	75.0	5.5	10.6	-5.1
5	100.0	5.5	10.0	-4.5
6	125.0	5.5	10.4	-4.9
7	150.0	5.5	9.6	-4.1
8	175.0	5.5	8.5	-3.0
9	200.0	5.5	8.7	-3.2
10	225.0	5.5	9.2	-3.7
11	250.0	5.5	8.3	-2.8
12	275.0	5.5	8.8	-3.3
		<b>Layer 1</b>	<b>Layer 2</b>	
<b>Velocities used</b>		1457.	5176.	

Table B3. HFT-2: Shotpoint information, geophone data, and arrival times. Times are in msec.

	SP	Elev (ft)	X Loc (ft)	Y Loc (ft)	Depth (ft)					
	F	4.9	-25.0	0.0	0.0					
	M	3.7	138.5	15.0	0.0					
	R	5.5	300.0	0.0	0.0					

Geo	Elev (ft)	X Loc (ft)	Y Loc (ft)	SP	F	SP	M	SP	R
1	4.9	0.0	0.0	16.0	1	38.0	2	70.8	2
2	4.9	25.0	0.0	18.6	2	34.0	2	64.4	2
3	4.5	50.0	0.0	25.8	2	31.0	2	60.0	2
4	3.9	75.0	0.0	31.0	2	25.0	2	54.6	2
5	3.9	100.0	0.0	32.3	2	18.2	2	49.5	2
6	3.8	125.0	0.0	40.1	2	14.6	2	44.9	2
7	3.6	150.0	0.0	44.3	2	15.2	1	42.0	2
8	3.8	175.0	0.0	48.2	2	18.8	2	37.0	2
9	4.0	200.0	0.0	50.0	2	21.5	2	30.0	2
10	4.3	225.0	0.0	57.0	2	27.2	2	26.0	2
11	5.0	250.0	0.0	52.3	2	32.2	2	21.0	2
12	5.5	275.0	0.0	67.4	2	39.0	2	16.0	1



Table B4. BFI-2: Smoothed position of layers beneath shotpoints and geophones.

SP	Position	Surface Elev (ft)	Layer 2	
			Depth (ft)	Elev (ft)
F	-25.0	4.9	10.7	-5.8
M	138.5	3.7	8.5	-4.8
R	300.0	5.5	9.7	-4.2
Geophone				
1	0.0	4.9	10.5	-5.6
2	25.0	4.9	8.8	-3.9
3	50.0	4.5	9.9	-5.4
4	75.0	3.9	9.3	-5.4
5	100.0	3.9	7.2	-3.3
6	125.0	3.8	8.2	-4.4
7	150.0	3.6	8.7	-5.1
8	175.0	3.8	8.8	-5.0
9	200.0	4.0	6.1	-2.1
10	225.0	4.3	7.7	-3.4
11	250.0	5.0	9.0	-4.0
12	275.0	5.5	9.9	-4.4
		Layer 1	Layer 2	
Velocities used		1438.	5378.	

Table B5. WT-2: Shotpoint information, geophone data, and arrival times. Times are in msec.

	SP	Elev (ft)	X Loc (ft)	Y Loc (ft)	Depth (ft)				
	F	5.0	-25.0	0.0	0.0				
	M	5.0	137.5	15.0	0.0				
	R	5.5	300.0	0.0	0.0				

Geo	Elev (ft)	X Loc (ft)	Y Loc (ft)	SP	F	SP	M	SP	R
1	5.0	0.0	0.0	14.0	1	35.0	2	68.8	2
2	4.8	25.0	0.0	18.0	2	30.8	2	64.8	2
3	4.7	50.0	0.0	24.2	2	26.0	2	61.0	2
4	4.6	75.0	0.0	28.5	2	19.0	2	48.9	2
5	4.7	100.0	0.0	33.0	2	15.0	2	48.9	2
6	5.0	125.0	0.0	39.0	2	12.8	1	45.0	2
7	4.9	150.0	0.0	42.5	2	13.2	1	38.8	2
8	4.9	175.0	0.0	50.0	2	17.5	2	33.5	2
9	5.2	200.0	0.0	53.8	2	20.0	2	28.0	2
10	5.4	225.0	0.0	59.0	2	25.0	2	23.8	2
11	5.4	250.0	0.0	64.0	2	30.4	2	19.8	2
12	5.5	275.0	0.0	69.0	2	37.0	2	15.2	1

Table B6. BWT-2: Smoothed position of layers beneath shotpoints and geophones.

SP	Position	Surface Elev (ft)	Layer 2	
			Depth (ft)	Elev (ft)
F	-25.0	5.0	6.8	-1.8
M	137.5	5.0	7.1	-2.1
R	300.0	5.5	7.8	-2.3
Geophone				
1	0.0	5.0	6.8	-1.8
2	25.0	4.8	7.5	-2.7
3	50.0	4.7	8.4	-3.7
4	75.0	4.6	6.8	-2.2
5	100.0	4.7	6.6	-1.9
6	125.0	5.0	7.1	-2.1
7	150.0	4.9	7.1	-2.2
8	175.0	4.9	7.7	-2.8
9	200.0	5.2	6.3	-1.1
10	225.0	5.4	6.7	-1.3
11	250.0	5.4	7.4	-2.0
12	275.0	5.5	7.8	-2.3
		Layer 1	Layer 2	
Velocities used		1609.	4966.	



Table B8. CT-1: Smoothed position of layers beneath shotpoints and geophones.

SP	Position	Surface Elev (ft)	Layer 2	
			Depth (ft)	Elev (ft)
A	-10.0	6.8	4.3	2.5
M	137.5	6.4	5.9	0.5
B	285.0	6.0	7.0	-1.0
<b>Geophone</b>				
1	0.0	7.0	4.6	2.4
2	25.0	6.5	6.6	-0.1
3	50.0	6.1	6.9	-0.8
4	75.0	6.1	6.3	-0.2
5	100.0	6.3	6.2	0.1
6	125.0	6.6	6.4	0.2
7	150.0	6.3	5.5	0.8
8	175.0	6.3	5.9	0.4
9	200.0	6.2	6.5	-0.3
10	225.0	6.4	4.0	2.4
11	250.0	6.8	6.5	0.3
12	275.0	7.0	7.9	-0.9
		Layer 1	Layer 2	
<b>Velocities used</b>		1538.	5122.	



Table B10. CT-2: Smoothed position of layers beneath shotpoints and geophones.

SP	Position	Surface Elev (ft)	Layer 2	
			Depth (ft)	Elev (ft)
A	-10.0	7.0	7.8	-0.8
M	137.5	4.5	5.6	-1.1
B	285.0	4.3	7.9	-3.6
Geophone				
1	0.0	7.0	7.8	-0.8
2	25.0	6.3	7.2	-0.9
3	50.0	4.8	5.0	-0.2
4	75.0	4.5	4.2	0.3
5	100.0	4.5	4.5	0.0
6	125.0	4.5	5.1	-0.6
7	125.0	4.5	6.1	-1.6
8	175.0	4.5	6.7	-2.2
9	200.0	4.6	7.5	-2.9
10	225.0	4.4	7.4	-3.0
11	250.0	4.2	8.2	-4.0
12	275.0	4.2	7.6	-3.4
		Layer 1	Layer 2	
Velocities used		1479.	5275.	





Table B12. FE-1: Smoothed position of layers beneath shotpoints and geophones.

SP	Position	Surface Elev (ft)	Layer 2	
			Depth (ft)	Elev (ft)
A	-10.0	3.0	4.5	-1.5
M	138.5	2.5	4.8	-2.3
B	285.0	4.0	5.7	-1.7
Geophone				
1	0.0	3.0	4.6	-1.6
2	25.0	3.0	5.5	-2.5
3	50.0	2.8	5.9	-3.1
4	75.0	3.0	4.6	-1.6
5	100.0	2.7	6.0	-3.3
6	125.0	2.5	6.2	-3.7
7	150.0	2.6	3.8	-1.2
8	175.0	2.7	3.0	-0.3
9	200.0	3.1	3.1	-0.0
10	225.0	3.3	4.9	-1.6
11	250.0	3.7	4.9	-1.2
12	275.0	4.0	5.6	-1.6
		Layer 1	Layer 2	
Velocities used:		1500.	5213.	



Table B14. FE-1A: Smoothed position of layers beneath shotpoints and geophones.

SP	Position	Surface Elev (ft)	Layer 2	
			Depth (ft)	Elev (ft)
A	-3.0	3.0	1.7	1.8
M	138.5	2.5	5.8	-3.8
B	280.0	4.0	5.4	-1.4
<b>Geophone</b>				
1	0.0	3.0	1.9	1.1
2	25.0	3.0	4.1	-1.1
3	50.0	2.8	3.7	-0.9
4	75.0	3.0	4.5	-1.5
5	100.0	2.7	5.6	-2.9
6	125.0	2.5	6.3	-3.8
7	150.0	2.6	5.5	-2.9
8	175.0	2.7	3.6	-0.9
9	200.0	3.1	1.7	1.4
10	225.0	3.3	1.4	1.9
11	150.0	3.7	4.2	-0.5
12	275.0	4.0	5.5	-1.5
<b>Velocities used:</b>		<b>Layer 1</b>	<b>Layer 2</b>	
		1774.	4995.	

Table B15. FE-2A: Shotpoint information, geophone data, and arrival times. Times are in msec.

	SP	Elev (ft)	X Loc (ft)	Y Loc (ft)	Depth (ft)								
	F	4.0	-15.0	0.0	0.0								
	A	4.0	-5.0	0.0	0.0								
	M	5.3	137.5	15.0	0.0								
	B	6.3	280.0	0.0	0.0								
	R	6.8	290.0	0.0	0.0								

Geo	Elev (ft)	X Loc (ft)	Y Loc (ft)	SP	F	SP	A	SP	M	SP	B	SP	R
1.	4.0	0.0	0.0	9.8	1	4.5	1	33.5	2	62.5	2	66.5	2
2	4.1	25.0	0.0	12.1	2	13.2	2	28.0	2	55.6	2	61.0	2
3	4.4	50.0	0.0	15.0	2	15.6	2	24.0	2	52.4	2	51.0	2
4	4.7	75.0	0.0	18.8	2	21.4	2	20.0	2	46.4	2	49.1	2
5	5.0	100.0	0.0	26.0	2	29.0	2	15.5	2	37.5	2	42.0	2
6	5.2	125.0	0.0	38.5	2	33.8	2	14.5	1	36.0	2	39.3	2
7	5.6	150.0	0.0	39.3	2	38.0	2	14.5	1	29.0	2	36.5	2
8	5.7	175.0	0.0	45.2	2	41.0	2	18.2	2	24.5	2	33.1	2
9	5.8	200.0	0.0	50.5	2	46.0	2	19.0	2	18.0	2	27.8	2
10	6.0	225.0	0.0	51.5	2	32.5	2	25.1	2	16.0	2	25.2	2
11	6.1	250.0	0.0	59.5	2	61.0	2	28.1	2	13.8	2	20.2	2
12	6.3	275.0	0.0	66.0	2	66.2	2	34.5	2	3.8	1	12.6	1

Table B16. FE-2A: Smoothed position of layers beneath shotpoints and geophones.

SP	Position	Surface Elev (ft)	Layer 2	
			Depth (ft)	Elev (ft)
A	-5.0	4.0	5.6	-1.6
M	137.5	5.3	6.4	-1.1
B	280.0	6.3	9.2	-2.9
Geophone				
1	0.0	4.0	5.6	-1.6
2	25.0	4.1	5.2	-1.1
3	50.0	4.4	4.5	-0.1
4	75.0	4.7	4.0	0.7
5	100.0	5.0	4.7	0.3
6	125.0	5.2	6.5	-1.3
7	150.0	5.5	6.4	-0.9
8	175.0	5.7	6.5	-0.8
9	200.0	5.8	5.5	0.8
10	225.0	6.0	6.5	-0.5
11	250.0	6.1	8.4	-2.3
12	275.0	6.8	9.2	-2.9
Velocities used:		Layer 1 1307.	Layer 2 5271.	



Table B18. JM-1: Smoothed position of layers beneath shotpoints and geophones.

SP	Position	Surface Elev (ft)	Layer 2	
			Depth (ft)	Elev (ft)
A	-10.0	5.2	5.5	-0.5
M	137.5	5.0	6.8	-1.8
B	285.0	4.0	7.1	-3.1
Geophone				
1	0.0	5.2	5.5	-0.3
2	25.0	5.0	6.7	-1.7
3	50.0	5.0	5.2	-0.2
4	75.0	5.1	4.7	0.4
5	100.0	5.0	5.5	-0.5
6	125.0	5.0	6.4	-1.4
7	150.0	4.9	7.1	-2.2
8	175.0	4.8	7.5	-2.7
9	200.0	4.8	7.1	-2.3
10	225.0	4.5	7.0	-2.5
11	250.0	4.1	7.4	-3.3
12	275.0	4.0	7.1	-3.1
		Layer 1	Layer 2	
Velocities used		1522.	4997.	





Table B20. TPT-1: Smoothed position of layers beneath shotpoints and geophones.

SP	Position	Surface Elev (ft)	Layer 2	
			Depth (ft)	Elev (ft)
A	-10.0	4.5	4.0	-0.4
M	139.0	4.5	7.0	-2.5
B	285.0	4.5	7.4	-2.9
Geophone				
1	0.0	4.5	5.0	-0.5
2	25.0	4.5	5.3	-0.8
3	50.0	4.5	6.4	-1.9
4	75.0	4.5	6.3	-1.8
5	100.0	4.5	6.2	-1.7
6	125.0	4.5	6.8	-2.3
7	150.0	4.5	7.1	-2.6
8	175.0	4.5	7.2	-2.7
9	200.0	4.5	6.5	-2.0
10	225.0	4.5	6.4	-1.9
11	250.0	4.5	7.5	-3.0
12	275.0	4.5	7.3	-2.8
		Layer 1	Layer 2	
Velocities used		1310.	4967.	



Table B22. TPT-2: Smoothed position of layers beneath shotpoints and geophones.

SP	Position	Surface Elev (ft)	Layer 2	
			Depth (ft)	Elev (ft)
A	-10.0	4.5	6.4	-1.9
M	140.0	4.6	6.1	-1.5
B	285.0	5.2	6.7	-1.5
Geophone				
1	0.0	4.5	6.4	-1.9
2	25.0	4.6	7.6	-3.0
3	50.0	4.6	6.6	-2.0
4	75.0	4.7	6.6	-1.9
5	100.0	4.6	7.1	-2.5
6	125.0	4.6	6.2	-1.6
7	150.0	4.6	6.0	-1.4
8	175.0	4.8	5.5	-0.7
9	200.0	5.0	7.1	-2.1
10	225.0	5.0	7.1	-2.1
11	250.0	5.1	7.6	-2.5
12	275.0	5.2	6.6	-1.4
		Layer 1	Layer 2	
Velocities used		1363.	4930.	



Table B24. TPT-3: Smoothed position of layers beneath shotpoints and geophones.

SP	Position	Surface Elev (ft)	Layer 2	
			Depth (ft)	Elev (ft)
A	-10.0	4.5	5.7	-1.2
M	139.0	6.1	7.1	-1.0
B	285.0	6.0	6.5	-0.5
Geophone				
1	0.0	4.5	5.7	-1.2
2	25.0	5.1	6.3	-1.2
3	50.0	5.7	7.2	-1.5
4	75.0	6.2	6.6	-0.4
5	100.0	6.4	7.7	-1.3
6	125.0	6.4	7.7	-1.3
7	150.0	5.8	6.6	-0.8
8	175.0	6.1	6.8	-0.7
9	200.0	6.3	7.7	-1.4
10	225.0	6.7	6.3	0.4
11	250.0	6.4	6.8	-0.4
12	275.0	6.0	6.5	-0.5
		Layer 1	Layer 2	
Velocities used		1266.	5088.	



Table B26. TPT-4: Smoothed position of layers beneath shotpoints and geophones.

SP	Position	Surface Elev (ft)	Layer 2	
			Depth (ft)	Elev (ft)
A	-10.0	6.2	9.6	-3.4
M	137.5	4.0	8.4	-4.4
B	285.0	4.0	11.3	-7.3
Geophone				
1	0.0	6.0	9.5	-3.5
2	25.0	5.5	9.1	-3.6
3	50.0	4.8	8.6	-3.8
4	75.0	3.4	6.8	-3.4
5	100.0	3.5	7.6	-4.0
6	125.0	3.8	8.5	-4.7
7	150.0	4.2	8.4	-4.2
8	175.0	4.4	9.3	-4.9
9	200.0	3.9	9.8	-5.9
10	225.0	4.3	9.2	-4.9
11	250.0	4.5	10.6	-6.1
12	275.0	4.0	11.1	-7.1
		Layer 1	Layer 2	
Velocities used		1398.	5867.	

Table B27. JT-1: Shotpoint information, geophone data, and arrival times. Times are in msec.

	SP	Elev (ft)	X Loc (ft)	Y Loc (ft)	Depth (ft)								
	F	5.0	-25.0	0.0	0.0								
	A	5.0	-10.0	0.0	0.0								
	M	4.6	137.5	10.0	0.0								
	B	6.5	285.0	0.0	0.0								
	R	6.5	300.0	0.0	0.0								

Geo	Elev (ft)	X Loc (ft)	Y Loc (ft)	SP	F	SP	A	SP	M	SP	B	SP	R
1	5.1	0.0	0.0	13.5	1	8.0	1	36.0	2	66.0	2	71.0	2
2	5.8	25.0	0.0	19.2	2	14.5	2	31.8	2	61.0	2	66.0	2
3	5.7	50.0	0.0	23.9	2	20.0	2	27.0	2	56.0	2	62.0	2
4	5.5	75.0	0.0	28.5	2	25.0	2	22.0	2	52.3	2	56.8	2
5	5.2	100.0	0.0	36.3	2	31.5	2	17.4	2	47.8	2	53.5	2
6	4.9	125.0	0.0	38.8	2	36.0	2	11.3	1	41.0	2	47.5	2
7	4.3	150.0	0.0	45.0	2	42.5	2	11.3	1	37.0	2	42.0	2
8	4.5	175.0	0.0	50.2	2	47.0	2	14.8	2	32.0	2	37.0	2
9	4.6	200.0	0.0	53.5	2	51.0	2	19.0	2	26.0	2	31.5	2
10	5.0	225.0	0.0	59.8	2	57.0	2	25.4	2	21.2	2	27.0	2
11	5.8	250.0	0.0	64.8	2	61.5	2	30.4	2	18.1	2	22.0	2
12	6.5	275.0	0.0	68.2	2	65.0	2	35.5	2	8.8	1	16.5	1



Table B28. TT-1: Smoothed position of layers beneath shotpoints and geophones.

SP	Position	Surface Elev (ft)	Layer 2	
			Depth (ft)	Elev (ft)
A	-10.0	5.0	4.4	0.6
M	157.5	4.6	6.6	-2.0
B	285.0	6.5	6.1	0.4
Geophone				
1	0.0	5.1	4.8	0.3
2	25.0	5.8	5.2	0.6
3	50.0	5.7	5.5	0.2
4	75.0	5.5	5.9	-0.4
5	100.0	5.2	7.5	-2.3
6	125.0	4.9	6.7	-1.8
7	150.0	4.3	6.5	-2.2
8	175.0	4.5	6.6	-2.1
9	200.0	4.6	5.5	-0.9
10	225.0	5.0	6.4	-1.4
11	250.0	5.8	6.7	-0.9
12	275.0	6.5	6.2	0.3
		Layer 1	Layer 2	
Velocities used		1431.	4962.	



Table B30. TI-2: Smoothed position of layers beneath shotpoints and geophones.

SP	Position	Surface Elev (ft)	Layer 2	
			Depth (ft)	Elev (ft)
A	-10.0	6.5	7.1	-0.6
M	138.5	8.6	5.4	3.2
B	285.0	12.4	7.3	5.1
Geophone				
1	0.0	6.5	6.8	-0.3
2	25.0	6.5	6.8	-0.3
3	50.0	7.0	7.7	-0.7
4	75.0	7.4	6.2	1.2
5	100.0	8.0	5.7	2.3
6	125.0	8.5	4.7	3.8
7	150.0	8.9	6.1	2.8
8	175.0	8.6	6.2	2.4
9	200.0	8.5	7.5	1.0
10	225.0	8.8	7.7	1.1
11	250.0	9.2	7.3	1.9
12	275.0	12.7	7.7	5.0
		Layer 1	Layer 2	
Velocities used		1131.	5550.	

Table B31. BST-1: Shotpoint information, geophone data, and arrival times.  
Times are in msec.

	SP	Elev (ft)	X Loc (ft)	Y Loc (ft)	Depth (ft)								
	F	3.0	-25.0	0.0	0.0								
	A	3.5	-10.0	0.0	0.0								
	M	3.3	137.5	10.0	0.0								
	B	4.9	285.0	0.0	0.0								
	R	4.9	300.0	0.0	0.0								

Geo	Elev (ft)	X Loc (ft)	Y Loc (ft)	SP	F	SP	A	SP	M	SP	B	SP	R
1	3.5	0.0	0.0	14.5	1	8.4	1	37.5	2	62.0	3	63.5	3
2	4.7	25.0	0.0	20.8	2	19.0	2	33.0	2	59.5	3	61.0	3
3	4.4	50.0	0.0	26.6	2	24.2	2	28.7	2	55.0	3	57.2	3
4	4.2	75.0	0.0	33.0	2	29.5	2	24.0	2	52.0	2	54.5	2
5	3.8	100.0	0.0	35.0	2	32.8	2	15.4	2	43.6	2	46.5	2
6	3.4	125.0	0.0	40.2	2	37.3	2	11.0	1	39.4	2	41.0	2
7	3.3	150.0	0.0	44.5	2	43.0	2	11.0	1	35.2	2	37.5	2
8	3.3	175.0	0.0	49.0	2	46.5	2	14.5	2	29.5	2	32.5	2
9	3.7	200.0	0.0	53.0	2	50.0	2	20.6	2	24.2	2	27.0	2
10	4.5	225.0	0.0	58.2	3	55.0	2	25.5	2	18.6	2	22.5	2
11	4.7	250.0	0.0	62.0	3	58.0	3	29.2	2	14.0	2	17.4	2
12	4.9	275.0	0.0	66.0	3	63.3	3	34.0	2	8.1	1	13.0	1

Table B32. BST-1: Smoothed position of layers beneath shotpoints and geophones.

SP	Position	Surface Elev (ft)	Layer 2		Layer 3	
			Depth (ft)	Elev (ft)	Depth (ft)	Elev (ft)
A	-10.0	3.5	9.9	-6.4	53.9	-50.4
M	137.5	3.3	7.4	-4.1	52.7	-49.4
B	285.0	4.9	7.9	-3.0	48.7	-43.8
Geophone						
1	0.0	3.5	9.7	-6.2	53.8	-50.3
2	25.0	4.7	9.6	-4.9	54.8	-50.1
3	50.0	4.4	10.3	-5.9	54.4	-50.0
4	75.0	4.2	10.6	-6.4	54.3	-50.1
5	100.0	3.8	7.5	-3.7	53.4	-49.4
6	125.0	3.4	7.3	-3.9	52.9	-49.5
7	150.0	3.3	7.5	-4.2	52.7	-49.4
8	175.0	3.3	6.8	-3.5	52.5	-49.1
9	200.0	3.7	6.2	-2.5	52.8	-49.1
10	225.0	4.5	6.1	-1.6	53.2	-48.7
11	250.0	4.7	5.9	-1.2	50.0	-45.3
12	275.0	4.9	6.9	-2.0	48.3	-43.4
			Layer 1	Layer 2	Layer 3	
Velocities used			1497.	5110.	6343.	



Table B34. BST-2: Smoothed position of layers beneath shotpoints and geophones.

SP	Position	Surface Elev (ft)	Layer 2		Layer 3	
			Depth (ft)	Elev (ft)	Depth (ft)	Elev (ft)
A	-10.0	4.7	6.4	-1.7	48.9	-44.2
M	136.5	5.2	9.9	-4.7	60.2	-55.0
B	285.0	6.2	7.2	-1.0	52.5	-46.3
Geophone						
1	0.0	4.9	7.0	-2.1	48.3	-43.4
2	25.0	4.9	9.1	-4.2	49.2	-44.3
3	50.0	4.1	9.9	-5.8	49.4	-45.3
4	75.0	4.3	9.1	-4.8	47.4	-43.1
5	100.0	4.5	9.3	-4.8	44.6	-40.1
6	125.0	4.9	9.5	-4.6	57.4	-52.5
7	150.0	5.2	10.0	-4.8	63.1	-57.9
8	175.0	5.6	9.8	-4.2	63.8	-57.9
9	200.0	6.1	6.8	-0.7	64.2	-58.1
10	225.0	6.1	6.3	-0.2	64.1	-58.0
11	250.0	6.4	6.4	-0.0	64.1	-57.7
12	275.0	6.2	6.5	-0.3	51.6	-45.4
			Layer 1	Layer 2	Layer 3	
Velocities used			1443.	4936.	12074.	





Table B36. B3T-3: Smoothed position of layers beneath shotpoints and geophones.

SP	Position	Surface Elev (ft)	Layer 2		Layer 3	
			Depth (ft)	Elev (ft)	Depth (ft)	Elev (ft)
A	-10.0	6.2	6.4	-0.2	56.5	-50.3
M	137.0	5.2	7.3	-2.1	59.6	-54.4
B	285.0	7.0	9.0	-0.2	32.4	-25.4
Geophone						
1	0.0	6.2	6.6	-0.4	51.6	-45.4
2	25.0	6.2	8.1	-1.9	54.0	-47.8
3	50.0	5.8	6.6	-0.8	62.9	-57.1
4	75.0	5.5	8.5	-3.0	58.5	-53.0
5	100.0	5.2	7.5	-2.3	54.1	-48.9
6	125.0	5.2	6.8	-1.6	50.0	-44.8
7	150.0	5.2	7.8	-2.6	70.1	-64.9
8	175.0	5.7	6.6	-0.9	57.4	-51.7
9	200.0	6.0	5.3	0.7	51.3	-45.3
10	225.0	6.7	6.2	0.5	45.5	-38.8
11	250.0	6.8	7.5	-0.7	39.2	-32.4
12	275.0	6.9	8.9	-2.0	35.1	-28.2
			Layer 1	Layer 2	Layer 3	
Velocities used			1486.	5530.	7432.	

Table B37. BWT-1: Shotpoint information, geophone data, and arrival times.  
Times are in msec.

	SP	Elev (ft)	X Loc (ft)	Y Loc (ft)	Depth (ft)				
	F	5.5	-25.0	0.0	0.0				
	M	4.2	139.5	10.0	0.0				
	R	1.7	300.0	0.0	0.0				

Geo	Elev (ft)	X Loc (ft)	Y Loc (ft)	SP	F	SP	M	SP	R
1	5.5	0.0	0.0	13.5	1	35.5	2	64.2	3
2	5.3	25.0	0.0	19.0	2	31.0	2	58.8	3
3	5.4	50.0	0.0	25.5	2	27.5	2	55.3	2
4	5.2	75.0	0.0	30.8	2	22.0	2	51.3	2
5	5.0	100.0	0.0	38.3	2	18.3	2	46.0	2
6	4.5	125.0	0.0	40.4	2	12.2	1	40.2	2
7	3.8	150.0	0.0	45.1	2	11.2	1	34.4	2
8	3.5	175.0	0.0	49.5	2	16.6	2	28.8	2
9	3.2	200.0	0.0	56.4	2	22.0	2	25.1	2
10	3.1	225.0	0.0	60.2	3	27.0	2	20.0	2
11	2.0	250.0	0.0	63.2	3	29.5	3	13.2	2
12	1.7	275.0	0.0	66.9	3	33.3	3	8.4	1

Table B38. BWT-1: Smoothed position of layers beneath shotpoints and geophones.

SP	Position	Surface Elev (ft)	Layer 2		Layer 3	
			Depth (ft)	Elev (ft)	Depth (ft)	Elev (ft)
F	-25.0	5.5	3.1	2.4	98.3	-92.8
M	139.5	4.2	9.2	-5.0	57.3	-53.1
R	300.0	1.7	2.3	-0.6	16.7	-15.0
Geophone						
1	0.0	5.5	4.4	1.1	92.4	-86.9
2	25.0	5.3	7.0	-1.7	86.3	-81.0
3	50.0	5.4	8.8	-3.4	80.5	-75.1
4	75.0	5.2	9.7	-4.5	74.3	-69.1
5	100.0	5.0	11.0	-6.0	68.2	-63.2
6	125.0	4.5	10.0	-5.5	61.8	-57.3
7	150.0	3.8	8.5	-4.7	53.8	-50.0
8	175.0	3.5	8.3	-4.8	46.3	-42.6
9	200.0	3.2	9.3	-6.1	42.5	-39.3
10	225.0	3.1	8.2	-5.1	37.5	-34.4
11	250.0	2.0	3.8	-1.8	27.8	-25.8
12	275.0	1.7	3.1	-1.4	22.5	-20.8
			Layer 1	Layer 2	Layer 3	
Velocities used			2043.	4913.	6013.	

Table B39 CL-1: Shotpoint information, geophone data, and arrival times.  
Times are in msec.

	SP	Elev (ft)	X Loc (ft)	Y Loc (ft)	Depth (ft)					
	F	5.0	-25.0	0.0	0.0					
	M	6.5	140.0	25.0	0.0					
	R	6.5	300.0	0.0	0.0					

Geo	Elev (ft)	X Loc (ft)	Y Loc (ft)	SP	F	SP	M	SP	R
1	5.0	0.0	0.0	15.0	1	31.0	2	65.0	3
2	5.0	25.0	0.0	20.9	2	26.5	2	60.4	2
3	5.2	50.0	0.0	25.0	2	20.3	2	55.8	2
4	6.2	75.0	0.0	30.2	2	17.5	2	52.7	2
5	6.5	100.0	0.0	33.0	2	14.5	2	47.0	2
6	6.5	125.0	0.0	43.3	2	14.2	1	43.8	2
7	6.5	150.0	0.0	47.6	2	17.0	1	40.5	2
8	6.5	175.0	0.0	51.2	2	19.0	2	31.6	2
9	6.5	200.0	0.0	54.2	2	23.5	2	30.4	2
10	6.5	225.0	0.0	59.8	3	28.6	2	25.6	2
11	6.5	250.0	0.0	61.6	3	34.0	2	17.3	2
12	6.5	275.0	0.0	65.0	3	41.8	2	12.0	1

Table B40. Cl-1: Smoothed position of layers beneath shotpoints and geophones.

SP	Position	Surface Elev (ft)	Layer 2		Layer 3	
			Depth (ft)	Elev (ft)	Depth (ft)	Elev (ft)
F	-25.0	5.0	1.7	3.3	48.9	-43.9
M	140.0	6.5	11.3	-4.8	97.9	-91.4
R	300.0	6.5	17.5	-11.0	108.0	-101.5
Geophone						
1	0.0	5.0	2.7	2.3	55.6	-50.6
2	25.0	5.0	6.1	-1.1	60.4	-55.4
3	50.0	5.2	5.8	-0.6	67.7	-62.5
4	75.0	6.2	7.5	-1.3	75.7	-69.5
5	100.0	6.5	7.5	-1.0	83.1	-76.6
6	125.0	6.5	11.1	-4.6	90.2	-83.7
7	150.0	6.5	11.5	-5.0	103.0	-96.5
8	175.0	6.5	11.5	-5.0	103.6	-97.1
9	200.0	6.5	12.4	-5.9	103.2	-96.7
10	225.0	6.5	13.2	-6.7	100.3	-93.8
11	250.0	6.5	13.9	-7.4	103.9	-97.4
12	275.0	6.5	16.6	-10.1	107.4	-100.9
			Layer 1	Layer 2	Layer 3	
Velocities used			1847.	5210.	9338.	



Table B67. DSJCT: Smoothed position of layers beneath shotpoints and geophones.

SP	Position	Surface Elev (ft)	Layer 2		Layer 3	
			Depth (ft)	Elev (ft)	Depth (ft)	Elev (ft)
A	-10.0	9.0	4.2	4.8	14.5	-5.5
M	137.5	9.0	7.8	1.2	59.9	-50.9
B	285.0	9.0	4.4	4.6	52.2	-43.2
Geophone						
1	0.0	9.0	4.4	4.6	17.5	-8.5
2	25.0	8.5	5.9	2.6	37.9	-29.4
3	50.0	8.0	4.1	3.9	49.9	-41.9
4	75.0	7.5	1.4	6.1	52.4	-44.9
5	100.0	8.0	6.1	1.9	55.3	-47.3
6	125.0	9.0	7.7	1.3	58.7	-47.3
7	150.0	9.0	7.8	1.2	61.1	-52.1
8	175.0	8.5	6.0	2.5	63.0	-54.5
9	200.0	9.0	5.0	4.0	56.9	-47.9
10	225.0	9.0	2.4	6.6	52.8	-43.8
11	250.0	9.0	6.1	2.9	54.5	-45.5
12	275.0	9.0	4.7	4.3	53.0	-44.0
		Layer 1	Layer 2	Layer 3		
Velocities used		1273.	5439.	8720.		





Table B44. IS5GT: Smoothed position of layers beneath shotpoints and geophones.

SP	Position	Surface Elev (ft)	Layer 2		Layer 3	
			Depth (ft)	Elev (ft)	Depth (ft)	Elev (ft)
A	-10.0	8.5	9.6	-1.1	58.9	-50.4
M	137.5	8.5	9.9	-1.4	57.4	-48.9
B	285.0	8.5	10.5	-2.0	10.5	-2.0
<b>Geophone</b>						
1	0.0	8.5	9.6	-1.1	59.0	-50.5
2	25.0	8.5	9.7	-1.2	57.2	-48.7
3	50.0	8.5	8.5	-0.0	55.3	-46.8
4	75.0	8.5	7.2	1.3	60.8	-52.3
5	100.0	8.5	10.3	-1.8	59.5	-51.0
6	125.0	8.5	9.9	-1.4	58.3	-49.8
7	150.0	8.5	9.9	-1.4	56.6	-48.1
8	175.0	8.5	9.5	-1.0	45.1	-36.6
9	200.0	8.5	7.6	0.9	33.0	-24.5
10	225.0	8.5	7.3	1.2	21.0	-12.5
11	250.0	8.5	10.0	-1.5	13.7	-5.2
12	275.0	8.5	10.4	-1.9	10.4	-1.9
			<b>Layer 1</b>	<b>Layer 2</b>	<b>Layer 3</b>	
<b>Velocities used</b>			1228.	5096.	7146.	



Table B46. EPT-1: Smoothed position of layers beneath shotpoints and geophones.

SP	Position	Surface Elev (ft)	Layer 2		Layer 3	
			Depth (ft)	Elev (ft)	Depth (ft)	Elev (ft)
A	-10.0	4.5	8.9	-4.4	36.2	-31.7
M	136.0	4.2	7.2	-3.0	59.1	-54.9
B	285.0	1.8	2.2	-0.4	55.4	-53.6
Geophone						
1	0.0	4.5	8.8	-4.3	38.1	-33.6
2	25.0	5.2	8.3	-3.1	40.8	-35.6
3	50.0	4.3	7.8	-3.5	42.0	-37.7
4	75.0	4.3	7.3	-3.0	47.6	-43.3
5	100.0	4.4	7.6	-3.2	52.6	-48.2
6	125.0	4.2	7.2	-3.0	62.0	-57.8
7	150.0	4.1	7.1	-3.0	55.3	-51.2
8	175.0	3.8	7.0	-3.2	49.0	-45.2
9	200.0	3.4	6.2	-2.8	45.6	-42.2
10	225.0	3.0	4.9	-1.9	52.1	-49.1
11	250.0	2.0	5.0	-3.0	52.9	-50.9
12	275.0	2.0	3.0	-1.0	54.8	-52.8
			Layer 1	Layer 2	Layer 3	
Velocities used:			1435.	4906.	6852.	



Table B48. EFT-2: Smoothed position of layers beneath shotpoints and geophones.

SP	Position	Surface Elev (ft)	Layer 2		Layer 3	
			Depth (ft)	Elev (ft)	Depth (ft)	Elev (ft)
A	-25.0	2.0	3.8	-1.8	54.1	-52.1
M	140.0	3.3	4.1	-0.8	58.7	-55.4
B	285.0	7.3	8.3	-1.0	57.2	-49.9
Geophone						
1	0.0	2.0	2.9	-0.9	54.8	-52.8
2	25.0	3.7	3.3	0.4	58.4	-54.7
3	50.0	3.7	1.9	1.8	60.2	-56.5
4	75.0	2.1	2.3	-0.2	60.4	-58.3
5	100.0	2.7	3.0	-0.3	62.7	-60.0
6	125.0	3.3	4.0	-0.7	62.3	-59.0
7	150.0	3.3	4.2	-0.9	56.3	-53.0
8	175.0	6.4	6.0	0.4	53.4	-47.0
9	200.0	7.1	7.3	-0.2	50.8	-43.7
10	225.0	7.0	9.4	-2.4	50.6	-43.6
11	250.0	7.0	10.1	-3.1	53.0	-46.0
12	275.0	7.3	8.6	-1.3	56.3	-49.0
			Layer 1	Layer 2	Layer 3	
Velocities used:			1558.	5190.	7274.	



Table B50. EPT-3: Smoothed position of layers beneath shotpoints and geophones.

SP	Position	Surface Elev (ft)	Layer 2		Layer 3	
			Depth (ft)	Elev (ft)	Depth (ft)	Elev (ft)
A	-10.0	7.2	9.2	-2.0	55.0	-47.8
M	137.5	7.5	6.5	1.0	56.6	-49.1
B	285.0	8.0	4.2	3.8	44.0	-36.0
Geophone						
1	0.0	7.3	8.5	-1.2	56.3	-49.0
2	25.0	7.1	7.8	-0.7	58.2	-51.1
3	50.0	7.7	6.6	1.1	60.8	-53.1
4	75.0	7.7	6.1	1.6	62.6	-54.9
5	100.0	7.7	6.5	1.2	59.8	-52.1
6	125.0	7.2	6.6	0.6	57.3	-50.1
7	150.0	7.2	5.8	1.4	55.4	-48.2
8	175.0	7.5	6.4	1.1	55.9	-48.4
9	200.0	7.5	4.9	2.6	63.2	-55.7
10	225.0	4.9	3.7	1.2	58.4	-53.5
11	250.0	4.9	3.1	1.8	36.2	-31.3
12	275.0	4.9	1.6	3.3	40.7	-35.8
			Layer 1	Layer 2	Layer 3	
Velocities used:			1484.	4954.	9536.	

Table B51. EPT-4: Shotpoint information, geophone data, and arrival times.  
Times are in msec.

	SP	Elev (ft)	X Loc (ft)	Y Loc (ft)	Depth (ft)				
	F	4.9	-10.0	0.0	0.0				
	M	7.6	137.5	10.0	0.0				
	R	8.6	285.0	0.0	0.0				

Geo	Elev (ft)	X Loc (ft)	Y Loc (ft)	SP	F	SP	M	SP	R
1	4.9	0.0	0.0	7.0	2	33.0	3	60.0	3
2	8.0	25.0	0.0	10.0	2	31.0	3	55.5	3
3	8.0	50.0	0.0	15.0	2	28.5	2	53.4	3
4	7.8	75.0	0.0	22.0	2	22.0	2	52.0	2
5	7.6	100.0	0.0	29.0	2	16.0	2	47.0	2
6	7.4	125.0	0.0	34.7	2	12.5	1	44.0	2
7	8.1	150.0	0.0	41.0	2	12.5	1	37.6	2
8	8.1	175.0	0.0	44.0	2	19.0	2	29.0	2
9	8.1	200.0	0.0	50.0	2	20.0	2	23.0	2
10	8.7	225.0	0.0	52.6	3	26.0	2	22.0	2
11	8.7	250.0	0.0	56.3	3	31.0	2	18.0	2
12	8.8	275.0	0.0	58.0	3	37.0	2	12.0	2



Table B52. BPT-4: Smoothed position of layers beneath shotpoints and geophones.

SP	Position	Surface Elev (ft)	Layer 2		Layer 3	
			Depth (ft)	Elev (ft)	Depth (ft)	Elev (ft)
F	-10.0	4.9	2.2	2.7	38.9	-34.0
M	137.5	7.6	8.5	-0.9	44.7	-37.1
R	285.0	8.6	7.0	1.6	51.1	-42.5
Geophone						
1	0.0	4.9	1.6	3.3	40.7	-35.8
2	25.0	8.0	3.5	4.5	44.2	-36.2
3	50.0	8.0	6.9	1.1	44.6	-36.6
4	75.0	7.8	7.8	0.0	50.9	-43.1
5	100.0	7.6	8.3	-0.7	44.8	-37.2
6	125.0	7.4	8.5	-1.1	41.9	-34.5
7	150.0	8.1	8.9	-0.8	47.9	-39.8
8	175.0	8.1	7.4	0.7	49.5	-41.4
9	200.0	8.1	5.8	2.3	48.9	-40.8
10	225.0	8.7	6.7	2.0	49.0	-40.3
11	250.0	8.7	7.4	1.3	50.1	-41.4
12	275.0	8.8	7.3	1.5	51.2	-42.4
			Layer 1	Layer 2	Layer 3	
Velocities used:			1281.	4734.	6654.	



Table B54. 7E-2: Smoothed position of layers beneath shotpoints and geophones.

SP	Position	Surface Elev (ft)	Layer 2		Layer 3	
			Depth (ft)	Elev (ft)	Depth (ft)	Elev (ft)
A	-10.0	4.0	3.3	0.7	40.6	-36.6
M	137.5	5.3	3.4	1.9	48.3	-43.0
B	285.0	6.3	5.6	0.7	33.9	-27.6
Geophone						
1	0.0	4.0	3.0	1.0	41.1	-37.1
2	25.0	4.1	2.4	1.7	42.5	-38.4
3	50.0	4.4	1.8	2.6	44.1	-39.7
4	75.0	4.7	2.0	2.7	45.8	-41.1
5	100.0	5.0	2.8	2.2	47.4	-42.4
6	125.0	5.2	3.1	2.1	48.9	-43.7
7	150.0	5.5	3.7	1.8	47.7	-42.2
8	175.0	5.7	3.5	2.2	50.1	-44.4
9	200.0	5.8	2.1	3.7	52.6	-46.8
10	225.0	6.0	2.4	3.6	49.9	-43.9
11	250.0	6.1	3.5	2.6	40.5	-34.3
12	275.0	6.3	4.8	1.5	34.6	-28.3
			Layer 1	Layer 2	Layer 3	
Velocities used:			920.	5335.	6874.	



Table B56. FE-3: Smoothed position of layers beneath shotpoints and geophones.

SP	Position	Surface Elev (ft)	Layer 2		Layer 3	
			Depth (ft)	Elev (ft)	Depth (ft)	Elev (ft)
A	-5.0	6.3	4.6	1.7	35.8	-29.5
M	137.0	7.4	6.3	1.1	46.1	-38.7
N	138.0	7.4	6.3	1.1	46.2	-38.8
B	280.0	8.0	5.9	2.1	58.6	-50.6
Geophone						
1	0.0	4.0	2.5	1.5	32.3	-28.3
2	25.0	4.1	4.5	-0.4	30.6	-26.5
3	50.0	4.4	3.6	0.8	29.1	-24.7
4	75.0	4.7	3.1	1.6	36.3	-31.6
5	100.0	5.0	4.5	0.5	40.6	-35.6
6	125.0	5.2	4.3	0.9	42.9	-37.7
7	150.0	5.5	4.1	1.4	45.3	-39.8
8	175.0	5.7	3.6	2.1	47.7	-42.0
9	200.0	5.8	3.6	2.2	49.2	-43.4
10	225.0	6.0	3.7	2.3	51.6	-45.6
11	250.0	6.1	3.8	2.3	54.0	-47.9
12	275.0	6.3	4.3	2.0	56.5	-50.2
			Layer 1	Layer 2	Layer 3	
Velocities used:			887.	5176.	8125.	



Table B58. II-1: Smoothed position of layers beneath shotpoints and geophones.

SP	Position	Surface Elev (ft)	Layer 2		Layer 3	
			Depth (ft)	Elev (ft)	Depth (ft)	Elev (ft)
A	-10.0	5.1	6.8	-1.7	77.8	-72.7
M	140.0	5.9	8.2	-2.3	82.0	-76.1
B	285.0	7.0	8.2	-1.2	83.5	-76.5
Geophone						
1	0.0	5.2	6.9	-1.7	78.0	-72.8
2	25.0	5.4	8.1	-2.7	79.0	-83.6
3	50.0	5.6	7.7	-2.1	80.1	-74.5
4	75.0	5.6	7.6	-2.0	78.4	-72.8
5	100.0	5.7	7.6	-1.9	80.0	-74.3
6	125.0	5.8	8.3	-2.5	81.2	-75.4
7	150.0	6.0	8.2	-2.2	84.1	-77.7
8	175.0	6.4	8.7	-2.2	84.1	-77.7
9	200.0	6.5	7.6	-1.1	85.1	-78.6
10	225.0	6.7	7.7	-1.0	83.1	-76.4
11	250.0	6.9	6.2	0.7	83.4	-76.5
12	275.0	7.0	7.4	-0.4	83.5	-76.5
			Layer 1	Layer 2	Layer 3	
Velocities used			1335.	5066.	9299.	

Table B59. IR-2: Shotpoint information, geophone data, and arrival times. Times are in msec.

	SP	Elev (ft)	X Loc (ft)	Y Loc (ft)	Depth (ft)								
	F	7.0	-25.0	0.0	0.0								
	A	7.0	-10.0	0.0	0.0								
	M	8.4	141.0	10.0	0.0								
	B	10.0	285.0	0.0	0.0								
	R	10.0	300.0	0.0	0.0								

Geo	Elev (ft)	X Loc (ft)	Y Loc (ft)	SP	F	SP	A	SP	M	SP	B	SP	R
1	7.0	0.0	0.0	17.4	1	9.0	1	42.0	2	64.8	3	68.6	3
2	7.1	25.0	0.0	22.3	2	19.0	2	39.0	2	63.4	3	65.8	3
3	7.5	50.0	0.0	26.2	2	20.0	2	33.0	2	59.7	2	61.4	2
4	7.8	75.0	0.0	29.5	2	23.0	2	27.5	2	51.5	2	56.3	2
5	8.0	100.0	0.0	35.8	2	32.5	2	22.0	2	46.0	2	51.7	2
6	8.3	125.0	0.0	39.2	2	37.0	2	14.2	1	33.0	2	45.3	2
7	8.6	150.0	0.0	44.8	2	43.5	2	12.3	1	29.0	2	40.5	2
8	9.2	175.0	0.0	50.8	2	50.2	2	22.2	2	26.6	2	35.9	2
9	9.4	200.0	0.0	54.0	2	52.0	2	22.8	2	25.0	2	32.1	2
10	9.5	225.0	0.0	58.0	2	58.0	2	26.5	2	23.2	2	30.0	2
11	10.0	250.0	0.0	63.6	3	63.3	3	37.0	2	21.6	2	27.3	2
12	10.0	275.0	0.0	67.7	3	67.0	3	41.5	2	13.0	1	20.2	1



Table B60. CR-2: Smoothed position of layers beneath shotpoints and geophones.

SP	Position	Surface Elev (ft)	Layer 2		Layer 3	
			Depth (ft)	Elev (ft)	Depth (ft)	Elev (ft)
A	-10.0	7.0	6.9	0.1	83.5	-76.5
M	141.0	8.4	5.5	2.9	73.0	-64.6
B	285.0	10.0	10.5	-0.5	47.6	-37.6
Geophone						
1	0.0	7.0	7.4	-0.4	83.5	-76.5
2	25.0	7.1	9.5	-2.4	83.5	-76.4
3	50.0	7.5	8.0	-0.5	83.9	-76.4
4	75.0	7.8	6.2	1.2	82.7	-74.9
5	100.0	8.0	6.8	1.2	80.7	-72.7
6	125.0	8.3	4.8	3.5	76.1	-67.8
7	150.0	8.6	6.0	2.6	71.4	-62.8
8	175.0	9.2	7.0	2.2	67.1	-57.9
9	200.0	9.4	6.2	3.2	62.4	-53.0
10	225.0	9.5	7.5	2.0	57.6	-48.1
11	250.0	10.0	10.9	-0.9	54.2	-44.2
12	275.0	10.0	10.2	-0.2	49.5	-39.5
			Layer 1	Layer 2	Layer 3	
Velocities used			1163.	5239.	8213.	

Table B61. LWT-1: Shotpoint information, geophone data, and arrival times. Times are in msec.

	SP	Elev (ft)	X Loc (ft)	Y Loc (ft)	Depth (ft)								
	F	6.7	-25.0	0.0	0.0								
	A	6.7	-10.0	0.0	0.0								
	M	7.0	137.5	10.0	0.0								
	B	8.0	285.0	0.0	0.0								
	R	7.5	300.0	0.0	0.0								

Geo	Elev (ft)	X Loc (ft)	Y Loc (ft)	SP	F	SP	A	SP	M	SP	B	SP	R
1	6.7	0.0	0.0	14.4	1	9.1	1	34.5	2	62.5	3	64.0	3
2	6.7	25.0	0.0	17.6	2	19.5	2	31.4	2	60.5	3	63.0	3
3	6.5	50.0	0.0	19.1	2	21.0	2	26.2	2	57.6	3	59.3	3
4	6.1	75.0	0.0	23.4	2	23.5	2	21.0	2	51.0	2	55.3	2
5	5.8	100.0	0.0	25.3	2	25.0	2	17.6	2	49.0	2	48.0	2
6	5.6	125.0	0.0	27.8	2	29.0	2	12.5	1	44.5	2	46.0	2
7	6.8	150.0	0.0	38.4	2	37.0	2	13.0	1	42.7	2	39.6	2
8	9.5	175.0	0.0	48.3	2	47.5	2	15.9	2	34.4	2	31.0	2
9	10.5	200.0	0.0	56.0	3	54.2	3	21.0	2	26.5	2	21.5	2
10	10.5	225.0	0.0	60.0	3	59.5	3	30.0	2	18.5	2	18.0	2
11	10.0	250.0	0.0	65.0	3	64.5	3	36.9	2	15.0	2	17.3	2
12	9.5	275.0	0.0	68.0	3	69.0	3	40.0	2	9.5	1	14.5	1

Table B62. LWT-1: Smoothed position of layers beneath shotpoints and geophones.

SP	Position	Surface Elev (ft)	Layer 2		Layer 3	
			Depth (ft)	Elev (ft)	Depth (ft)	Elev (ft)
A	-10.0	6.7	5.6	1.1	45.2	-38.5
M	137.5	7.0	7.8	-0.8	75.4	-68.4
B	285.0	8.0	8.1	-0.1	98.0	-90.0
Geophone						
1	0.0	6.7	5.1	1.6	42.1	-35.4
2	25.0	6.7	6.7	-0.0	45.6	-38.9
3	50.0	6.5	4.4	2.1	46.5	-40.0
4	75.0	6.1	3.7	2.4	50.5	-44.4
5	100.0	5.8	5.6	0.2	59.2	-53.4
6	125.0	5.6	6.7	-1.1	69.0	-63.4
7	150.0	6.8	7.2	-0.4	80.1	-73.3
8	175.0	9.5	8.7	0.8	85.7	-76.2
9	200.0	10.5	7.4	3.1	88.6	-78.1
10	225.0	10.5	8.6	1.9	89.4	-78.9
11	250.0	10.0	10.9	-0.9	93.9	-83.9
12	275.0	9.5	9.6	-0.1	98.3	-88.8
			Layer 1	Layer 2	Layer 3	
Velocities used			1358.	4692.	6827.	



Table B64. LWT-2: Smoothed position of layers beneath shotpoints and geophones.

SP	Position	Surface Elev (ft)	Layer 2		Layer 3	
			Depth (ft)	Elev (ft)	Depth (ft)	Elev (ft)
A	-10.0	8.6	6.7	1.9	6.7	1.9
M	137.0	6.6	6.0	0.6	42.0	-35.4
B	285.0	6.7	5.8	0.9	43.5	-36.8
Geophone						
1	0.0	8.6	6.8	1.8	6.8	1.8
2	25.0	7.1	6.0	1.1	43.7	-36.6
3	50.0	7.1	4.1	3.0	47.5	-40.4
4	75.0	7.0	4.9	2.1	54.1	-47.1
5	100.0	6.8	4.7	2.1	60.5	-53.7
6	125.0	6.4	6.0	0.4	47.9	-41.5
7	150.0	6.8	6.0	0.8	35.7	-28.9
8	175.0	7.1	3.8	3.3	45.6	-38.5
9	200.0	8.6	4.6	4.0	37.3	-28.7
10	225.0	6.7	5.4	1.3	74.0	-67.3
11	250.0	6.7	6.4	0.3	49.8	-43.1
12	275.0	6.7	5.1	1.6	42.1	-35.4
			Layer 1	Layer 2	Layer 3	
Velocities used			1343.	4847.	10259.	



Table B66. N-1: Smoothed position of layers beneath shotpoints and geophones.

SP	Position	Surface Elev (ft)	Layer 2		Layer 3	
			Depth (ft)	Elev (ft)	Depth (ft)	Elev (ft)
A	-10.0	5.6	3.1	2.5	55.7	-50.1
M	137.5	5.3	6.4	-1.1	67.8	-62.5
B	285.0	5.5	5.1	0.4	50.8	-45.3
Geophone						
1	0.0	5.1	2.9	2.2	55.9	-50.8
2	25.0	5.3	3.5	1.8	58.3	-53.0
3	50.0	5.4	4.0	1.4	60.6	-55.2
4	75.0	5.6	5.0	0.6	58.7	-53.1
5	100.0	5.3	5.8	-0.5	60.7	-55.4
6	125.0	5.3	6.7	-1.4	66.9	-61.6
7	150.0	5.4	6.1	-0.7	68.8	-63.4
8	175.0	5.2	5.2	-0.0	68.3	-63.1
9	200.0	5.0	3.7	1.3	67.6	-62.6
10	225.0	5.1	3.7	1.4	62.4	-57.3
11	250.0	5.3	5.4	-0.1	53.2	-47.9
12	275.0	5.5	5.1	0.4	52.3	-46.8
			Layer 1	Layer 2	Layer 3	
Velocities used			1320.	4922.	7155.	





Table B68. NT-2: Smoothed position of layers beneath shotpoints and geophones.

SP	Position	Surface Elev (ft)	Layer 2		Layer 3	
			Depth (ft)	Elev (ft)	Depth (ft)	Elev (ft)
A	-10.0	4.5	5.2	-0.7	74.0	-69.5
M	136.0	6.1	8.1	-2.0	69.4	-63.3
B	285.0	5.8	4.2	1.6	72.4	-66.6
Geophones						
1	0.0	4.2	4.9	-0.7	73.3	-69.1
2	25.0	3.5	5.5	-2.0	72.6	-69.1
3	50.0	3.5	8.1	-4.6	72.6	-69.1
4	75.0	4.7	7.8	-3.1	73.8	-69.1
5	100.0	5.5	6.0	-0.5	74.6	-69.1
6	125.0	6.1	8.3	-2.2	68.2	-62.1
7	150.0	6.1	7.9	-1.8	71.0	-65.4
8	175.0	6.0	6.9	-0.9	71.4	-65.4
9	200.0	6.0	7.2	-1.2	72.0	-66.0
10	225.0	6.0	7.4	-1.4	72.5	-66.5
11	250.0	6.0	6.5	-0.5	72.5	-66.5
12	275.0	5.8	4.4	1.4	72.3	-66.5
			Layer 1	Layer 2	Layer 3	
Velocities used			1331.	5343.	6927.	



Table B70. N-3: Smoothed position of layers beneath shotpoints and geophones.

SP	Position	Surface Elev (ft)	Layer 2		Layer 3	
			Depth (ft)	Elev (ft)	Depth (ft)	Elev (ft)
A	-10.0	6.5	9.6	-3.1	79.0	-72.5
M	137.5	6.5	6.5	-0.0	95.6	-89.1
B	285.0	5.6	5.2	0.4	106.7	-101.1
Geophone						
1	0.0	6.3	9.3	-3.0	79.9	-73.6
2	25.0	6.0	8.1	-2.1	82.1	-76.1
3	50.0	5.7	6.0	-0.3	84.3	-78.6
4	75.0	5.8	9.9	-4.1	86.9	-81.1
5	100.0	6.0	8.6	-2.6	89.5	-83.5
6	125.0	6.2	6.9	-0.7	93.7	-87.5
7	150.0	7.0	6.4	0.6	97.6	-90.6
8	175.0	7.8	9.5	-1.7	98.0	-90.2
9	200.0	6.3	9.7	-3.4	99.0	-92.7
10	225.0	6.0	7.8	-1.8	101.2	-95.2
11	250.0	5.2	7.5	-2.3	102.9	-97.7
12	275.0	5.5	5.1	0.4	105.7	-100.2
			Layer 1	Layer 2	Layer 3	
Velocities used:			1428.	5881.	8453.	



Table B72. NC-4: Smoothed position of layers beneath shotpoints and geophones.

SP	Position	Surface Elev (ft)	Layer 2		Layer 3	
			Depth (ft)	Elev (ft)	Depth (ft)	Elev (ft)
A	-10.0	5.3	6.7	-1.4	77.5	-72.2
M	137.5	5.0	4.2	0.8	62.7	-57.7
B	285.0	5.0	8.0	-3.0	10.0	-5.0
Geophone						
1	0.0	5.5	6.8	-1.3	77.4	-71.9
2	25.0	5.3	6.0	-0.7	72.5	-67.2
3	50.0	5.1	6.4	-1.3	67.5	-62.4
4	75.0	5.0	6.6	-1.6	75.9	-70.9
5	100.0	4.9	5.1	-0.2	76.7	-71.8
6	125.0	4.9	4.4	0.5	67.8	-62.9
7	150.0	5.0	3.9	1.1	57.4	-52.4
8	175.0	5.0	4.1	0.9	47.0	-42.0
9	200.0	5.0	4.9	0.1	36.5	-31.5
10	225.0	5.0	6.7	-1.7	27.3	-22.3
11	250.0	5.0	8.4	-3.4	22.9	-17.9
12	275.0	5.0	7.6	-2.6	13.5	-8.5
			Layer 1	Layer 2	Layer 3	
Velocities used:			1303	6033.	9810.	



Table B74. PT-1: Smoothed position of layers beneath shotpoints and geophones.

SP	Position	Surface Elev (ft)	Layer 2		Layer 3	
			Depth (ft)	Elev (ft)	Depth (ft)	Elev (ft)
A	-10.0	4.8	7.4	-2.6	14.6	-9.8
M	140.0	6.0	6.3	-0.3	26.5	-20.5
B	285.0	5.0	6.6	-1.6	22.6	-17.6
Geophone						
1	0.0	5.3	7.8	-2.5	15.8	-10.5
2	25.0	5.6	7.3	-1.7	18.0	-12.4
3	50.0	5.7	6.5	-0.8	20.0	-14.3
4	75.0	5.9	7.3	-1.4	21.1	-15.2
5	100.0	6.0	6.9	-0.9	23.2	-17.2
6	125.0	6.0	6.9	-0.9	25.3	-19.3
7	150.0	4.8	4.6	0.2	26.1	-21.3
8	175.0	5.2	4.1	1.1	28.5	-23.3
9	200.0	5.8	5.4	0.4	31.1	-25.3
10	225.0	5.6	6.4	-0.8	22.0	-16.4
11	250.0	5.5	6.3	-0.8	22.7	-17.2
12	275.0	5.3	6.7	-1.4	23.4	-18.1
			Layer 1	Layer 2	Layer 3	
Velocities used:			1218.	4908.	5373.	

Table B75. PT-2: Shotpoint information, geophone data, and arrival times. Times are in msec.

	SP	Elev (ft)	X Loc (ft)	Y Loc (ft)	Depth (ft)								
	F	4.2	-25.0	0.0	0.0								
	A	4.2	-10.0	0.0	0.0								
	M	4.5	137.5	10.0	0.0								
	B	5.4	285.0	0.0	0.0								
	R	5.6	300.0	0.0	0.0								

Geo	Elev (ft)	X Loc (ft)	Y Loc (ft)	SP	F	SP	A	SP	M	SP	B	SP	R
1	4.2	0.0	0.0	13.0	2	8.6	1	35.4	2	66.0	3	69.0	3
2	4.0	25.0	0.0	19.0	2	16.2	2	31.0	2	62.0	3	65.0	3
3	4.0	50.0	0.0	24.0	2	21.9	2	27.0	2	56.0	3	59.3	3
4	4.0	75.0	0.0	30.0	2	26.6	2	22.5	2	52.0	3	55.5	3
5	4.9	100.0	0.0	35.5	2	33.6	2	18.0	2	47.3	2	51.0	2
6	4.5	125.0	0.0	40.8	2	38.5	2	13.4	1	40.8	2	45.3	2
7	4.3	150.0	0.0	45.8	2	44.3	2	13.5	1	37.5	2	41.2	2
8	4.7	175.0	0.0	51.5	3	50.6	2	18.5	2	34.0	2	37.0	2
9	4.7	200.0	0.0	54.2	3	53.5	3	21.0	2	26.4	2	29.2	2
10	4.7	225.0	0.0	58.3	3	58.3	3	26.0	2	21.0	2	25.5	2
11	5.0	250.0	0.0	66.1	3	63.6	3	31.2	2	16.2	2	23.0	2
12	5.5	275.0	0.0	72.0	3	68.8	3	38.4	2	10.0	1	17.0	2



Table B76. PI-2: Smoothed position of layers beneath shotpoints and geophones.

SP	Position	Surface Elev (ft)	Layer 2		Layer 3	
			Depth (ft)	Elev (ft)	Depth (ft)	Elev (ft)
A	-10.0	4.2	4.2	-0.0	16.0	-11.8
M	137.5	4.5	6.6	-2.1	31.3	-26.8
B	285.0	5.4	6.0	-0.6	42.4	-37.0
Geophone						
1	0.0	4.2	4.3	-0.1	17.1	-12.9
2	25.0	4.0	4.9	-0.9	18.8	-14.8
3	50.0	4.0	5.6	-1.6	20.8	-16.8
4	75.0	4.0	5.9	-1.9	22.8	-18.8
5	100.0	4.9	6.3	-1.4	25.7	-20.8
6	125.0	4.5	6.2	-1.7	32.7	-28.2
7	150.0	4.3	6.7	-2.4	29.7	-25.4
8	175.0	4.7	7.5	-2.8	33.0	-28.3
9	200.0	4.7	4.3	0.4	35.0	-30.3
10	225.0	4.7	4.4	0.3	36.9	-32.2
11	250.0	5.0	5.5	-0.5	39.2	-34.2
12	275.0	5.3	6.1	-0.8	41.5	-36.2
			Layer 1	Layer 2	Layer 3	
Velocities used:			1136.	4949.	5128.	



Table B78. PT-3: Smoothed position of layers beneath shotpoints and geophones.

SP	Position	Surface Elev (ft)	Layer 2		Layer 3	
			Depth (ft)	Elev (ft)	Depth (ft)	Elev (ft)
A	-10.0	4.3	3.9	0.4	34.5	-30.2
M	139.5	4.3	6.4	-2.1	42.9	-38.6
B	285.0	4.0	4.6	-0.6	25.5	-21.5
<b>Geophone</b>						
1	0.0	4.4	4.2	0.2	35.3	-30.9
2	25.0	4.5	4.7	-0.2	36.4	-31.9
3	50.0	4.6	3.8	0.8	37.6	-33.0
4	75.0	4.2	3.5	0.7	39.9	-35.7
5	100.0	4.2	4.5	-0.3	42.6	-38.4
6	125.0	4.3	7.5	-3.2	42.8	-38.5
7	150.0	4.5	5.9	-1.4	43.3	-38.8
8	175.0	4.7	5.6	-0.9	43.3	-38.6
9	200.0	3.7	6.3	-2.6	42.2	-38.5
10	225.0	4.0	8.5	-4.5	41.4	-37.4
11	250.0	4.2	4.3	-0.1	28.7	-24.5
12	275.0	4.0	4.6	-0.6	26.9	-22.9
			Layer 1	Layer 2	Layer 3	
Velocities used:			1208.	4846.	5837	



Table B80. ST-1: Smoothed position of layers beneath shotpoints and geophones.

SP	Position	Surface Elev (ft)	Layer 2		Layer 3	
			Depth (ft)	Elev (ft)	Depth (ft)	Elev (ft)
A	-10.0	2.8	5.0	-2.2	39.6	-36.8
M	137.5	4.1	6.6	-2.5	28.6	-24.5
B	285.0	5.5	6.4	-0.9	17.8	-12.3
<b>Geophone</b>						
1	0.0	2.8	4.7	-1.9	38.7	-35.9
2	25.0	3.2	5.3	-2.1	37.4	-34.2
3	50.0	3.3	5.2	-1.9	35.9	-32.6
4	75.0	3.5	5.2	-1.7	39.4	-35.9
5	100.0	3.8	6.3	-2.5	36.5	-32.7
6	125.0	4.1	6.8	-2.7	29.8	-25.7
7	150.0	4.2	6.5	-2.3	27.6	-23.4
8	175.0	5.5	7.3	-1.8	26.6	-21.1
9	200.0	5.5	6.7	-1.2	24.3	-18.8
10	225.0	6.5	5.9	0.6	23.1	-16.6
11	250.0	6.0	5.4	0.6	19.5	-13.5
12	275.0	5.7	5.5	0.2	15.2	-9.5
			Layer 1	Layer 2	Layer 3	
<b>Velocities used:</b>			1329.	5111.	5938.	



Table B82. S<sub>1</sub>-2: Smoothed position of layers beneath shotpoints and geophones.

SP	Position	Surface Elev (ft)	Layer 2		Layer 3	
			Depth (ft)	Elev (ft)	Depth (ft)	Elev (ft)
A	-10.0	5.8	5.5	0.3	16.9	-11.1
M	137.5	4.1	9.2	-5.1	46.6	-42.5
B	285.0	3.5	5.5	-2.0	9.3	-5.8
Geophone						
1	0.0	5.7	5.6	0.1	15.2	-9.5
2	25.0	5.2	7.7	-2.5	21.7	-16.5
3	50.0	4.3	8.1	-3.8	37.3	-33.0
4	75.0	4.3	9.7	-5.4	29.5	-25.2
5	100.0	4.3	10.8	-6.5	25.5	-21.2
6	125.0	4.2	10.0	-5.8	34.5	-30.3
7	150.0	4.1	8.5	-4.4	58.8	-54.7
8	175.0	4.4	8.7	-4.3	54.9	-50.5
9	200.0	4.2	10.8	-6.6	30.4	-26.2
10	225.0	4.1	11.5	-7.4	19.6	-15.5
11	250.0	4.0	7.8	-3.8	16.5	-12.5
12	275.0	4.0	6.0	-2.0	11.3	-7.3
			Layer 1	Layer 2	Layer 3	
Velocities used:			1119.	4743.	5802.	





Table B84. ST-3: Smoothed position of layers beneath shotpoints and geophones.

SP	Position	Surface Elev (ft)	Layer 2		Layer 3	
			Depth (ft)	Elev (ft)	Depth (ft)	Elev (ft)
A	-10.0	4.0	6.8	-2.8	13.4	-9.4
M	137.5	4.1	5.2	-1.1	44.6	-40.5
B	285.0	6.0	4.1	1.9	26.1	-20.1
<b>Geophone</b>						
1	0.0	4.0	6.0	-2.0	11.3	-7.3
2	25.0	4.0	6.0	-2.0	7.6	-3.6
3	50.0	4.0	5.3	-1.3	16.7	-12.7
4	75.0	3.8	5.0	-1.2	33.1	-29.3
5	100.0	3.9	5.9	-2.0	38.2	-34.3
6	125.0	4.1	5.2	-1.1	42.5	-38.4
7	150.0	4.2	5.3	-1.1	46.7	-42.5
8	175.0	4.3	5.0	-0.7	51.0	-46.7
9	200.0	5.0	4.0	1.0	44.7	-39.7
10	225.0	4.5	4.6	-0.1	56.4	-51.9
11	250.0	6.3	4.7	1.6	28.1	-21.8
12	275.0	6.0	3.9	2.1	23.9	-17.9
			Layer 1	Layer 2	Layer 3	
<b>Velocities used:</b>			1341.	5437.	7106.	



Table B86. IT-4: Smoothed position of layers beneath shotpoints and geophones.

SP	Position	Surface Elev (ft)	Layer 2		Layer 3	
			Depth (ft)	Elev (ft)	Depth (ft)	Elev (ft)
A	-10.0	6.1	4.2	1.9	25.6	-19.5
M	135.0	5.7	-0.8	36.9	32.0	
B	285.0	5.3	6.3	-1.0	6.3	-1.0
<b>Geophone</b>						
1	0.0	6.0	3.9	2.1	23.9	17.9
2	25.0	5.8	4.2	1.6	29.2	-23.4
3	50.0	5.6	4.5	1.1	34.5	-28.9
4	75.0	5.4	4.6	0.8	34.8	-29.4
5	100.0	5.0	4.9	0.1	35.5	-30.5
6	125.0	4.8	5.5	-0.7	36.4	-31.6
7	150.0	4.9	6.0	-1.1	37.6	-32.7
8	175.0	4.9	4.6	0.3	34.4	-29.5
9	200.0	5.0	2.9	2.1	26.7	-21.7
10	225.0	5.1	3.9	1.2	20.2	-15.1
11	250.0	5.3	5.8	-0.5	17.0	-11.7
12	275.0	5.3	6.2	-0.9	6.2	-0.9
			Layer 1	Layer 2	Layer 3	
Velocities used:			1232.	5665.	6254.	

Table B87. ST-5: Shotpoint information, geophone data, and arrival times. Times are in msec.

	SP	Elev (ft)	X Loc (ft)	Y Loc (ft)	Depth (ft)								
	F	3.6	-25.0	0.0	0.0								
	A	3.0	-10.0	0.0	0.0								
	M	6.5	136.0	10.0	0.0								
	B	3.5	285.0	0.0	0.0								
	R	2.8	300.0	0.0	0.0								

Geo	Elev (ft)	X Loc (ft)	Y Loc (ft)	SP	F	SP	A	SP	M	SP	B	SP	R
1	2.6	0.0	0.0	12.8	2	9.0	2	33.0	2	62.0	3	60.5	3
2	2.8	25.0	0.0	18.5	2	13.1	2	28.7	2	56.0	3	65.0	3
3	3.1	50.0	0.0	21.5	2	18.5	2	25.0	2	52.4	3	52.5	3
4	5.0	75.0	0.0	26.0	2	24.0	2	21.2	2	49.0	3	50.0	3
5	6.7	100.0	0.0	32.4	2	30.3	2	16.5	2	45.0	3	45.6	3
6	6.6	125.0	0.0	39.0	2	37.3	2	13.4	1	42.0	2	42.1	3
7	6.5	150.0	0.0	45.5	2	43.0	2	12.5	1	37.5	2	39.3	2
8	6.6	175.0	0.0	50.5	2	47.8	2	18.5	2	32.0	2	34.0	2
9	7.9	200.0	0.0	54.0	3	51.0	3	23.0	2	25.5	2	28.8	2
10	8.6	225.0	0.0	60.0	3	55.5	3	28.0	2	20.5	2	23.2	2
11	9.5	250.0	0.0	63.0	3	60.4	3	32.5	2	15.5	2	17.5	2
12	9.0	275.0	0.0	68.2	3	64.3	3	38.5	2	9.8	2	18.2	2

Table B88. HT-5: Smoothed position of layers beneath shotpoints and geophones.

SP	Position	Surface Elev (ft)	Layer 2		Layer 3	
			Depth (ft)	Elev (ft)	Depth (ft)	Elev (ft)
A	-10.0	3.0	4.2	-1.2	4.2	-1.2
M	136.0	6.5	8.2	-1.7	19.4	-12.9
B	285.0	3.5	2.2	1.3	2.2	1.3
Geophone						
1	0.0	2.6	3.7	-1.1	3.7	-1.1
2	25.0	2.8	3.9	-1.1	3.9	-1.1
3	50.0	3.1	3.7	-0.6	3.7	-0.6
4	75.0	5.0	4.1	0.9	4.1	0.9
5	100.0	6.7	5.4	1.3	5.4	1.3
6	125.0	6.6	7.7	-1.1	16.4	-9.8
7	150.0	6.5	9.1	-2.6	23.4	-16.9
8	175.0	6.6	9.1	-2.5	21.4	-14.8
9	200.0	7.9	8.9	-1.0	19.8	-11.9
10	225.0	8.6	8.5	0.1	17.6	-9.0
11	250.0	9.5	8.3	1.2	15.2	-5.7
12	275.0	9.0	8.0	1.0	8.0	1.0
Velocities used:		Layer 1 1243.	Layer 2 4924.	Layer 3 5434.		



Table B90. ST-6: Smoothed position of layers beneath shotpoints and geophones.

SP	Position	Surface Elev (ft)	Layer 2		Layer 3	
			Depth (ft)	Elev (ft)	Depth (ft)	Elev (ft)
A	-10.0	6.6	7.9	-1.3	12.5	-5.9
M	137.5	5.0	9.5	-4.5	56.2	-51.2
B	285.0	2.8	4.8	-2.0	38.0	-35.2
<b>Geophone</b>						
1	0.0	6.6	8.1	-1.5	15.6	-9.0
2	25.0	6.6	8.4	-1.8	23.0	-16.4
3	50.0	6.3	8.2	-1.9	33.3	-27.0
4	75.0	5.8	8.3	-2.5	36.4	-30.6
5	100.0	5.5	8.5	-3.0	44.8	-39.3
6	125.0	4.5	8.8	-4.3	53.4	-48.9
7	150.0	3.2	8.0	-4.8	56.8	-53.6
8	175.0	3.1	7.0	-3.9	55.9	-52.8
9	200.0	3.0	6.1	-3.1	49.3	-46.3
10	225.0	3.2	5.8	-2.6	44.3	-41.1
11	250.0	3.0	5.6	-2.6	41.3	-38.3
12	275.0	2.8	4.7	-1.9	38.7	-35.9
			Layer 1	Layer 2	Layer 3	
<b>Velocities used:</b>			1359.	5048	5973.	





Table B92. FBC-1: Smoothed position of layers beneath shotpoints and geophones.

SP	Position	Surface Elev (ft)	Layer 2		Layer 3	
			Depth (ft)	Elev (ft)	Depth (ft)	Elev (ft)
A	-10.0	4.9	6.1	-1.2	54.9	-50.0
M	137.0	4.9	7.0	-2.1	76.8	-71.9
B	285.0	3.7	6.2	-2.5	68.7	-65.0
Geophone						
1	0.0	4.9	6.2	-1.3	56.2	-51.3
2	25.0	4.6	5.5	-0.9	60.1	-55.5
3	50.0	4.4	5.4	-1.0	57.9	-53.5
4	75.0	4.5	4.8	-0.3	60.7	-56.2
5	100.0	4.7	6.0	-1.3	67.2	-62.5
6	125.0	4.9	6.7	-1.8	73.8	-68.9
7	150.0	5.1	7.4	-2.3	80.0	-74.9
8	175.0	5.3	9.6	-4.3	72.9	-67.6
9	200.0	5.5	10.1	-4.6	71.5	-66.0
10	225.0	5.3	6.8	-1.5	69.8	-64.5
11	250.0	5.1	7.9	-2.8	71.0	-65.9
12	275.0	3.9	6.5	-2.6	69.5	-65.6
			Layer 1	Layer 2	Layer 3	
Velocities used:			1621.	5857.	10250.	



Table B94. TIC-2; Smoothed position of layers beneath shotpoints and geophones.

SP	Position	Surface Elev (ft)	Layer 2		Layer 3	
			Depth (ft)	Elev (ft)	Depth (ft)	Elev (ft)
A	-10.0	3.8	3.3	0.5	192.9	-189.1
M	137.5	7.0	7.4	-0.4	104.2	-97.2
B	285.0	6.5	6.9	-0.4	27.9	-21.4
<b>Geophone</b>						
1	0.0	3.9	3.5	0.4	186.0	-182.1
2	25.0	5.0	4.3	0.7	169.9	-164.9
3	50.0	5.5	5.6	-0.1	153.1	-147.6
4	75.0	6.3	7.0	-0.7	136.6	-130.3
5	100.0	6.4	7.1	-0.7	119.4	-113.0
6	125.0	6.5	7.2	-0.7	102.2	-95.7
7	150.0	7.0	7.1	-0.1	105.7	-98.7
8	175.0	7.0	5.6	1.4	84.9	-77.9
9	200.0	7.5	5.1	2.4	63.9	-56.4
10	225.0	7.0	7.0	-0.0	41.9	-34.9
11	250.0	6.9	8.3	-1.4	24.2	-17.3
12	275.0	6.9	8.3	-1.4	23.5	-16.6
			Layer 1	Layer 2	Layer 3	
<b>Velocities used:</b>			1616.	5124.	8538.	



Table B96. TIC-3: Smoothed position of layers beneath shotpoints and geophones.

SP	Position	Surface Elev (ft)	Layer 2		Layer 3	
			Depth (ft)	Elev (ft)	Depth (ft)	Elev (ft)
A	-10.0	6.9	8.3	-1.4	23.8	-16.9
M	137.5	5.8	8.8	-3.0	77.0	-71.2
B	285.0	6.7	7.5	-0.8	74.3	-67.6
Geophone						
1	0.0	6.9	8.3	-1.4	23.5	-16.6
2	25.0	6.3	5.1	1.2	34.8	-28.5
3	50.0	6.1	7.8	-1.7	40.5	-34.4
4	75.0	5.9	9.0	-3.1	51.0	-45.1
5	100.0	5.7	8.8	-3.1	61.2	-55.5
6	125.0	5.7	9.1	-3.4	71.7	-66.0
7	150.0	6.0	8.5	-2.5	82.5	-76.5
8	175.0	4.8	6.2	-1.4	91.8	-87.0
9	200.0	5.2	6.5	-1.3	91.6	-86.4
10	225.0	5.3	4.8	0.5	79.9	-74.6
11	250.0	5.5	5.0	0.5	79.2	-73.7
12	275.0	6.6	5.7	0.9	76.3	-69.7
			Layer 1	Layer 2	Layer 3	
Velocities used:			1259.	5107.	7108.	



Table B98. CHC-4: Smoothed position of layers beneath shotpoints and geophones.

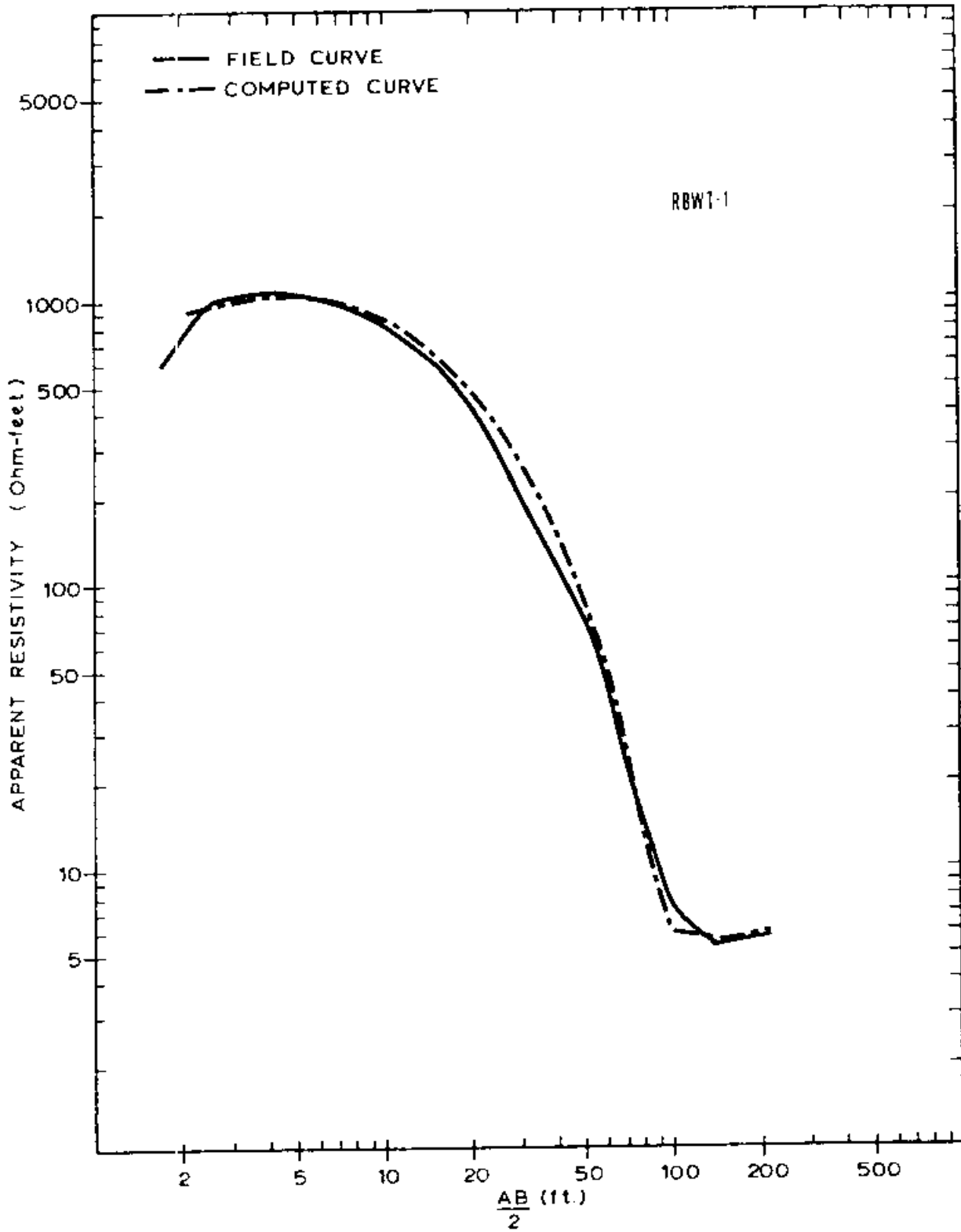
SP	Position	Surface Elev (ft)	Layer 2		Layer 3	
			Depth (ft)	Elev (ft)	Depth (ft)	Elev (ft)
A	-10.0	5.8	5.0	0.8	77.1	-71.3
M	137.5	7.8	6.8	1.0	56.9	-49.1
B	285.0	8.5	3.9	4.6	55.3	-46.8
<b>Geophone</b>						
1	0.0	6.6	5.8	0.8	76.3	-69.7
2	25.0	7.0	10.2	-3.2	71.4	-64.4
3	50.0	7.5	10.8	-3.3	66.6	-59.1
4	75.0	8.0	9.9	-1.9	61.8	-53.8
5	100.0	7.7	6.4	1.3	68.2	-60.5
6	125.0	7.2	6.2	1.0	55.7	-48.5
7	150.0	7.6	6.5	1.1	57.2	-49.6
8	175.0	6.5	5.4	1.1	56.0	-49.5
9	200.0	8.5	6.2	2.3	57.7	-49.2
10	225.0	4.3	2.2	2.1	54.2	-49.9
11	250.0	5.1	3.8	1.3	53.6	-48.5
12	275.0	8.5	4.1	4.4	55.5	-47.0
			Layer 1	Layer 2	Layer 3	
Velocities used:			1379.	5227.	9743.	



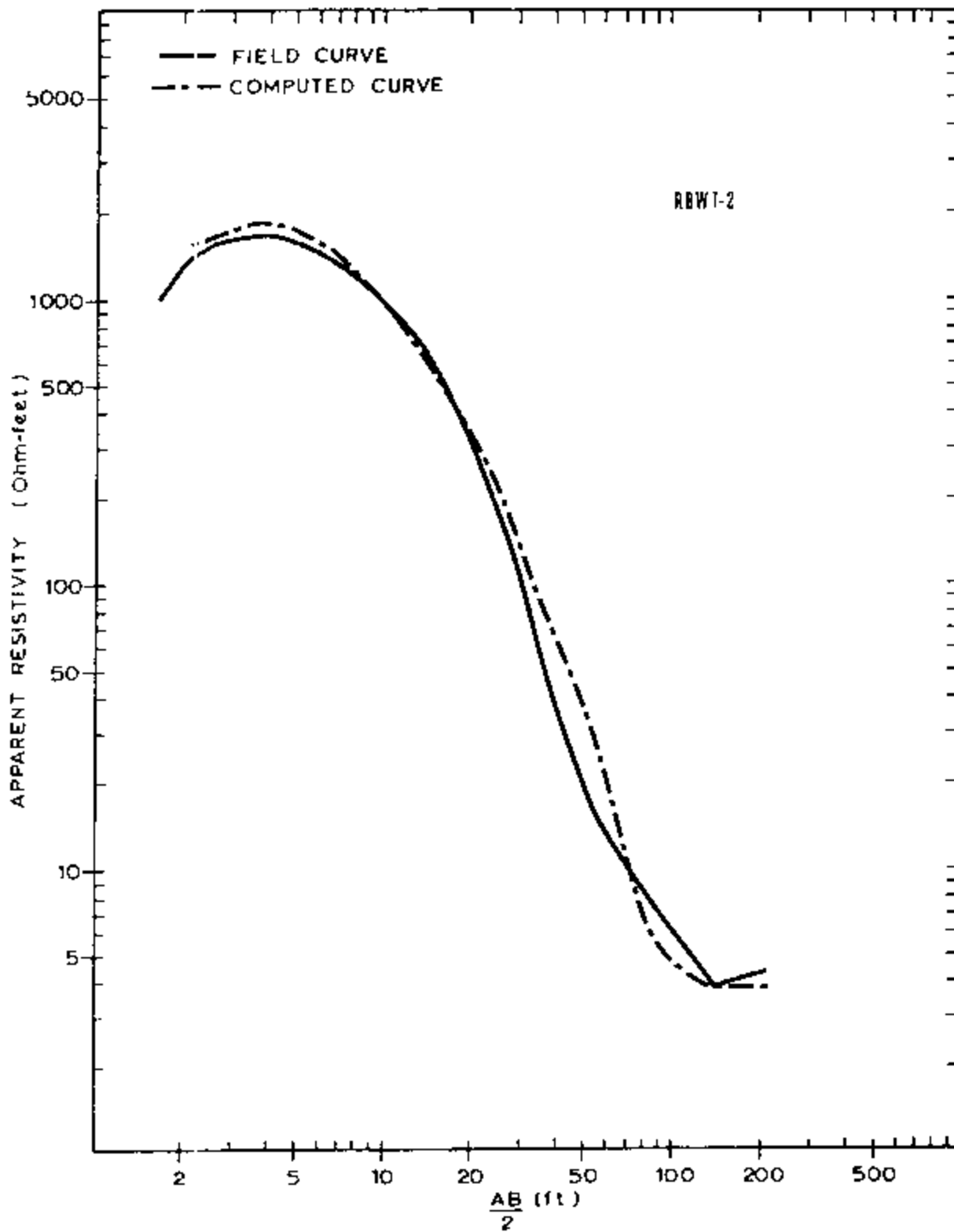


Table B100. 1HC-5: Smoothed position of layers beneath shotpoints and geophones.

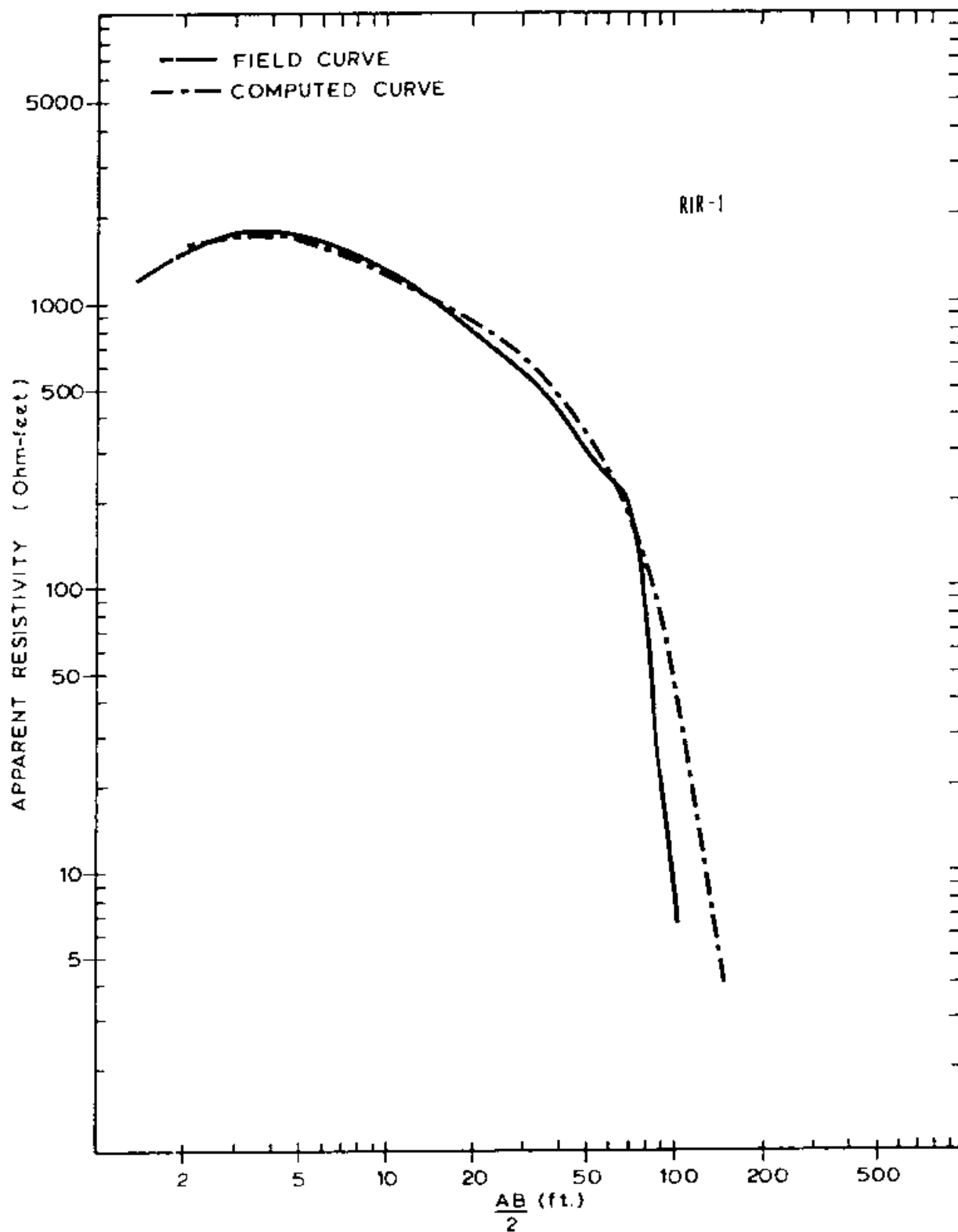
SP	Position	Surface Elev (ft)	Layer 2		Layer 3	
			Depth (ft)	Elev (ft)	Depth (ft)	Elev (ft)
A	-10.0	7.5	5.3	2.2	5.3	2.2
M	140.0	5.7	4.3	1.4	69.0	-63.3
B	285.0	6.1	3.8	2.3	98.3	-92.2
Geophone						
1	0.0	5.4	3.1	2.3	3.1	2.3
2	25.0	4.9	3.3	1.6	28.6	-23.7
3	50.0	4.2	2.9	1.3	38.9	-34.7
4	75.0	4.8	1.8	3.0	46.0	-41.2
5	100.0	5.4	2.6	2.8	55.1	-49.7
6	125.0	5.9	3.7	2.2	64.1	-58.2
7	150.0	6.4	5.5	0.9	73.1	-66.7
8	175.0	7.0	5.2	1.8	85.7	-78.2
9	200.0	7.0	5.0	2.0	105.3	-98.3
10	225.0	6.4	4.8	1.6	82.3	-75.9
11	250.0	6.3	5.1	1.2	89.7	-83.4
12	275.0	6.1	3.8	2.3	97.0	-90.9
			Layer 1	Layer 2	Layer 3	
Velocities used:			1096.	5633.	12361.	



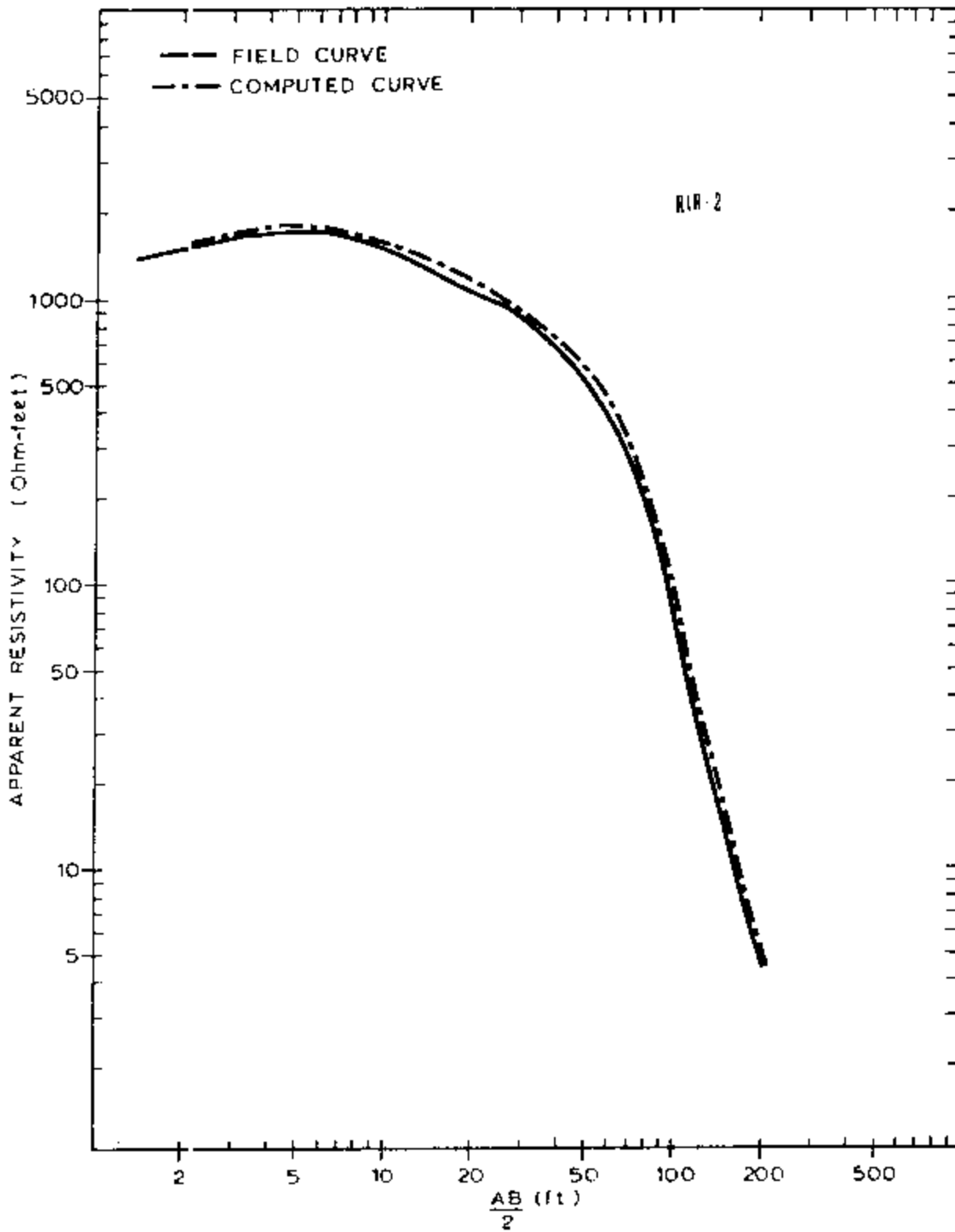
Station 1: field VES curve and computed VES curve.



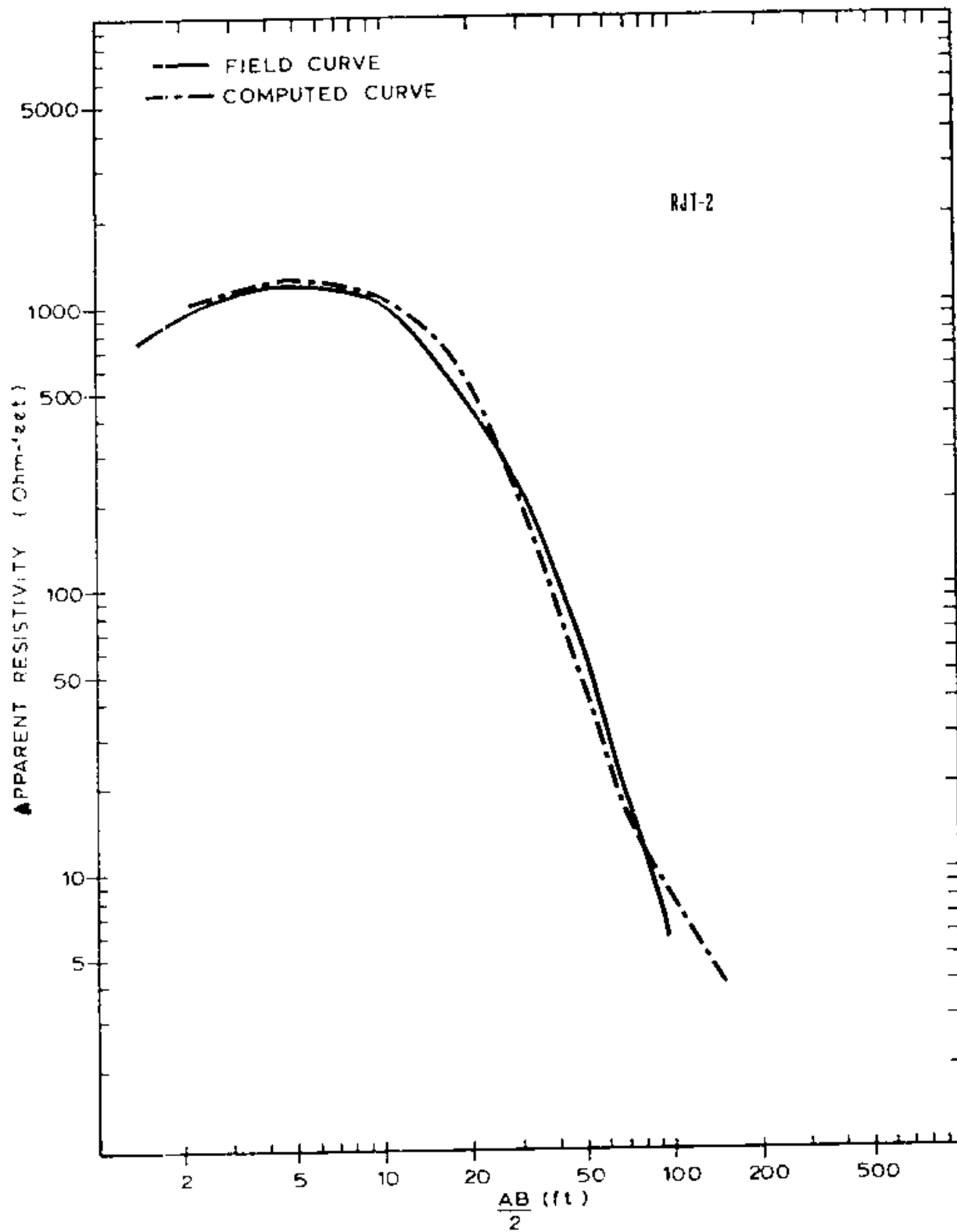
Station 2: Field VES curve and computed VES curve.



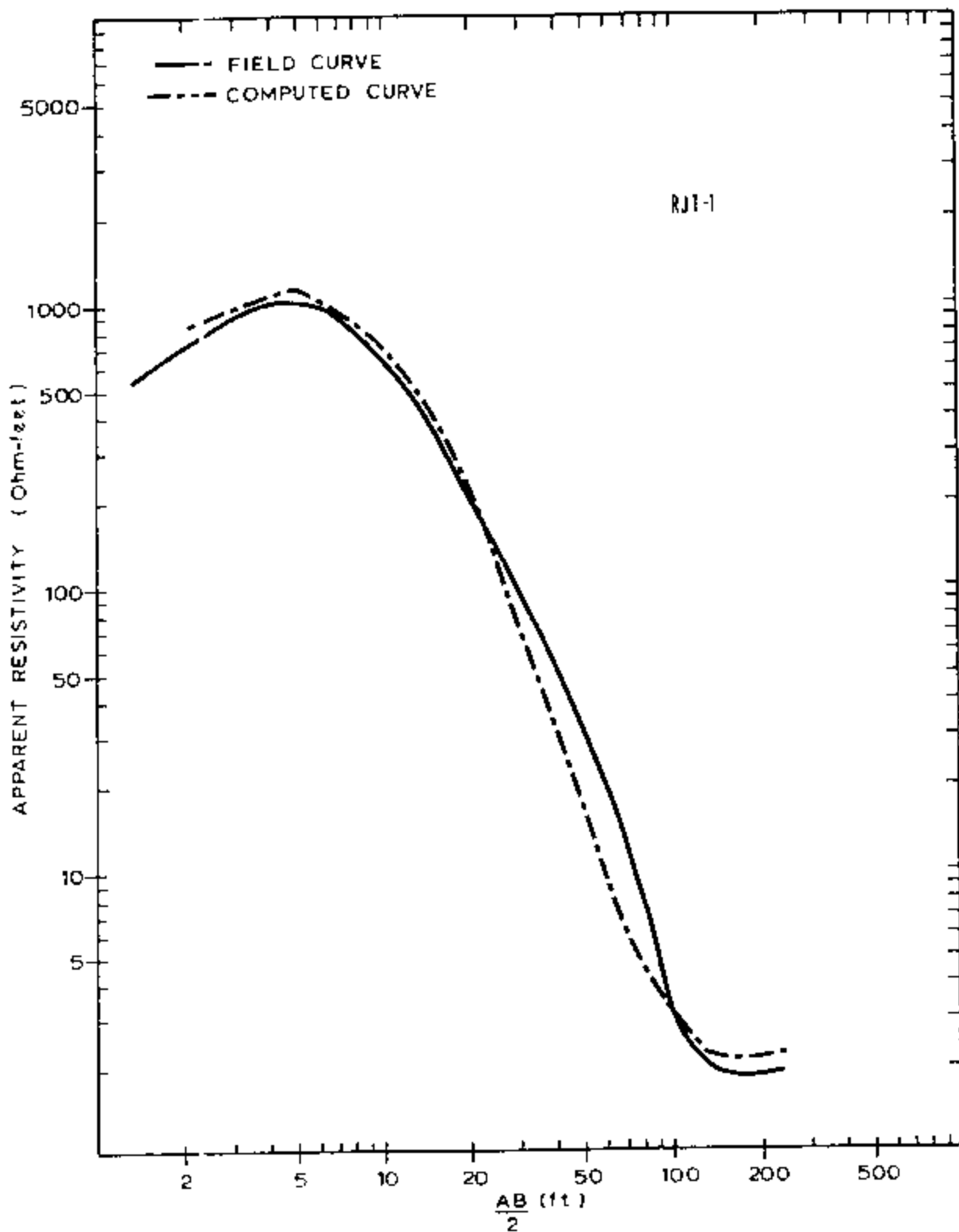
Station 3: Field VES curve and computed VES curve.



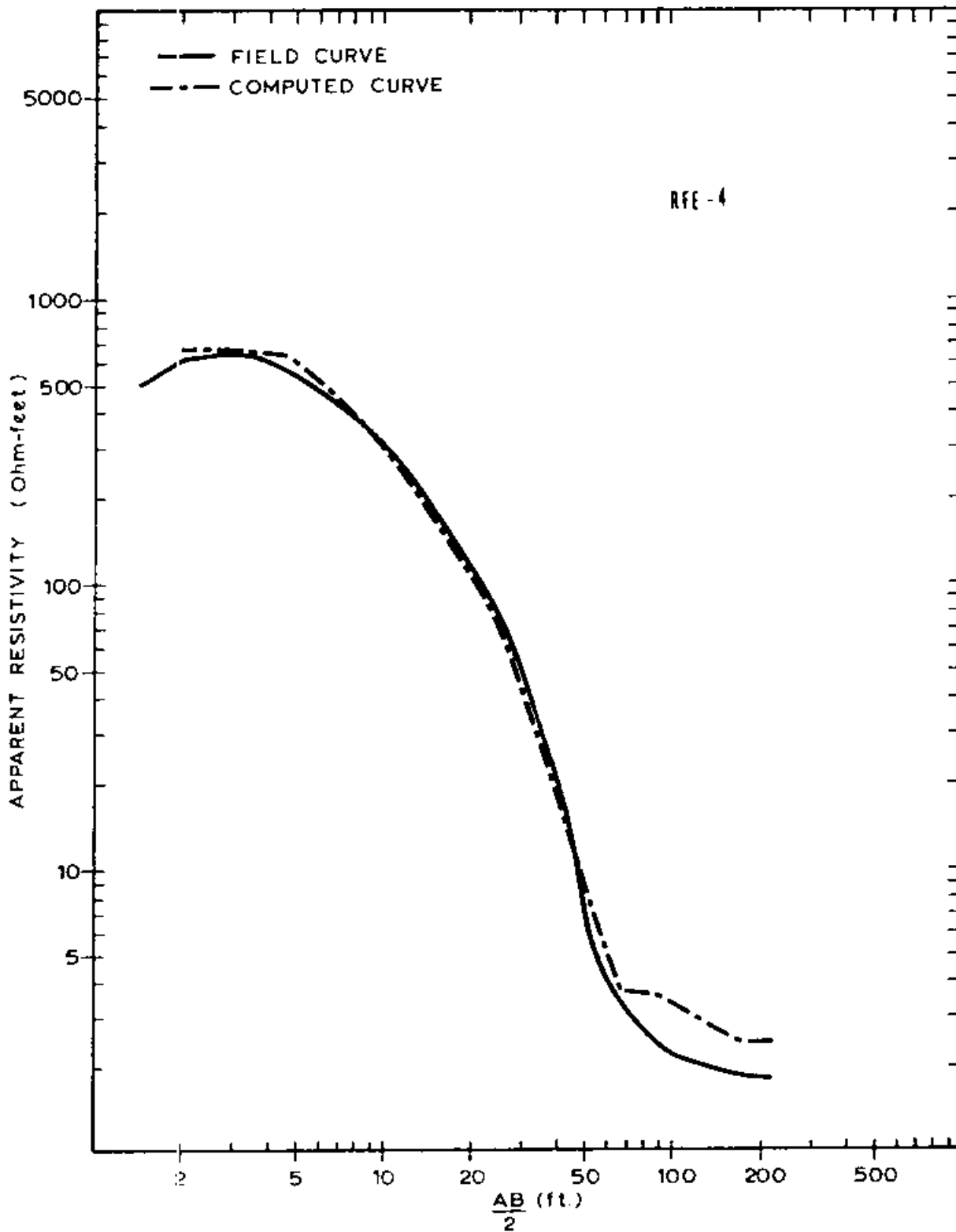
Station 4: Field VES curve and computed VES curve.



Station 5: Field VES curve and computed VES curve.

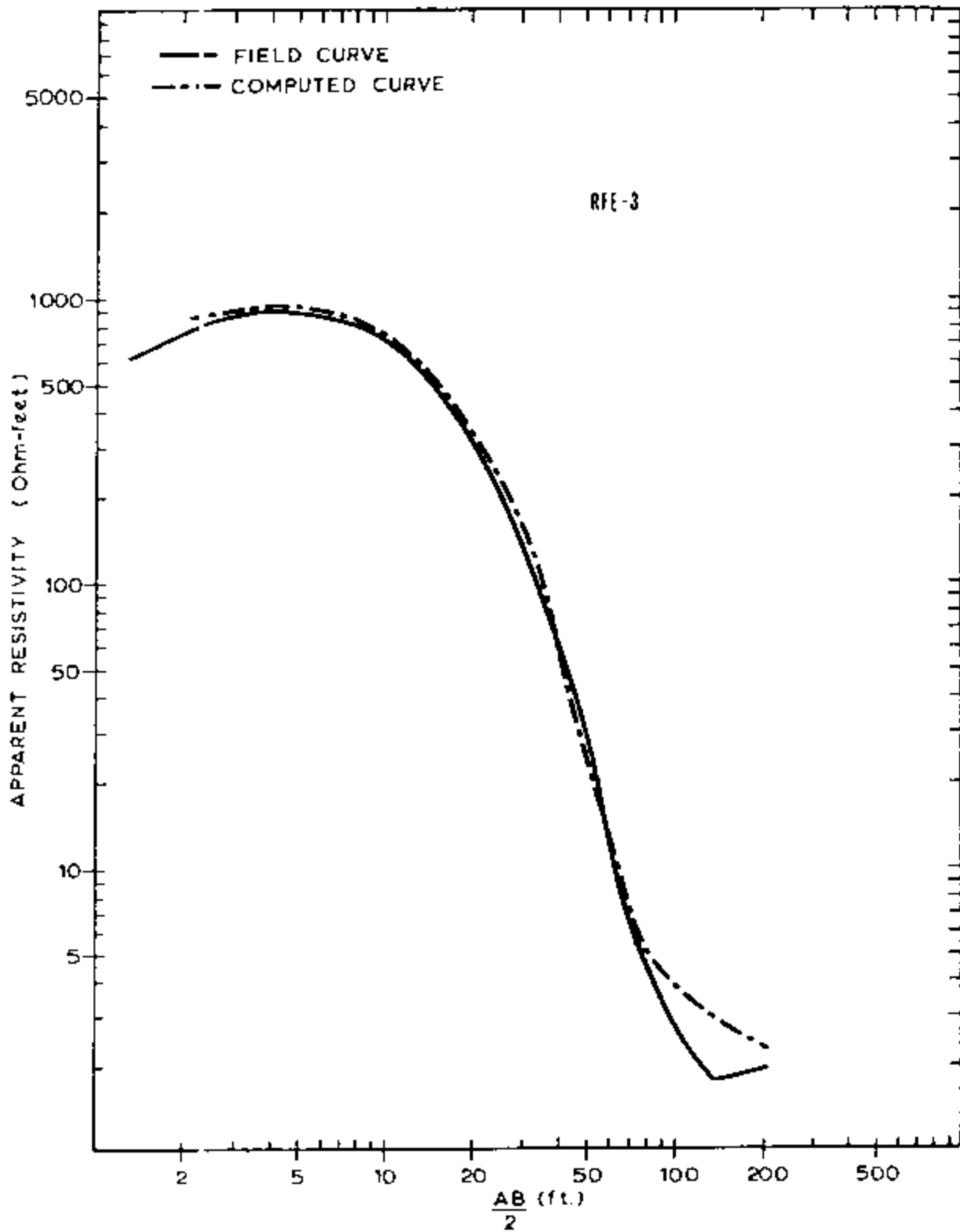


Station 6: Field VES curve and computed VES curve.

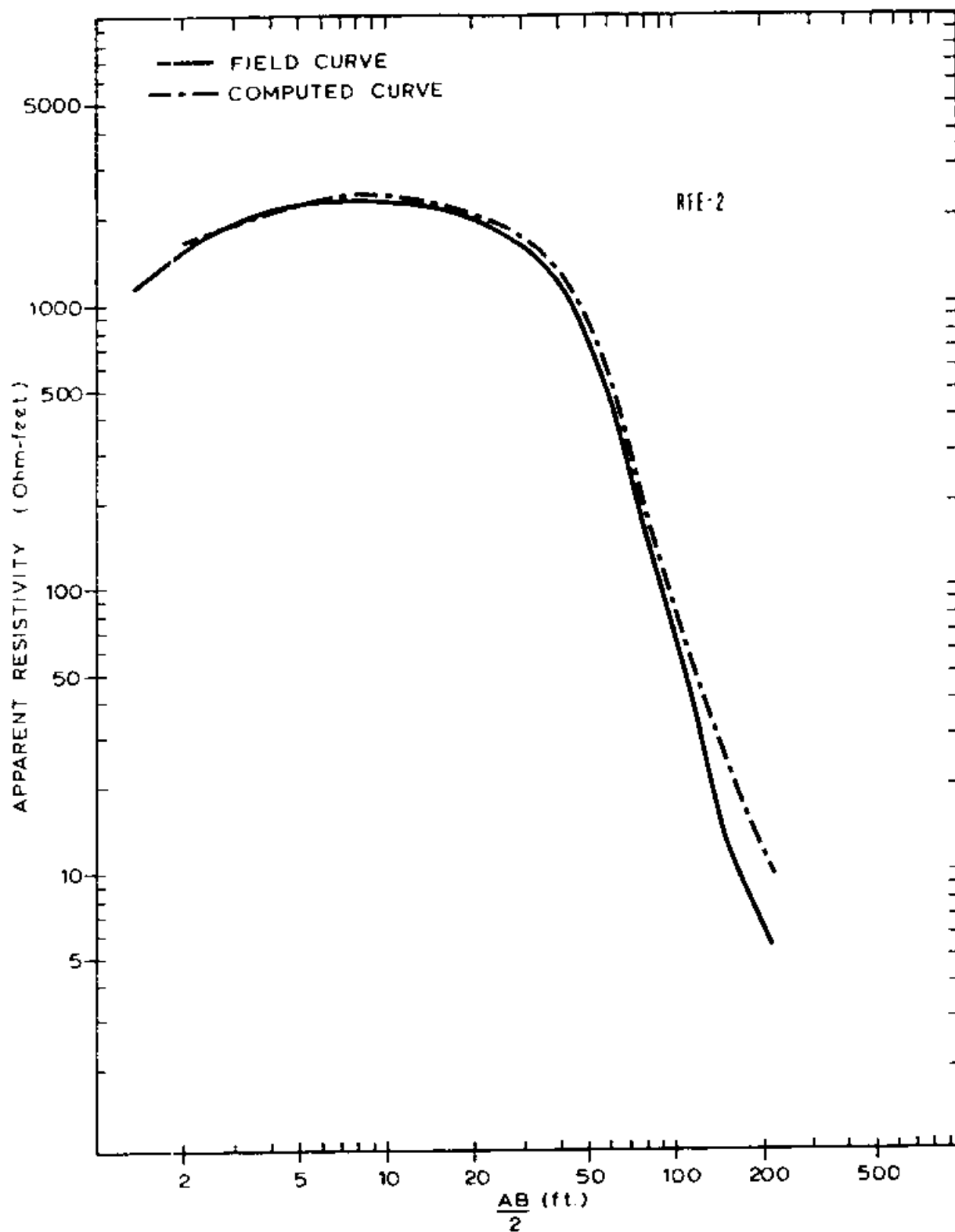


Station 7: Field VES curve and computed VES curve.

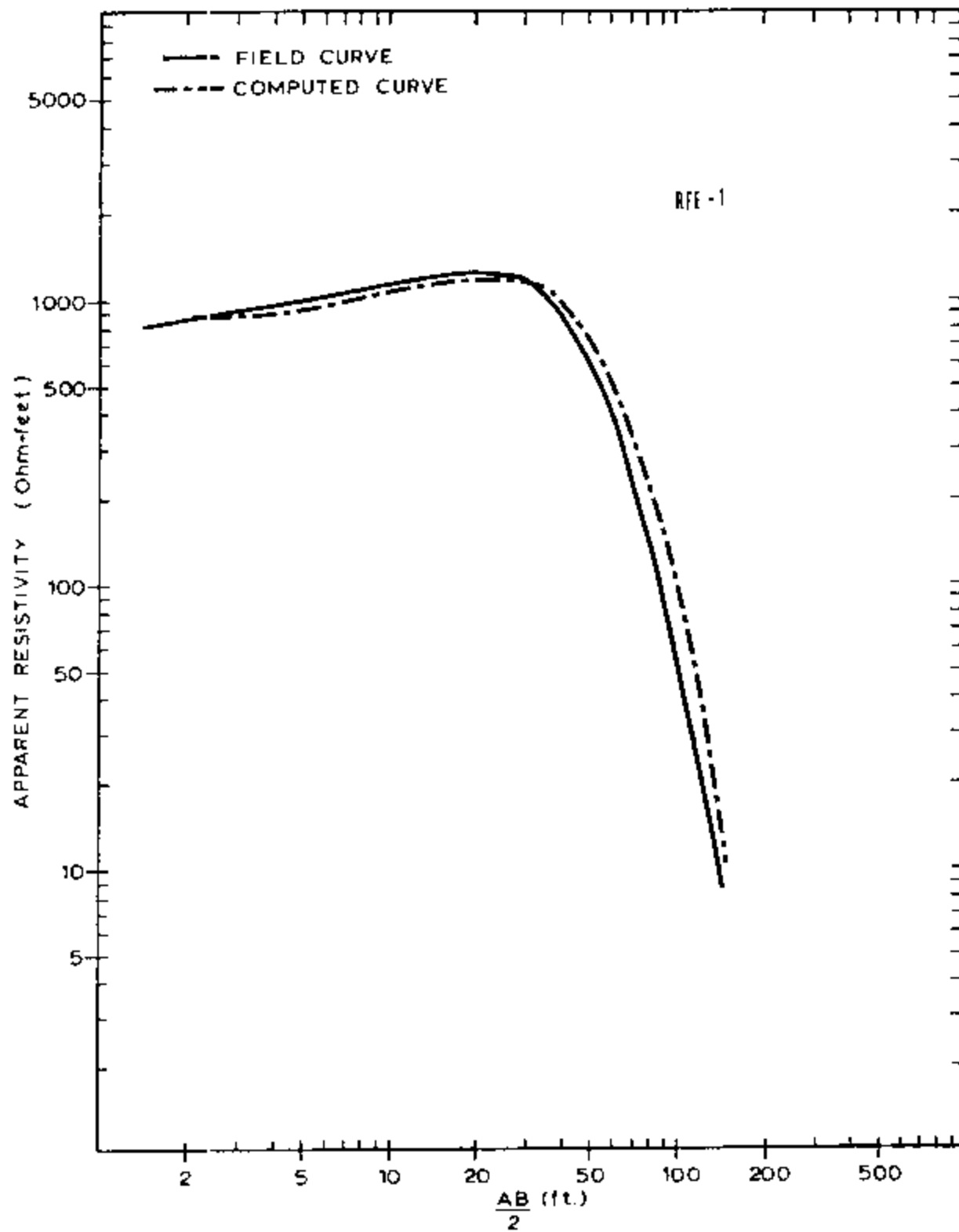




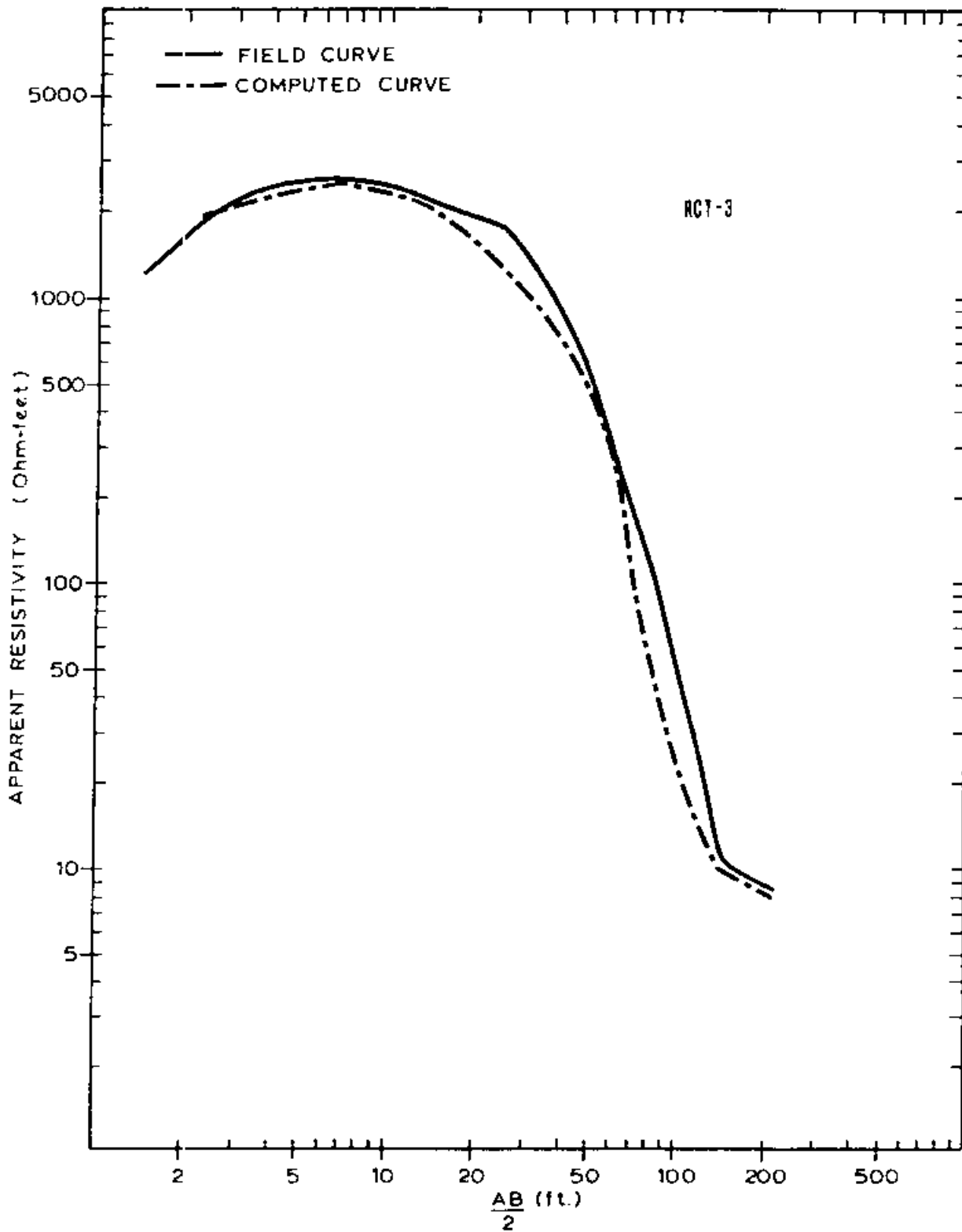
Station 8: Field VES curve and computed VES curve.



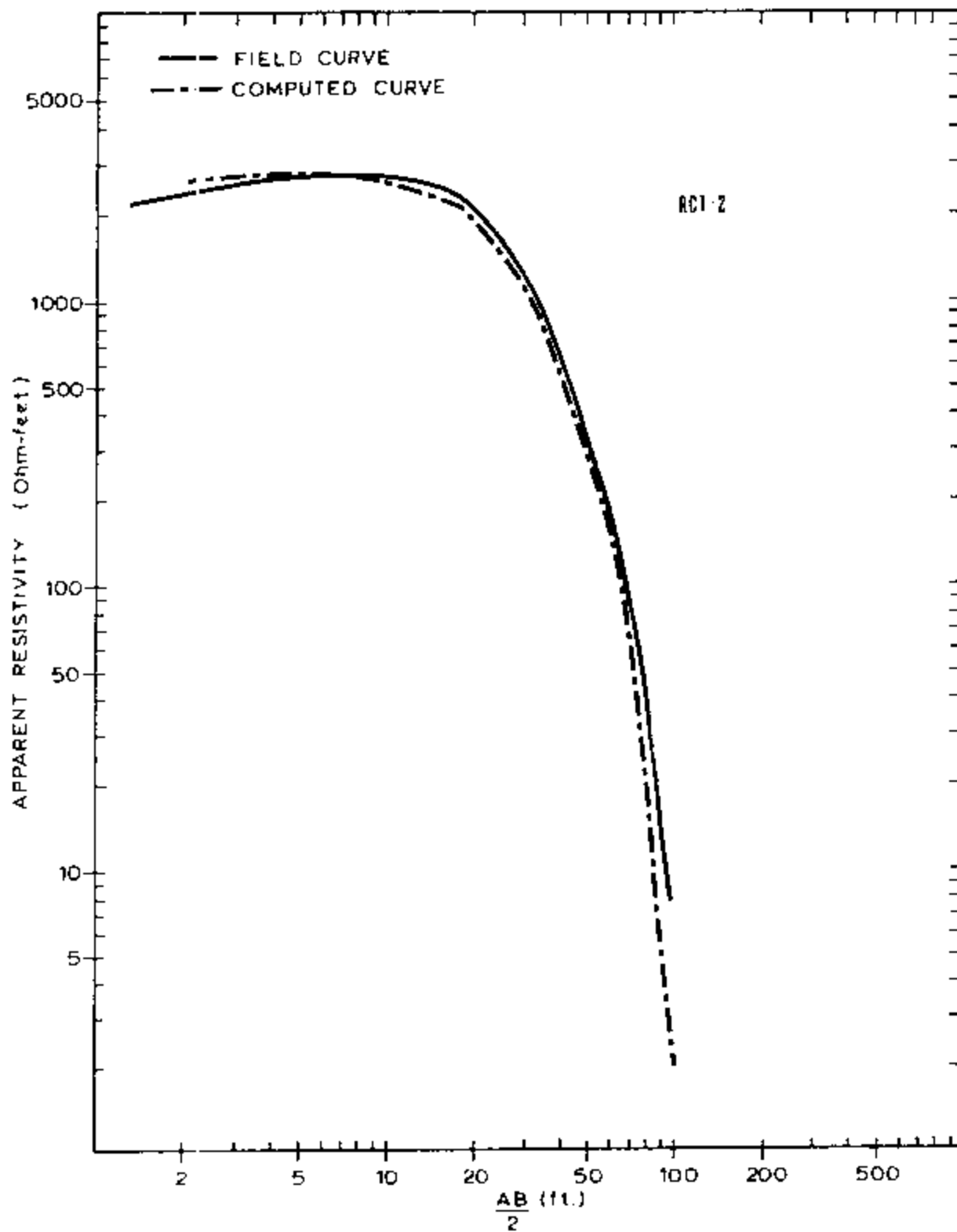
Station 9: Field VES curve and computed VES curve.



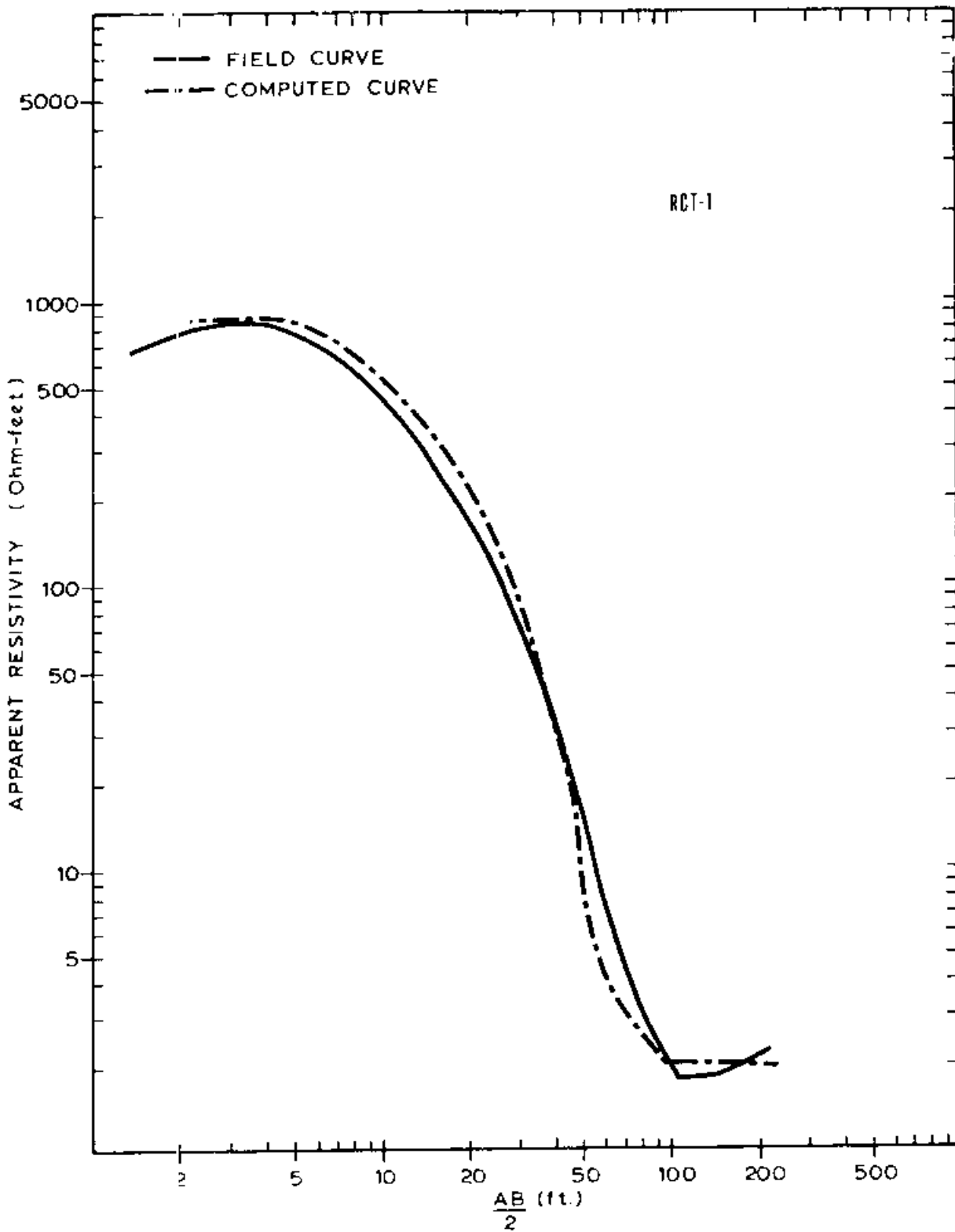
Station 10: Field VES curve and computed VES curve.



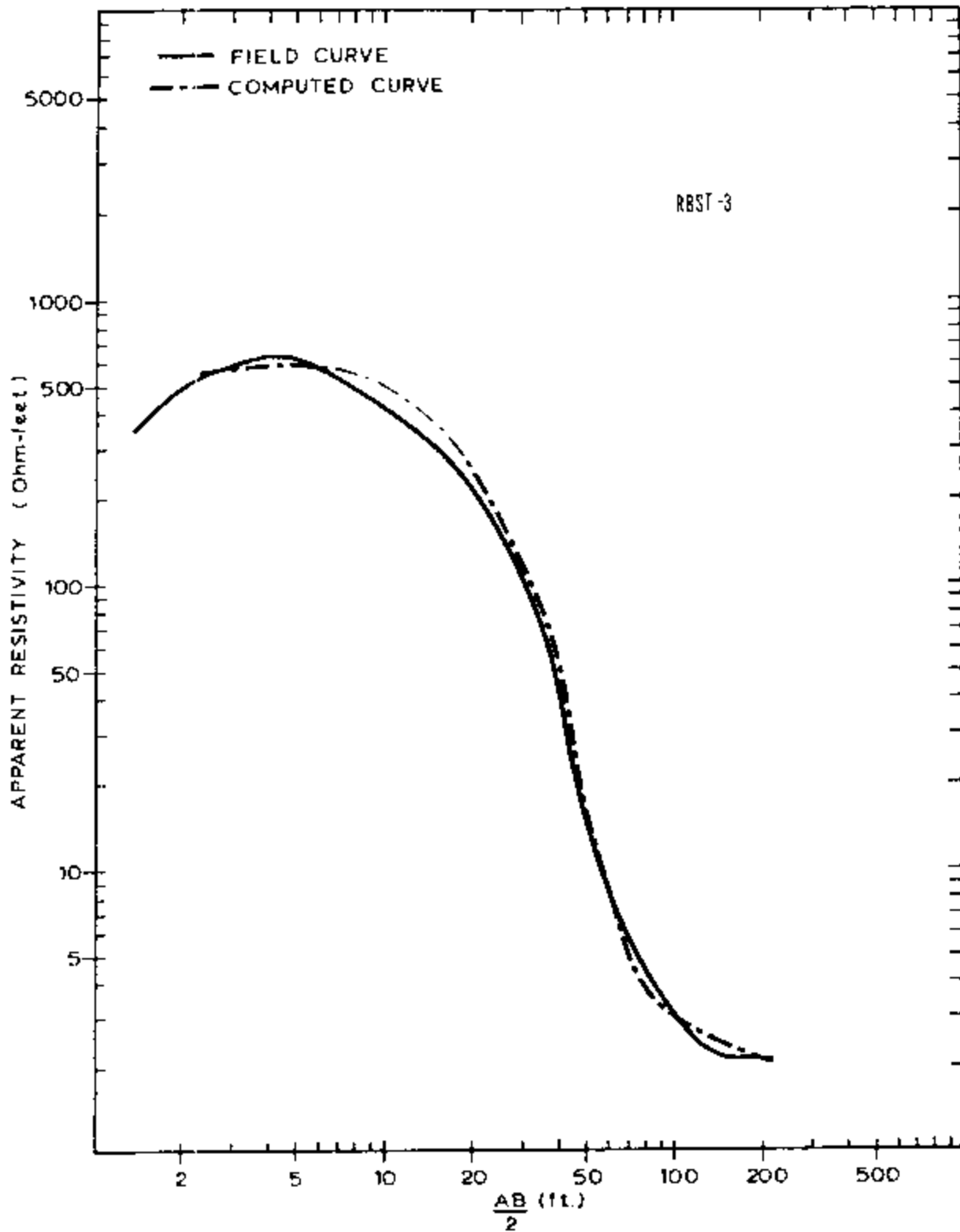
Station 11: Field VES curve and computed VES curve.



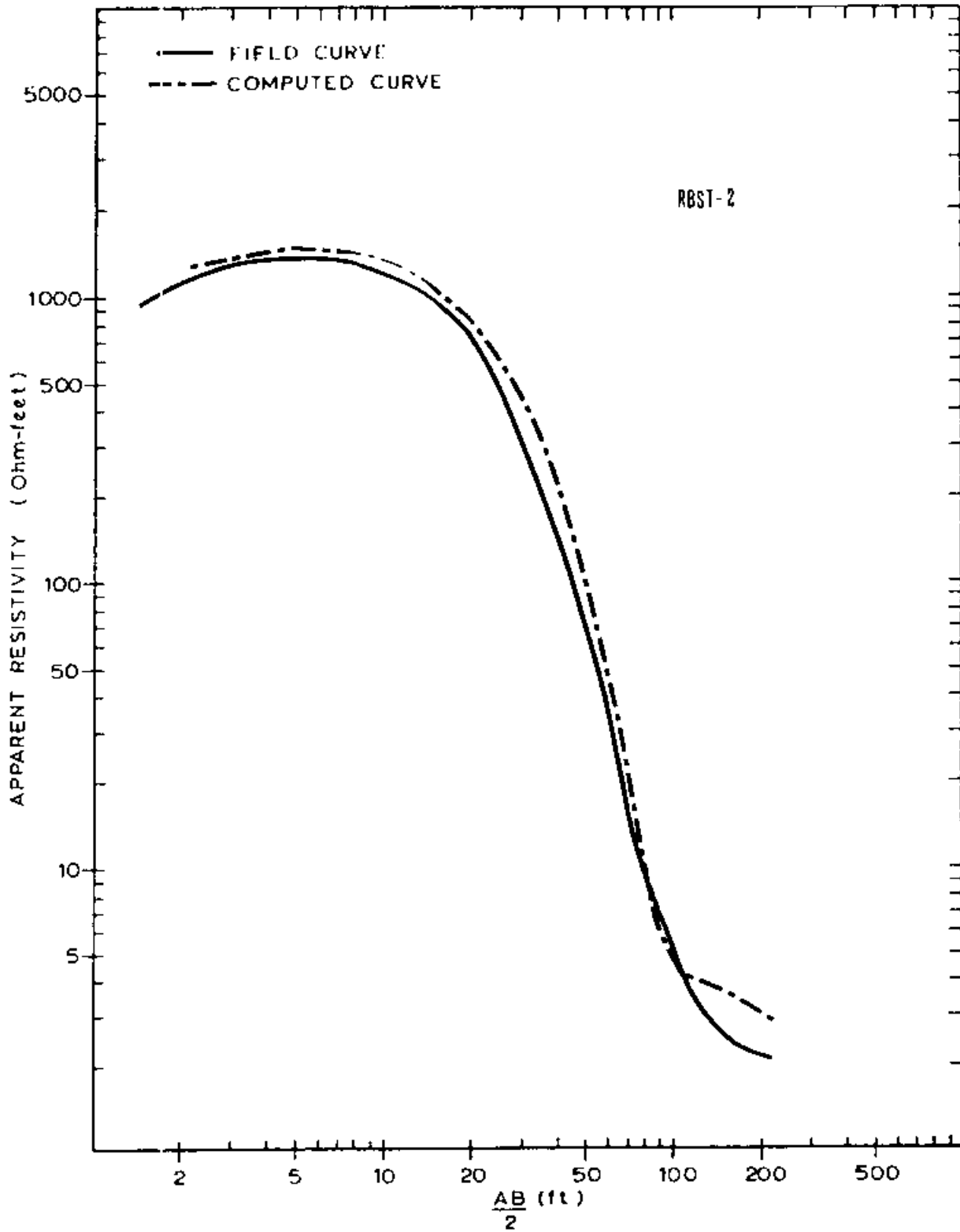
Station 12: Field VES curve and computed VES curve.



Station 13: Field VES curve and computed VES curve.

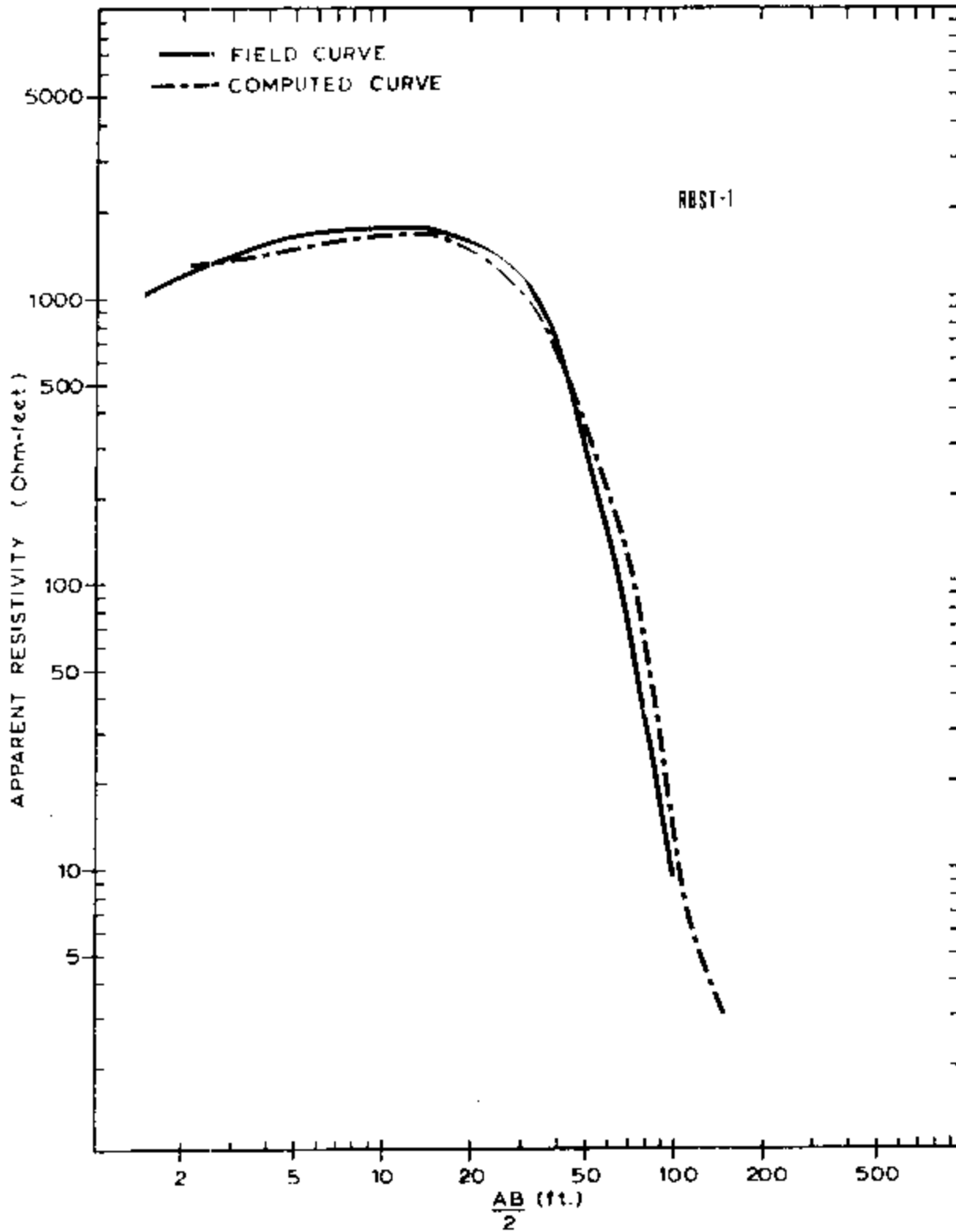


Station 14: Field VES curve and computed VES curve.



Station 15: Field VES curve and computed VES curve.





Station 16: Field VES curve and computed VES curve.

## APPENDIX C

## CONTENTS

Page

## Descriptions of Stratigraphic Sections

Stratigraphic section at DS3 drill site.....	290
Stratigraphic section at DS4 drill site.....	291
Stratigraphic section at A6 drill site.....	292
Stratigraphic section at Pz1 drill site.....	293
Stratigraphic section at Pz2 drill site.....	294

## Drilling Logs

Drilling log from DS1.....	295
Drilling log from DS2.....	296
Drilling log from DS3.....	297
Drilling log from DS4.....	300
Drilling log from DS5.....	302
Drilling log from PS1.....	303
Drilling log from PS2.....	304
Drilling log from PS3.....	305
Drilling log from PS4.....	307
Drilling log from PS5.....	308

## Sample Descriptions

Sample description for PG 1-1.....	309
Sample description for PG 3-2.....	310
Sample description for PG 4-1.....	311
Sample description for PG 5-2.....	312
Sample description for PG 6-1.....	313
Sample description for PG 7-2.....	314
Sample description for PG 8-1.....	315
Sample description for PG 9-1.....	316
Sample description for PG 11-2B.....	317
Sample description for PGA 2A.....	318
Sample description for PGA 6B.....	319
Sample description for PGA 7.....	320
Sample description for PGA 10B.....	321
Sample description for PGA 13A.....	322

## Figure -- Location Map

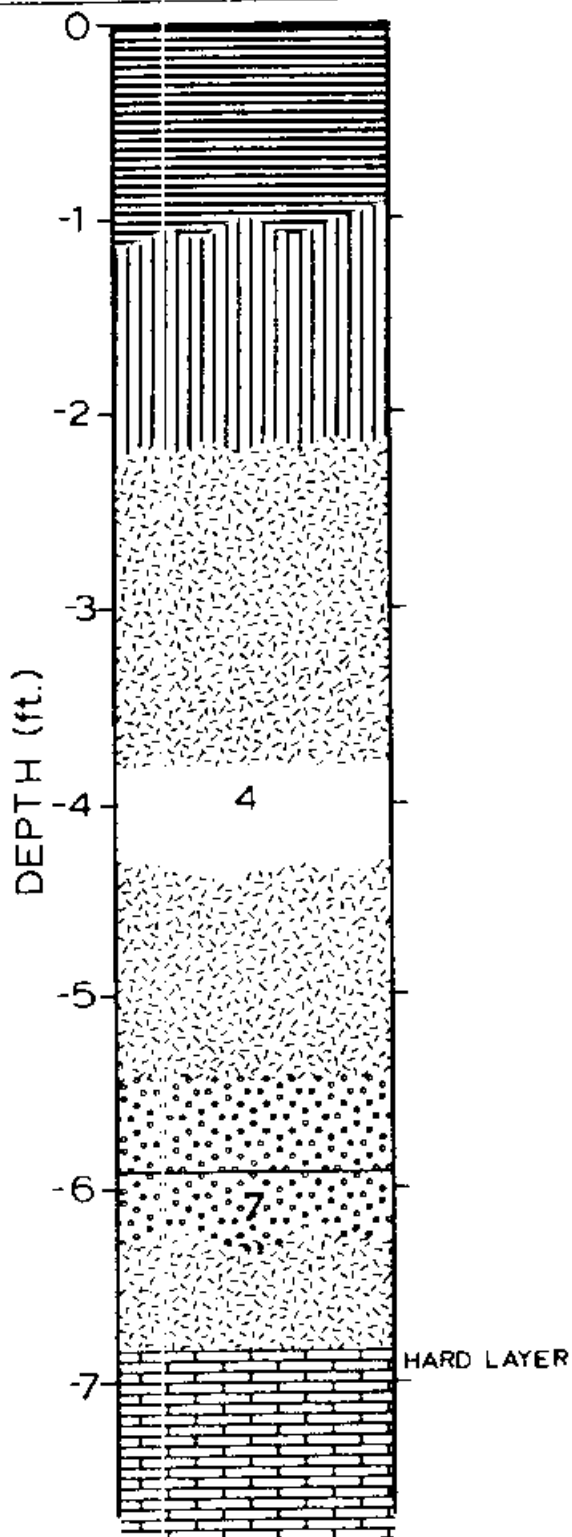
C1. Map of Deke Island showing the location of collection sites for sediment size analysis.....	323
---	-----

## Tables -- Sieve Analysis

C1. Sample no. 1: sieve analysis.....	324
---------------------------------------	-----

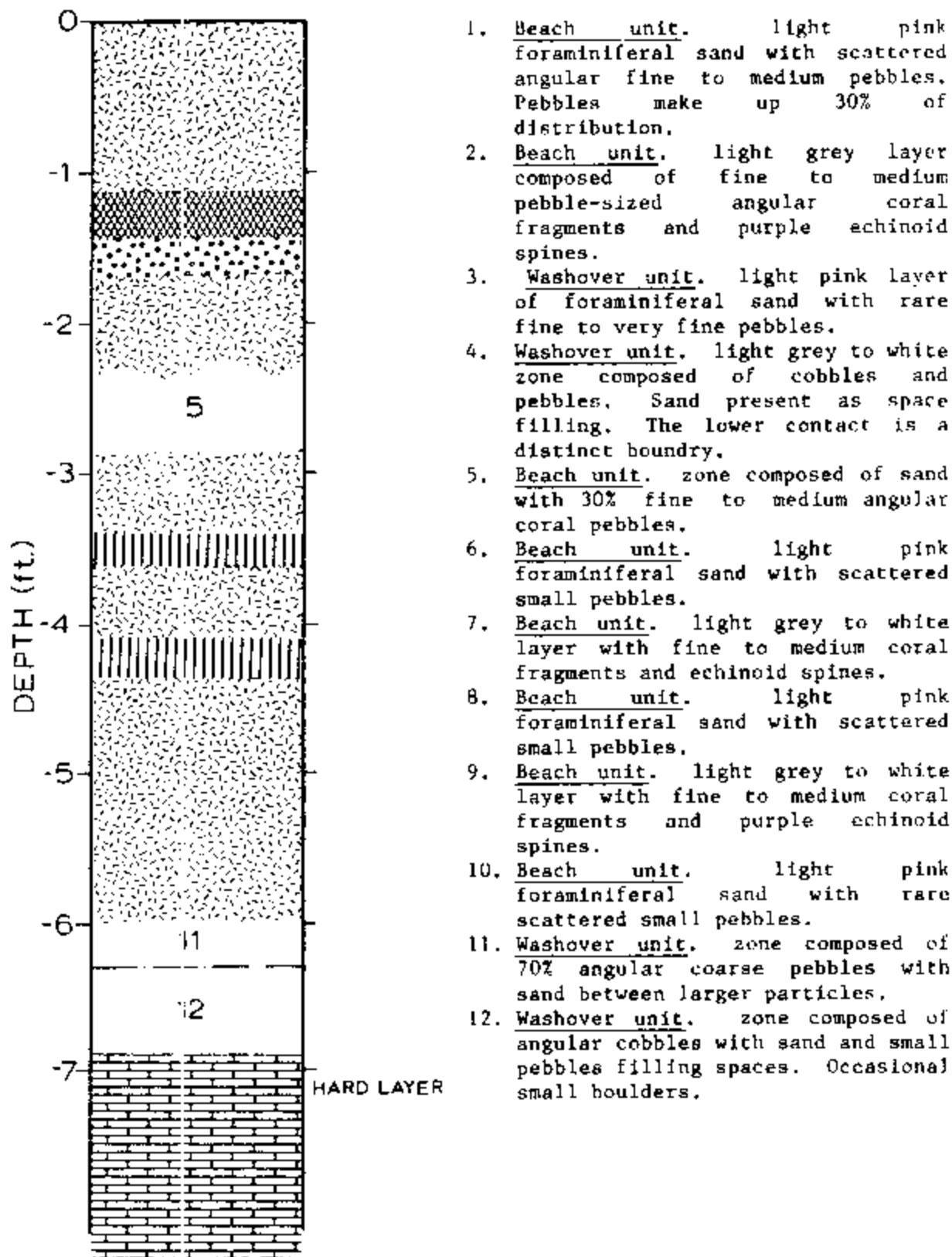
C2.	Sample no. 2:	sieve analysis.....	325
C3.	Sample no. 3:	sieve analysis.....	326
C4.	Sample no. 4:	sieve analysis.....	327
C5.	Sample no. 5:	sieve analysis.....	328
C6.	Sample no. 6:	sieve analysis.....	329
C7.	Sample no. 7:	sieve analysis.....	330
C8.	Sample no. 8:	sieve analysis.....	331
C9.	Sample no. 9:	sieve analysis.....	332
C10.	Sample no. 10:	sieve analysis.....	333
C11.	Sample no. 11:	sieve analysis.....	334
C12.	Sample no. 12:	sieve analysis.....	335
C13.	Sample no. 13:	sieve analysis.....	336
C14.	Sample no. 14:	sieve analysis.....	337
C15.	Sample no. 15:	sieve analysis.....	338
C16.	Sample no. 16:	sieve analysis.....	339
C17.	Sample no. 17:	sieve analysis.....	340
C18.	Sample no. 18:	sieve analysis.....	341
C19.	Sample no. 19:	sieve analysis.....	342
C20.	Sample no. 20:	sieve analysis.....	343
C21.	Sample no. 21:	sieve analysis.....	344
C22.	Sample no. 22:	sieve analysis.....	345
C23.	Sample no. 24:	sieve analysis.....	346
C24.	Sample no. 25:	sieve analysis.....	347
C25.	Sample no. 26:	sieve analysis.....	348
C26.	Sample no. 27:	sieve analysis.....	349
C27.	Sample no. 28:	sieve analysis.....	350
C28.	Sample no. 29:	sieve analysis.....	351
C29.	Sample no. 30:	sieve analysis.....	352

## Stratigraphic section at DS-3 drill site.

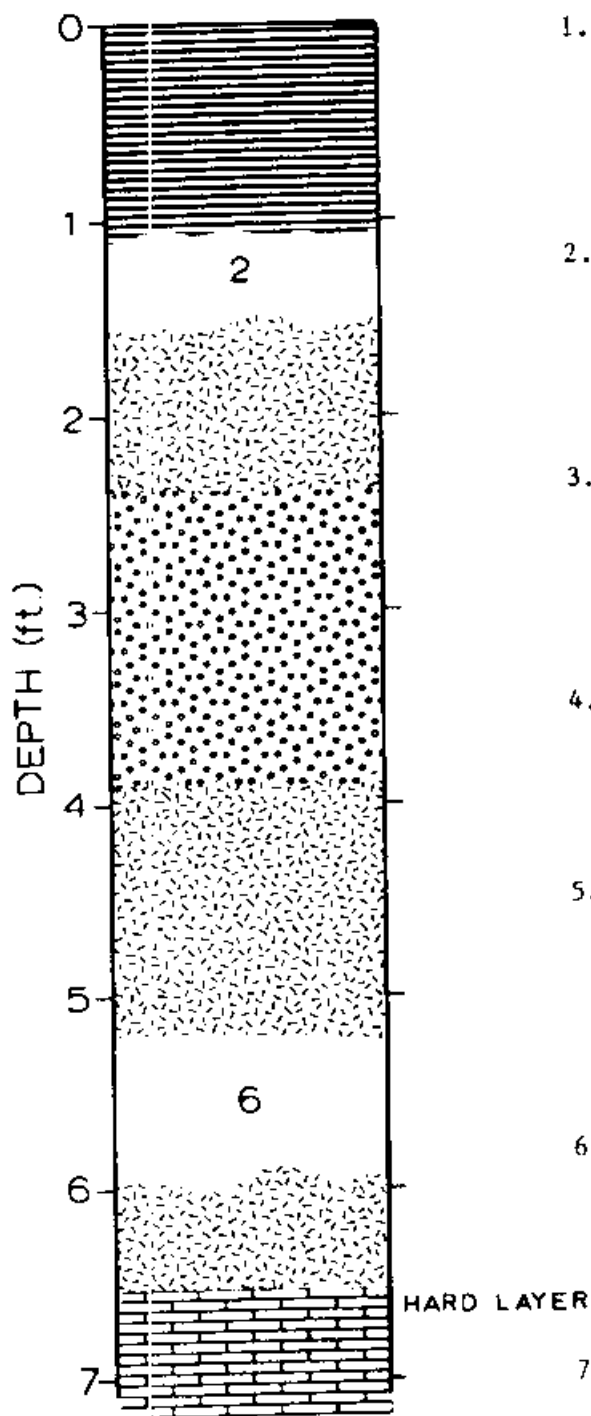


1. Washover unit. Dark brown to black soil zone containing 30 to 40% foraminiferal sand with 60 to 70% medium to coarse pebbles and rare small cobbles. Root fragments and root casts are common.
2. Washover unit. light grey to white zone composed of 20% foraminiferal sand and 80% medium to coarse pebbles with small cobbles. Sharp contact with the underlying stratigraphic unit.
3. Beach unit. light pink zone composed of foraminiferal sand, layers 3 to 4 inches thick alternating with 1 inch layers of fine to very fine coral pebbles.
4. Washover unit. Grey to light brown zone containing 60% medium to coarse gravel and 40% foraminiferal sand as filling. Root fragments and root casts are common.
5. Beach unit. light pink zone composed of 60% foraminifera sand with scattered very fine pebbles in 3" to 4" layers, alternating with 1" thick fine pebble layers.
6. Washover unit. light pink zone composed of 60% fine to very coarse pebbles with scattered small cobbles and 40% foraminifera sand filling spaces between pebbles.
7. Washover unit. light pink zone composed of 60% fine to very coarse pebbles with scattered small cobbles and 40% foraminiferal sand filling spaces between pebbles. This zone is loosely cemented.
8. Light pink zone containing 60% foraminiferal sand with 1" thick discontinuous fine to very fine pebble layers.

## Stratigraphic section at DS-4 drill site.

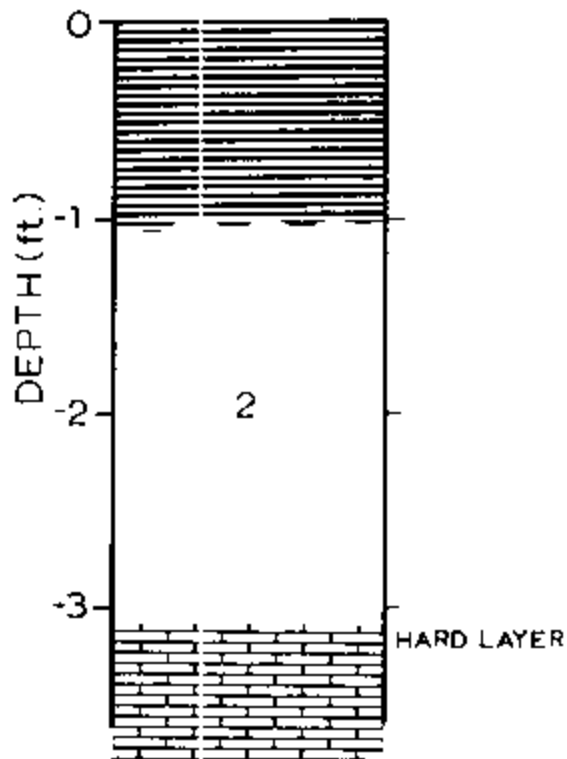


## Stratigraphic section at A6 test pit.



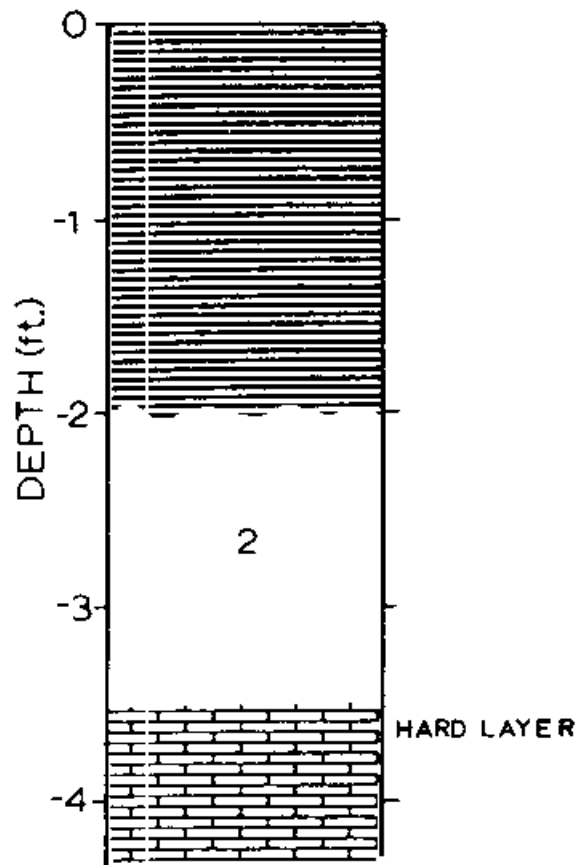
1. Washover unit. dark brown to black soil zone containing 30% foraminiferal sand sand 70% medium to coarse pebbles with common small cobbles. Roots and root casts are common.
2. Washover unit. light grey zone composed of 35 to 40% foraminiferal sand and 60 to 65% medium to coarse pebbles with common small cobbles. Roots and root casts are less abundant.
3. Beach unit. light pink zone composed of alternating 3"-4" layers of foraminifera sand with 1" to 1.5" well-sorted, very fine pebble layers. Pebble layers dip 2 to 3 degrees toward Southeast.
4. Washover unit. light pink to white zone containing angular medium to very coarse pebbles with cobbles. foraminiferal sand filling spaces between larger particles.
5. Beach unit. light pink zone composed of alternating 3"-4" layers of foraminiferal sand with 1" to 1.5" thick well-sorted, very fine pebble layers. Pebble layers dip 5 to 7 degrees toward Southeast.
6. Washover unit. light grey to pink zone composed of 60% angular coarse to very coarse pebbles and abundant cobbles with rare small boulders. Foraminiferal sand composes remaining 40% as space filling.
7. light pink foraminiferal sand with scattered very fine to medium pebbles. Pebbles compose 20 to 30% of the distribution.

## Stratigraphic section at Pz-1 drill site.



1. Dark brown to black soil zone composed of large cobbles of angular coral fragments in grain supported matrix. Pebbles and sand are found filling spaces between larger particles. Roots are abundant.
2. Light pink to grey zone composed of large cobbles of angular coral fragments in grain supported matrix. Pebbles and sand are found filling spaces between larger particles. Roots are rare.

## Stratigraphic section at Pz-2 drill site.



1. Dark brown soil zone composed of cobbles and small boulder size angular coral fragments in grain supported matrix. Pebbles and sand are found as fillings. Roots are quite large and very common.
2. Light pink to grey zone composed of cobbles and small boulder-size angular coral fragments in grain supported matrix. Sand is more abundant in this zone. Sand and pebbles are found filling spaces between the larger grains. Roots are quite rare.



## DEKE ISLAND DRILLING LOG

Drill Site: DS1                      Drilling Dates: 20 and 21 February  
 Core Diameter: 1" and split-      Total Depth Drilled: 15 ft.  
    spoon  
 Total Core Recovery: 0              Depth From Surface to Hard Layer: not found

Depth (Below Hard Layer)	Run No.	Recovery (ft)	Drilling Characteristics
15 ft from surface	1 and 2	0	unconsolidated sediments; Primarily <u>Baculogypsina</u> and <u>calcarina</u> sands; Core drill and split spoon sampling not successful; excessive caving and saturated sediments.

## DEKE ISLAND DRILLING LOG

Drill Site: DS2

Drilling Dates: 25 and 26 February

Core Diameter: 1" and split-  
spoon

Total Depth Drilled: 15 ft.

Total Core Recovery: 0

Depth From Surface to Hard Layer: not found

Depth (Below Hard Layer)	Run No.	Recovery (ft)	Drilling Characteristics
0-15'	1	0	Unconsolidated sediments; primarily <u>Baculogypsina</u> and <u>calcarina</u> sands; core drill sampling not successful.
from 5-7' below surface	2	2	split spoon sample of sediments collected by driving sampler into sediments at base of pipe mount casing; sediments were from caving of hole after core drilling attempts; 2 samples, taken-at upper 1' and lower 1' of sampled section. Lower 1' sediments contain more small to medium pebbles, which were near water table.

## DEKE ISLAND DRILLING LOG

Drill Site: DS3

Drilling Dates: 3, 5, 6, and 8 March

Core Diameter: 1"

Total Depth Drilled: 61 ft.

Total Core Recovery: 15.5 ft. Depth From Surface to Hard Layer: 7.5 ft.

Depth (Below Hard Layer)	Run No.	Recovery (ft)	Drilling Characteristics
0-5	1	4.7	very hard drilling; no cavities; few natural breaks; compact recent reef with cemented <u>Baculogypsina</u> and <u>calcarina</u> sands; encrusting foraminifera, <u>Tridacna</u> shell, very sparse coralline algae.
5-10	2	1.3	0.5 ft. hard drilling, broke thru hard layer and lost circulation; 1 ft sandy pocket; easy drilling with some crunchy drilling (sand or gravel?).
10-15	3	0.8	2 ft. easy drilling; 3 ft. of easy drilling with medium hard layers of 1 to 3" thickness; 75 psi for easy drill and 100 psi for harder drilling (marine pump).
15-20	4	1.0	1 ft. cave in with possible sand/gravel; easy drilling with few medium hard thin layers; 50-60 psi (marine pump).
20-25	5	1.4	2.5 ft of cave in with possible sand/gravel; easy drilling with thin medium hard layer and hard layer at 22 ft.

## DEKE ISLAND DRILLING LOG

Drill Site: DS3 continued      Drilling Dates: 3, 5, 6, and 8 March

Core Diameter: 1"              Total Depth Drilled: 61 ft.

Total Core Recovery: 15.5 ft. Depth From Surface to Hard Layer: 7.5 ft.

Depth (Below Hard Layer)	Run No.	Recovery (ft)	Drilling Characteristics
25-30	6	1.1	2.5 ft of cave in with possible sand/gravel; there was 8" hard (coral) in caved material; alternating easy and medium hard layers ranging from 2-8" thick; 95 psi (marine pump).
30-35	7	0	5 ft. of cave-in, feels like gravel-drilled pipe to starting depth; very easy drill from 30-35 ft. with thin crunchy layers; 75 psi (marine pump).
35-40	8	0.5	hole closed from 27 to 29 ft., gravel (?) and open from 29 to 34 ft; 1 ft easy drilling; 4 ft of alternating easy and medium hard drilling; 65 psi (marine pump).
40-45	9	0.8	hole closed from 26 to 29 ft, gravel (?) and partly to mostly open to 40 ft; alternating easy drilling and thin medium hard layers.
45-51	10	1.2	back filled to 27 ft with few open pockets to 45 ft.; 2 ft easy drilling with a thin hard layers; 3 ft alternating easy to thin medium hard layers; 1 ft of rough bouncy drilling; 55-60 psi (marine pump); possible facies change at 51 ft.

## DEKE ISLAND DRILLING LOG

Drill Site: DS3 continued      Drilling Dates: 3, 5, 6, and 8 March

Core Diameter: 1"      Total Depth Drilled: 61 ft.

Total Core Recovery: 15.5 ft. Depth From Surface to Hard Layer: 7.5 ft.

Depth (Below Hard Layer)	Run No.	Recovery (ft)	Drilling Characteristics
51-61	11	2.7	back filled at 25 ft. and 34 ft. with few open pockset to 51 ft.; 2 ft. medium hard drilling at 400-500 psi (freshwater pump); 2 ft. alternating medium hard and easy drilling layers; 2 ft. alternating thin very hard and easy drilling layers; 4 ft. alternating easy drilling and thin medium hard layers at 70-75 psi (marine pump); Halimeda rich facies.

## DEKE ISLAND DRILLING LOG

Drill Site: DS4

Drilling Dates: 12, 13, and 14 March

Core Diameter: 1"

Total Depth Drilled: 70 ft.

Total Core Recovery: 15.3 ft. Depth From Surface to Hard Layer: 10 ft.

Depth (Below Hard Layer)	Run No.	Recovery (ft)	Drilling Characteristics
0-4.7	1	1.5	hard layer 2.7 ft thick, with hard to very hard drilling; lost circulation below base hard layer; pocket of <u>Calcarina</u> sand with few rough spots (sandy layer with cobbles); 80 psi marine pump; hard layer material similar to DS3.
4.7-9.7	2	2.2	Easy drilling with few thin medium hard to hard layers and rough spots.
9.7-19.7	3	0.8	Easy drilling with 6-8" hard layer and few rough spots.
19.7-29.7	4	0.9	backfilled 0.5 ft, possible sand/gravel; alternating easy drilling with medium hard layers; few thin (1 to 2") hard layers; few small crunchy zones-like gravel; 80 psi (marine pump).
29.7-39.7	5	1.5	back filled 10ft., possible sand and gravel with few protrusions wall of along hole; alternating easy drilling and thin hard layers; 4 ft. rough bouncy drilling with few rough spots from 4-10 ft. of run.

## DEKE ISLAND DRILLING LOG

Drill Site: DS4 continued      Drilling Dates:  
 Core Diameter:                      Total Depth Drilled:  
 Total Core Recovery:              Depth From Surface to Hard Layer:

Depth (Below Hard Layer)	Run No.	Recovery (ft)	Drilling Characteristics
39.7-49.7	6	2.0	backfilled to 30 ft. level, rough crunchy material like pea gravel; at 38 ft. sandy (soft); 2 ft. of easy drilling with few hard layers; 6 ft. alternating easy drilling and medium hard layers with some rough bouncy drilling, change in facies- <u>Halimeda</u> rich; 50-65 psi (marine pump).
49.7-59.7	7	2.2	back filled to 36 ft. level; 2 ft. easy drilling with few thin hard layers at 50-60 psi (marine pum); 2 ft. crunchy (gravel) and slightly bouncy medium hard drilling; 2 ft. of thinly layered easy drilling and bouncy medium to hard layers; 4 ft. of alternating medium hard bouncy to hard layers at 70 psi (marine pump).
59.7-69.7	8	4.3	backfilled to 37 ft. level; jammed core barrel with <u>calcarina</u> sand in cleaning of hole; 10 ft. of alternating easy crunchy drilling and medium hard layers with few rough and bouncy spots; sand packing around bit; 70-75 psi (marine pump).

## DEKE ISLAND DRILLING LOG

Drill Site: DSS

Drilling Dates: 14 March

Core Diameter: 1"

Total Depth Drilled: 17 ft.

Total Core Recovery: 3.8 ft. Depth From Surface to Hard Layer: 8.4 ft.

Depth (Below Hard Layer)	Run No.	Recovery (ft)	Drilling Characteristics
0-1.8	1	1.8	hard layer, very hard drilling; rough and bouncy; difficulty with drilling at 1.8 ft., very rough drilling; hard layer material similar to DS3 and DS4.
1.8-6.8	2	2.0	very hard drilling in hard layer; broke thru at 4 ft. and lost circulation, recovery from run all hard layer material; below hard layer easy drilling (sand).
6.8-16.8	3	0	backfilled 2 ft., to lower level of hard layer, 4 ft.; 10 ft. easy drilling with only one medium hard layer (fragment of <u>Tridacna</u> shell); sand packing around bit, very difficult to retrieve; after pull-out, hole caved in to base hard layer.



## DEKE ISLAND DRILLING LOG

Drill Site: PS1                      Drilling Dates: 23 February  
 Core Diameter: 1/2"                Total Depth Drilled: 3 ft.  
 Total Core Recovery: 2.7 ft.      Depth From Surface to Hard Layer: Reef flat, 0

Depth (Below Hard Layer)	Run No.	Recovery (ft)	Drilling Characteristics
0-3	1	2.7	Reef flat at edge of steep sloped beach; very hard drilling with small cavity at 2.5-2.7 ft.; top 2" core is 1" diameter, coral; finished with smaller bit, because 1' bit coupler bent; Recent reef material similar to DS3, DS4, DS5; cavity area had more <u>Heliopora</u> coral; did not break thru hard layer.

## DEKE ISLAND DRILLING LOG

Drill Site: PS2

Drilling Dates: 1 March

Core Diameter: 1/2"

Total Depth Drilled: 2.5 ft.

Total Core Recovery: 2.5 ft. Depth From Surface to Hard Layer: hard layer  
in DS3, 7.5 ft.

Depth (Below Hard Layer)	Run No.	Recovery (ft)	Drilling Characteristics
0-2	1	2.0	hard layer in open pit at DS3, prior to cementing drill mounting pipe; surface of hard layer smooth and solid; very hard drilling; Layers of cemented <u>calcarina</u> sands and <u>Heliopora</u> coral; encrusting foraminifera, <u>Homotrema</u> , <u>Carpenteria</u> and <u>Sporadotrema</u> .
2-2.5	2	0.5	hard layer; very hard, slightly rough drilling; sand binding bit; material same as in run 1; drilled thru <u>Tridacna</u> shell.

## DEKE ISLAND DRILLING LOG

Drill Site: PS3

Drilling Dates: 11 and 14 March

Core Diameter: 1/2"

Total Depth Drilled: 8 ft.

Total Core Recovery: 4.9 ft. Depth From Surface to Hard Layer: 3 ft.

Depth (Below Hard Layer)	Run No.	Recovery (ft)	Drilling Characteristics
Surface sediments			sediments are gravel and white sand with surface soil layer of 3-4", beds of cobble and sand, then sand, with layer of large coral clasts near hard layer contact; fresh water ponded on surface.
0-1.7	1	1.5	hard layer; smooth surface with no visible breaks or cavities; very hard drilling; <u>Calcarina</u> sands and <u>Heliopora</u> coral, very little coralline algae, mollusk debris, coral interstices infilled with white "mud"; hard layer material similar to DS3, DS4, DS5, and PS1, PS2.
1.7-3.5	2	1.7	hard layer with hard to medium hard drilling, slightly rough in spots; <u>Calcarina</u> sands, abundant <u>Heliopora</u> coral (medium hard) which is bored and infilled with white "mud"; coral not <u>in situ</u> ; lower 6" is mostly cemented foraminiferal sand ( <u>Calcarina</u> , <u>Baculogypsina</u> , and few <u>Amphistegina</u> ).

## DEKE ISLAND DRILLING LOG

Drill Site: PS3 continued      Drilling Dates: 11 and 14 March

Core Diameter: 1/2"              Total Depth Drilled: 8 ft.

Total Core Recovery: 4.9 ft.      Depth From Surface to Hard Layer: 3 ft.

Depth (Below Hard Layer)	Run No.	Recovery (ft)	Drilling Characteristics
3.5-5.5	3	1.2	Hard layer with hard to medium hard drilling and few easy drilling spots, slightly rough drilling in spots; lost circulation at 5.3 ft, base of hard layer; cemented <u>Calcarina</u> sand, appears bedded; fragments of eroded <u>Heliopora</u> .
5.5-7.5	4	0.5	Alternating easy drilling and hard to medium hard layers, below hard layer; <u>Heliopora</u> coral and cemented fine grained rubble, encrusters; no <u>Calcarina</u> sand; water bubbling and "hissing" out of hole.

## DEKE ISLAND DRILLING LOG

Drill Site: PS4

Drilling Dates: 15 March

Core Diameter: 1/2"

Total Depth Drilled: 5.5 ft.

Total Core Recovery: 1.6 ft. Depth From Surface to Hard Layer: 3 ft.

Depth (Below Hard Layer)	Run No.	Recovery (ft)	Drilling Characteristics
0-1.5	1	0.8	hard layer, very hard to hard drilling with few rough spots; hard layer about 1.5 ft. thick; cemented fine grained sediments with rubble, coarse sand, some <u>Calcarina</u> sands, and coralline encrustations on coral fragments; maybe bedded.
1.5-3.5	2	0.5	Alternating layers of easy and medium hard drilling; coral and cemented <u>Calcarina</u> sand.
3.5-5.5	3	0.3	Easy drilling with few rough spots (coral rubble); possible sand/gravel layer; water bubbling and "hissing" out of hole.

## DEKE ISLAND DRILLING LOG

Drill Site: PS5

Drilling Dates: 16 March

Core Diameter: 1/2"

Total Depth Drilled: 4 ft.

Total Core Recovery: 0.2 ft. Depth From Surface to Hard Layer: about 4 ft.

Depth (Below Hard Layer)	Run No.	Recovery (ft)	Drilling Characteristics
0-4	1	0.2	Drilled into surface of taro pit; surface hard layer, top slightly irregular with coral rubble and encrusting coralline algae; 4" moderate drilling, remainder easy drilling; lost circulation at 0.8 ft; water bubbled out and stood above hard layer; core contained coral fragments, <u>Heliopora</u> , <u>Porolithon</u> fragment, no cemented sand.

Slab Sample: PG 1-1

Field Relations: Sample was taken from the reef flat surface at the junction of two fractures, approximately 1200 feet along traverse 1.

Constituents: Predominantly Acropora (in growth position?), the lower portion is encrusted by coralline algae, Homotrema and Sporadotrema. Below this encrusted zone, infilling of the coral has taken place. Above the encrustation are several small pockets within Acropora that contain sand fill. This sand fill consists mainly of Baculogypsina (about 1mm in longest dimension), coralline algae, echinoid spines, Calcarina, and fine-grained cement. Acropora coral pieces are also found dispersed throughout (4 to 5 mm in diameter).

Geometry, sorting etc. The sands are poorly sorted and some clasts are large, the largest being echinoid spines and Acropora branches. Orientation of grains is random, suggesting little or no reworking. Larger grains are not in contact, but separated by the finer foram sand and cement. The infilled sediment below the coral and encrusted layer is clearly a skeletal grainstone.

Some worm borings with yellow-brown rings are found in coralline algal stringers (encrusted zone). Worm borings and other bioerosion is common along edges with fewer borings in center.

Vugs are less common than on most other reef flat rocks; highly cemented. Coral geometry suggests a growth position with encrustation before sediment influx took place.

Slab Sample: PG 3-2

Field Relation: Cemented rubble ridge 25 feet seaward from the toe of the beach.

Constituents: Pocillopora is main constituent. Other corals, Acropora and Porites, are also present. Coralline material as a whole makes up about 60% of the rock. Baculogypsina, Calcarina, and coralline algae are loosely cemented between interstices of coral. Minor grain components include echinoid spines, Homotrema, and benthonic forams.

Geometry, sorting, etc.: Coralline rubble and interstitial grainstone lack an obvious arrangement. Sorting in sands is minimal. The foram grainstone portion is within the .75-1 mm size range; where as the coralline algae is commonly 2 mm or more in diameter.

Porosity may be as high as 20-25%, due to general lack of cement. In Addition, unfilled borings in the coralline material adds to the porosity.



Slab Sample: PG 4-1

Field Relation: Sample taken on reef flat, about 45 feet along traverse 4 in a buttress zone elevated above remainder of the reef flat.

Constituents. Similar grains as seen in PG 11-2B; the foram Calcarina dominates over Baculogypsina. However, the major constituents are corals: Acropora, Heliopora, and other undifferentiated corals (20 to 30 percent of the slab). Coralline algae is also common (10 to 20 percent). The remainder of the rock is foram sand tightly cemented with cryptocrystalline carbonate (30 to 40 percent of the volume). Porosity constituents about 10 to 20 percent of slab. A minor component of the slab includes Homotrema, which is dispersed as detrital grains throughout foram sand areas. Cerithid gastropods, bivalves, and other gastropods are uncommon in the cemented foram sand and are volumetrically unimportant.

Geometry, sorting, etc.: A grainstone on two scales typifies PG 4-1. Size of clasts are generally smaller than PG 11-2B; they are usually 5 mm in diameter or width. However, some larger pieces of coral are present but not common. Cryptocrystalline carbonate or cement characterizes some areas. This can be observed most readily in the area surrounding partially filled worm burrows.

No unusual arrangement of grains; sorting is minimal with sand (1mm and less) filling interstices between larger grains. Shelter porosity is common with other porosity types found as vugs or borings, which are partially filled with foram sand and coralline algal debris.

Slab Sample: PG 5-2

Field Relation: Sample taken from edge of reef plate between Pingelap and Deke islands. Portions of plate extend as fingers, lagoonward.

Constituents: Acropora coral (not in situ) has been intensely bio-eroded, producing porosity of 10-15%, and perhaps higher than normal permeability, especially where larger borings are interconnected. The large worm borings, up to 8x5 mm, are usually infilled with mud. Some of these show excellent geopetal structures. The exterior portion has small borings but with much closer spacing. The bio-eroded surface is blackish to yellow in color. Boring by Lithophaga bivalve.

Geometry, sorting, etc.: Coral shows extensive replacement by infilling of borings with yellow and white mud. Structure of coral mostly altered. Large borings show several generations of fine sediment infilling and cementation.

Slab Sample. PG 6-1

Field Relation: Sample taken on the reef flat along a fracture edge. Surface of the specimen was covered with a filamentous algal mat and abundant forams. Location approximately 1700 feet along transverse 6.

Constituents: Acorpora coral is the major constituent, possibly in growth position. Coral material is truncated in part and abutted with obvious detrital grains consisting of coralline algae (some round in cross section and chalky white) and forams (usually no more than 1 mm in greatest dimension). Coral fragments, approximately the size of most of the coralline algal fragments (3 to 5 mm in diameter), are common in this detrital mixture. Encrusting forams; and Tubopora coral are fairly sparse. Exterior edge of slab shows some algal laminations with minor worm borings.

Geometry, sorting etc.: Coral is possibly in situ, where as, other grains have been transported; slight indication of imbrication towards the center of the slab directly above the coral mass. Sorting is poor within the detrital or grainstone portion.

Slab Sample: PG 7-2

Field Relation: On outer reef flat within an exposed buttress zone. There are some raised algal(?) polygonal networks within vicinity of sampling site.

Constituents: Transported Acropora coral and other corals are major constituents. Vuggy porosity is commonly very large (5-7 mm in width and up to 3 cm in length). Most of the vugs are open, those that are partially filled contain cemented coral fragments, Baculogypsina, cerithid gastropods, Sporadotrema encrustations, and echinoid spines. Grains average 1 mm to 2 mm in size. Encrusting coralline algae appears as stringers across slab, commonly 2 mm wide, but up to 4 mm or slightly larger.

Outside of vugs, echinoid spines, Sporadotrema and other forams are common but are rarely in grain to grain contact. The majority of the slab is a coralline boundstone, with grainstone inside of the vugs.

Worm borings are commonly filled with very fine, white mud. A concentration of yellow to brown ringed borings is found within the white stringers of coralline algae, otherwise borings may be filled and lack color bands around the perimeter.

Geometry, sorting, etc.: Sorting is good in the coarse sand that infills vugs. In the massive portions of the slab, sorting is not much of a factor, since there are only a few forams and pieces of coralline algae. These grains appear to be distributed randomly. The slab is tightly cemented.

Slab Sample: PG 8-1

Field Relation: Sample taken on reef flat, about 1,000 feet along traverse B on seaward edge of a cemented rubble lobe.

Constituents: Helipora and Acropora corals constitute about 25% of sample. Both coral types show boring by blue-green algae and some of the bores are infilled with light (very white) mud.

Sands filling interstices makes up about 60% of rock. The larger coralline algal pieces, taken as a single component make up 10-15% of the rock volume. The coralline algae is found as solid cylinder or as an encruster (most pieces are 1 mm thick zones with yellow-brown ringed worm borings). The sands are finer grained (.5-.75 mm) compared to most other reef flat rubble zones. Calcarina, Baculogypsina and coralline algae are the most common sand components. In addition, lesser amounts of echinoid spines, and Homotrema are present.

Geometry, sorting, etc.: Individual lenses and pockets of sand are, relatively, well sorted. Fine white carbonate cements are pervasive throughout, especially in coralline algal/foram sands (grainstone). This sample of rubble zone grainstone can be considered as "two grainstones in one" - large grains and a finer grained sandy portion which fills the interstices between larger grains.

Slab Sample: PG 9-1

Field Relation: Sample taken on reef flat area within a buttress zone, approximately 45 feet along traverse 9.

Constituents: Acropora coral makes up about 70% of slab. Heliopora coral has been encrusted (<30%) and then overgrown by Acropora. Both corals are apparently in growth position, a fine grained foram (Baculogypsina, Calcarina, and Homotrema) grainstone fills the interstices of chalky, white coralline algae. This filling is in abrupt contact with Acropora portion of slab. Bioerosion around the outside portion, probably by blue-green algae and worms is very prevalent.

A similar slab for thin sectioning of PG 9-1 revealed a control that worm burrows had an arrangement of various constituents. The zone of white coralline algal encrustation on Heliopora and through parts of the Acropora mass had yellow-brown filled and unfilled worm borings (.5 to .75 mm in diameter) that are limited only to this surface. Larger worm borings are infilled with mostly well cemented foram grainstone (very fine .75 mm or less in diameter). Since most of the slab is coral, small portions show a tendency towards grainstone. Cementation is good and corals appear to be highly replaced.

Slab Sample: PG 11-2B

Field Relation: Collected on a cemented rubble ridge apron, at 10 cm above low tide water level.

Constituents: Pocillopora coral rubble makes up 50 to 60 percent of the slab. Other large clasts, which constitute 10 to 20 percent of the slab, include echinoid spines, and coralline algae. Sands found between coral branches are mostly foram sands, dominated by Calcarina. Baculogypsina is present but subordinate to Calcarina sands. Rarer constituents include Caulastrea coral, Heliopora coral and forams Heterostegina and Homotrema.

Geometry, sorting etc.: The arrangement of the rubble grains is chaotic with an imbrication of coralline material. These larger coral clasts are 5 to 8 mm in narrowest dimension and about 10 to 20 mm in the longest dimension. Foram sand between the coral is typically 1 to 1.5 mm in size, dependent on foram species. The whole rock can be considered a grainstone; both larger clasts and other sand filling in interstices.

Porosity is found in various forms; mostly shelter, intraparticle (in corals), and vuggy. All these porosity types combined produce 10 to 20 percent total porosity throughout the whole slab.

Boring algae has contributed to the porosity of the slab, this is most noticeable as a red outline at the upper most portion (edge) of the slab. In addition, many of the corals have been bored by other bioeroders and refilled with sediment.

Cementation is rather good even though this material is from a reef flat rubble zone. Initially most rubble was friable and currently this sample is in later stages of cementation.

Slab Sample: PGA 2-A

Field Relations: Abandoned taro pit on Oke Island. The surface of "hard layer" is very uneven as opposed to other surfaces in taro pits. The irregularity of the surface is possibly defined by patchy cementation of coarse rubble.

Constituents: Porites? coral head, probably in growth position. The foram sands around the coral base are accreted onto the periphery of the coral. The sand fraction is dominated by coralline algae (Porolithon), Calcarina, Baculogypsina, coral fragments, echinoid spine fragments, Cerithid gastropods, and Homotrema. Serpulid worm tubes are present on base of coral.

Geometry, sorting, etc.: The foram sand is well sorted with a  $\phi$  range from 0 to .5. This sand is loosely cemented, for the most part. Arrangement of foram grainstone or sands suggests material filtered down to base of coral and filled interstices before eventually completely burying coral. Some minor worm borings in the coral contribute to porosity; However, most is intraparticle and shelter porosity within coral and at base of coral, respectively.



Slab Sample: PCA 6B

Field Relation: Sample taken from a taro pit on Deke Island. Collection of sample was from 12 cm below surface of "hard layer". Coral heads were found within a coarse matrix of cemented debris.

Constituents: A large Tridacna bivalve is encrusted and bored. The outer encrustation is a similar material which fills a large bore. The Tridacna was bored prior to burial with a detrital material which filled voids and accreted around the shell. Most of this material is a detrital sand dominated by Calcarina, Baculogypsina, coralline algae and lesser amounts of Homotrema, Marginopora, and echnioid spines.

Geometry, sorting, etc.: These sands can be classed as an algal/foram grainstone. The average grain size is controlled by foram test size (usually 1 to 1.5 mm). Some of the coralline algal grains are larger. This cemented sand makes a very well indurated rock.

Slab Sample: PGA-7

Field Relation: A cemented layer 30 cm below the floor of a double taro pit on Deke Island. The upper zone above the layer has 5 cm of clean, foram sand. The slab surface is generally smooth with a slight undulatory relief. This "hard layer" is exceptionally hard below the uppermost layer which is chalky, bored, and lacks any indurated crust. The rock surface was covered with abundant bulbous coralline algae along (Porolithon), with Heliopora coral and other small coral fragments.

Constituents: Most of the corals show evidence of transport and are not in growth position. They constitute the major component of the slab. Coralline algae, seen as round to elliptical, chalky white masses are also prevalent. Towards the center of the slab is a foram grainstone that fills the interstices between the larger coral mass. Echinoid spines and Nomotrema are interdispersed throughout.

Geometry, sorting etc.: The foram grainstone portion is generally poorly sorted with the exception of a few "clean" zones with  $\phi$  range of 0.0 to -0.5. Imbrication, especially in the foram grainstone suggests flow from left to right.

Porosity is mainly vuggy with average vugs rarely more than 1.5 or 2 mm in diameter. However, some large vugs up to 5 mm wide occur. Intraparticle porosity is well developed in most foram tests and to a lesser extent in corals.

This sample is in a very indurated condition and contains very fine cements. Although some vugs are common in places, overall this slab has less pore space than most rocks found on the reef flat which contain detritus or rubble.

Slab Sample: PGA 10B

Field Relation: Sample taken at D-1 site. Thin layer with a fairly sharp contact, level top that grades into gravel and an uncemented zone.

Constituents: Well cemented Acropora coral head, in possible growth position. Coralline algae encrusts exterior of coral. Few small borings in edges of coral, generally not filled.

Geometry, sorting, etc.: Porosity is mainly intraparticle.

Slab Sample: PGA 13A

Field Relation: In a hand-dug pit on Deke Island. Sample was extracted from a cemented layer that appeared to be discontinuous unlike the typical "hard layer" that commonly is indurated and has much greater lateral continuity. This lightly cemented or encrusted rubble was from an interval 20 to 30 cm below the water table at low tide (March 21, 1984). Not all portions of this layer appeared to be rubble, some evidence suggested in situ growth position.

Constituents: Acropora (at bottom of slab) and Favites? or Goniastera? constitute the coral material which makes up the bulk of the slab. Most corals are encrusted with coralline algae and minor Homotrema. Outer edges of coral have a thin rind of secreted foram and coralline algae sands. Worm borings are rare.

Geometry Sorting, etc.: This slab suggests in situ growth of corals and associated encrusting algae. Although field observation does not suggest that this is the "hard layer" it is possibly more than a rubble deposit. Perhaps it is an incipient "hard layer" in early stages of cementation or has been exposed to dissolution or may be a water table cemented layer. Some portions of the slab show vuggy porosity, but generally intraparticle porosity is prevalent in Acropora and less in the other corals.

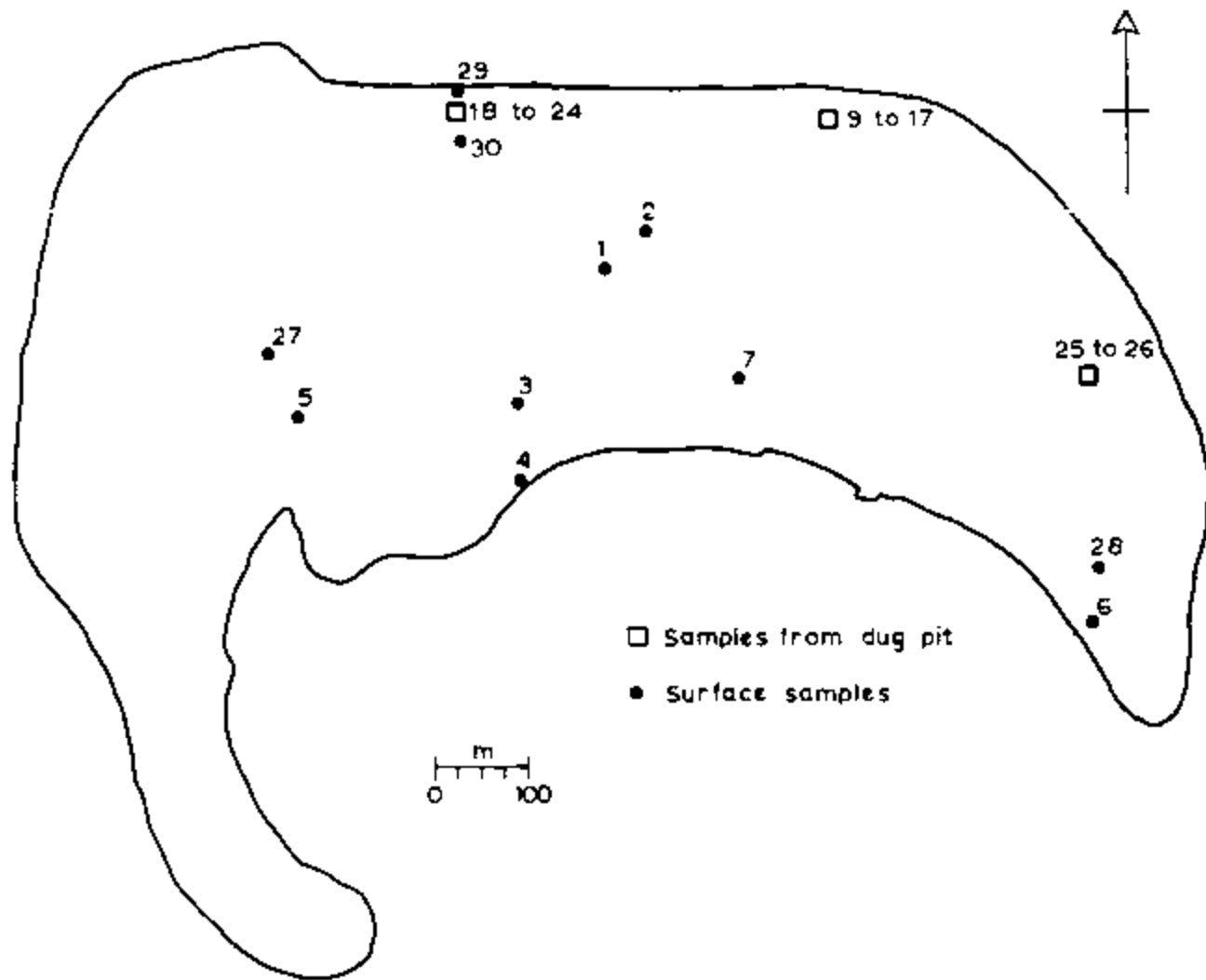


Figure C1. Map of Deke Island showing the location of collection sites for sediment size analysis.

Table C1. Sample no. 1: Sieve analysis.

	Class (phi)	Fraction Wt. (gm)	Weight (%)	Cumulative Wt. (%)
	-4.22	49.05	18.4	18.4
G	-3.66	29.73	11.2	29.6
R	-2.68	24.23	9.1	38.6
A	-2.35	9.65	3.6	42.3
V	-1.76	9.08	3.4	45.6
E	-1.24	11.01	4.1	49.8
L	-0.61	11.24	4.2	54.0
	-0.22	14.31	5.4	59.4
	0	6.63	2.5	61.9
	0.50	35.08	13.2	75.0
	0.75	13.82	5.2	80.2
S	1.75	6.28	2.4	82.6
A	2.33	24.24	9.1	91.7
N	2.74	10.04	3.8	95.4
D	3.24	4.22	1.6	97.0
	3.74	2.06	0.8	97.8
	4.04	1.16	0.4	98.2
	Pan	4.65	1.7	99.9
Percent Gravel:		59.4		
Percent Sand:		38.8		
Percent Pan:		1.7		

Table C2. Sample no. 2: Sieve analysis.

	Class (phi)	Fraction Wt. (gm)	Weight (%)	Cumulative Wt. (%)
	-4.22	8.1	4.3	4.3
G	-3.66	23.1	12.2	16.5
R	-2.68	9.9	5.2	21.7
A	-2.35	5.4	2.8	24.6
V	-1.76	2.6	1.3	25.9
E	-1.24	3.5	1.8	27.8
L	-0.61	4.5	2.4	30.1
	-0.22	9.0	4.8	34.9
	0	6.2	3.3	38.2
	0.50	47.1	24.9	63.1
	0.75	22.7	12.0	75.1
S	1.75	8.8	4.6	79.7
A	2.33	24.5	12.9	92.6
N	2.74	7.9	4.1	96.8
D	3.24	3.0	1.6	98.4
	3.74	1.6	0.9	99.2
	4.04	0.9	0.4	99.7
	Pan	0.6	0.3	100
Percent Gravel:		34.9		
Percent Sand:		64.8		
Percent Pan:		0.3		

Table C3. Sample no. 3: Sieve analysis.

	Class (phi)	Fraction Wt. (gm)	Weight (%)	Cumulative Wt. (%)
	-4.22	19.9	17.8	17.8
G	-3.66	6.2	5.6	23.3
R	-2.68	11.0	9.9	33.2
A	-2.35	4.7	4.2	37.4
V	-1.76	3.8	3.4	40.9
E	-1.24	2.9	2.6	43.5
L	-0.61	3.9	3.5	47.0
	-0.22	6.4	5.7	52.7
	0	3.8	3.4	56.1
	0.50	19.8	17.7	73.8
	0.75	9.0	8.1	81.9
S	1.75	2.8	2.5	84.5
A	2.33	8.2	7.3	91.8
N	2.74	4.2	3.8	95.5
D	3.24	1.9	1.7	97.2
	3.74	1.4	1.2	98.4
	4.04	0.7	0.6	99.1
	Pan	1.0	0.9	100.0
Percent Gravel:		52.7		
Percent Sand:		46.4		
Percent Pan:				



Table C4. Sample no. 4: Sieve analysis.

	Class (phi)	Fraction Wt. (gm)	Weight (%)	Cumulative Wt. (%)
	-4.22	39.8	23.1	23.1
G	-3.66	18.6	10.8	24.0
R	-2.68	26.4	15.4	49.4
A	-2.35	5.6	3.3	52.6
V	-1.76	4.4	2.6	55.2
E	-1.24	4.1	2.4	57.6
L	-0.61	6.6	3.8	61.5
	-0.22	6.3	3.7	66.1
	0	1.7	1.0	66.1
	0.50	18.3	10.6	76.7
	0.75	12.4	7.3	84.1
S	1.75	4.4	2.5	86.6
A	2.33	11.6	6.7	93.4
N	2.74	4.1	2.4	95.7
D	3.24	3.4	2.0	97.7
	3.74	2.0	1.2	98.9
	4.04	1.0	0.6	99.4
	Pan	1.0	0.9	100.0
Percent Gravel:		65.1		
Percent Sand:		34.6		
Percent Pan:		0.3		

Table C5. Sample no. 5: Sieve analysis.

	Class (phi)	Fraction Wt. (gm)	Weight (%)	Cumulative Wt. (%)
	-4.22	68.6	27.4	24.4
G	-3.66	52.3	20.9	48.4
R	-2.68	24.4	9.8	58.1
A	-2.35	4.7	1.9	60.0
V	-1.76	3.2	1.3	61.3
E	-1.24	2.4	1.0	62.2
L	-0.61	4.1	1.6	63.9
	-0.22	5.1	2.0	65.9
	0	2.8	1.1	67.0
	0.50	16.2	6.5	73.5
	0.75	18.4	7.3	80.9
S	1.75	8.8	3.5	84.4
A	2.33	22.4	8.9	93.3
N	2.74	8.0	3.2	96.5
D	3.24	3.5	1.4	97.9
	3.74	2.7	1.1	99.0
	4.04	1.4	0.6	99.6
	Pan	1.0	0.4	100.0
Percent Gravel:		65.9		
Percent Sand:		33.6		
Percent Pan:		0.4		

Table C6. Sample no. 6: Sieve analysis.

	Class (phi)	Fraction Wt. (gm)	Weight (%)	Cumulative Wt. (%)
	-4.22	9.1	4.4	4.4
G	-3.66	16.8	8.1	12.4
R	-2.68	34.4	16.5	28.9
A	-2.35	5.0	2.4	31.3
V	-1.76	4.3	2.1	33.4
E	-1.24	4.0	1.9	35.3
L	-0.61	4.2	2.0	37.3
	-0.22	4.1	2.0	39.3
	0	1.2	0.6	39.9
	0.50	16.1	7.7	47.6
	0.75	26.6	12.8	60.4
S	1.75	14.6	7.0	67.4
A	2.33	46.4	22.3	89.6
N	2.74	11.9	5.7	95.3
D	3.24	3.7	1.8	97.1
	3.74	2.4	1.1	98.3
	4.04	1.8	0.9	99.1
	Pan	1.8	0.9	100.0
Percent Gravel:		39.3		
Percent Sand:		59.8		
Percent Pan:		0.9		

Table C7. Sample no. 7: Sieve analysis. Sample depth 0.6 ft.

	Class (phi)	Fraction Wt. (gm)	Weight (%)	Cumulative Wt. (%)
	-4.22	189.8	57.6	57.6
G	-3.66	53.5	16.2	73.8
R	-2.68	25.2	7.7	81.5
A	-2.35	3.7	1.1	82.6
V	-1.76	2.3	0.7	83.3
E	-1.24	3.4	1.0	84.4
L	-0.61	4.1	1.2	85.6
	-0.22	4.4	1.3	86.9
	0	1.7	0.5	87.4
	0.50	6.5	2.0	89.4
	0.75	6.6	2.0	91.4
S	1.75	2.9	0.9	92.3
A	2.33	10.6	3.2	95.5
N	2.74	7.8	2.4	97.9
D	3.24	3.0	0.9	98.8
	3.74	1.1	0.3	99.5
	4.04	0.7	0.2	99.9
	Pan	0.7	0.2	100.0
Percent Gravel:		86.9		
Percent Sand:		12.9		
Percent Pan:		0.2		

Table C8. Sample no. 8: Sieve analysis. Sample depth 1.2 ft.

	Class (phi)	Fraction Wt. (gm)	Weight (%)	Cumulative Wt. (%)
	-4.22	20.1	7.9	7.9
G	-3.66	92.4	36.2	44.1
R	-2.68	88.9	34.9	79.0
A	-2.35	5.1	2.0	81.0
V	-1.76	2.7	1.1	82.1
E	-1.24	2.2	0.9	83.0
L	-0.61	2.2	0.8	83.8
	-0.22	2.2	0.9	84.7
	0	2.1	0.8	85.5
	0.50	4.9	1.9	87.4
	0.75	6.5	2.6	90.0
S	1.75	2.9	1.1	91.1
A	2.33	11.4	4.5	95.6
N	2.74	6.0	2.3	97.9
D	3.24	2.8	1.0	99.0
	3.74	1.6	0.6	99.6
	4.04	0.8	0.3	99.9
	Pan	0.1	0.1	100.0
Percent Gravel:		84.7		
Percent Sand:		15.2		
Percent Pan:		0.1		

Table C9. Sample no. 9: Sieve analysis. Sample depth 1.8 ft.

	Class (phi)	Fraction Wt. (gm)	Weight (%)	Cumulative Wt. (%)
	-4.22	148.7	45.2	45.2
G	-3.66	44.9	13.6	58.8
R	-2.68	19.7	13.6	64.8
A	-2.35	2.9	0.9	64.7
V	-1.76	2.3	0.7	66.4
E	-1.24	3.3	1.0	67.4
L	-0.61	4.9	1.5	68.9
	-0.22	6.8	2.1	71.0
	0	3.6	1.1	72.1
	0.50	32.0	9.7	81.8
	0.75	23.4	7.1	88.9
S	1.75	9.5	2.9	91.8
A	2.33	19.3	5.9	97.7
N	2.74	4.1	1.3	99.0
D	3.24	1.1	0.3	99.3
	3.74	1.3	0.4	99.7
	4.04	0.7	0.2	99.9
	Pan	0.7	0.2	100.0
Percent Gravel:		71.0		
Percent Sand:		28.9		
Percent Pan:		0.2		

Table C10. Sample no. 10: Sieve analysis. Sample depth 2.8 ft.

	Class (phi)	Fraction Wt. (gm)	Weight (%)	Cumulative Wt. (%)
	-4.22	56.5	24.0	24.0
G	-3.66	36.0	15.3	39.2
R	-2.68	31.4	13.3	52.6
A	-2.35	10.9	4.6	57.2
V	-1.76	10.7	4.5	61.8
E	-1.24	7.6	3.2	65.0
L	-0.61	7.0	3.0	67.9
	-0.22	10.0	4.2	72.2
	0	5.9	2.5	74.7
	0.50	16.8	7.1	81.3
	0.75	9.7	4.1	86.0
S	1.75	4.7	2.0	88.0
A	2.33	18.7	7.9	95.9
N	2.74	4.0	1.7	97.6
D	3.24	1.6	0.7	98.3
	3.74	1.2	0.5	98.8
	4.04	0.8	0.3	99.1
	Pan	2.0	0.8	100.0
Percent Gravel:		72.2		
Percent Sand:		27.0		
Percent Pan:		0.8		

Table C11. Sample no. 11: Sieve analysis. Sample depth 4.6 ft.

	Class (phi)	Fraction Wt. (gm)	Weight (%)	Cumulative Wt. (%)
	-4.22	45.2	16.7	16.7
G	-3.66	13.0	4.8	21.5
R	-2.68	30.8	11.4	32.9
A	-2.35	10.3	3.8	36.8
V	-1.76	7.6	2.8	39.5
E	-1.24	10.3	3.8	43.3
L	-0.61	9.8	3.6	47.0
	-0.22	18.6	6.9	53.9
	0	15.0	5.6	59.4
	0.50	40.0	14.8	74.2
	0.75	23.4	8.7	82.9
S	1.75	10.3	3.8	86.7
A	2.33	27.6	10.2	97.0
N	2.74	4.3	1.6	98.6
D	3.24	1.5	0.6	99.1
	3.74	1.3	0.5	99.6
	4.04	0.7	0.2	100.9
	Pan	2.0	0.1	100.0
Percent Gravel:		53.9		
Percent Sand:		46.0		
Percent Pan:		0.1		



Table C12. Sample no. 12: Sieve analysis. Sample depth 3.8 ft.

	Class (phi)	Fraction Wt. (gm)	Weight (%)	Cumulative Wt. (%)
	-4.22	43.9	24.7	24.7
G	-3.66	22.2	12.5	37.2
R	-2.68	6.1	3.4	40.6
A	-2.35	6.8	3.8	44.4
V	-1.76	5.5	3.1	47.5
E	-1.24	5.1	2.9	50.4
L	-0.61	14.0	7.9	58.2
	-0.22	2.6	1.5	59.7
	0	8.1	4.5	64.2
	0.50	25.2	14.2	78.4
	0.75	8.3	4.6	83.0
S	1.75	5.0	2.8	85.9
A	2.33	17.8	10.0	95.9
N	2.74	3.5	2.0	97.9
D	3.24	1.3	0.7	98.6
	3.74	1.2	0.7	99.3
	4.04	0.7	0.4	99.7
	Pan	0.5	0.3	100.0
Percent Gravel:		59.7		
Percent Sand:		40.0		
Percent Pan:		0.3		

Table C13. Sample no. 13: Sieve analysis. Sample depth 4.2 ft.

	Class (phi)	Fraction Wt. (gm)	Weight (%)	Cumulative Wt. (%)
	-4.22	67.0	31.5	31.5
G	-3.66	15.4	7.2	38.7
R	-2.68	15.0	7.0	45.8
A	-2.35	3.3	1.6	47.3
V	-1.76	6.7	3.1	50.5
E	-1.24	7.6	3.6	54.1
L	-0.61	7.1	3.3	57.4
	-0.22	11.8	5.5	62.9
	0	8.1	3.8	66.7
	0.50	24.9	11.7	78.4
	0.75	8.9	4.2	82.6
S	1.75	4.5	2.1	84.7
A	2.33	22.2	10.4	95.1
N	2.74	5.3	2.5	97.6
D	3.24	1.9	0.9	98.5
	3.74	1.3	0.6	99.1
	4.04	1.1	0.5	99.6
	Pan	0.8	0.4	100.0
Percent Gravel:		62.9		
Percent Sand:		36.7		
Percent Pan:		0.4		

Table C14. Sample no. 14: Sieve analysis. Sample depth 5.6 ft.

	Class (phi)	Fraction Wt. (gm)	Weight (%)	Cumulative Wt. (%)
	-4.22	0.0	0.0	0.0
G	-3.66	0.0	0.0	0.0
R	-2.68	8.9	18.4	18.4
A	-2.35	1.4	3.0	21.4
V	-1.76	1.9	3.9	25.3
E	-1.24	3.0	6.2	31.5
L	-0.61	3.5	7.3	38.8
	-0.22	6.3	13.3	52.1
	0	2.4	4.9	57.0
	0.50	9.7	20.0	77.1
	0.75	3.9	8.1	85.2
S	1.75	1.7	3.5	88.6
A	2.33	4.0	8.3	96.9
N	2.74	0.8	1.8	98.7
D	3.24	0.2	0.5	99.2
	3.74	0.2	0.3	99.5
	4.04	0.1	0.2	99.7
	Pan	0.1	0.3	100.0
Percent Gravel:		52.1		
Percent Sand:		47.6		
Percent Pan:		0.3		

Table C15. Sample no. 15: Sieve analysis. Sample depth 5.9 ft.

	Class (phi)	Fraction Wt. (gm)	Weight (%)	Cumulative Wt. (%)
	-4.22	26.7	15.6	15.6
G	-3.66	22.7	13.3	28.9
R	-2.68	30.0	17.6	46.5
A	-2.35	6.8	4.0	50.5
V	-1.76	6.1	3.6	54.1
E	-1.24	5.3	3.1	57.2
L	-0.61	5.9	3.4	60.7
	-0.22	13.5	7.9	68.6
	0	6.7	3.9	72.5
	0.50	20.7	12.1	84.6
	0.75	9.3	5.4	90.1
S	1.75	3.6	2.1	92.2
A	2.33	9.6	5.6	97.8
N	2.74	1.8	1.0	98.9
D	3.24	0.6	.4	99.2
	3.74	0.5	.3	99.5
	4.04	0.4	.2	99.8
	Pan	0.4	.2	100.0
Percent Gravel:		68.6		
Percent Sand:		31.2		
Percent Pan:		.2		

Table C16. Sample no. 16: Sieve analysis. Sample depth 6.2 ft.

	Class (phi)	Fraction Wt. (gm)	Weight (%)	Cumulative Wt. (%)
	-4.22	91.2	36.6	36.6
G	-3.66	14.8	5.9	42.5
R	-2.68	16.6	6.6	49.1
A	-2.35	6.3	2.5	51.7
V	-1.76	2.9	1.2	52.9
E	-1.24	4.8	1.9	54.9
L	-0.61	5.3	2.1	56.9
	-0.22	12.9	5.2	62.1
	0	6.3	2.5	64.6
	0.50	25.5	10.2	74.8
	0.75	14.9	6.0	80.8
S	1.75	7.0	2.8	83.6
A	2.33	28.1	11.3	94.8
N	2.74	5.1	2.0	96.9
D	3.24	4.3	1.7	98.6
	3.74	1.9	.8	99.4
	4.04	0.8	.3	99.7
	Pan	0.7	.3	100.0
Percent Gravel:		62.1		
Percent Sand:		37.6		
Percent Pan:		.3		

Table C17. Sample no. 17: Sieve analysis. Sample depth 5.1 ft.

	Class (phi)	Fraction Wt. (gm)	Weight (%)	Cumulative Wt. (%)
	-4.22	5.7	9.4	9.4
G	-3.66	6.3	10.5	19.9
R	-2.68	5.7	9.5	29.4
A	-2.35	1.6	2.7	32.1
V	-1.76	0.8	1.3	33.4
E	-1.24	1.4	2.3	35.7
L	-0.61	2.2	3.7	39.4
	-0.22	5.0	8.3	47.8
	0	3.3	5.5	53.3
	0.50	18.1	29.9	83.2
	0.75	3.8	6.4	89.6
S	1.75	1.2	1.9	91.5
A	2.33	3.5	5.8	97.3
N	2.74	0.8	1.3	98.6
D	3.24	0.2	.4	99.0
	3.74	0.4	.6	99.7
	4.04	0.4	.2	99.8
	Pan	0.1	.1	100.0
Percent Gravel:		47.8		
Percent Sand:		52.1		
Percent Pan:		.1		

Table C18. Sample no. 18: Sieve analysis. Sample depth 1.5 ft.

	Class (phi)	Fraction Wt. (gm)	Weight (%)	Cumulative Wt. (%)
	-4.22	0.0	0.0	0.0
G	-3.66	0.0	0.0	0.0
R	-2.68	3.0	.4	.4
A	-2.35	1.2	1.3	4.7
V	-1.76	1.7	1.9	6.7
E	-1.24	2.2	2.5	9.1
L	-0.61	4.3	4.9	14.0
	-0.22	14.8	16.8	30.8
	0	10.8	12.2	43.1
	0.50	42.9	48.8	91.9
	0.75	4.5	5.1	97.0
S	1.75	1.0	1.1	98.0
A	2.33	1.0	1.2	99.2
N	2.74	0.2	.2	99.4
D	3.24	0.1	.1	99.6
	3.74	0.1	.1	99.7
	4.04	0.1	.1	99.8
	Pan	0.2	.2	100.0
Percent Gravel:		30.8		
Percent Sand:		69.0		
Percent Pan:		.2		

Table C19. Sample no. 19: Sieve analysis. Sample depth 2.2 ft.

	Class (phi)	Fraction Wt. (gm)	Weight (%)	Cumulative Wt. (%)
	--4.22	50.7	26.3	26.3
G	--3.66	69.4	36.1	62.4
R	--2.68	18.3	9.5	71.9
A	--2.35	1.7	0.9	72.8
V	--1.76	1.7	0.9	73.7
E	--1.24	1.7	0.9	74.6
L	--0.61	1.3	0.7	75.3
	--0.22	5.5	2.9	78.2
	0	3.5	1.8	80.0
	0.50	25.6	13.3	93.3
	0.75	5.4	2.8	96.2
S	1.75	1.2	0.6	96.8
A	2.33	3.5	1.8	98.6
N	2.74	1.2	0.6	96.8
D	3.24	0.4	0.2	99.5
	3.74	0.3	0.1	99.6
	4.04	0.1	0.1	99.7
	Pan	0.6	.3	100.0
Percent Gravel:		78.2		
Percent Sand:		21.5		
Percent Pan:		.3		



Table C20. Sample no. 20: Sieve analysis. Sample depth 2.6 ft.

	Class (phi)	Fraction Wt. (gm)	Weight (%)	Cumulative Wt. (%)
	-4.22	12.8	7.9	7.9
G	-3.66	9.5	5.9	13.8
R	-2.68	17.9	11.1	24.8
A	-2.35	4.3	2.7	27.5
V	-1.76	3.6	2.2	29.7
E	-1.24	2.3	1.4	31.1
L	-0.61	3.3	2.0	33.2
	-0.22	9.0	5.5	38.7
	0	8.4	5.2	43.9
	0.50	31.1	19.2	63.1
	0.75	15.1	9.3	72.4
S	1.75	6.9	4.3	76.0
A	2.33	30.3	18.7	95.5
N	2.74	0.1	0.0	95.5
D	3.24	6.1	3.7	99.3
	3.74	0.6	0.4	99.7
	4.04	0.3	0.2	99.9
	Pan	0.2	0.1	100.0

Percent Gravel: 38.7  
 Percent Sand: 61.2  
 Percent Pass: .1

Table C21. Sample no. 21: Sieve analysis. Sample depth 1.5 ft.

	Class (phi)	Fraction Wt. (gm)	Weight (%)	Cumulative Wt. (%)
	-4.22	138.0	45.2	45.2
G	-3.66	50.4	16.5	61.7
R	-2.68	34.1	11.2	72.9
A	-2.35	9.0	2.9	75.8
V	-1.76	9.8	3.2	79.1
E	-1.24	7.7	2.5	81.6
L	-0.61	7.1	2.3	83.9
	-0.22	8.4	2.8	86.7
	0	6.0	2.0	88.7
	0.50	19.0	6.2	94.9
	0.75	5.5	1.8	96.7
S	1.75	1.3	0.4	97.1
A	2.33	5.1	1.7	98.8
N	2.74	1.8	0.6	99.3
D	3.24	0.7	0.2	99.5
	3.74	0.6	0.2	99.7
	4.04	0.4	0.1	99.8
	Pan	0.3	0.1	99.9
Percent Gravel:		86.7		
Percent Sand:		13.2		
Percent Pan:		.1		

Table C22. Sample no. 22: Sieve analysis. Sample depth 5.8 ft.

	Class (phi)	Fraction Wt. (gm)	Weight (%)	Cumulative Wt. (%)
	-4.22	0.0	0.0	0.0
G	-3.66	0.0	0.0	0.0
R	-2.68	0.6	0.8	0.8
A	-2.35	0.4	0.5	1.3
V	-1.76	1.0	1.3	2.6
E	-1.24	2.0	2.7	5.3
L	-0.61	2.5	3.2	8.5
	-0.22	9.0	11.8	20.3
	0	7.0	9.2	29.5
	0.50	39.7	52.1	81.6
	0.75	2.2	2.9	84.5
S	1.75	2.7	3.5	88.0
A	2.33	7.3	9.6	97.6
N	2.74	1.0	1.4	99.0
D	3.24	0.3	.4	99.4
	3.74	0.2	.3	99.7
	4.04	0.1	.1	99.8
	Pan	0.2	.2	100.0
Percent Gravel:		20.3		
Percent Sand:		79.5		
Percent Pan:		.2		

Table C23. Sample no. 24: Sieve analysis. Sample depth 4.0 ft.

	Class (phi)	Fraction Wt. (gm)	Weight (%)	Cumulative Wt. (%)
	-4.22	12.5	19.3	19.3
G	-3.66	0.0	0.0	19.3
R	-2.68	2.9	6.0	25.3
A	-2.35	5.3	8.1	33.4
V	-1.76	8.4	12.9	46.3
E	-1.24	8.6	13.2	59.5
L	-0.61	5.2	8.0	67.5
	-0.22	6.32	9.6	77.1
	0	2.7	4.2	81.6
	0.50	6.1	9.4	91.0
	0.75	1.3	2.1	93.1
S	1.75	0.6	.9	94.0
A	2.33	2.3	3.5	97.5
N	2.74	1.1	1.7	99.2
D	3.24	0.4	.6	99.8
	3.74	0.2	.2	100.0
	4.04	0.1	.1	100.1
	Pan	0.1	.1	100.3
Percent Gravel:		59.5		
Percent Sand:		40.3		
Percent Pan:		.2		

Table C24. Sample no. 25: Sieve analysis. Sample depth 1.5 ft.

	Class (phi)	Fraction Wt. (gm)	Weight (%)	Cumulative Wt. (%)
	-4.22	55.4	29.9	29.9
G	-3.66	31.3	16.9	46.8
R	-2.68	22.5	12.1	58.9
A	-2.35	2.6	1.4	60.3
V	-1.76	5.8	3.1	63.4
E	-1.24	6.2	3.4	66.8
L	-0.61	7.5	4.1	70.9
	-0.22	8.0	4.3	75.2
	0	3.8	2.9	77.2
	0.50	17.6	9.5	86.7
	0.75	10.7	5.8	92.5
S	1.75	2.7	1.4	93.9
A	2.33	6.3	3.4	97.3
N	2.74	2.1	1.1	98.4
D	3.24	1.6	0.8	99.2
	3.74	0.7	0.4	99.6
	4.04	0.1	0.1	99.7
	Pan	0.1	0.1	99.8

Percent Gravel: 75.2  
 Percent Sand: 0.0  
 Percent Pan: .1

Table C25. Sample no. 26: Sieve analysis. Sample depth 2.5 ft.

	Class (phi)	Fraction Wt. (gm)	Weight (%)	Cumulative Wt. (%)
	-4.22	165.6	39.9	39.9
G	-3.66	18.9	4.5	44.4
R	-2.68	33.8	8.1	52.5
A	-2.35	12.5	3.0	55.5
V	-1.76	10.2	2.4	57.9
E	-1.24	10.9	2.6	60.5
L	-0.61	12.1	2.9	63.4
	-0.22	20.6	5.0	68.4
	0	17.9	4.3	72.7
	0.50	45.0	10.8	83.5
	0.75	22.3	5.4	88.9
S	1.75	8.8	2.1	91.0
A	2.33	22.5	5.4	96.4
N	2.74	6.2	1.5	97.9
D	3.24	3.8	0.9	98.8
	3.74	1.7	0.4	99.2
	4.04	1.6	0.4	99.6
	Pan	0.8	0.2	99.8
Percent Gravel:		68.4		
Percent Sand:		31.4		
Percent Pan:		.2		

Table C.6. Sample no. 27: Sieve analysis.

	Class (phi)	Fraction Wt. (gm)	Weight (%)	Cumulative Wt. (%)
	-4.22	0.0	0.0	0.0
G	-3.66	17.0	6.1	6.1
R	-2.68	18.5	6.7	12.8
A	-2.35	4.4	1.6	14.4
V	-1.76	4.4	1.6	16.0
E	-1.24	5.8	2.1	18.1
L	-0.61	8.2	3.0	21.1
	-0.22	14.4	5.2	26.3
	(	10.7	3.9	30.2
	0.50	45.4	16.4	46.6
	0.75	29.6	10.7	57.3
S	1.75	13.1	4.7	62.0
A	2.33	55.9	20.2	82.2
N	2.74	28.6	10.3	92.5
D	3.24	13.4	4.8	97.3
	3.74	4.7	1.7	99.0
	4.04	1.5	0.5	99.5
	Pan	0.8	0.2	100.0
Percent Gravel:		26.3		
Percent Sand:		73.2		
Percent Pan:		.5		

Table (27). Sample no. 28: Sieve analysis.

	Class (phi)	Fraction Wt. (gm)	Weight (%)	Cumulative Wt. (%)
	-4.22	128.5	31.0	31.0
G	-5.66	67.5	16.3	47.3
R	-7.68	22.7	5.5	52.8
A	-9.35	3.9	.9	53.7
V	-11.76	4.8	1.2	54.9
E	-14.24	6.1	1.5	56.4
L	-16.61	9.6	2.3	60.3
	-19.22	9.6	2.3	60.3
	0	2.8	.7	61.0
	0.50	27.5	6.6	67.6
	0.75	31.4	7.6	75.2
S	1.75	14.9	3.6	78.8
A	2.33	50.6	12.2	91.0
N	2.74	25.7	6.1	97.1
D	3.24	6.0	1.4	98.5
	3.74	2.8	.7	99.2
	4.04	1.4	.3	99.5
	Pan	0.4	.3	99.8
Percent: Gravel:		60.3		
Percent: Sand:		39.4		
Percent: Pan:		.3		



Table C28. Sample no. 29: Sieve analysis.

	Class (phi)	Fraction Wt. (gm)	Weight (%)	Cumulative Wt. (%)
	-4.22	16.4	5.8	5.8
G	-3.66	0.0	0.0	5.8
R	-2.68	5.2	1.8	7.6
A	-2.35	1.2	.4	8.0
V	-1.76	2.1	.8	8.8
E	-1.24	2.2	.7	8.8
L	-0.61	3.2	1.1	10.6
	-0.22	13.2	4.7	15.3
	0	15.6	5.5	20.8
	0.50	148.1	57.5	73.3
	0.75	45.6	16.2	89.5
S	1.75	8.9	3.1	92.6
A	2.33	16.5	5.9	98.5
N	2.74	1.8	.6	99.1
D	3.24	.6	.2	99.3
	3.74	.6	.2	99.5
	4.04	.3	.1	99.6
	Pan	.7	.2	99.8
Percent Gravel:		15.3		
Percent Sand:		84.3		
Percent Pan:		.2		

Table C29. Sample no. 30: Sieve analysis.

	Class (phi)	Fraction Wt. (gm)	Weight (%)	Cumulative Wt. (%)
	-4.22	56.5	13.0	13.0
G	-3.66	95.0	21.9	34.9
R	-2.68	39.3	9.1	44.0
A	-2.35	4.7	1.1	45.1
V	-1.76	3.7	.9	46.0
E	-1.24	3.9	.9	46.0
L	-0.61	5.1	1.2	48.1
	-0.22	15.4	3.5	51.6
	0	10.5	2.4	54.0
	0.50	66.1	15.2	69.2
	0.75	46.2	10.7	79.9
S	1.75	14.5	3.3	83.2
A	2.33	45.0	10.4	93.6
N	2.74	19.3	4.4	98.0
D	3.24	4.5	1.0	99.0
	3.74	3.0	0.7	99.7
	4.04	1.7	0.4	100.1
	Pan	1.0	0.2	100.3
Percent Gravel:		51.6		
Percent Sand:		48.2		
Percent Pan:		0.2		

## APPENDIX D

## CONTENTS

	Page
Figure -- Introduction	
D1. Calibration curve of specific conductance vs. chloride- ior concentration.....	354
Table -- Salinity - Profile Data from DS3	
D1. Specific-conductance measurements and estimated chloride- ior concentrations with depth.....	355
Figures -- Probability Plots of Relative Salinity for DS3	
D2. Profile 1 - March 6; 0900 hrs.....	357
D3. Profile 2 - March 7; 1330 hrs.....	358
D4. Profile 3 - March 9; 0930 hrs.....	359
D5. Profile 4 - March 13; 0830.....	360
D6. Profile 5 and 6 - March 14; 0810 hrs and 1730 hrs.....	361
D7. Profile 7 - March 15; 0830 hrs.....	362
D8. Profile 8 - March 16; 0830 hrs.....	363
D9. Profile 9 and 10 - March 17; 0800 hrs and 1545 hrs.....	364
D10. Profile 11 and 12 - March 18; 1115 hrs and 1515 hrs.....	365

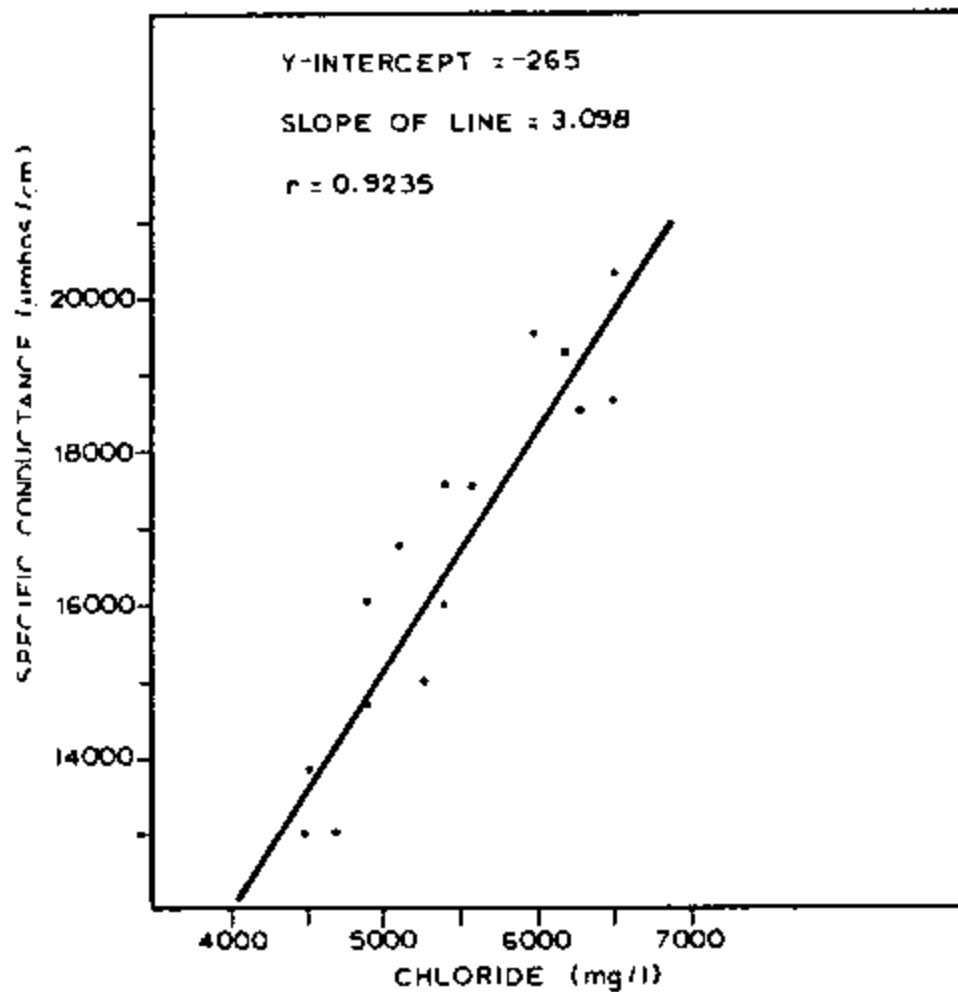


Figure D1. Calibration curve of specific conductance vs. chloride-ion concentration. Curve is used for  $Cl^-$  determination in collected water samples and borehole conductance measurements.

Table D1. Depth related specific-conductance and estimated chloride-ion data for DS3.

Depth below max water table (ft.)	Profile 1		Profile 2		Profile 3		Profile 4		Profile 5		Profile 6	
	Date: 3-6-84		Date: 3-7-84		Date: 3-9-84		Date: 3-13-84		Date: 3-14-84		Date: 3-14-84	
	Time: 0900		Time: 1330		Time: 0930		Time: 0830		Time: 0810		Time: 1730	
	S.Cond.	Chl	S.Cond.	Chl	S.Cond.	Chl	S.Cond.	Chl	S.Cond.	Chl	S.Cond.	Chl
1												
2												
3												
4	2725	705	120	>100	1800	385	6500	2005	3900	1110	2050	470
5			3400	935					6500	2005	2050	470
6	2725	705	3425	945	1950	435	5250	1575	6500	2005	2025	460
7			3425	955					6250	1920	2025	460
8	2750	710	3050	955	2000	455	2450	610	3200	865	2025	460
9			2450	610					2450	610	2100	490
10	2400	590	2275	550	2100	490						
11									2300	555	2200	520
12	2300	555	2275	550	2200	540	2350	575	2250	575	2250	540
13							2350	575				
14	2600	660	2350	575	3000	800	2450	610	2400	590	2600	660
15							2500	625				
16	2950	780	2650	675	2550	645	2500	625	3100	830		
17			3050	815			2650	675				
18	5500	1660	3650	1020	7000	2175	3500	970	3000	830	6500	2005
19							4500	1315	3600	1005	7500	2350
20	7050	2195	6000	1835	13000	4245	8250	2610	8000	2520	12000	4245
21			9050	2885			10300	3315	12500	4075	17000	5625
22	16000	5280			20000	6660	18000	5970	17000	5625	20000	6660
23	20500	6835					20000	6660	19500	6490	22500	7525
24	25000	8385			26250	8815	25500	8560	25000	8385	26750	8990
25							29000	9765	27500	9245	29500	9935
26					30000	10110	30250	10195	29250	9850	30250	10195
27							31250	10540	30250	10195	30500	10280
28					31000	10455	32000	10800	31250	10540	30750	10370

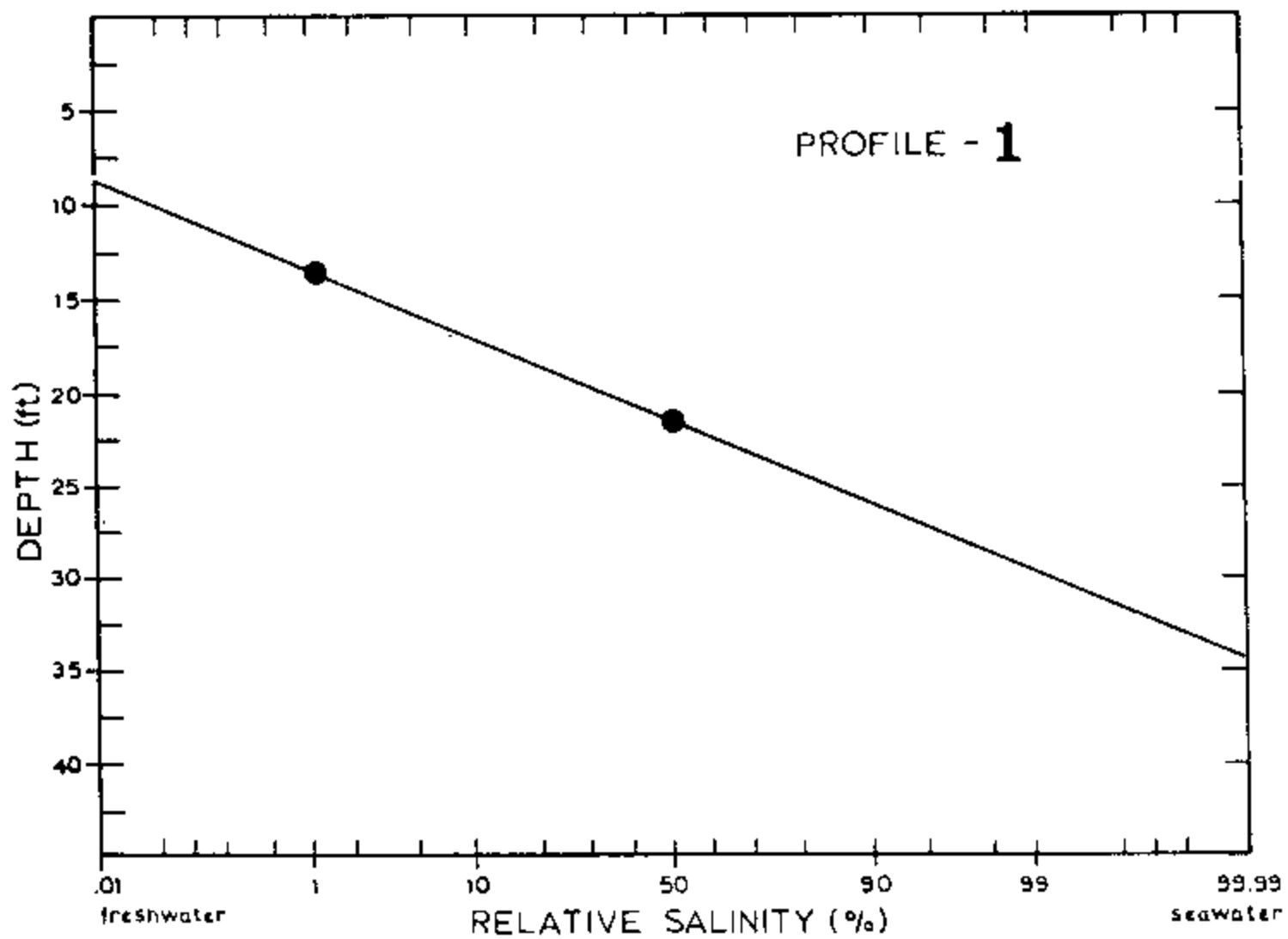
\* S. Cond. - Specific conductance,  $\mu\text{mhos/cm}$ .

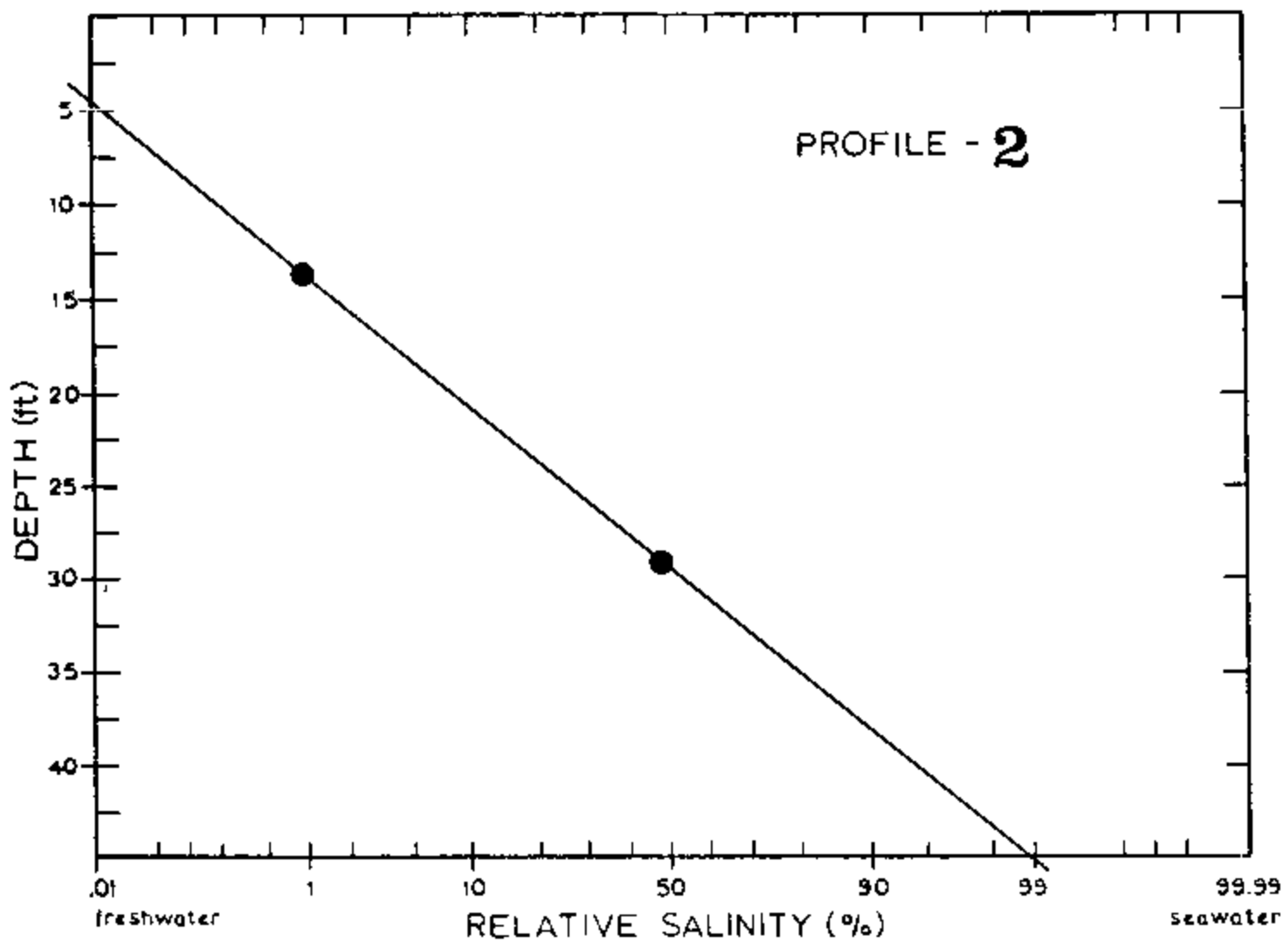
\*\* Chl. - estimated chloride (mg/l), based on graphical data.

Table D1. Continued

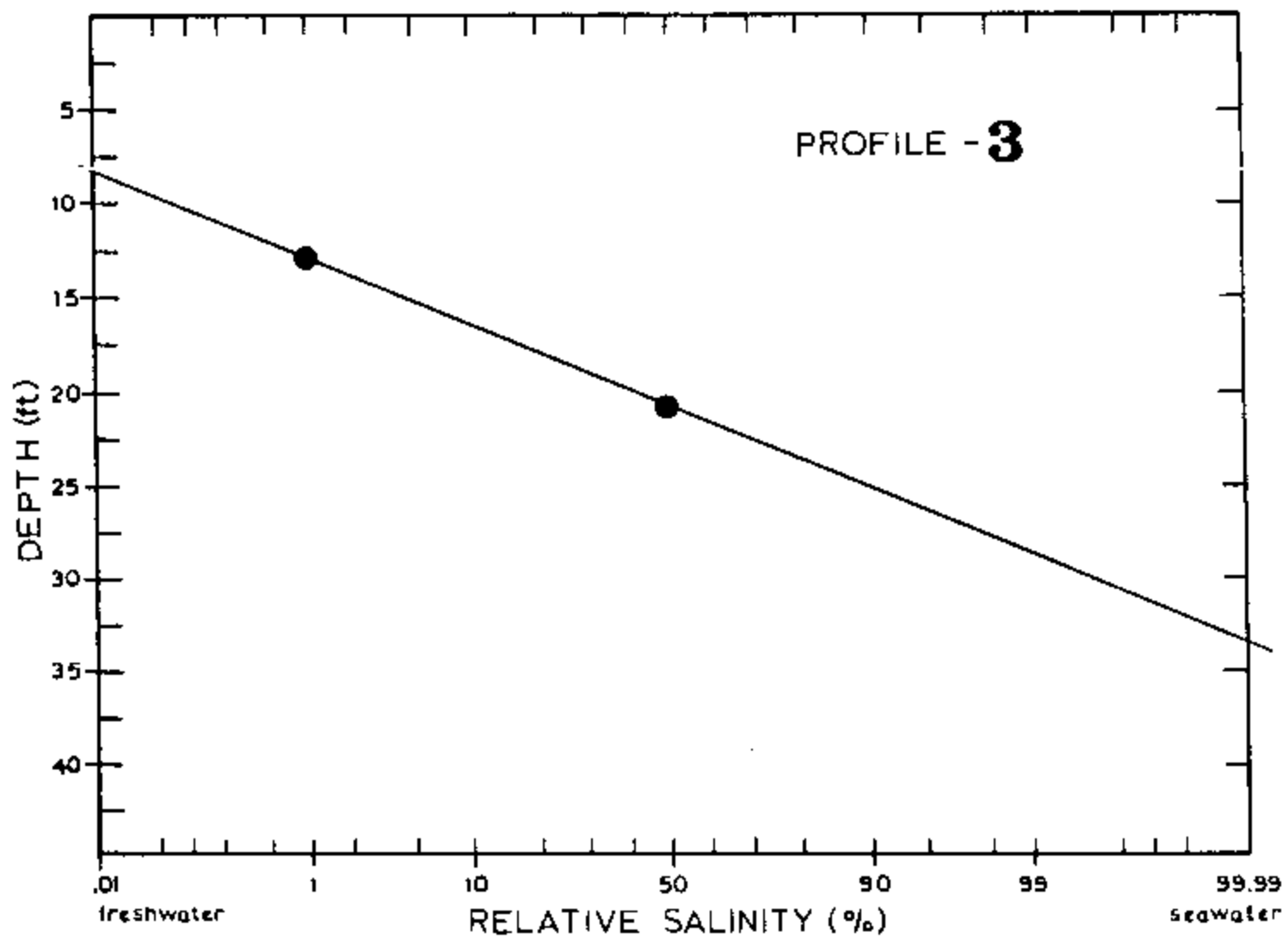
Depth below max water table (ft)	Profile 7 Date: 3-15-84 Time: 0830		Profile 8 Date: 3-16-84 Time: 0830		Profile 9 Date: 3-17-84 Time: 0800		Profile 10 Date: 3-17-84 Time: 1545		Profile 11 Date: 3-18-84 Time: 1115		Profile 12 Date: 3-18-84 Time: 1515	
	S.Cond.*	Chl**	S.Cond.	Chl.	S.Cond.	Chl	S.Cond.	Chl	S.Cond.	Chl	S.Cond.	Chl
1											3500	970
2							2175	515			3500	970
3							2225	530			3550	990
4	185	<100	400	<100	dry		2350	575	305	<100	3550	990
5	2800	730	1500	280	1350	230	2375	580	1300	<100	3575	995
6	2975	790	2400	590	2300	555	2375	580	2300	555	3575	995
7	3175	860	2550	645	2300	555	2400	590	2375	580	3575	995
8	2750	710	2575	650	2325	565	2400	590	2375	580	3600	1005
9	2450	610	2475	615	2450	610	2375	580	2450	610	3600	1005
10	2400	590	2475	615	2475	615	2400	590	2475	615	3600	1005
11	2375	580	2500	625	2500	625	2425	600	2500	625	3650	1020
12	2400	590	2525	635	2600	660	2475	615	2525	635	3700	1040
13	2400	590	2600	660	2875	755	3250	885	2700	695	4400	1175
14	2400	590	2600	660	2875	755	3250	885	2700	695	4400	1280
15	2450	610	2725	705	3000	800	3500	970	2800	730	4500	1315
16	2500	625	2750	710	3250	885	3575	995	2850	745	4550	1330
17	3000	800	3000	800	3100	830	5500	1660	3000	800	5000	1490
18	3500	970	3600	1005	4700	1385	8000	2520	3400	935	7800	2455
19	6000	1835	8000	2520	6250	1920	8750	2780	4050	1160	8500	2695
20	800	2520	10000	3210	11750	3820	13000	4245	8250	2610	13500	4420
21	12500	4075	14000	4590	15750	5195	17000	5625	12250	3990	18000	5970
22	17000	5625	18000	5970	19000	6315	19750	6570	17000	5625	20000	6660
23	19500	6490	20000	6660	20750	6920	23000	7695	19250	6400	23750	7955
24	24750	8300	26000	8730	27000	9075	28000	9420	24500	8215	28000	9420
25	27500	9245	28000	9420	29000	9765	30000	10110	27750	9335	31000	10455
26	29500	9935	29000	9765	30750	10370	31000	10455	30000	10110	32000	10800
27	30000	10110	30000	10110	31250	10540	31500	10625	30750	10370	32500	10970
28	3025	10280	32000	10800	31500	10625	31500	10625	3100	10455	32500	10970

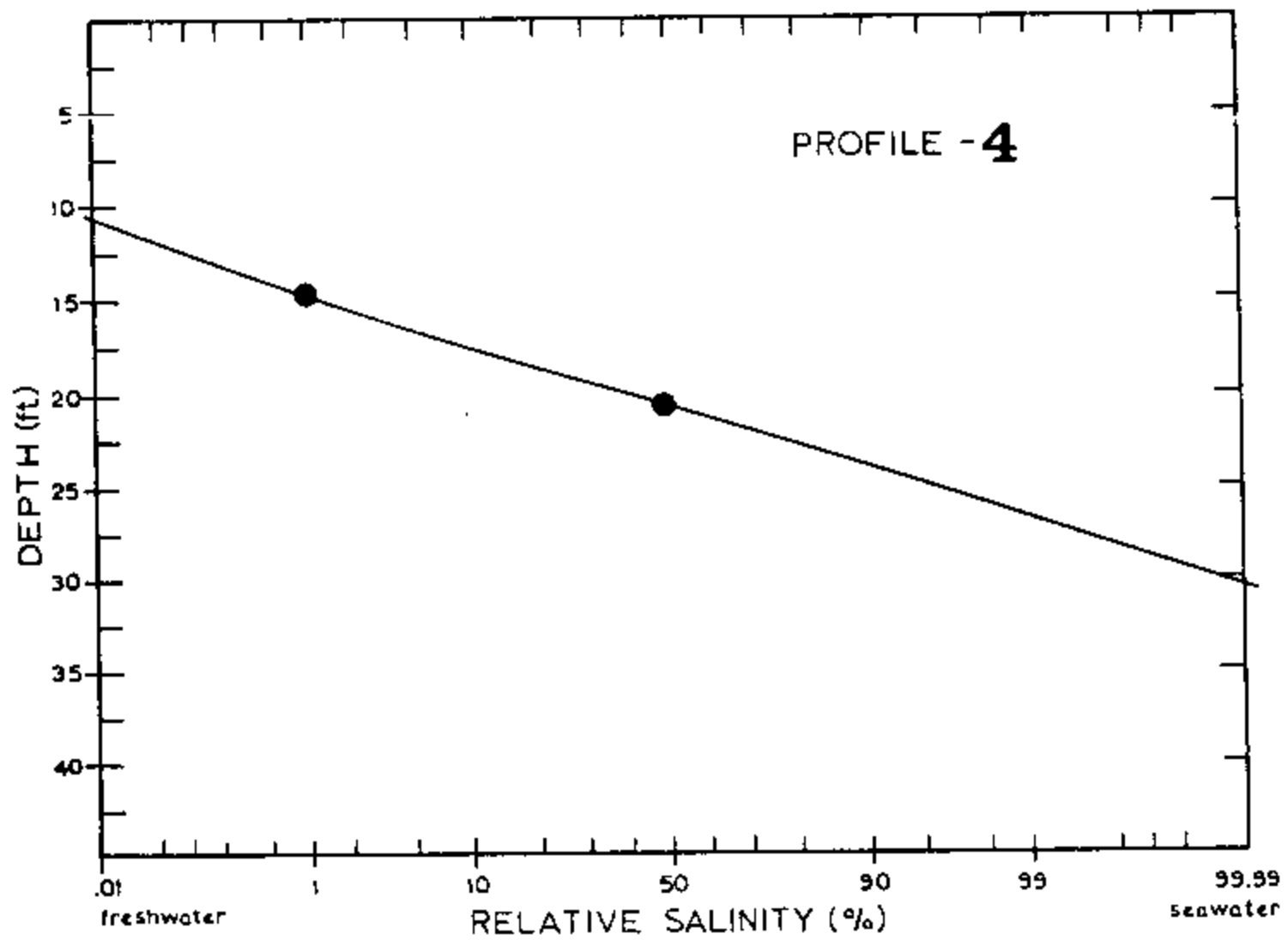
\* S. Cond. - Specific conductance in  $\mu\text{mhos/cm}$

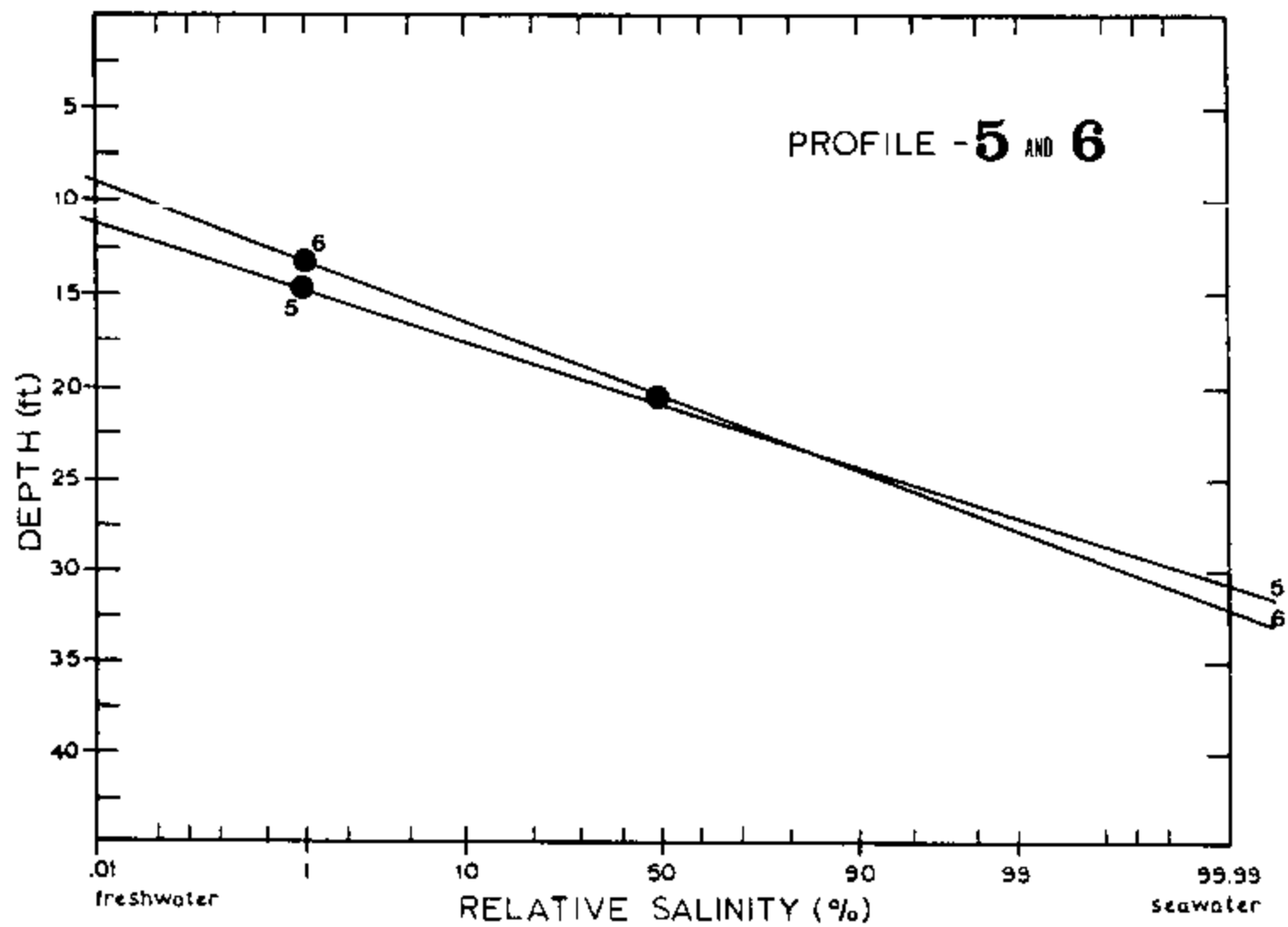


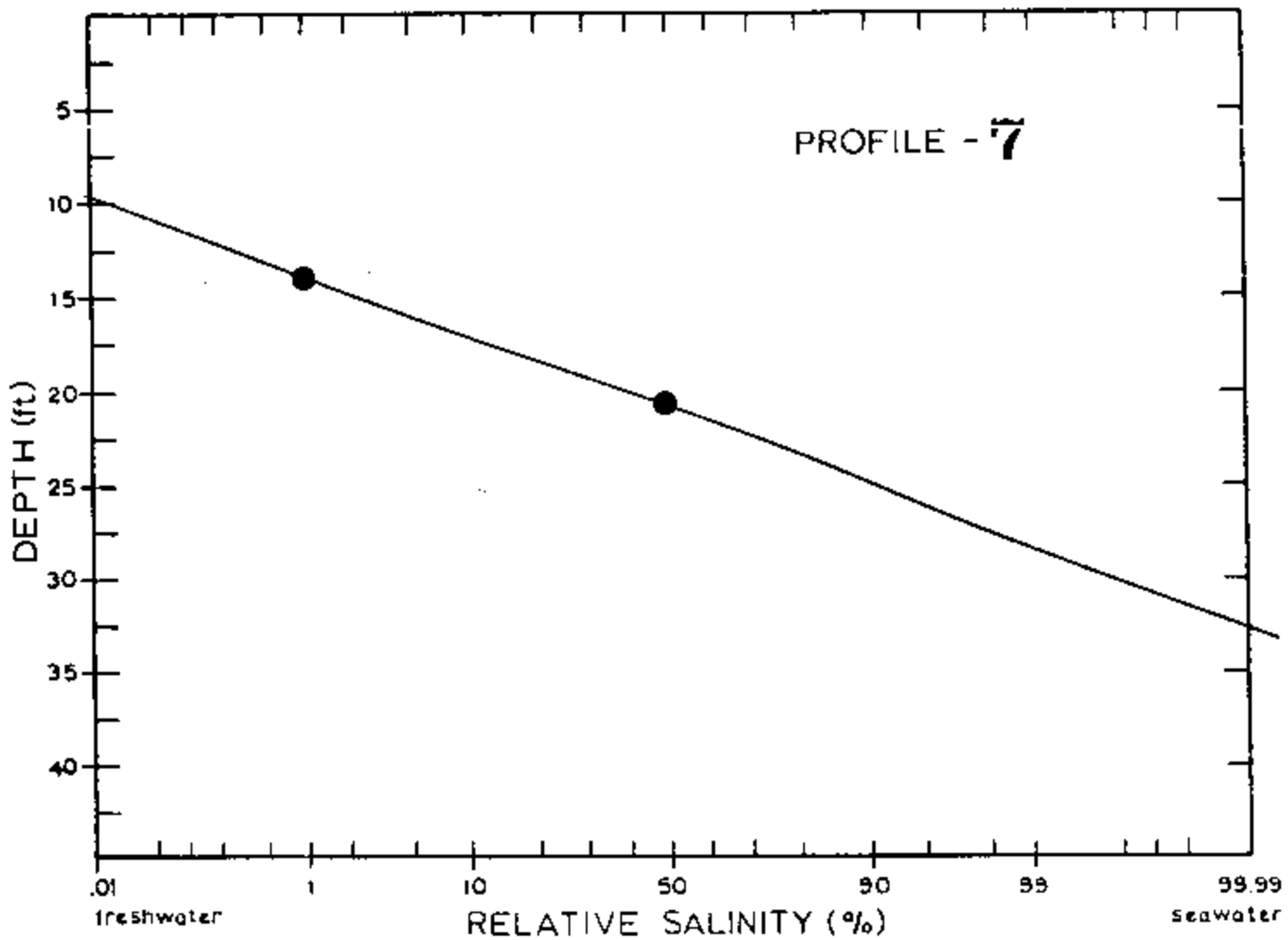


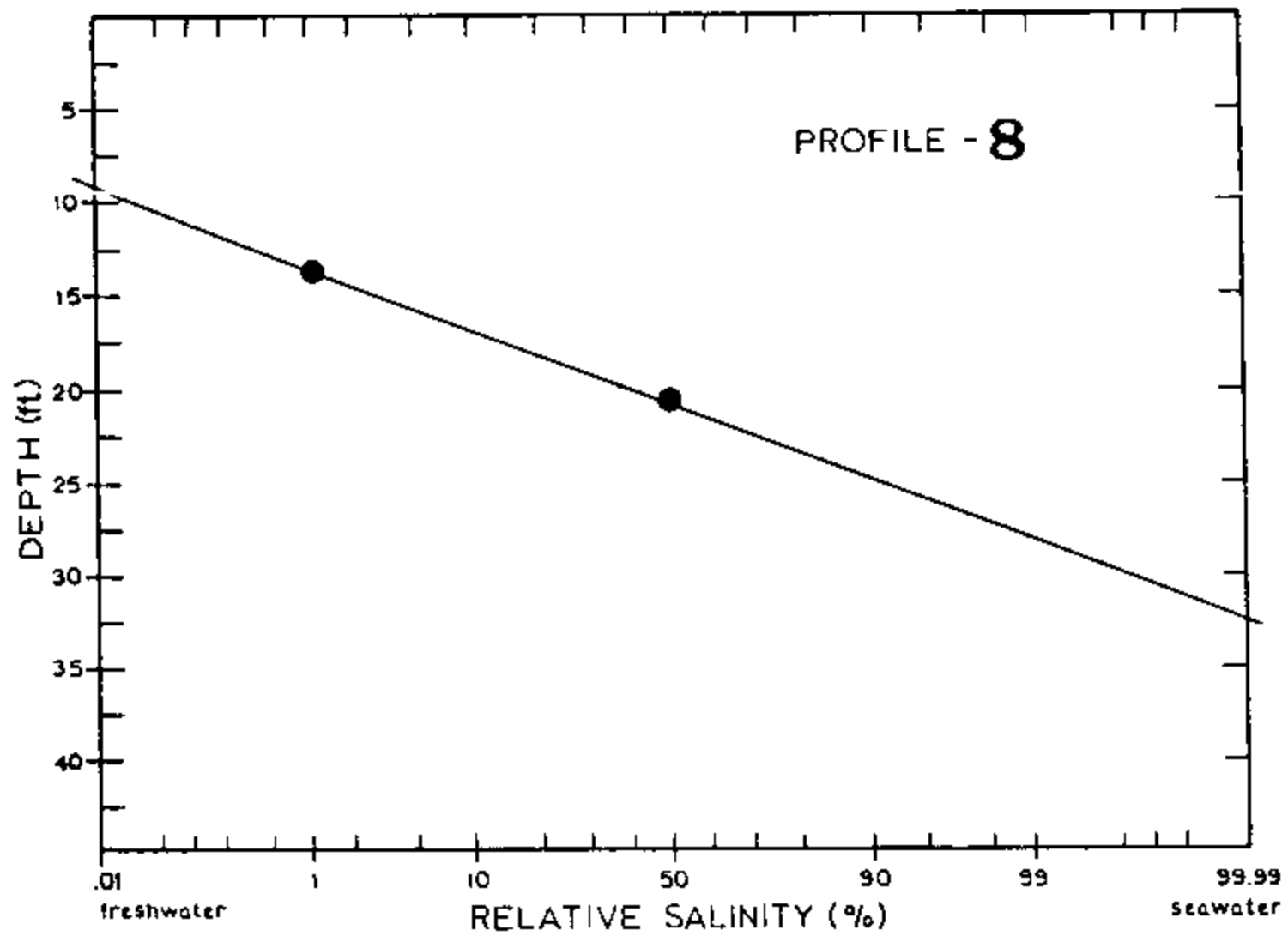


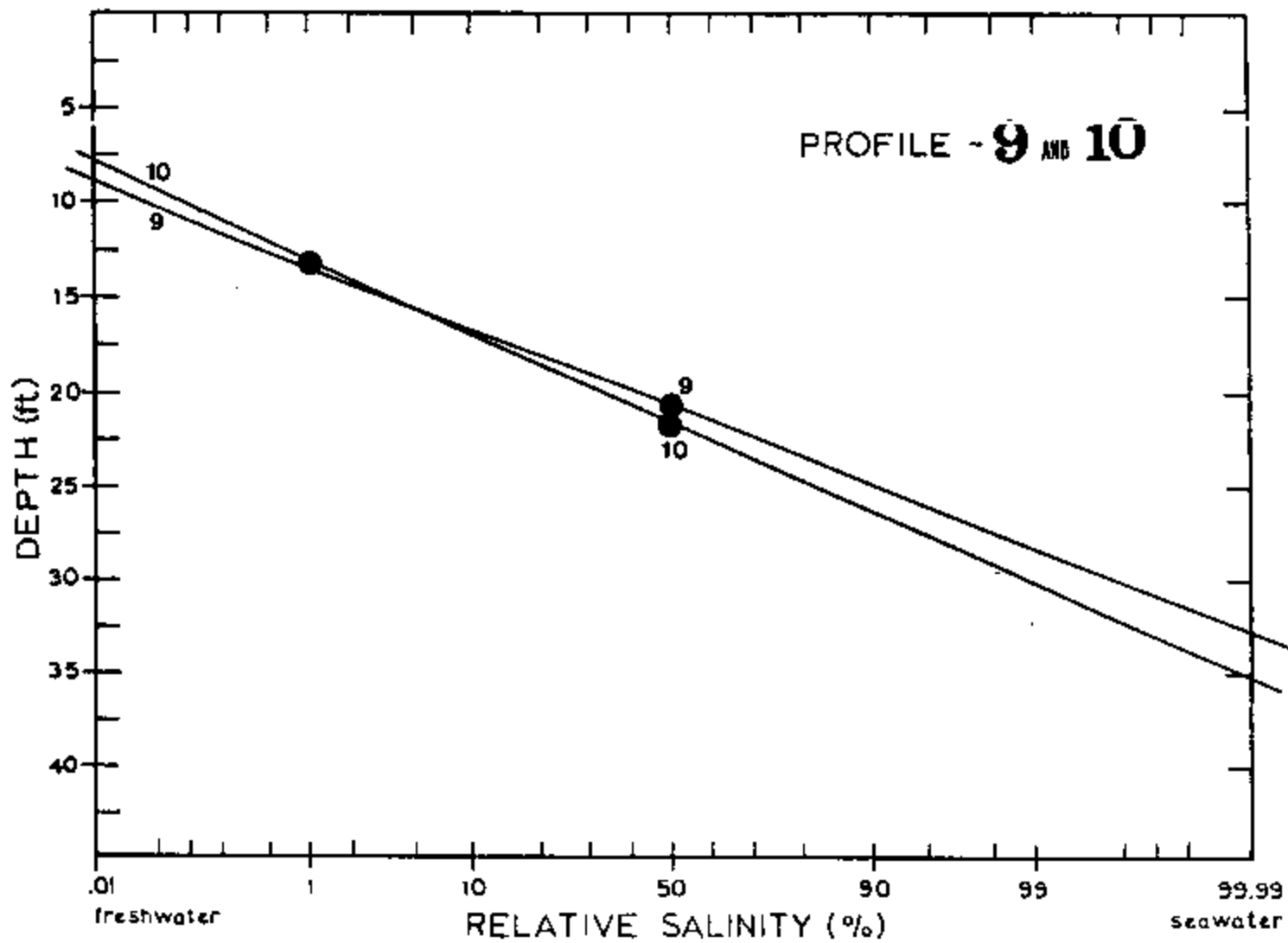












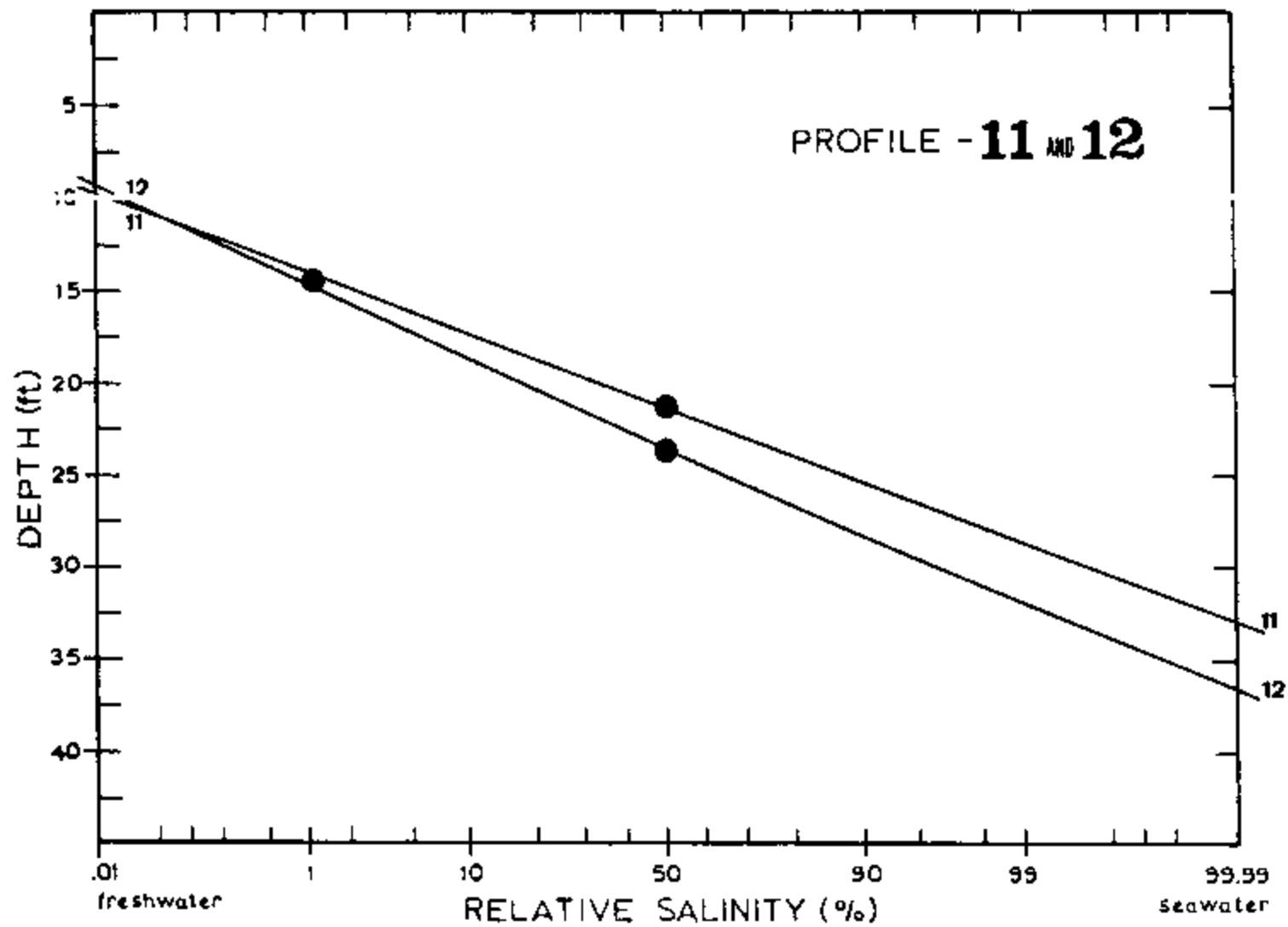


Table D2. Depth related specific-conductance and estimated chloride-ion data for DS4.

Depth below max water table (ft)	Profile 1 Date: 3-15-84 Time: 0845		Profile 2 Date: 3-16-84 Time: 0805		Profile 3 Date: 3-17-84 Time: 0740		Profile 4 Date: 3-18-84 Time: 0512	
	S.Cond.	Chl**	S.Cond.	Chl	S.Cond.	Chl	S.Cond.	Chl
1	205	<100	118	<100	dry		dry	
2	2075	480	2000	455	190	<100	145	<100
3	2050	470	2150	505	1900	420	1800	385
4	2125	495	2375	580	2450	610	2300	555
5	6500	2005	6900	2145	8800	2800	7500	2350
6	12000	3900	13750	4505	16000	5280	15750	5195
7	12750	4160	14000	4590	16250	5365	16500	5455
8	12750	4160	14000	4590	16250	5365	16500	5455
9	12750	4160	13750	4505	16250	5365	16500	5280
10	13250	4335	14000	4590	16750	5540	16250	5365
11	15250	5025	16000	5280	18000	5970	17000	5625
12	17500	5800	16250	5365	18000	5970	17750	5885
13	19250	6400	17000	5625	20000	6660	18000	5970
14	21000	7005	19000	6315	24000	8040	18500	6145
15	21250	7090	20000	6660	24500	8215	19000	6315
16	22000	7350	20750	6920	25000	8385	19250	6400
17	22000	7350	21250	7180	25500	8560	20000	6660
18	22000	7350	21250	7180	25500	8560	20000	6660
19	22250	7435	21500	7265	25500	8560	20000	6660
20	22250	7435	21750	7265	25500	8560	20250	6745
21	22250	7435	22000	7350	25750	8645	20250	6475
22	22250	7435	22000	7350	25750	8645	20500	6835
23	22250	7435	22000	7350	26000	8730	20500	6835
24	22250	7435	22000	7350	26000	8730	20500	6835

\* S. Cond. - Specific conductance,  $\mu\text{mhos/cm}$ .

\*\* Chl. - estimated chloride (mg/l), based on graphical data.